Statistical, Electrical and Mathematical Analysis of Water Treed Cross-Linked Polyethylene Cable Insulation

Elfrith Foottit

Bachelor of Engineering (Electronics) (Hons) \
Bachelor Information Technology (Computer Science) (Dist),
QUT, Brisbane, Australia, 2003

This thesis was submitted
as part of the requirements for the degree of

Doctor of Philosophy

in the

School of Engineering Systems
Science and Engineering Faculty

at the

Queensland University of Technology
Brisbane, Australia.

2015

Abstract

This work presents the results of an accelerated wet ageing test that was designed to examine the effects of water treeing on commercially available XLPE cable. The test was performed on samples of modern construction XLPE cable, as well as older style cable as found currently in-service in many electrical networks. The older style cable was treated with silicone oil 'restoration' fluid, as may be performed on in-service cable of this type. Electrical measurements were taken on the samples, and after a specified ageing period, they were broken down by an ACBD step test.

The samples were then analysed post-mortem in order to correlate the electrical measurements with the internal morphology of the cable, specifically with the type, number and length of water trees found. An improved technique of optical post-mortem analysis was developed, which enabled a large population of water trees to be measured.

Statistical tests were performed on the populations measured, with the result that the field-aged and treated samples were shown to have a higher number of water trees with a greater length, correlating to a lower breakdown strength. A population model was created, suggesting that the lognormal distribution gives a better fit than the Weibull distribution when considering the length of bow tie trees grown in XLPE.

A new ageing factor was proposed - the degree of non-linearity. This factor requires simple, off the shelf hardware to compute, and may be used to give a classification of in-service XLPE cable. While there may be several confounding factors in a given sample, it was found that the degree of non-linearity did correlate to the length of water trees found in the samples in this test.

Finally, a mathematical model was created to remove confounding factors in electrical measurements. This model isolated the phenomena of dielectrophoresis as a mechanism for the change in morphology of XLPE, this change

in morphology causing the non-linear response. It was found that the simulated samples did show an increase in non-linearity with increasing water tree length as was found in the electrical measurements, however the order of magnitude of change was much smaller in the simulations than the electrical measurements.

Contents

List of Figures

List of Tables

Declaration

The work contained in this thesis has not been previously submitted for a degree or diploma at any higher education institution. To the best of my knowledge and belief, the thesis contains no material previously published or written by another person except where due reference is made.

Signed: QUT Verified Signature **Date:** 6.7.2015

Previously Published Material

The following papers have been published or presented, and contain material based on the content of this dissertation:

[1] F. Foottit, J. Lyall, D. Birtwhistle, P. Wickramasuriya, R. Gilbert, L. Powell, and T. Saha. An accelerated wet ageing test on meduim voltage xlpe cables. *Australian Universities Power Engineering Conference (AUPEC)*, 2004.

[2] B. Oyegoke, F. Foottit, D. Birtwhistle, J. Lyall, and P. Wickramasuriya. Condition assessment of xlpe insulated cables using isothermal relaxation current technique. In *Power Engineering Society General Meeting, 2006. IEEE*, page 6 pp., 0-0 2006.

The following papers utilise data gained from the facility described in this document and maintained by the author of this thesis.

[1] A. Thomas and T. Saha. Statistical analysis of diagnostic indicators during an accelerated ageing experiment for xlpe cable specimens. *Dielectrics and Electrical Insulation, IEEE Transactions on*, 19(1):274 –282, february 2012.

[2] A. Thomas and T. Saha. A new dielectric response model for water tree degraded xlpe insulation - part a: model development with small sample verification. *Dielectrics and Electrical Insulation, IEEE Transactions on*, 15(4):1131 –1143, august 2008.

[3] A. Thomas and T. Saha. Frequency domain dielectric relaxation in water tree degraded xlpe cables. In *Power Engineering Conference, 2007. AUPEC 2007. Australasian Universities*, pages 1 –6, dec. 2007.

[4] A. Thomas and T. Saha. A theoretical investigation for the development of a water tree dielectric response model. In *Electrical Insulation and Dielectric Phenomena, 2006 IEEE Conference on*, pages 369 –372, oct. 2006.

[5] A. Thomas and T. Saha. The analysis of dc and ac conductivity in the detection of water tree degradation in xlpe cables. In *Power Engineering Society General Meeting, 2005. IEEE*, pages 87 – 94 Vol. 1, june 2005.

[6] J. Yew, T. Saha, and A. Thomas. Impact of temperature on the frequency domain dielectric spectroscopy for the diagnosis of power transformer insulation. In *Power Engineering Society General Meeting, 2006. IEEE*, page 7 pp., 0-0 2006.

Acknowledgements

First and foremost, I must thank the team at Ergon Energy, especially the staff at the testing workshop in Virginia, whose skill and dedication enabled this project to proceed.

Secondly, the members of the research team : Dr Jim Lyall, A/Prof David Birtwhistle, Prof Tapan Saha, Dr Bolarin Oyegoke, and Dr Andrew Thomas. For providing advice, inspiration and direction to this project and this thesis. A special mention to Dr Jim Lyall, whose tireless dedication to this thesis far exceeded its original time-line and who provided direction and encouragement beyond the boundaries of this project.

The members involved in research at QUT: Arnold, Dave, Simon, Maree, Shui, Reza, Richard, Hilary, Keith, and the coffee club - you helped me survive the 'abyss' of writing, and find the inspiration to continue when quitting would have been so much easier. And I would especially like to thank Dr Dan Mueller for giving me his LaTeX thesis template, without which I would have been using Word.

And finally, I must thank my family for allowing me the time to achieve this milestone. Renae, you can have your husband back now!

> "It is not the mountain we conquer, but ourselves." -Sir Edmund Hilliary

Chapter 1

Introduction

Scientia Potentia Est
Knowledge is power

Old Proverb

1.1 Overview of Work

Ergon Energy is an electrical distributor located in northern Queensland, Australia. While they service a relatively modest number of subscribers compared to urban network operators, the area covered by their network is extensive. Therefore, efficient monitoring and maintenance of their network is of prime importance.

They have commissioned this work to investigate methods of assessing the condition of their XLPE distribution network. The goal of this project is to gain a better understanding of the processes involved in the ageing of XLPE, investigate how these processes may be measured non-destructively, and suggest a testing regime that allows the use of 'just in time' maintenance practices and prioritisation of replacement of in-service underground XLPE cable based on condition monitoring.

Furthermore, this project aimed to shed some light on the effects of a typical cable treatment program designed to 'cure' XLPE cables of water treeing by chemically changing water trees into a form that can withstand significant

voltage stress. This process is not well documented in published literature, but it has gained widespread acceptance in several countries. Anecdotal studies of the effects of the curing process have been published, yet firm conclusions remain elusive [13, 31, 88, 92].

Despite the measurably different electrical characteristics of XLPE post treatment, it is common practice to apply the same diagnostic procedures to cable that has been treated. The measurements and analysis of the samples in this test highlight the need for revision of 'normal' parameters in cable that has been treated with curing agents. In particular, the treatment process increases the electrical losses of the sample, making it appear to have a more severe infestation of water trees. Isothermal relaxation current measurements in particular are affected by the change in response of the sample.

Currently, there are two methods of testing XLPE non-destructively in common usage: time domain methods and frequency domain methods. The installation on which this work is based encompasses the use of both time and frequency domain methods, however this document is focused on the use of time domain measurements to assess the condition of water treed XLPE. For a detailed analysis of the effectiveness of frequency domain techniques, the interested reader is directed to [102].

This work describes the use of time domain measuring equipment and statistical analysis to better understand the internal structure of water treed XLPE cable. By improving understanding of the relationship of the internal structure to the electrical measurements, the state of the insulation may be estimated. New XLPE is a high quality material that displays many characteristics of an ideal dielectric (high resistivity, low dispersion, low permittivity). Ageing by water treeing can be likened to adding impurities to virgin XLPE, thus degrading its electrical performance. In particular, the low dispersion of XLPE is affected when impregnated with water.

However, the chemical properties of XLPE are such that the continuing presence of water requires an external driving force. It is proposed that the external electrical field applied to a cable under load provides this force - literally squeezing the water into small cracks and weak points in the insulation. When the external force is removed, the compressive internal forces of the insulation will push the water out of the water tree, causing it to collapse, leaving a tree-shaped potential space inside the insulation.

The field-dependant change in water tree structure can be used as a tool to examine a cable for the presence of water trees. In a sample with few water trees, the change will be close to zero. However, as the number and length of water trees increases, this change in the morphology of the sample will create a larger deviation from the 'ideal' response. This increasing deviation of the sample from a linear response gives an indication as to the state of the insulation.

Rather than observing a linear increase in measured current when increasing the applied voltage, there will be an element of non-linearity to the response in water treed XLPE. By contrast, it is expected that virgin insulation will maintain a linear response to increasing voltage (within the level of stresses applied in the proposed tests)[1].

The primary goal of this work is analysing this *degree of non-linearity* (DONL). This factor, calculated from non destructive tests at multiple voltage levels, is based on the proposed mechanism that the amount of water in a sample of XLPE will be related to the magnitude of the external driving field and its effect on any water trees present. Undamaged XLPE should show a linear increase in current to an increasing applied voltage, as approximated by an ideal dielectric. By analysing the deviation of a sample from this ideal response, a new means of diagnostic assessment has been developed that uses simple equipment that can be used to classify aged XLPE cables in situ.

A proposed mechanism for the change in internal morphology is a phenomenon known as *dielectrophoresis*. Dielectrophoretic force is a mechanical force applied to uncharged dielectric molecules when a potential field is constructed. In a non-uniform electric field, materials with a higher permittivity (water) than the surrounding medium (XLPE) will be attracted to regions with a high electric field [86, 85].

A commonly held view is that water trees are made up of channels with some degree of plasticity, meaning an applied force may cause water trees to change their length, depending on the magnitude of the applied field. The diagnostic approach developed here is based on dielectrophoresis and analysis of the information gained from time-domain effects to classify the state of the insulation non destructively.

[1] It is well known that dielectric materials display non-linear behaviour at very high stresses, however the applied voltages are an order of magnitude lower than the dielectric breakdown level where these phenomenon occur.

An accelerated ageing facility was constructed according to IEEE standard 1407 [1] in order to study the effects of water treeing on time and frequency domain measurements. The facility was also intended to study the effectiveness of the silicon restoration treatment process on aged samples of XLPE. This work does not focus on the effectiveness of the treatment specifically, but rather the effects of the fluid on the internal morphology of the insulation and the effects of the treatment on the electrical measurements. This topic is discussed in chapter 3.

One aspect of the work presented here that differs from many of the other tests based on this same standard is the lack of water inserted into the conductor core of the samples. This treatment was not possible due to the terminations of the treated samples having a water-proof seal. Inserting water would require breaking the seal, and possibly removing some of the injected fluid in order to gain access. It was considered that the terminations used should be as close as possible to those that would be applied in the field, and as such there could be no water inserted into the conductor interstitium on these samples. In order to maintain consistency, there was no water inserted into the other sample groups.

This difference may have a significant effect on the amount of water trees grown. The samples in this test aged somewhat less rapidly than those in other tests, and this is considered to be one of the major contributing factors to the relatively good quality of the insulation at the termination of the test. This key point of difference makes the results of this test difficult to compare to other, otherwise similar, tests.

After 400 days of effective ageing, the samples were broken down in a high voltage step breakdown test. An analysis of the breakdown voltages was performed to correlate the measurements taken directly before the breakdown test with the forensic analysis performed directly afterwards. The forensic analysis estimated the length of the longest water tree and compared it to the breakdown strength and the condition of the sample predicted by non-destructive electrical measurements.

A computer model was constructed in order to isolate the proposed mechanisms of ageing. This model uses a novel technique for computing a time varying electric field in three dimensional space, referred to here as the *flux balance method*. This tool was developed at QUT for use in teaching field theory to

undergraduate engineers [64]. The use of a custom tool allowed the model to focus on the unique effects of water and XLPE interaction in an applied field.

The simulation was used to analyse the effect of polymer morphology on electrical measurements, specifically the effect of the size of water trees on the linearity of the response to an applied electrical field. The model used measurements taken from the ageing facility in order to more closely correlate the results of the model with the forensic analysis of the broken down samples. This model correctly produced a non-linear response in samples with changing water tree lengths, although the magnitude of the response is somewhat smaller than measured in the samples.

Finally, the samples were analysed forensically, with a new procedure for analysing significantly greater quantities of insulation developed. The method used in this work was used to analyse approximately 0.5% of the total insulation length in the test (microscopic analysis of approximately 600mm of insulation overall was performed). This is a far greater amount than typically published, and the detailed examination presented allowed for a more rigorous statistical analysis of water tree lengths in aged XLPE.

Despite the absence of water in the conductor interstitium, water trees were found throughout both groups of samples. However it is possible that the water trees are shorter and fewer in number than might otherwise have been found, as similar tests have grown water trees to approximately the thickness of the insulation in this time period [99].

The forensic analysis examined the effects of the CableCure process on both the qualitative and quantitative properties of water trees. Quantitatively, its effect on the length and number of water trees was analysed. Qualitatively, the presence of 'old' and 'new' water trees was inferred by the discovery of two water tree types appearing in the treated samples, and only a single type being found in the untreated samples.

The statistical review of the data obtained in this ageing test forms a significant part of the contribution of this work. While other tests have been done in a similar manner, the development of a new forensic analysis technique has allowed the examination of a much larger number of samples than previously, and the resulting increase in confidence of the conclusions provides some insight into new directions for research.

Specifically, this work presents a detailed analysis of the statistical distri-

bution of the lengths and location of bow tie water trees. This represents an original contribution, as no detailed studies on the properties of bow tie tree populations was found in the literature.

The statistical analysis produced evidence supporting the currently accepted theory that water trees lower the breakdown strength of XLPE. This supports the current consensus that an accelerated ageing test will grow water trees of non-trivial sizes, and these water trees will affect the properties of the insulation, specifically the AC breakdown strength of the samples. The analysis also gave support for the use of the log-normal probability distribution for modelling the length of bow tie trees grown in commercial XLPE.

The statistical analysis produced evidence for the use of the log-normal distribution when modelling the length of bow tie water trees in aged XLPE. This statistical model more closely follows the data gained from the test than the two most common alternatives: Weibull and normal (Gaussian).

When analysing and comparing the length of the longest water tree (considered by many to be the most significant factor), Weibull extreme value analysis was used, with the samples indicating a detectable difference in water tree length that may explain the difference in breakdown values of the two groups. This method of analysis (and indeed, this experimental method) does not allow for analysis of remaining lifespan, rather the undamaged insulation thickness is used as a proxy for insulation age.

It was found that water trees are not uniformly distributed throughout the bulk insulation (that is, the location of the centers of the bow tie water trees did not follow a uniform distribution), and the location of a water tree has no correlation to its length. This somewhat surprising result suggests there may be an interplay of factors involved in the initiation of water trees, rather than a simple 'field strength' or 'impurity' distribution. Ultimately, at the conclusion of this work, the distribution of water trees within the cable still remains unknown. The analysis and data that led to this conclusion can be found in chapter 4.

Chapter 4 describes the extreme value analysis of the water tree length and the AC breakdown strength of the samples. The extreme value analysis supports the prevailing theory that longer water trees lead to lower breakdown strength. There is a change in the Weibull shape parameter of the samples treated with silicone restoration fluid that may improve the lifespan of treated

samples by modifying the distribution of the water tree lengths in treated samples. The exact nature and effect of the change on the statistical distribution is still unknown. It is assumed that this effect is beneficial due to the positive experiences described in the literature, but the evidence indicated in this work is not conclusive in that regard.

Following this, chapter 6 describes the results of a computer model constructed to analyse the effects of water tree length on dielectric measurements. It was found that modifying the lengths of vented water trees gave a similar non-linear effect as found in the measurements taken on the samples during the test, albeit with significantly lower magnitude in the simulations than the sample measurements.

The theory on which the model is based is well established and the model will yield a behaviour according to the established theorems of electromagnetic theory. The most significant area of deviation of the model from reality is in the functions used to define material behaviour. It was found that time domain material properties of virgin XLPE and water were not easily found in the literature. As such, the approximations used in the model are based on measurements taken from the samples in the test, which almost certainly contain errors related to time, temperature, and environmental conditions that are not well controlled in a large scale experiment (compared with taking very accurate measurements on very pure samples in the laboratory).

In summary, the major contributions of this work are the following:

- Statistical evidence for bow tie water trees not being uniformly distributed inside the bulk insulation
- Statistical evidence for the length of bow tie trees being independent of location within the bulk insulation
- Statistical evidence for the length of bow tie trees being log-normally distributed
- Qualitative evidence for the existence of two separate type of water trees in bulk XLPE treated by silicone restoration fluid
- Qualitative evidence, supported by numerical modelling, of a change in the linearity of the response of XLPE being related to the presence and length of vented water trees in the insulation

The work presented here has focused on presenting the most reliable and well-supported data taken from the ageing test. It is the nature of such a test to have many confounding factors both foreseen and unforeseen. Furthermore, the significant downtime experienced in this test frustrated attempts to analyse the effects of ageing time on the samples. Thus the principal contribution of this work is the statistical analysis, which has the most reliable data. The electrical measurements provide some insight into the effects of water treeing on XLPE, but with less certainty. The correlation of the measurements with the simulation lends extra weight to the proposed mechanisms, but these still remain firmly in the bounds of 'working hypothesis', rather than 'strongly supported' theory.

Chapter 2

Water Treeing in Underground Cables - A Review

> Imagination is more important than knowledge.
>
> *Albert Einstein*

2.1 Underground Cable

The use of underground cable for distribution of electrical power is common due to the benefits it affords compared to overhead power lines, especially in built up areas. The principle benefits are improved appearance and fewer catastrophic interactions (vehicle crashes, lightning strikes, storms, etc.). The cost of this concealment is increased difficulty in monitoring the state of the insulation, combined with ongoing exposure to a damaging environment. Furthermore, the inhomogeneity of the environment poses challenges related to localised defects; for example, when determining the load capacity of the cable, localised heating effects may be the most significant factor in assessing the safe operating load. In the case of a direct buried polymeric insulated cable subjected to a wet or humid environment, localised concentrations of water can cause repeated failures in one segment of cable, while other segments of the same cable remain in 'almost new' condition. These localised effects pose

a significant challenge - an entire cable may be rendered unserviceable due to localised failure in one region, and electrical measurements on XLPE cable usually consider the whole length as a whole. As such, localised defects are 'averaged out' and can be undetectable, while still presenting clear danger to the cable as a whole.

2.1.1 Types of Underground Cable

There are three types of underground distribution cables in common use: Oil-Paper Insulated, Gas filled, and Polymeric. The appropriateness of an insulation type for a particular facility is based on several factors that may not be particularly related to insulation performance. As a general rule, non-polymeric installations require significantly greater expense to install and maintain, and are typically used in very high voltage and high power delivery installations, where polymeric insulation has not been extensively tested. In contrast, the main benefit of polymeric insulation is a low maintenance life-cycle and lower electrical losses, with relatively lower power delivery, and it is becoming the preferred choice for high voltage installations as well as distribution networks. There are two main types of polymeric insulation, cross-linked polyethylene (XLPE) and ethylene propylene rubber (EPR). In general terms, XLPE insulation is stronger physically and has a lower loss factor. EPR on the other hand is more flexible, making it easier to work with inside installations. As such, XLPE is commonly used for longer runs and in outdoor settings, while EPR is used more often indoors and in confined spaces.

2.1.2 Cross-Linked Polyethylene Cable (XLPE)

XLPE is the most commonly used polymeric insulation. Compared to oil-paper insulation (which it often replaces), XLPE has better durability, lower electrical losses, easier handling and simpler termination requirements. Compared to ethylene propylene rubber, XLPE has lower losses and tougher physical characteristics, albeit at a cost in flexibility. For this reason EPR is often used inside installations, and XLPE for longer distribution runs [14].

Much research has been focused on increasing the voltage rating of polymeric insulation, and is is starting to be considered as a replacement in high and extra-high voltage installations. The relatively maintenance free life-cycle

of XLPE make it an attractive alternative to gas filled insulation. The hazardous chemicals used in oil-filled insulation provide an environmental danger that must be managed, which is not the case in polymeric insulation.

2.1.2.1 Cable Construction

Modern XLPE is manufactured by drawing polyethylene pellets (see figure 2.1) onto an internal conducting cable (typically aluminium or copper), with the inner semiconductor, outer semiconductor and insulation layer being all formed in a single action on an extrusion line (triple extruded). In early manufacturing processes the polyethylene was 'cured' (cross-linked) using pressure and temperature provided by steam, but this method was found to be detrimental to the lifespan of the cable, as the steam curing allowed a lot of moisture to collect inside the bulk insulation [73], leading to rapid infestation by water trees and subsequent premature failure.

The use of pellets in the manufacture of XLPE is significant due to the distribution of impurities it creates. While efforts are made to ensure cleanliness of the entire manufacturing process, it is a certainty that particles will be drawn into the extrusion plant while attached to the pellets. Virtually all XLPE contains impurities in the form of sodium salt (NaCl), other metal salts and oxidised polyethylene. Much of the advancement in improving XLPE resistance to water treeing is derived from improved cleanliness in manufacturing.

A typical single phase XLPE insulated distribution cable is constructed as shown in figure 2.2. Table 3.1 shows the electrical properties of the 22kV distribution cable used in this test.

2.1.2.2 XLPE Properties

Cross-linked polyethylene (XLPE) is a non-polar dielectric with high resistivity and low electrical permittivity. These properties combine to make an insulation with a low loss factor, making it economical for long runs [50].

The modern XLPE plant cross-links the polyethylene chemically (using peroxide or other proprietary chemicals) with a high pressure nitrogen environment. The result is a tough, impact and stress resistant plastic with good temperature performance and excellent electrical characteristics. Once the polyethylene has been cross-linked, the material becomes highly resistant to

Figure 2.1: Polyethylene pellets, as used in the manufacture of XLPE.

temperature effects, with no ill effects below 90°C, and generally no issues with brief excursions of temperature up to 120°C [105].

Bulk XLPE is significantly hydrophobic, with a solubility in water of approximately 2.65 mg/100mL [35]. This low solubility means liquid water will concentrate in cracks and voids rather than diffuse throughout the polymer. The effect of this concentrating property is to provide an initiation site for the development of *water trees*.

2.1.3 Failure Modes of XLPE Insulated Cable

When subjected to electrical, chemical and mechanical stresses, XLPE cables have been observed to fail in the following ways:

1. Mechanical Stress: Tearing/breakage of metallic screen, jacket damage causing corrosion and water ingress, electrical field enhancement due to direct trauma.

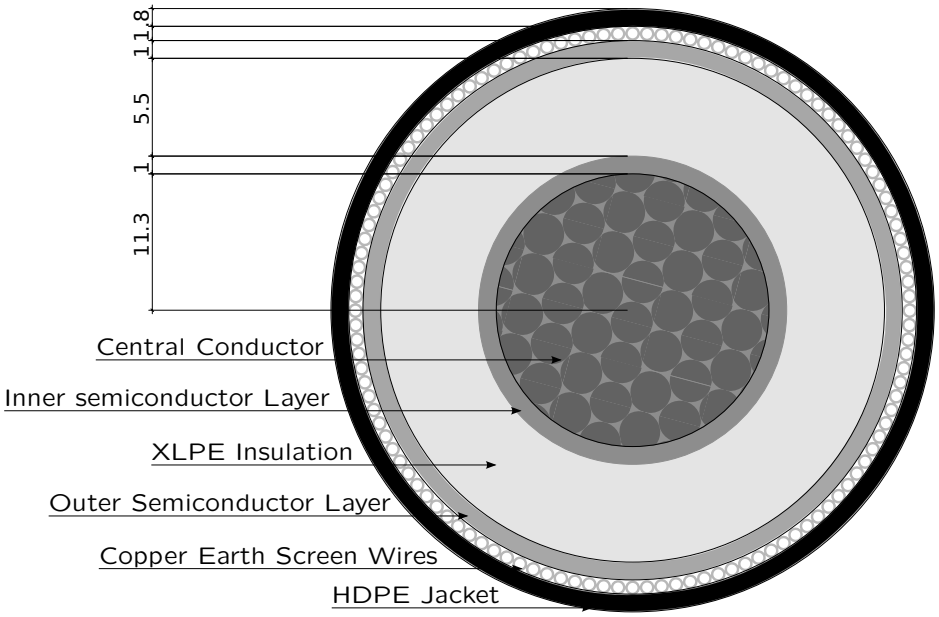

Figure 2.2: An example of a typical XLPE insulated cable cross section, with dimensions consistent with the samples used in this test. Note that the samples in this test did not have the metallic screen (as found in some modern installations) that would render them impervious to water.

2. Chemical Stress: Corrosion of metallic screen, oxidation of insulation, inclusions/intrusions of substances that accelerate water treeing.

3. Electrical Stress: Water treeing, electrical treeing, arcing damage at screen/semiconductor interface, partial discharge leading to electrical treeing.

The two most common causes of failure of in-service XLPE cable are water treeing leading to electrical treeing, and damage/corrosion of the metallic screen leading to arcing [3].

2.2 Water Treeing

Water trees, so called due to their tree or bush-like appearance on microscopy (see figures 2.4 2.5 2.6 2.7 2.8 2.9) are the primary age related cause of failure of XLPE insulated cable.

With the first discovery of water trees causing failures in the 1970s, and the subsequent realisation that they have become the primary failure mode of XLPE

cable [105], a lot of time and money has been spent researching the effects, causes and prevention of water treeing in XLPE.

The general structure of a water tree is that of a branched 'tree' like structure with a narrow 'trunk' section fanning out into a series of smaller channels (the 'branches') - see figure 2.3 [94]. In many respects they resemble a bush - with a lot of closely packed smaller branches, and fewer larger branches [26].

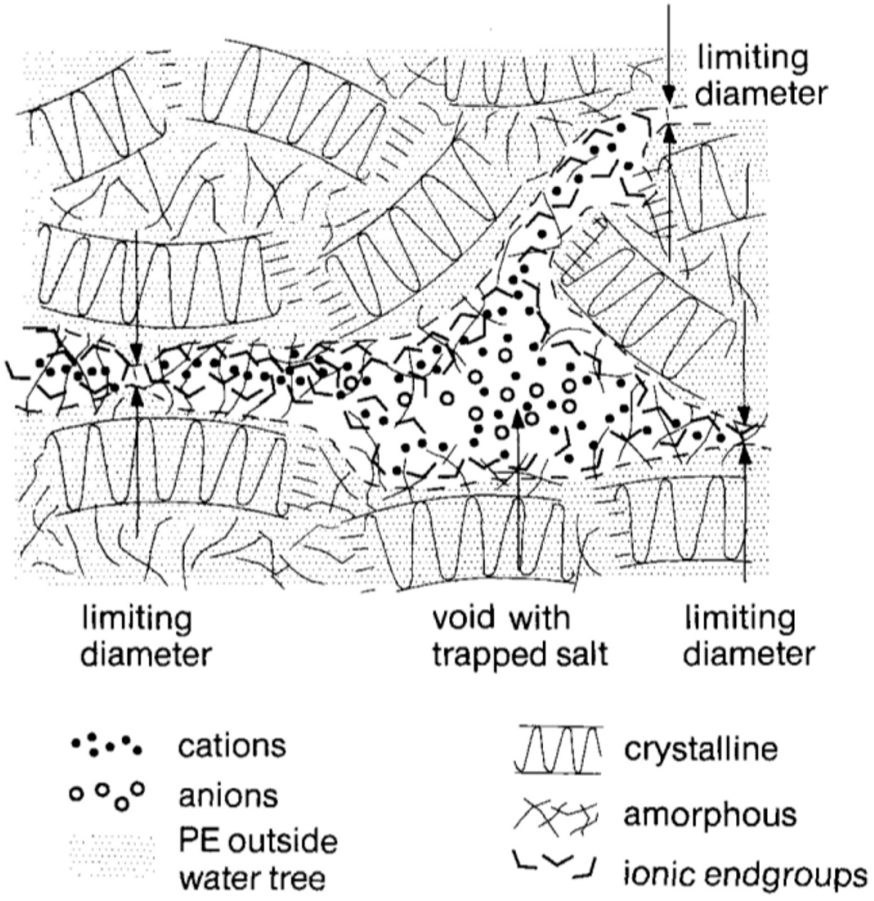

Figure 2.3: A diagram of a water tree, after Ross, 1998 ([94]).

Water trees are universally divided into two types: those originating at an insulation boundary (so-called 'vented trees') and those originating inside the bulk insulation ('bow tie' trees). The focus of most research is into vented water trees, as these are considered the most dangerous. Bow tie trees are thought to stop growing at a certain size, and as such are not considered as dangerous.

There is some suggestion that multiple bow tie trees could combine to form a very long water tree, or even reach a boundary and 'transform' into a vented tree. The probability of this occurring is related to the number of bow tie trees

and their distribution. As such, it will be based on the ageing environment to a significant extent. There were no 'linked' bow tie trees observed in this test, however there were trees found within close proximity.

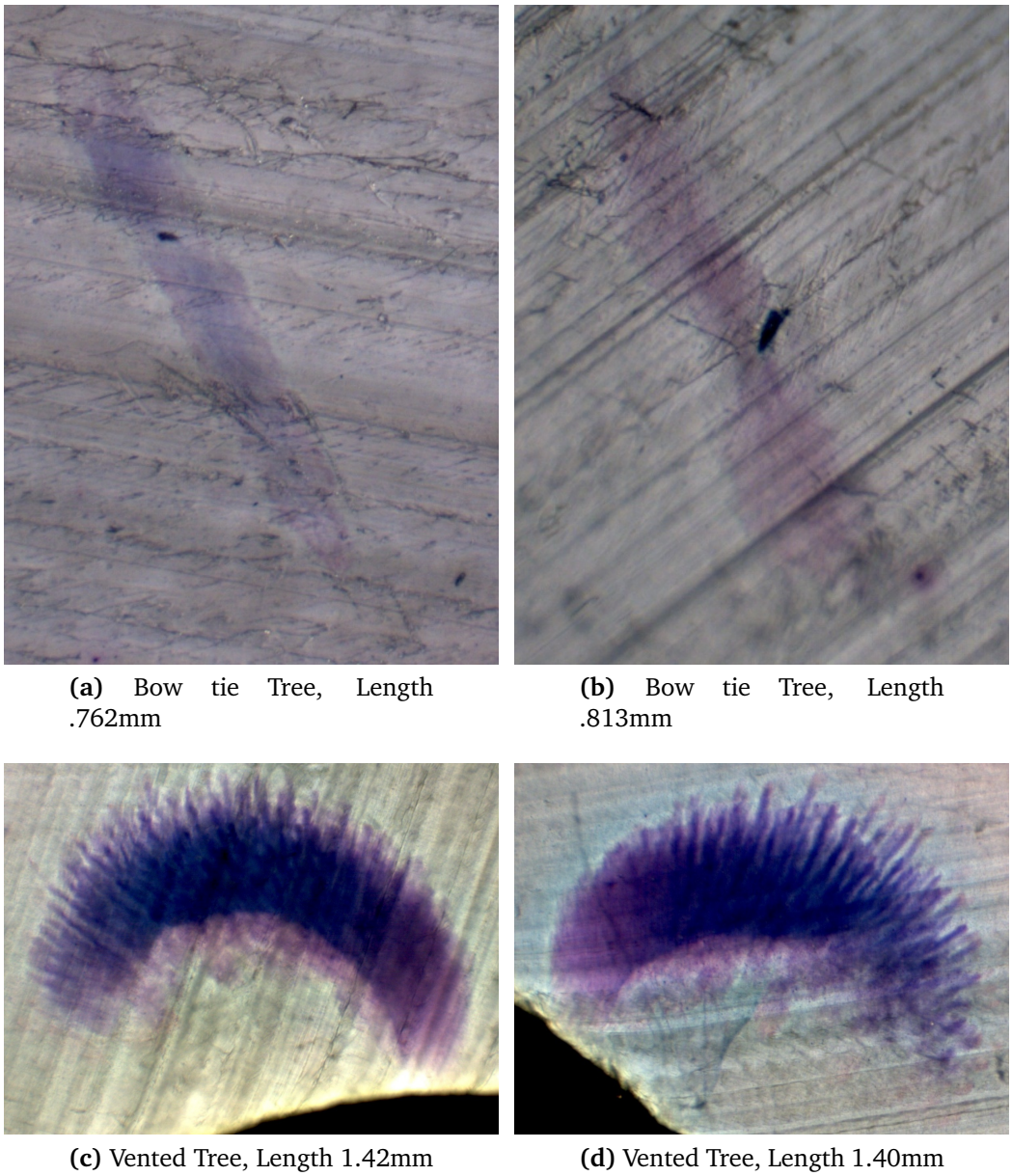

(a) Bow tie Tree, Length .762mm

(b) Bow tie Tree, Length .813mm

(c) Vented Tree, Length 1.42mm

(d) Vented Tree, Length 1.40mm

Figure 2.4: Water trees grown in XLPE and stained with Methylene Blue. (Courtesy of Novinium, Inc.)

(a) Vented water tree from 2.5c after staining with methylene blue.

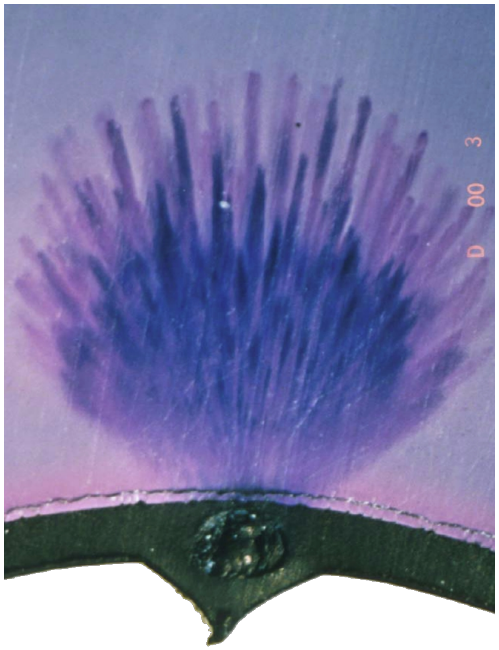

(b) Vented water tree grown in XLPE. The initiating defect is clearly visible in the semiconductor layer.

(c) A large vented water tree growing in XLPE.

Figure 2.5: Various vented water trees grown in XLPE. (Courtesy of Novinium, Inc.)

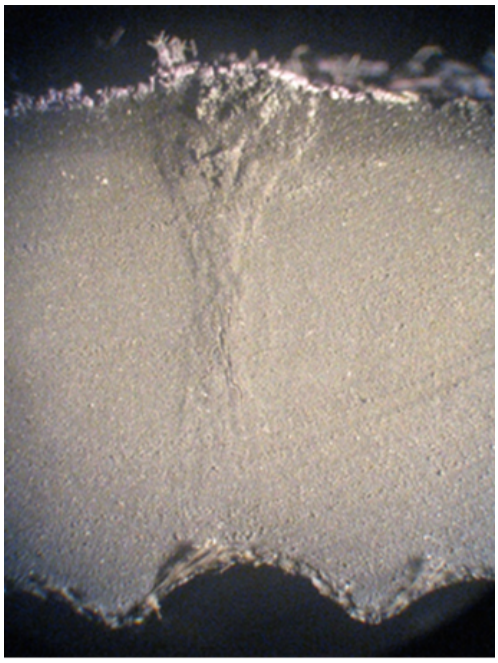

(a) Vented water tree in EPR.

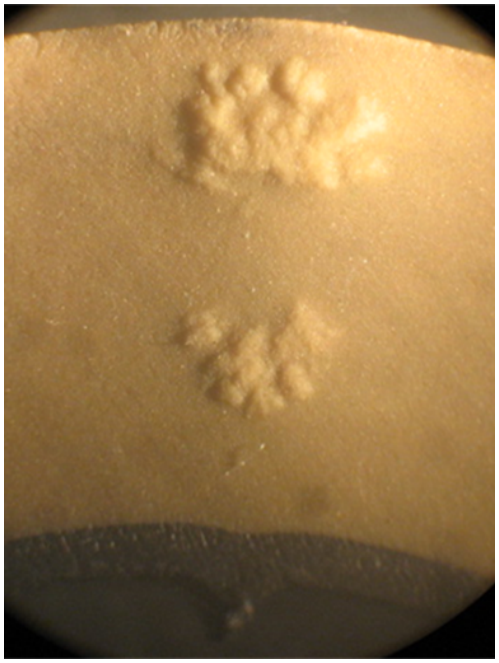

(b) Bow tie water tree in EPR.

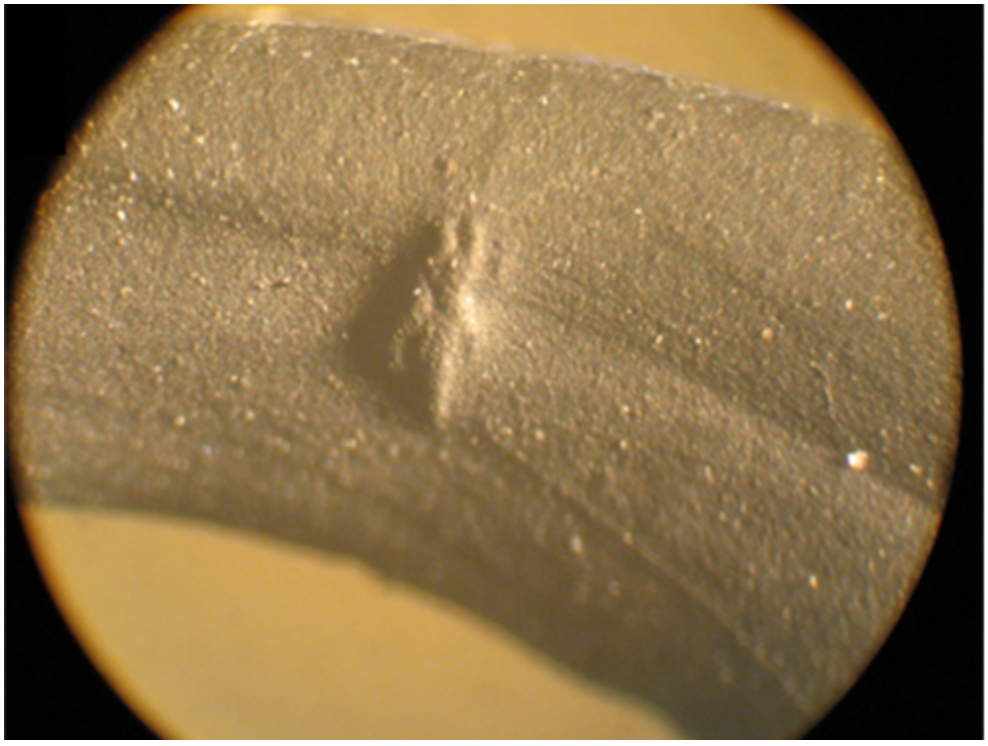

(c) Smaller bow tie tree in EPR

Figure 2.6: Water trees grown in EPR insulation and shown in relief. Due to the opacity of EPR insulation, staining is not an effective technique for visualisation. (Courtesy of Novinium, Inc.)

(a) Bow tie tree, Length: 1.02mm

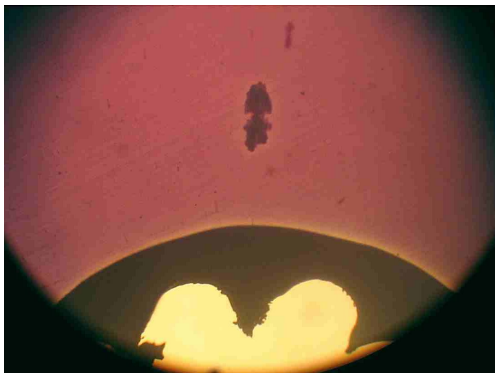

(b) Bow tie water tree

(c) Vented water tree

Figure 2.7: Water trees in XLPE. (Courtesy of Novinium, Inc.)

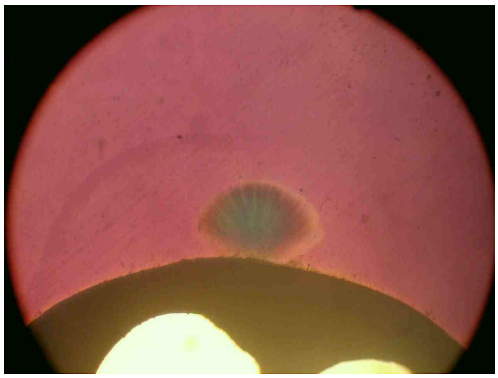

(a) Bow tie tree, length: 0.97mm

(b) Bow tie tree, length: 1.02mm

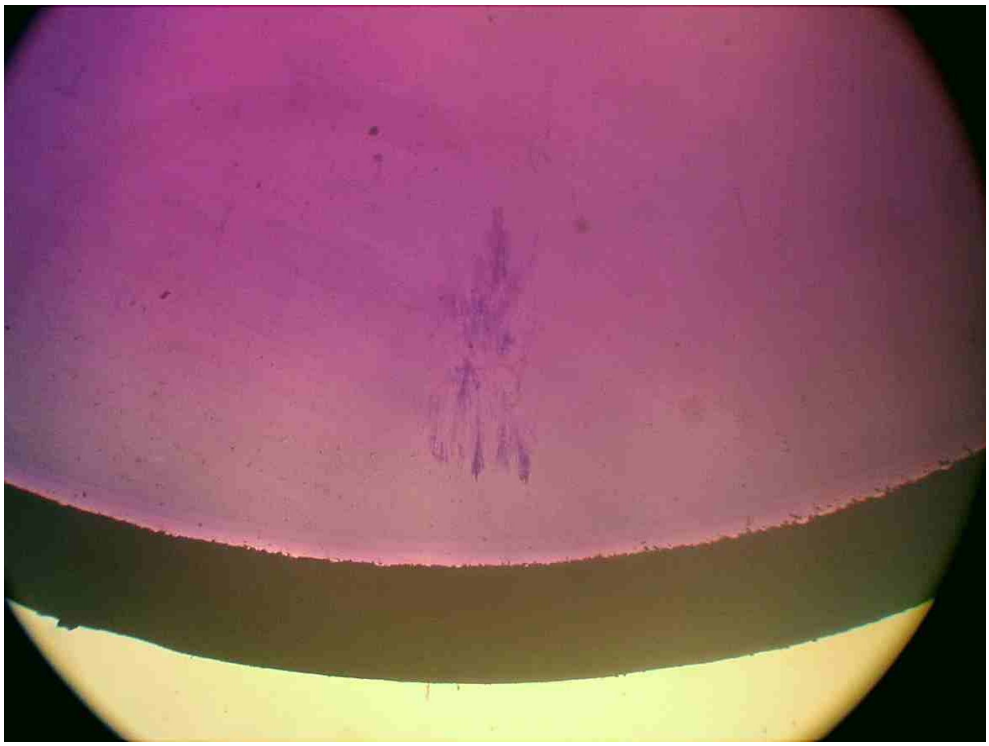

(c) Bow tie tree, length: 2.03mm

Figure 2.8: Water trees in XLPE. (Courtesy of Novinium, Inc.)

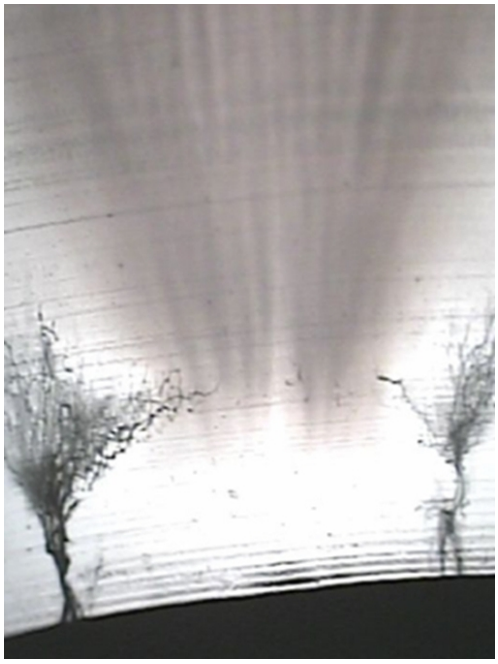

(a) Large vented water tree (center) with two electrical trees forming at the base.

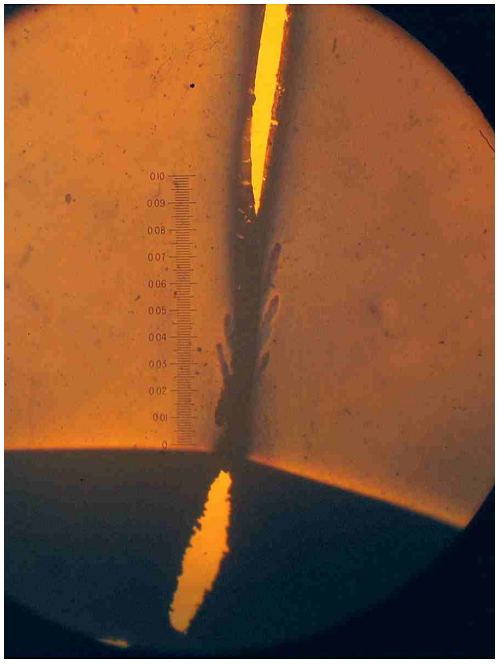

(b) A vented water tree that has caused a breakdown - note the damage to the insulation destroys the water tree that caused the breakdown.

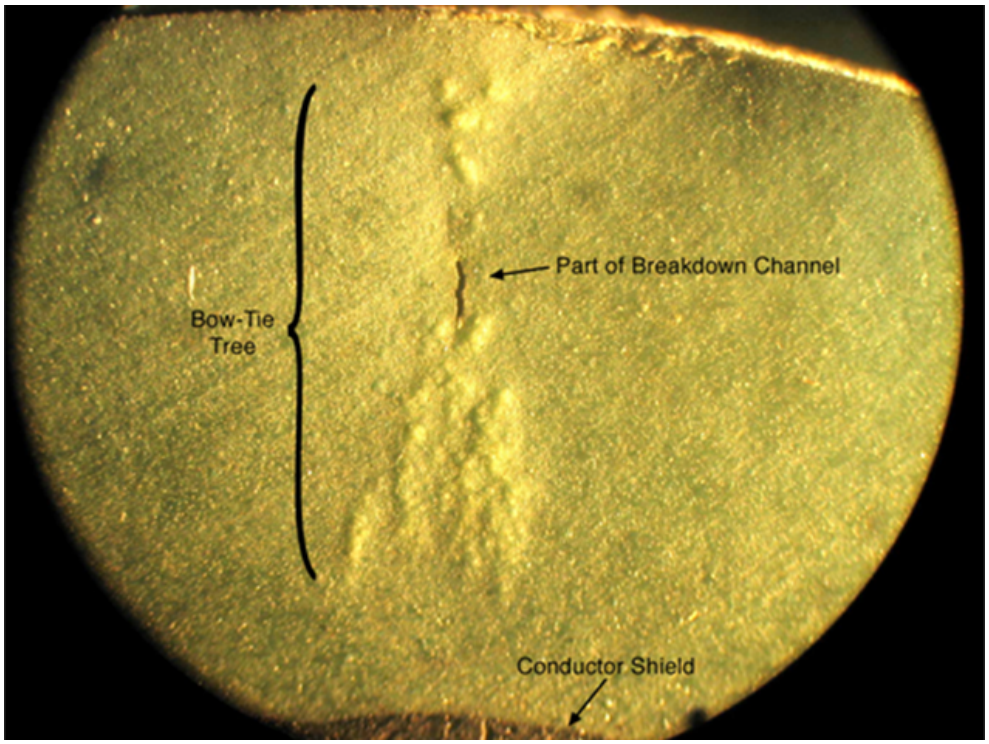

(c) Bow tie tree in EPR, this tree has 'converted' to a vented tree and the breakdown process (conversion to electrical tree) has begun.

Figure 2.9: Water trees leading to breakdown. (Courtesy of Novinium, Inc.)

(a) Vented Tree with Halo

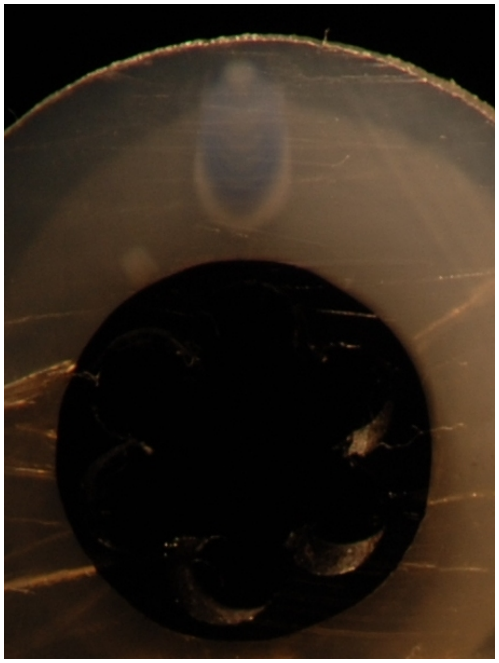

(b) Vented Tree with Halo

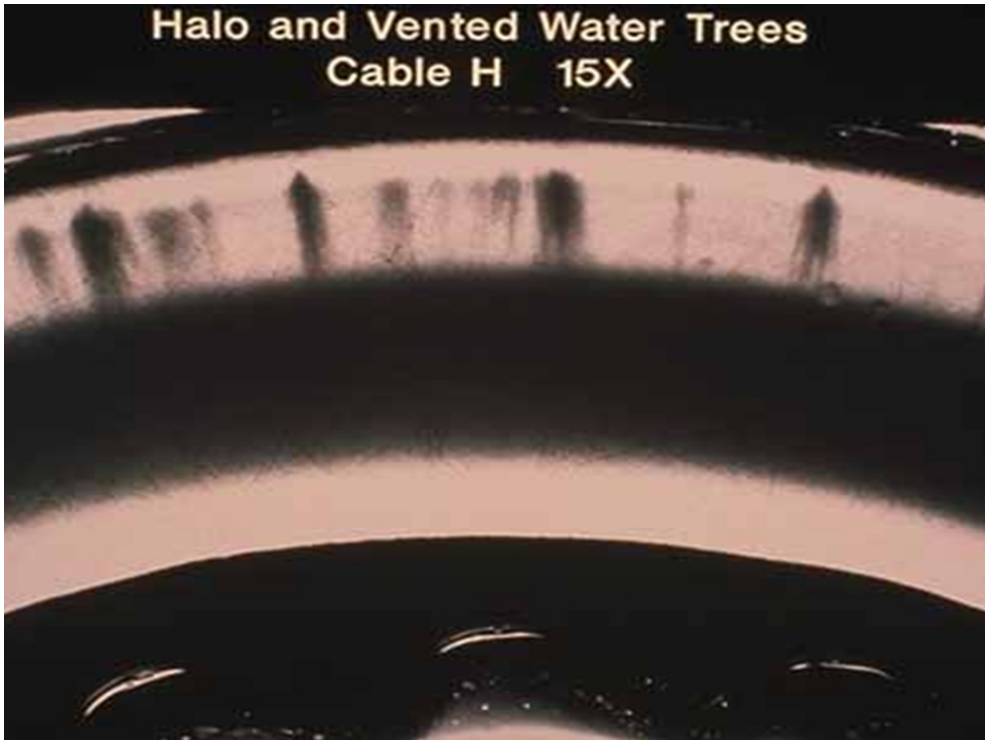

(c) Vented Trees with Halo

Figure 2.10: Halos and water trees are both signs of significantly contaminated insulation. These types of defects are normally discovered during manufacture, but occasionally appear as early failing cables. (Courtesy of Novinium, Inc.)

2.2.1 Definition

A precise definition of a 'water tree' is not completely agreed on, so taken directly from [94], the following definition will be used for this work:

> "Water trees are degradation structures in a polymer that are permanent, have grown due to at least humidity and an electric field, have a lower electrical strength than the original polymer when wet, but which are not a short circuit or local breakdown path, and are substantially more hydrophilic than the original polymer. A typical water content of wet water trees in polyethylene is $\geq$ 1%."
> -Robert Ross [94]

This definition, while not universally accepted, is generally understood. The terms 'vented water tree' and 'bow tie water tree' to denote water trees initiating from the edges of the insulation and the interior of the insulation respectively, will also be used. Although use of these terms in this manner is also not universally agreed, it is nearly universally understood [94].

2.2.2 Composition

Water tree composition has been extensively studied, and the environment in which the tree grows is known to affect both its chemical and electrical properties [91]. Techniques for examining both the morphology and chemical structure of water trees have been applied [108], and the chemical structure of water trees seems likely to be known in the near future.

What is currently suggested is that water trees initiate at a point of impurity, possibly a transition metal ion, or a salt inclusion. The water tree is then developed as a hydrophilic track, which often contains salt, but may also be related to oxidation or other chemical changes to the polymer. The finding of carbon in a water tree is a late sign and indicates the transition to an electrical tree.

2.2.3 Initiation and Growth

The means by which water trees initiate and grow is an area of some contention. What follows is a very brief overview of the theories surrounding water tree initiation and growth. This plethora of theories regarding the causes of

inception and growth of water trees lends some insight into the reason for the wildly differing results gained at various laboratories when the conditions are slightly different. Even under ostensibly identical conditions, the results vary for unknown reasons [99].

Of note is the nature of the statistical distribution of each of these causes. Causes based on the presence of impurities should yield a uniform distribution of water trees throughout the insulation. Those based on chemical effects should show some preference for water treeing in a particular segment of insulation. Thermal or electrical ageing would most likely concentrate near the conductor core, while mechanical effects would be felt at the outer radius of samples. Thus, by examining the location of water trees in a sample, it may be possible to infer the principle cause of water treeing in the sample.

Environmental Stress Cracking

The environmental stress cracking (ESC) theory states that the key means of growth of water trees is due to cracking caused by mechanical stress. For example, one variant suggests there is an electrokinetic force that acts on a dielectric under electrical stress that acts to 'expand' the polymer. This enables water to penetrate micro-cracks more easily, thus decreasing the inception time of water trees [83].

Residual Stresses/Bending

A cable that has been subjected to significant tensile stress tends to form water trees more quickly than one that has been subjected to compressive stress [100, 18]. The decrease in inception time may be due to the expansion of micro-cracks that would otherwise form a barrier to water due to surface tension.

Thus water trees form preferentially at the outside edge of bent cables [100]. It has also been shown that water trees grow more rapidly under moderate tensile stress. At 30% tensile stress, water trees grow approximately 100% faster [18]. However, increased stress beyond 30% has no discernible effect.

Field Induced Fracture

When an electric field is applied to a dielectric, several forces are initiated. If two materials of different permittivities (ϵ_1 and ϵ_2) are in contact with each

other, there will be an interfacial force per unit area according to:

$$k = \frac{1}{2}(\epsilon_1 - \epsilon_2)(E_{t1}^2 + \frac{\epsilon_1}{\epsilon_2}E_{n1}) \tag{2.1}$$

(where E_{t1} and E_{n1} are respectively the tangential and normal components of the field with respect to the boundary, and a positive k indicating force towards material 1 [100])

If a water filled void or crack is present, it will tend to concentrate the electrical field at the ends of the void, making the electrical field two to five times stronger than the applied field [24]. This force can lead to zones of crazing - a low density area with many micro-voids, susceptible to increased water treeing [100].

Fatigue

Water droplets will tend to deform under a high field [24], causing a water filled void in an alternating electric field to continually elongate and relax. This causes mechanical fatigue on the polymer surrounding a water droplet, eventually leading to the creation of micro-cracks, thus increasing the size of the water tree.

This theory suggests water tree growth should vary linearly with the frequency of the supply, however the exact relationship is not yet known. Increasing the frequency does increase the ageing rate, but the relationship is logarithmic rather than linear [24].

Contamination

Damage may also be caused to the polymer matrix by chemical processes. Although the quality of XLPE has improved greatly since its introduction, it would be somewhat optimistic to assume that there are no inclusions in a given commercial cable. It is virtually assured that there will be NaCl (common salt) ions in a given sample of commercial XLPE. But salt isn't the only contaminant, and some research suggests that other contaminants pose a greater threat to cable life [24, 47].

Condensation

Even without voids or inclusions in the polymer, water vapour may condense between the polymer strands and exert a hydraulic pressure. A 2% supersaturation of the air will exert a hydraulic pressure of 2.5 MPa - this is close to the rupture point of the molecular bonds of XLPE [83].

Additionally, inclusions of water soluble ions will lower the vapour pressure of water, which will increase the rate of condensation, decreasing the time to inception of water trees. If the relative humidity of the air in the vicinity of the insulation is above 75%, then conditions become favourable for the condensation of water around NaCl inclusions. As NaCl inclusions in the insulation are a practical certainty, 75% is considered the critical level of humidity for the initiation of water trees [95].

Lastly, thermodynamic theory states that water will condense preferentially in high field areas (e.g. voids). Thus in a humid environment (as that in which the network operated by Ergon Energy is located) the condensation of water around inclusions and other voids in the insulation is almost certain to occur, resulting in water trees being present in virtually all direct buried cable.

Osmosis

XLPE may be regarded as a semi-permeable membrane; water will tend to move from the surroundings into the insulation until a concentration equilibrium is established.

If there are any water soluble inclusions in the insulation, they will tend to attract water molecules and thus an osmotic pressure will build up. This pressure can lead to cracks in the polymer that will allow the water tree to grow [24].

Oxidation

Another hypothesised growth process of water trees is the bond scission that occurs due to electron injection or mechanical failure. Broken polymer chain ends allow for the release of free oxygen radicals that in turn may cause more bond scission.

The by-products of oxidation are also generally much more hydrophilic than the surrounding polymer. This lends some support to the theory that oxidation

plays a part in the growth of water trees [52, 19].

The evidence is not conclusive however; water tree initiation is not inhibited by an oxygen free environment, and studies have indicated that the level of oxidation in a water treed region is no greater than in the general polymer matrix [24][1]. More work on sensitive measurements of polymer properties may shed some light on this theory.

Dielectric Heating

Heat can accelerate the effects of chemical reactions and thus increase the rate of water tree growth as it relates to the chemical processes outlined above. Also, the polymer inside the insulation is usually not perfectly homogeneous. Thus, there are locations of electrical field enhancement. Under impulse conditions this field enhancement may cause excessive heating - causing polymer deformation or damage [24].

Dielectrophoresis

Dielectrophoresis is the tendency of polar molecules to move from a low field area to a high field area. As a water tree is a concentration of water molecules, diffusion pushes molecules away from the water tree. Dielectrophoresis opposes the diffusive force, keeping water molecules at the site of the water tree, and drawing more molecules to the water tree [86, 85].

Dielectrophoretic force is related to the shape of the particles, as well as the intensity of the electric fields.

For a field-aligned ellipsoid of radius r and length l ($r < l$) with complex dielectric constant ε_p^* in a medium with complex dielectric constant ε_m^* the time-dependent dielectrophoretic force is given by:

$$F_{\mathrm{DEP}} = \frac{\pi r^2 l}{3} \varepsilon_m \mathrm{Re}\left\{ \frac{\varepsilon_p^* - \varepsilon_m^*}{\varepsilon_m^*} \right\} \nabla \left| \vec{E} \right|^2 \tag{2.2}$$

The complex dielectric constant is $\varepsilon^* = \varepsilon + \frac{\sigma}{j\omega}$, where ϵ is the dielectric constant, σ is the electrical conductivity, ω is the field frequency, and j is the imaginary number.

[1] This reference, however indicates that a device for accurately measuring the amount of oxidation in XLPE is yet to become available, due to interference by water on the spectrographic measurements. As such, it is difficult to draw conclusions from this set of data alone.

One criticism of this theory is the fact that it should allow water trees to grow under a DC field. This has not been supported by evidence [24], instead it has been found that the rate of growth of water trees *increases* with higher frequencies of supply, while the dielectrophoretic force will decrease (as seen in equation 2.2).

However, this theory also suggests that short term morphological changes may occur in water treed XLPE when a DC electrical field is applied (e.g. a time-domain step test). Particularly relating to trapped charges (which tend to gather at the tips of water trees [61, 58, 62]), which will tend to maintain an electrical field in the absence of a continuously applied field, dielectrophoresis may significantly affect the internal morphology of water treed XLPE. Detecting and analysing a change in morphology is the basis for the DONL ageing factor presented in this work, thus the theory of dielectrophoresis is significant to this work, even if it is found not to contribute to the growth of water trees significantly.

Electro-Osmosis

If there is an anomaly in the insulation, whether it be a void, an inclusion or an intrusion, it will cause a field enhancement. Any water molecules that have diffused into the insulation will tend to move from the low field area to the high field area. This will create hydrostatic pressure and give the water tree a larger reservoir to draw from [24].

Electrostriction

Alternatively known as Maxwell's Forces, this theory comes from the fact that when an electrical field is applied to a dielectric liquid in a surrounding medium, a pressure change (ΔP) occurs. This change is related to both the permittivity of the dielectric and the applied field:

$$\Delta P = -\frac{E^2}{2} d \frac{\partial \epsilon_1}{\partial d} \tag{2.3}$$

Where d is the density of the liquid, ϵ_1 is its permittivity, and E is the electrical field [24].

When the field is time-varying, a water drop (which may be considered dielectric in this case) inside the polymer will continually expand and contract,

leading to fatigue and cracking.

2.3 Methods of Overcoming Water Treeing

In order to reduce or eliminate water trees from XLPE cables, a number of techniques have been created and implemented into distribution networks. The most successful method is eliminating water from the cable environment, using impermeable cable ducts or cable that contains a layer of aluminium below the outer jacket.

There are also methods of treating XLPE that chemically changes it into a form that is more resistant to water treeing. These methods result in a polymer that has similar characteristics of 'cured' XLPE, namely higher losses and a non linear response to applied voltage. The most successful modification to cable manufacture with regards to water treeing has been the introduction of 'dry curing' XLPE cable manufacture, as well as a significant reduction in the number of impurities in the bulk insulation as cleaner manufacturing techniques are developed.

2.3.1 Tree Retardant XLPE (TR-XLPE)

Treatment of XLPE to reduce the growth of water trees typically involves decreasing the hydrophobicity of the bulk insulation so the water disperses through the insulation rather than concentrating into water trees. The side effect of this treatment is the cable usually has significantly higher dielectric loss.

2.3.2 Silicone Oil Treatment

Silicone oil treatment of both new and previously water treed cables has been applied to several networks, often with good success. The use of silicon oil derivatives to attempt to 'treat' water tree affected XLPE cable is a relatively new process in Australia. While these methods have been somewhat successful in the United States [13, 88], there have been some issues when this technology has been applied in Europe [31].

The mechanism by which treatment with silicone oil derivatives treat water treeing inside the insulation is twofold. Firstly, the fluid attracts and binds water molecules into a stable structure with a comparatively high dielectric break-

down strength (oglimerisation). This reduces the field enhancement effects of water trees, prevents their further growth, and improves the breakdown characteristics of the insulation. Secondly, the process dries out the cable, by displacing water from the interior of the insulation and the conductor interstices, binding free environmental water, thus decreasing the available water for growing new water trees.

With many of the essential technical difficulties already ironed out of this (relatively mature) process, the question that remains is more economic in nature - does the cost of the treatment process give a commensurate increase in lifespan, or is laying new cable a better decision in the long term? Answering this question requires consideration of many factors not covered by the technical properties of the cable (for example, cable access, cost of installation and upgrade schedules), however the factors elucidated by this work may go some way in aiding the decision making process.

2.4 Detection of Water Trees

Several methods of detecting water trees have been proposed and tested both in the field and in the laboratory. The nature of solid dielectrics is that the polarisation and depolarisation of the material requires long periods of time and involves very low currents. Several techniques have been developed in laboratory settings that have not translated well to field measurements. Variables such as temperature and humidity, along with electrical interference render laboratory instruments unreliable in the field. As such, most current research is on gaining better information from more noise-tolerant instruments in order to make field measurements more viable.

2.4.1 Dielectric Response of XLPE

The dielectric response of XLPE is governed by the solid dielectric relaxation equations outlined by [43, 42]. In contrast to liquid dielectrics, the dipoles in a solid dielectric are constrained in their movement by the structure of the material. The presence of dipoles introduces a ‘screening’ effect, whereby more mobile charges are balanced somewhat by less mobile charges. The effect of screening is quite pronounced in XLPE, which is one reason for its low loss (and therefore excellent insulating performance). As the dipoles are constrained

and interactive, the dielectric relaxation of XLPE follows the 'many body' or 'universal relaxation' law.

This is in contrast to the discharge of an ideal capacitor, or indeed the response of liquid dielectrics. The decay response of a capacitor is normally defined by:

$$i(t) = -\frac{dP(t)}{dt} = \frac{P_0}{\tau} e^{\left(-\frac{t}{\tau}\right)} \tag{2.4}$$

(Where $P(t)$ is the polarisation function, P_0 the polarisation at $t = 0$, and τ the so-called 'time constant' of the capacitor)

Giving the characteristic loss peak:

$$\chi''(\omega) = \frac{\omega\tau}{1 + \omega^2\tau^2} = \omega\tau\chi'(\omega) \tag{2.5}$$

(Where ω is the frequency, and χ the frequency domain function)

This is the 'classic' or Debye relaxation, and is observed in materials where the charges are free to move without interacting with each other. In contrast, the proposed model of solid dielectric relaxation is the 'universal' law. The foundation of the universal law of relaxation is an observation that:

$$\frac{\chi''(\omega)}{\chi'(\omega)} = \cot\left(\frac{n\pi}{2}\right) = \text{const} \tag{2.6}$$

[Where n is a property of the material, varying from $0 - 1$, with higher values indicating lower losses. The value for n in XLPE is close to unity - it has very low losses, and the loss angle is close to being constant in the frequency domain.]

Stated another way, in solid dielectrics:

$$\frac{\text{energy lost per cycle}}{\text{energy stored}} = \text{const} \tag{2.7}$$

The general law for the relaxation of a dielectric upon removal of a driving field is given by:

$$i(t) = \frac{A(T)}{(\omega_p t)^{m+1} + (\omega_p t)^n} \tag{2.8}$$

[Where ω_p is the low frequency loss peak - a property of the material, n is as above, and m is a second material constant that defines the 'secondary' relax-

ation - after time $\frac{1}{\omega_p}$ a non-universal relaxation with greater rate of decay takes over (this region is not well defined and difficult to analyse experimentally)]

To summarise, XLPE as a solid dielectric does not follow a simple capacitive discharge curve, rather the many-body/universal solid dielectric relaxation law. The results of measurements taken on XLPE cable should be interpreted in this context.

2.4.2 Time-Domain Measurements

Time domain measurements are based on applying a defined voltage function to a sample and measuring the current response. There are three main types:

1. Isothermal Relaxation Current
2. Return Voltage Measurement (also discharge current measurement)
3. Polarisation/Depolarisation Current

The theory behind isothermal relaxation current is analysis of charges trapped during polarisation of a dielectric. When the potential is removed from the dielectric, different charge traps will release their charges at different times. The resulting current can be measured and analysed to estimate the condition of a sample of XLPE. Under strictly controlled laboratory conditions, this test gives a lot of information about the insulation.

Unfortunately, the variations (particularly thermal changes) which arise in the field make this test somewhat unreliable. IRC measurements were performed on these samples, but the issues with taking measurements outside a laboratory environment were notable, along with the restriction of the equipment not allowing the use of the raw measurement data [79].

Furthermore, the isothermal relaxation current method is based on Debye relaxation of the sample, and (as mentioned earlier) this is not a good fit for solid dielectric relaxation. There is some overlap between Debye and universal relaxation, so the model may give some approximation to the 'true' process.

Internally, the isothermal relaxation current equipment estimates the condition of a sample by computing several 'factors' by fitting a known function to the measured data. The question of the correctness of the function fit to the curve is secondary to the effectiveness of these factors in estimating the condition of the insulation. However, in several cases the equipment failed to

return a result, and this is possibly related to the deviation of the response of the samples from the classic Debye response. In contrast, oil based insulation should show a response more similar to the classic Debye response, and this may make the equipment more suitable for this type of insulation.

Return voltage measurement and discharge current measurements both measure the discharge current resulting from a charged dielectric being discharged. This method is somewhat more flexible in its approach, as it doesn't always attempt to compute parameters based on Debye relaxation. As such, the information is somewhat different to the isothermal relaxation current, and is similar in many ways to the polarisation/depolarisation current measurements.

The return voltage method uses the resistive properties of a sample to indirectly measure the current flowing by measuring the voltage between the electrodes after the input is applied. This method is thought to be more resistant to noise, as the reading of very small voltages is more accurate than reading very small currents.

The most significant disadvantage of the return voltage method is the fact that it requires the specimen to be ungrounded, which can result in distortion of the returned signal by leakage current flowing over the surface of the sample. The return voltage measurement equipment used in this test was still under development and was unable to reliably return a set of dielectric measurements on the samples. In this case, the accelerated ageing test bed acted as a development environment for the test equipment, rather than the test set providing insight into the condition of the samples.

The polarisation depolarisation current technique is the simplest, and is commonly used in assessing the condition of oil paper or oil pressboard insulation. The main disadvantage of this technique is the effects of electrical noise on the measurements that can overcome the very small signals being measured in XLPE cable.

This method attempts to characterise the state of the insulation by computing the resistivity of the sample. This may be computed directly, if the so-called 'steady state' charging stage is reached (the pseudo-DC state at which the sample is fully charged). However, reaching this state is not typically practical in high-resistivity samples such as XLPE. Rather, the difference between the charging and discharging current is used to estimate the resistivity (this procedure is outlined in chapter 6).

The equipment used to perform these measurements allowed for recording the applied voltage and current as the measurements were performed. This equipment was readily available 'off the shelf', comparatively cheap and reliable. Internally, the raw data measurements are available via a serial port on the device. Access to this data allows for analysis according to the universal relaxation law or the Debye model (or any other method desired) depending on the circumstances, making this the most flexible piece of equipment used in this test.

2.4.3 Frequency Domain Measurements

Frequency domain techniques have an advantage over time-domain techniques in terms of elimination of electrical interference. However, the equipment is large, complex and expensive in comparison to time-domain measurement devices. This test applied frequency domain testing to the samples, the results of which can be found in [103, 104, 102].

The frequency domain measurements can provide a lot of useful information, but it must be interpreted with care, as ambient humidity can affect the measurements to a significant degree. As with most of the methods discussed here, these measurements make the best contribution when used to assess the same sample over time.

2.4.4 Partial Discharge and Oscillating Wave Test

These tests were previously used to assess the condition of XLPE cable by applying a 'shaped' waveform and measuring the resulting returned waveform, but are no longer recommended as it has been found that they damage the cable under test [87].

2.4.5 Tan Delta Measurements

In recent times, analysis of the loss of cables at operating frequencies (so called 'tan-delta' measurements) have shown some promise with regards to predicting the breakdown strength of XLPE cable. The breakdown strength has been linked quite closely with the length of the longest water trees, as such this shows promise with regards to predicting the level of water treeing at a point in time. [44]

Chapter 3

Accelerated Ageing of XLPE Cable - Description of Test Facility and Procedures

> If you're doing an experiment, you should report everything that you think might make it invalid not only what you think is right about it.
>
> *Richard P. Feynman*

3.1 Rationale

Ergon Energy commissioned a test facility to be built to determine the effectiveness of silicone oil treatment of water treed XLPE cable. Furthermore, the facility was an excellent opportunity to develop and improve non-destructive testing methods for use on the underground network.

3.2 Test Facility

The test facility was built according to IEEE Standard 1407 [2]. The ageing parameters were temperature, voltage stress, and salt and water in contact with the insulation.

The facility was initially constructed with three sample groups in mind - new unaged cable, field aged (old) untreated cable directly from a site experiencing multiple failures, and old field aged cable treated with silicone restoration fluid ('CableCure').

However, the facility was unable to supply sufficient current to the sample groups to maintain the desired temperature. Calculations for the required current and rating of the current supplying transformer did not adequately account for the inductive load of the loops of cable. As such, the transformer was unable to supply the required current to heat all three tanks to the desired temperature, and a decision was made to remove the field aged untreated samples from the testing program.

3.2.1 Location

Construction of an accelerated ageing facility requires a substantial investment in floor space. Furthermore, the high voltages that are continuously applied create safety risks that must be carefully managed. Due to space and safety considerations, the test facility was unable to be built on-campus at the Queensland University of Technology. Instead, Ergon Energy offered use of a testing bay in their test and maintenance workshop located at Virginia, Queensland (a suburb of Brisbane in Australia).

The test bay was approximately 8m by 5m with a control room overlooking the test facility (see figure 3.1. There was a 2m chain link fence surrounding the bay, with safety interlocks on all the gates. If any gate was opened, the power to the test bay would be disconnected. The test bay is supplied by a high current three phase 50Hz supply, as well as standard 240V/10A 50Hz outlets.

3.2.2 Environment

The environment was intended to give an approximation of the environment the samples would experience in the field while increasing the severity of the

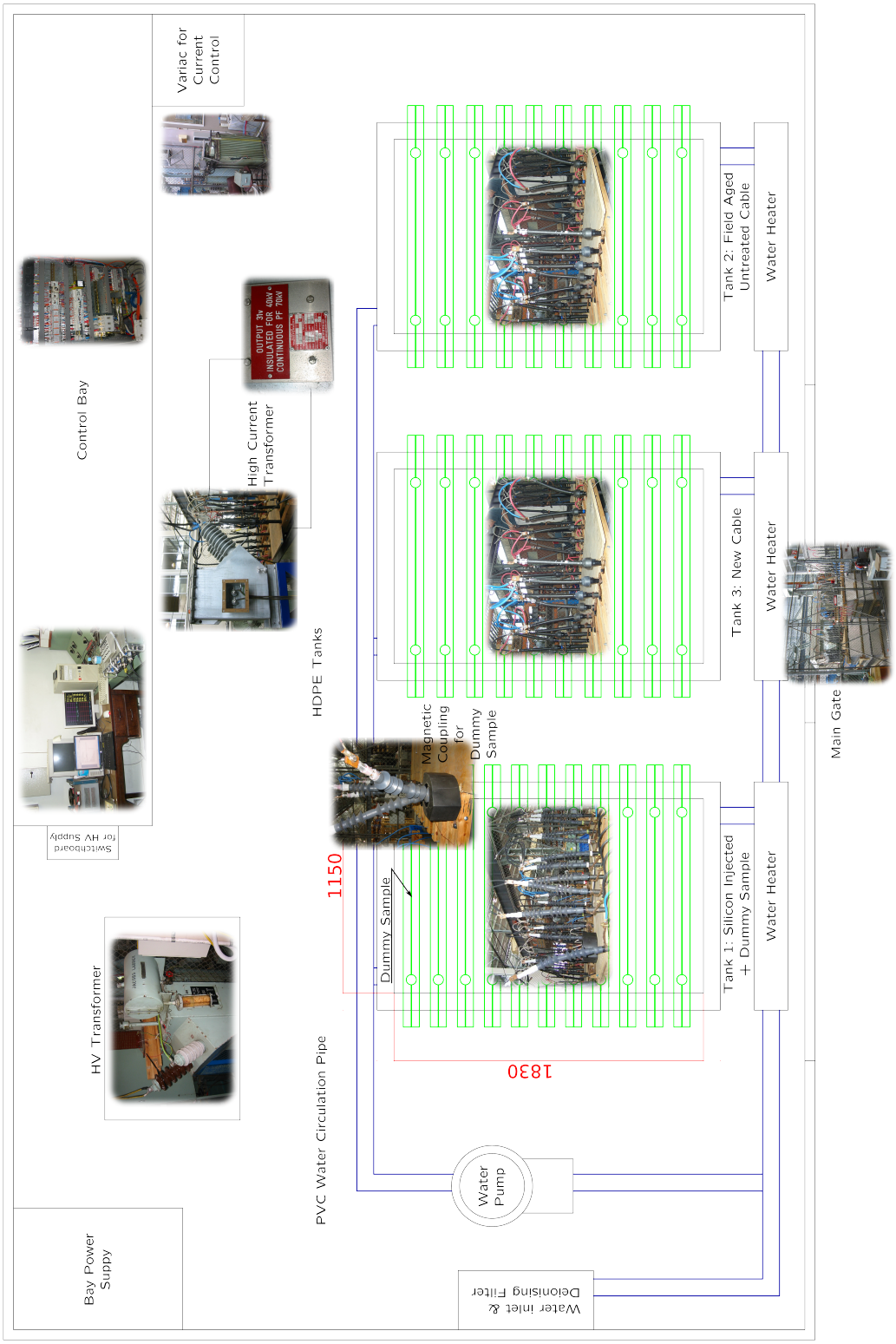

Figure 3.1: The layout of the test facility.

load to accelerate the ageing process.

3.2.2.1 Water

The water was intended to provide an approximation of the ionic content of the groundwater in which the network operates. It was sourced from the town water supply, with a deionising filter attached (thus it was referred to as deionised water). The initial fill of the tanks was via the filter, and the water was then cycled through the filter several times. Top up fills were applied via the filter.

The water purity was initially tested by measuring the resistivity of the water. Prior to the addition of the salt, the measured amount of contamination (based on electrical resistivity) was $<$10 ppm. The water analysing device was not able to accurately monitor concentrations above 100ppm, thus the 'salty' water was not monitored. As salt is not lost via evaporation, it was considered that the concentration would vary only with water level, and by maintaining the water level the concentration would remain constant.

Several water samples were taken from cables in the field and analysed for impurities:

Sample	Chloride [mg/L]	Nitrate [mg/L]	Sulphate [mg/L]
1	11	12	47
2	49	-	9
3	5	-	-
4	10	1	11
5	13	1	2
6	13	2	2
Tap Water	60	-	22

After the initial top up fill and de-ionisation, laboratory grade sodium chloride was added to the tanks to simulate the groundwater conditions of the region from which the samples were taken (a region near Innisfail in Queensland, Australia). It was decided to bring the ionic concentration of the water to 10mg/L of Chloride ions. Only a small amount of salt was required, per figure 3.2.

A significant difference between this test and other published tests (e.g. [99]) is the lack of water inside the conductor strands. Due to the termination requirements of the treated samples (sealed terminations to prevent water

Tank Dimensions = 1200 H $\times$ 1150 W $\times$ 1830 D
Tank Volume = 2.542 m^3
Tank Material: HDPE
Cable Dimensions = 7m (length) $\times$ 34mm (diameter)
Cable Volume = $17^2 \times \pi \times$ 7000mm = 6355mL = 6.4L

Water volume (no dummy) = 2344 L
Water volume (with dummy) = 2338 L

Amount of NaCl added:
NaCl = 1.65 mg/L (based on Na = 23 Da + Cl = 35.5 Da)

Intended concentration 10mg/L of Cl anions:
Weight to be added (dummy/no dummy): 38.6kg / 38.7kg

Figure 3.2: Calculation for the amount of NaCl to add to the tank water.

ingress and contain the treatment fluid within the conductor strands - see figure 3.3), it was decided not to expose any of the sample conductor strands to the salt water medium.

In order to minimise damage to the conductor strands, the HDPE outer jacket was left in-situ. However segments were removed every 1m to ensure adequate contact of water with the outer surface of the insulation.

The tanks were constructed from HDPE. It was noted that the tank material is a possible cause for changes in time to failure of samples, however this link has not been conclusively demonstrated. For the purposes of this test, as the samples are being directly compared under identical conditions, the composition of the tanks was not regarded as a significant factor.

In order to improve water access to the insulation, segments of the HDPE outer jacket were removed approximately every one metre. The jacket was not totally removed, as it was judged that the risk of damage to the samples would be too high.

This is a significant area of difference, and it makes the results of this test less comparable to other tests. Furthermore, this is likely a significant factor contributing to the good condition of the samples at the end of the ageing test.

Each tank was linked at the bottom by the inlet and outlet from the water pump, and at the top by overflow valves. The water was circulated throughout each tank at a constant 20L/min, governed by inlet flow restrictors (see figure

Figure 3.3: Image of a CableCure termination, showing the port (connected to the hose) into which the fluid is pumped into the cable.

3.4).

During the test, it was noted that, due to the high temperature of the water, the rate of evaporation was very high - on the order of 10-15mm per day. This initially caused the water level to drop significantly on two occasions, prompting the unused third tank to be added as extra storage. A small pump was installed to continuously pump water from the third storage tank to the other two tanks, with the overflow flowing back into the storage tank. This ensured the water level would remain at the maximum level.

3.2.2.2 Temperature

The temperature of the samples was elevated to the maximum that could safely be applied without causing a phase change to the polymer insulation, in order to accelerate the ageing as much as possible. There is some debate as to the safe operating temperature of XLPE, however it is generally accepted that ageing below 90 degrees Celsius will prevent thermal damage to the polymer. As such, the current in the conductors was varied (up to 400A) in order to maintain an internal temperature of 80 degrees Celsius.

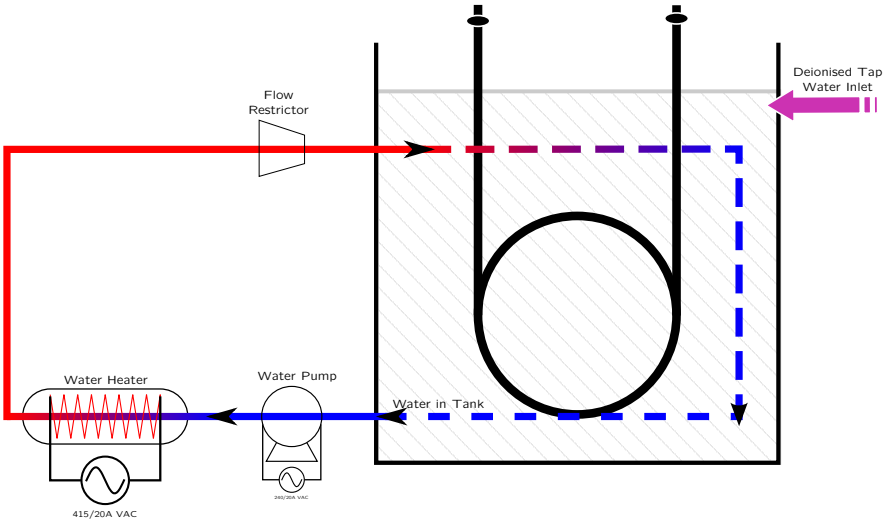

(a) The water flow in each tank.

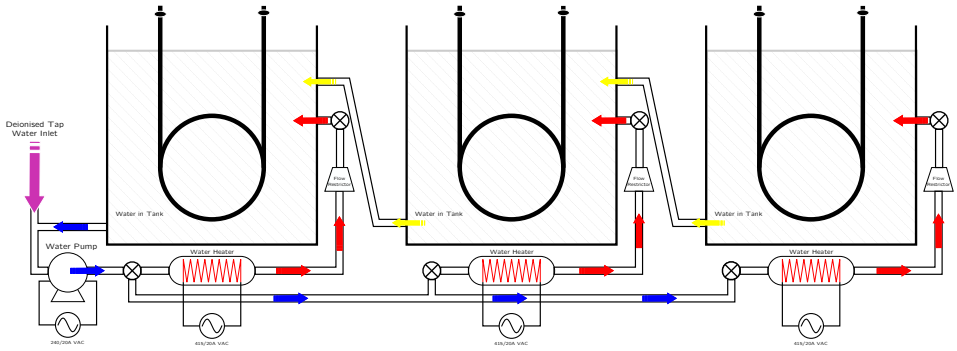

(b) The water flow between tanks.

Figure 3.4: The flow of the water in the tanks.

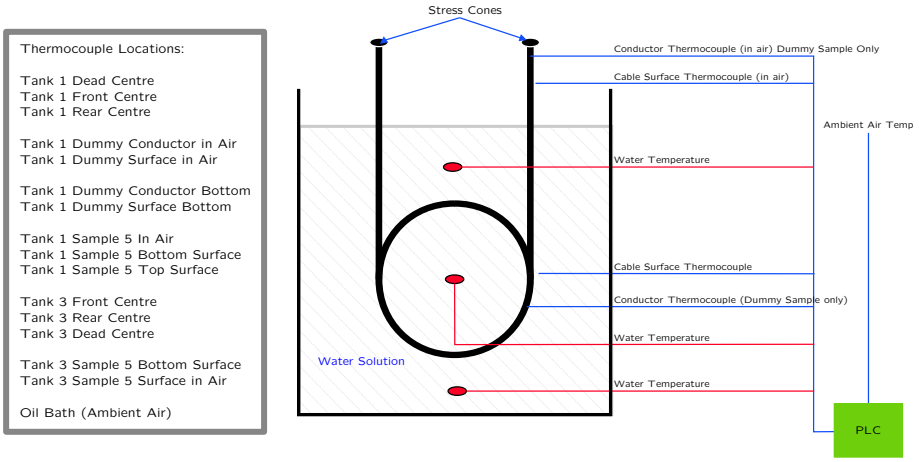

Figure 3.5: The locations in the tanks and the samples where the thermocouples were located.

Each tank had an inline heater that could be controlled independently. A total of 16 thermocouples were placed, with temperature being monitored in locations indicated in figure 3.5. In the duration of the test, several of the thermocouple inputs to the PLC failed. The cause of the thermocouple failures was never established, but was likely due to some kind of high-voltage transient that made its way along the thermocouple to the PLC - possibly when a sample broke down the water became briefly energised.

As well as monitoring the temperature of the water, several thermocouples were used to monitor the surface temperature of various samples. The procedure for attaching a thermocouple to the external surface of a sample was as follows:

- Cleaned sample area of water and dirt
- Applied a small amount of thermal conducting paste
- Thermocouple placed under a small copper pad, with the void filled with paste

- Approximately 5 - 7 layers of PVC electrical insulation tape applied to ensure the sensor is firmly fixed
- Tape or tie downs also used at a secondary location approx 100mm from site for mechanical strength

In the instances when the conductor temperature was being measured, a dummy sample was linked to the circuit using a 1:1 iron core. The induced current was measured to be approximately 95% of the measured applied current, thus it was assumed that the temperature of the dummy sample would provided a good representation of the temperature in the test samples.

The procedure for measuring conductor core temperature was as follows (see figure 3.6:

- Using a previously marked drill bit, a 4mm hole was drilled in the insulation with care being taken not to damage the conductor strands
- Hole filled with thermal conducting paste
- Thermocouple sensor inserted and taped into place using 5 - 7 layers of PVC electrical insulation tape
- Tape or tie downs also used at a secondary location approx 100mm from site for mechanical strength

Tape was applied in both instances (external and internal mounting) to add both mechanical strength and a small amount of thermal insulation to ensure the temperature reading was not adversely affected by the water temperature.

Throughout the four year time-frame of the test, there were seasonal variations in ambient temperature, but the in-line heaters kept the water temperature between 57°C and 61°C, with only a few significant changes when down-time of more than a few days was encountered (the water would cool to less than 20°C without active heating). The variation of the temperature inside the tank was very slight - with the pump circulating the water through each tank, the difference between the coldest thermocouple and the hottest was only around 1°C (excluding the core temperature measurements of course).

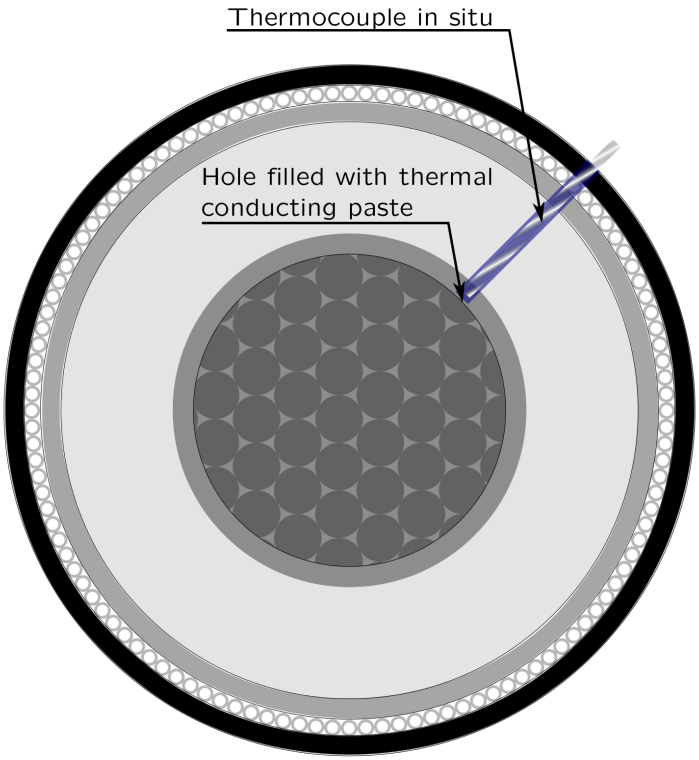

Figure 3.6: Diagram showing the location of the thermocouples used for measuring conductor ('core') temperature.

3.2.3 Ageing

The main application of ageing stress to the samples involved the use of a high voltage circuit to apply three times the rated voltage of the samples and a high current circuit to maintain an internal temperature of 80 degrees Celsius.

3.2.3.1 High Voltage Circuit

The high voltage circuit was applied to the sample as in figure 3.7

The magnitude of the voltage was three times the rated voltage (38kV), giving an electrical stress of 6.9 kV/mm.

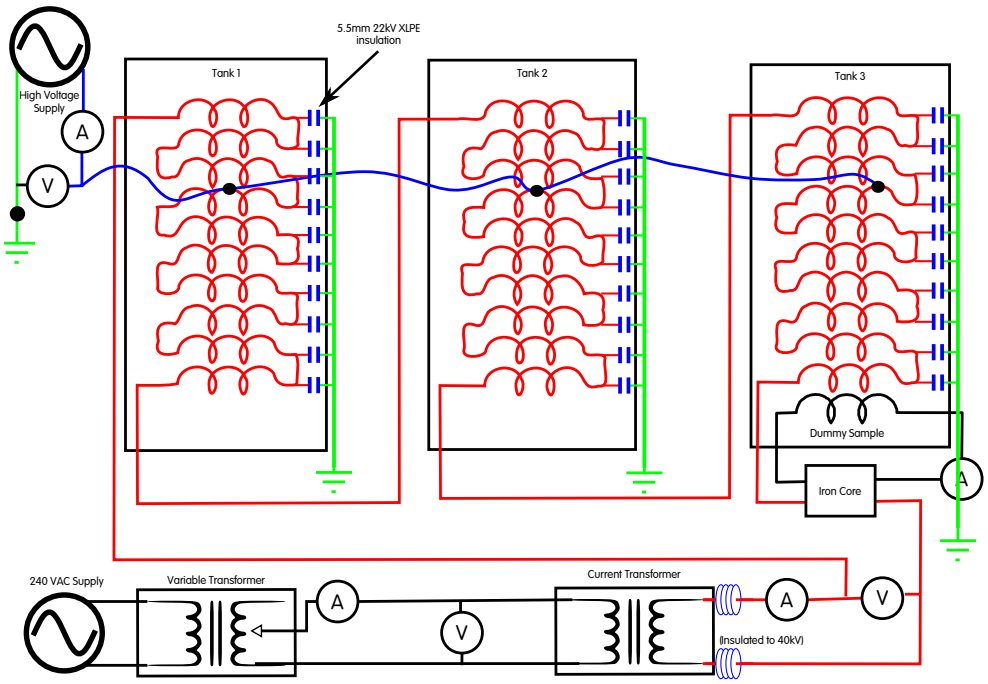

Figure 3.7: Diagram indicating the wiring of the high voltage and low voltage power connections to the samples.

3.2.3.2 Current/Heating Circuit

A heating current was applied to the samples as shown in figure 3.7. The heating current was cycled with a daily cycle - 8 hours on, 16 hours off, seven days a week. The temperature was monitored at several locations, both above the water line and below, however the 'key' measurement was the in-tank (under water) temperature of the dummy conductor core. This was the measurement used to control the temperature of the samples.

The current flowing in the dummy cable was not identical to that in the samples (due to losses in the linking iron core), however the measured current in the dummy sample was within 1% of the current in the main loop, therefore the temperature was assumed to be equivalent, given the precision of the instruments involved in measurement. A hysteresis controller was used to maintain a temperature of the hottest point between 79 degrees Celsius and 81 degrees Celsius. In practice, this temperature was below the waterline, however the temperatures above the waterline were measured in order to prevent thermal damage to the polymer.

The heating circuit required a custom built transformer that failed several

times during the test. Using a coil to induce the required current in the samples (as is the practice in cable proof testing) was not possible due to the inductance of the cable loops. The unusual requirements of this transformer were a key cause of the third sample group (field aged, untreated) being removed from the test.

3.3 Sample Properties

The samples had the following properties:

Cable Sample Details	New Sample	Field Aged Treated Sample
Period of Manufacture	late 1990s	1970s
Manufacturing process	Triple extruded	Triple extruded
Conductor	185mm^2 Compacted Stranded Aluminium Core, rated 400A continuous	
Inner Semiconductor	Fully Bonded	Fully Bonded
Insulation	5.5mm XLPE, rated 22kV phase, 12.7kV line	
Outer Semiconductor	Strippable	Fully Bonded
Earth Screen	Stranded Copper	Stranded Copper
Water Barrier	Wound Tape barrier	Nil
External Jacket	HDPE	HDPE
Termination Stress Control	Indoor stress cone	3M Weathershield sheds
Termination type	Crimp lugs and shear head lugs	CableCure crimp lugs and shear head lugs
Sample Length	Total Length, 7.5m, submerged length 7m	

Table 3.1: Test sample details.

3.4 Accelerated Ageing Program

3.4.1 Preconditioning

The newly manufactured cables were manufactured in 1994, and all samples for this test were cut from a single continuous length from a single roll. After sectioning, they were terminated using stress cones rated for 38kV, and crimp lugs rated to 400A. In order to remove any residual cross-linking by-products, the new samples were subjected to 40 hours preconditioning at 75°C after the cable was sectioned into samples. These samples formed the contents of tank 3. Throughout this work, these samples are referred to as *new* or *untreated*.

The two sets of field aged samples were taken from a direct-buried distribution cable that had been retired to due in-service failures. Twenty samples in total were taken from a single phase of the retired cable. These samples had standard outdoor weather shield stress grading applied, and ten were terminated with crimp lugs, while the other ten were subjected to the CableCure process (which requires custom terminations).

The field aged samples were considered to have been preconditioned in the field, and no further preconditioning was applied.

3.4.2 Electrical Measurements

During the course of the test, electrical measurements were made on the samples at regular intervals (see figure 3.8). Each week, the facility was taken offline for a day of testing. Frequency domain tests took approximately 90 minutes per sample, and were performed every week. It took four days to complete frequency domain tests of all the samples, therefore each sample was testing in this manner once every four weeks.

Time domain tests (polarisation/depolarisation) took 30 minutes per sample, so it was possible to test all the samples in a tank (ten samples) each week. Therefore each sample was tested every two weeks. Isothermal relaxation tests were performed during periods of downtime, however results from these tests were not good quality.

In order to avoid measurement artifacts, each sample was only tested with one methodology each week. Thus the samples undergoing time domain tests would not have frequency domain tests on the same day. This is to prevent the effects of space charge on the measurements, as it was thought that energisation for a week would eliminate any space charges that may have been left by DC testing.

The results of the frequency domain testing are reported in a thesis by Dr Andrew Thomas from the University of Queensland, representing the work he performed as part of a PhD program utilising the test facility described here, with a sole focus on frequency domain analysis of electrical measurements on XLPE cable.

There are published reports of undesirable effects on samples caused by ‘non-destructive’ testing (most notably high voltage DC testing or ‘thumping’, which is no longer performed). As such, the schedule of testing is reported here

to ensure the ability of future research to compare with the results obtained in this test.

3.4.3 Fault Detection

A significant challenge in a facility such as this is detection of a failed sample, due to the nature of water trees being a high impedance fault. The initial design was intended to shut down prior to the complete breakdown of a sample due to electrical treeing, however disengaging a sample after failure is a tricky problem. The use of fast blow fuses for each individual sample is the ideal method, but this requires a substantial installation and maintenance investment, as well as constant monitoring for 'false' fuse failures. In this test, a low current high speed circuit breaker was used on the primary side of the voltage transformer to ensure the power was cut as soon as possible in the case of a failure.

This method has the advantage of being simple and easy to maintain, however there is a larger amount of energy dissipated by a failed sample before the power is removed. In the ideal situation it may be possible to analyse the failure site with damage limited to a (high impedance) bridging electrical tree (or, with even more care, the higher impedance bridging *water tree*). If this were possible, a more confident assessment of the relationship of the length of a water tree to the breakdown voltage could be made. Unfortunately this level of detail was not possible in this test, but the fast acting circuit breaker was able to lessen the damage to the sample at the failure point somewhat.

One advantage of the damage caused by a fault is the visibility of the damage makes fault location a simple task. In the case of a high-impedance fault, just locating the fault can be an extremely challenging task. The reward for such a careful setup would be a significant new insight into the effect of water tree caused failure of XLPE, however this task was beyond the facilities available in this project.

3.5 AC Breakdown (ACBD) Test

Four years after the project was commissioned (approximately 400 days of applied ageing), with time constraints requiring the test to conclude, the samples were broken down in an AC breakdown test. Each sample was re-terminated

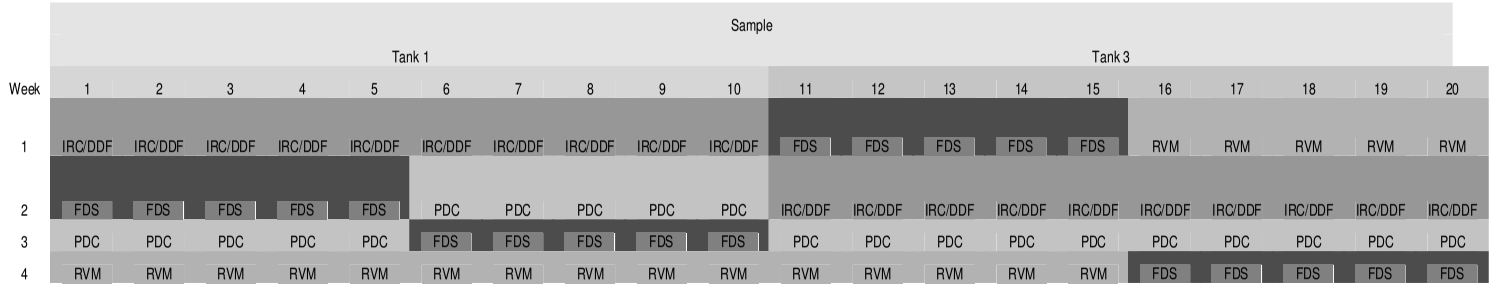

	Time per sample	Time for all Samples
IRC/DDF	0.75	15
PDC	0.5	10
RVM	0.5	10
FDS	1	20

Figure 3.8: The intervals of testing for the samples in the accelerated ageing test. Times are in hours. The use of the return voltage measurement was abandoned due to equipment failure. [IRC: Isothermal Relaxation Current DDF: Dielectric Dissipation Factor (50Hz) PDC: Polarisation/Depolarisation Current RVM: Return Voltage Method FDS: Frequency Domain Spectroscopy]

with a high voltage termination that was tested to withstand 130kV, and a voltage was applied in steps until each sample failed.

While the original goal of determining lifetime comparison between the samples was not possible using this method, it was possible to compare the electrical measurements taken directly before the breakdown tests with the post-mortem analysis of the samples with a much greater degree of confidence.

3.5.1 Procedure

Immediately prior to this final breakdown test, dielectric measurements were taken on each sample in order to correlate the final forensic assessment of the samples with the electrical measurements. The breakdown voltage of each sample was recorded, and this data was used in the analysis of the degradation of the samples. The results of the breakdown test, along with the forensic analysis is presented in chapter 4.

The samples were energised at the operating voltage overnight (8 hours) to remove any possible space charge left by the measurements prior to breakdown. Upon being de-energised, the sample was immediately removed from the tank and broken down within one hour. Minimising the time spent out of the tank was intended to ensure the results of the breakdown would be consistent with the maximum length water tree in the sample - it was considered that the breakdown would need to be performed before the water was allowed to dissipate from the water trees.

The breakdown test was performed in line with 'standard' procedure:

1. Final non-destructive test performed
2. Ageing stress applied for eight hours (overnight)
3. Ageing stress removed
4. Removed directly from tank
5. Energised at 1kV for one minute
6. Applied voltage increased by one kV at the end of each minute
7. Recorded voltage was the highest voltage that did not lead to breakdown within one minute

There was an emphasis on having samples broken down as soon as possible, to ensure the water trees are affected as little as possible by the removal of the high voltage field. There was an estimated 30 minutes from de-energising to breakdown. While the sample temperature was not measured at breakdown, they were able to be handled manually and were approximately room temperature. It is estimated that the core temperature would be between 25 and 35 degrees Celsius.

The analysis of failed samples of XLPE has been carried out since the original use of the material as an insulator. The current de facto standard for analysis is the 'hydrophilic stain' procedure [7]. The procedure involves heating thin slices of sample material in a hydrophilic stain (Rhodamine B was used in this project, Methylene Blue is another popular alternative), which 'fixes' the water trees and allows for the sample to be examined under an optical microscope. Typically a microtome is used to slice the samples to a thickness of between 10μm and 100μm.

Other methods of analysis include Fourier spectroscopy to determine the exact content of the water trees [96], novel stains to differentiate the different impurities in the samples [47], electron microscopy to visualise the microstructure of water trees [76, 93], and IR spectroscopy to analyse the condition of the polymer in the water tree [19].

These techniques focus on analysing the detailed structure of single water trees, often grown in specialised samples that allow for the complex technical processing required for the method to operate. This project, by contrast, examined the broad growth patterns of many water trees, measuring several thousand in an attempt to perform some statistical analysis that might give some insight into the growth patterns of water trees in real cable samples.

As such, only the optical analysis was performed on these samples. A new method of visualising the water trees was developed in order to process the samples more quickly and with better repeatability, and this allowed approximately 0.5% of the entire sample length to be analysed.

3.6 Post-mortem analysis of water-treed XLPE

3.6.1 Ageing

The samples were aged in a facility as described in chapter 3. In short, a facility was constructed for applying high voltage, high current ageing stress in a wet ionic environment. However, in contrast to other studies, the water (along with dissolved ions) was restricted to the outside of the samples with no water in the conductor interstitium. This is a significant point of difference in comparison to other similar studies, and was made necessary by the use of the treatment regime which requires a sealed conductor core.

The application of these stresses was intended to simulate field ageing at a more rapid rate than 'operational' ageing. However, there are likely to be differences in the morphology of the water trees grown in an accelerated ageing test compared to field aged samples.

During the early phases of the project, it was determined that the current supply transformer would be unable to supply sufficient current (taking into account resistive and reactive current requirements) to heat the conductors of thirty samples. As such, the decision was made to remove the field aged untreated samples from the test. This decision was made on the basis of the requirement of the test to compare treated aged samples with new samples in order to provide information for network management purposes.

There were two failures that occurred in the ageing test, and these were replaced by field aged untreated samples. These samples provided some invaluable data regarding the sectioning and staining process.

3.6.2 Breakdown

Having aged the samples for a constrained period of time, it was decided to break down the samples in order to compare the internal structure of the water treed samples to the dielectric measurements taken directly prior to breakdown. Ideally, an accelerated ageing test of this type would be performed according to a 'truncated time to failure' protocol. However, the design of the experiment as a time to failure model precluded breaking down samples during the test. At the time specified, the samples were broken down by an AC breakdown step test.

3.6.3 Analysis

There are several modes of analysis available when investigating water treed XLPE. The following options were explored in the design phase of this project.

Optical analysis is the mainstay of water tree investigations. Optical analysis of stained XLPE has been well described, and is utilised in laboratories throughout the world. The techniques for analysis tend to differ only in specific points of detail (e.g. the thickness of the slices, the type of stain used). In this test, the samples were stained with Rhodamine B, and sliced to a thickness of 0.1 mm. Most researchers slice the samples significantly thinner, in the range of 0.01 to 0.001 mm. The thicker slices in this test were a result of the 'spiral cutting' technique that produces a long spiral of sample which can be fed mechanically through a winding device that allows for rapid analysis of the water trees in a sample. The lathe used to turn the samples was capable of cutting 0.1 mm minimum thickness, and this was therefore the thickness used. With further refinements in this technique, improvements in contrast and detail of the image could allow more detailed measurements. The increased time involved in analysing thin slices may be offset by the use of computerised techniques to automatically measure and count the water trees in a sample.

3.6.4 Statistical Analysis

3.6.5 Population Models

Due to the difficulty and expense in creating an experimental test facility for growing water trees, there are few population studies of water trees beyond an examination and estimation of the density of water trees in a cable. A literature survey revealed many tests using test objects (small discs of polyethylene with an intruding needle), several using accelerated ageing tests on model samples, a few analyses of accelerated ageing tests on commercially available samples, and no well designed examinations of the populations of water trees grown in field aged cable.

There are two types of population analysis performed on the samples in this work: extreme value analysis (regarding the length of the longest water tree), and population distribution analysis (regarding the underlying population distribution of bow tie water trees). Analysis of the longest water tree is a well defined process that uses 'Extreme Value Analysis' in order to estimate the

longest water tree in a population by examining the longest water trees found in a series of samples. With a sufficiently large number of samples, the estimate of the longest water tree likely to be found in a population can be made with good accuracy.

The most commonly used statistical model for analysing the length of a population of water trees is the Weibull distribution [91], however the use of the log-normal distribution has also been proposed [6]. Determining population parameters of water treed XLPE is very difficult for several reasons - the samples are expensive and difficult to obtain, field aged samples are old and aged under unknown conditions, accelerated ageing has effects on the population parameters that may render these tests inapplicable to real networks, and finding and measuring water trees in XLPE is time consuming and expensive.

For these reasons, a model for the length of bow tie water trees is not well defined. The two models - log-normal and Weibull - have each been used, and each have been supported by experimental evidence. In the published literature, populations are typically sampled by 'bootstrapping' from a series of experimental measurements into a large data set for analysis of population parameters. While this technique is well known in statistical modelling, this work presents a large enough experimental data set that these 'data expanding' techniques are unnecessary.

3.6.6 Extreme Value Analysis

In general, the remaining life of a sample can be considered a function of the undamaged insulation thickness. That is, as the length of the longest water tree increases, the chance of a failure occurring increases. This relationship has been the subject of significant scrutiny, however an empirical relationship is yet to be found, and is likely to depend on many factors (temperature, applied stress, insulation morphology, etc.).

In this test, the remaining 'good' insulation thickness was estimated by performing an AC breakdown test of the samples - it has been indicated that the remaining insulation thickness is related to the remaining dielectric strength. The failure will occur at the weakest point in the insulation - being the point of the longest water tree - so this test was intended to give an indication of the longest tree present in the insulation.

Unfortunately, the test itself destroys the very object it is testing for - namely

the length of the longest water tree (see Figures 3.12 and 3.13). The charge dissipated by the breakdown generally causes a complete destruction of the point of initiation of failure. As such, it falls to the analysis of the remainder of the sample to provide an estimate as to the length of the water tree that caused the failure.

Computing the length of the longest tree in a sample is a somewhat challenging exercise, especially as the underlying distribution of water tree lengths has not been well studied. In this test, the samples followed an approximately log-normal distribution of lengths, however many other tests have not had the benefit of determining the underlying distribution of the population with any certainty, and have used alternative methods for estimating the length of the longest water tree. See chapter 4 for more detail regarding Figure 3.9 and the application of the log-normal distribution to the population of water trees found in this test.

The analysis of chapter 4 indicates that neither of the commonly accepted models (Weibull and log-normal) of analysing the length of water trees gives a perfect fit. Furthermore, in many tests performed in other laboratories, too few water trees are measured to make good estimates of the population parameters. In order to characterise the effect of water tree length on AC breakdown strength, an alternative method is required, which does not require a large number of samples.

As shown in figures 3.10 and 3.11, while the vast majority of water trees fall below a certain value (shown by the red line), the few trees longer than this length are significantly longer. If we assume that the breakdown voltage, and therefore the remaining life, is correlated to the length of the longest water tree, then this clearly shows that these deviations from the 'normal' values are very significant with regards to the remaining life of a sample.

In order to characterise these uncommon but significant events, we turn to *extreme value theory*.

The theory of extreme value statistics is well documented, what follows here is a brief introduction to the essential concepts. For more information, consult Kotz or Leadbetter ([54, 59] respectively) which were used extensively in preparing this section.

There is a well-known concept with regards to statistical modelling: the theory of 'central tendency'. This theory states that if a large group of random

Figure 3.9: Log-normal probability plots of the water tree length

. The log-normal probability distribution was found to have a slightly better fit, but the data is not conclusive.

Figure 3.10: The observed water tree lengths, with the Weibull 37% extreme value. Notice that the vast majority fall below this value, but the deviations above it can be significant.

Figure 3.11: The observed water tree lengths, with the Weibull 37% extreme value. Notice that the vast majority fall below this value, but the deviations above it can be significant.

sequences $X_1, X_2, X_3...$ are added together, the resulting distribution will be normal - even if none of the random sequences are normally distributed. Furthermore, it has been found that if the 'expected' value (the mean or average) of a group of random sequences is considered, the distribution of the 'expected' values will be normal.

The most commonly used distribution resulting from this theory is the Weibull distribution. It is used in lifetime estimations and reliability engineering. It is widely used in part because it can model several distributions simply by changing the shape parameter.

The 3-parameter Weibull pdf is given by:

$$f(t) = \frac{\beta}{\eta}\left(\frac{t-\gamma}{\eta}\right)^{\beta-1} e^{-\left(\frac{t-\gamma}{\eta}\right)^{\beta}} \tag{3.1}$$

where:

$f(t) \geq 0,$ when $t \geq (0$ or $\gamma)$

$\beta > 0$

$\eta > 0$

$-\infty \geq \gamma \geq +\infty$

and:

$\eta =$ scale parameter, or characteristic life

$\beta =$ shape parameter (or slope)

$\gamma =$ location parameter (or failure free life)

The 2-parameter Weibull pdf is obtained by setting $\gamma = 0$ and is given by:

$$f(t) = \frac{\beta}{\eta}\left(\frac{t}{\eta}\right)^{\beta-1} e^{-\left(\frac{t}{\eta}\right)^{\beta}} \tag{3.2}$$

The 1-parameter Weibull pdf is obtained by again setting $\gamma = 0$ and assuming $\beta = C =$ Constant assumed value or:

$$f(t) = \frac{C}{\eta}\left(\frac{t}{\eta}\right)^{C-1} e^{-\left(\frac{t}{\eta}\right)^{C}} \tag{3.3}$$

where the only unknown parameter is the scale parameter, η

In the formulation of the 1-parameter Weibull, the shape parameter β is defined by experience with the populations under test (or by previous models). This allows analysis of very limited data sets with few or no failures.

The distribution being applied in this case is the 2-parameter Weibull distribution. This is commonly expressed in terms of the cumulative density function:

$$F(t) = 1 - e^{-\left(\frac{t-\gamma}{\eta}\right)^{\beta}} \tag{3.4}$$

This is also referred to as unreliability and designated as $Q(t)$ by some authors.

The reliability function of a distribution is one minus the cdf, the reliability function for the 3-parameter Weibull distribution is therefore given by:

$$R(t) = e^{-\left(\frac{t-\gamma}{\eta}\right)^{\beta}} \tag{3.5}$$

And for the 2-parameter Weibull:

$$R(t) = e^{-\left(\frac{t}{\eta}\right)^{\beta}} \tag{3.6}$$

Of note, is the case $t = \eta$. This point represents the maximum of the probability density function - the expected value of the distribution. The probability of this value occurring is $1 - e^{-1} \approx .632$ hence the term *the 63% level*. This is used as the estimate for the most likely maximum value, and this is computed directly for the dielectric breakdown strength (as shown in table 4.2).

3.7 Novel Method of Analysing Failed XLPE Cable

This method was developed for use in this test in order to analyse a much greater proportion of the sample than has previously been published. Using this method, 510mm of the total cable length was analysed.

3.7.1 Sectioning

Although the supply current in the AC breakdown test was limited, the capacitance of the cable supplied sufficient current to cause a defect that could be located with the naked eye quite easily. Figures 3.12 and 3.13 show the appearance of the failure sites after the cable jacket has been removed.

The samples were rough-cut into sections approximately 700 mm long with the failure site in the middle. They were then turned on a lathe into sections

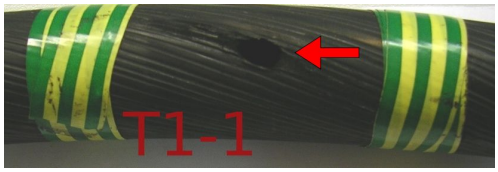

(a) Sample T1-1 Failure Point

(b) Sample T1-2 Failure Point

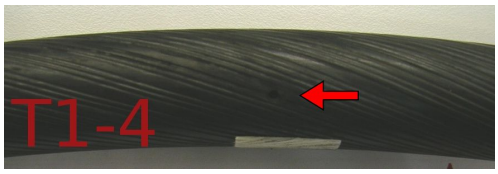

(c) Sample T1-4 Failure Point

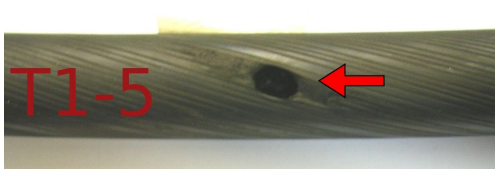

(d) Sample T1-5 Failure Point

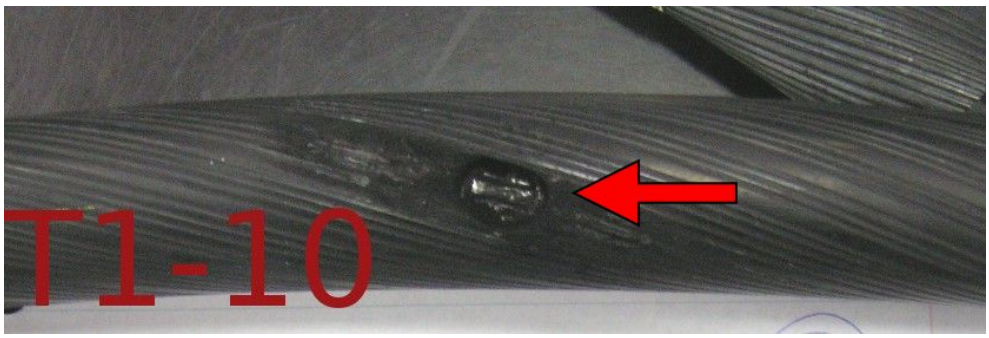

(e) Sample T1-10 Failure Point

Figure 3.12: Photographs of the failure points of the samples from Tank 1.

10mm thick at the locations indicated in figure 3.14.

At the failure site, this resulted in a series of concentric rings of insulation rather than the continuous spiral at the nearby sites.

3.7.2 Staining

The samples were stained using Rhodamine B in a water bath at 90 degrees Celsius. This is an adaptation of the original method created for visualisation of water trees [7]. Rather than requiring a basic environment for fixing the dye to the water trees, the use of Rhodamine B allows staining to take place in a neutral aqueous environment.

The samples were placed in a 1g/L solution of Rhodamine B, and warmed in a water bath at 75°C - 90°C for 6-8 hours. The time spent in the water bath was not as critical as the temperature reached. If the temperature did not exceed 80°C, the stain was faint and water trees difficult to see. In this case,

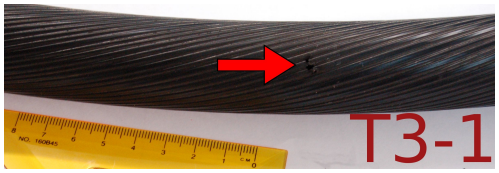

(a) Sample T3-1 Failure Point

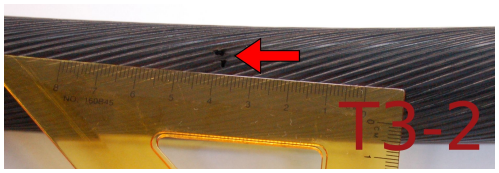

(b) Sample T3-2 Failure Point

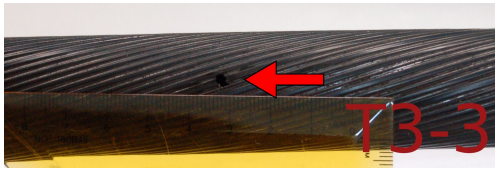

(c) Sample T3-3 Failure Point

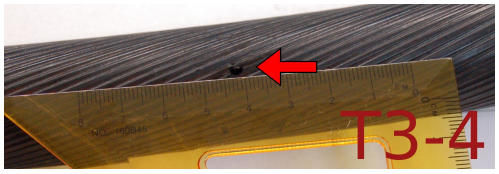

(d) Sample T3-4 Failure Point

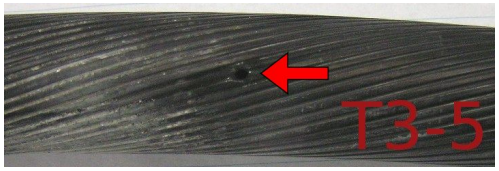

(e) Sample T3-5 Failure Point

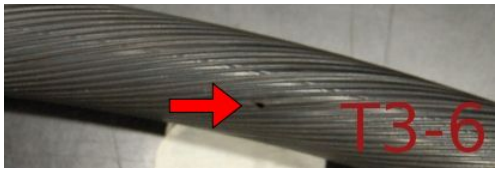

(f) Sample T3-6 Failure Point

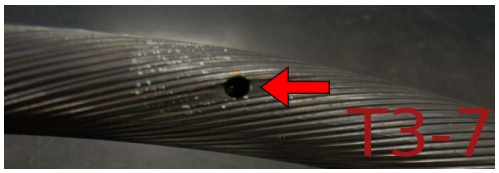

(g) Sample T3-7 Failure Point

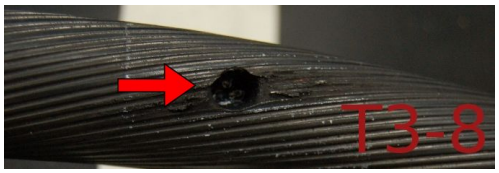

(h) Sample T3-8 Failure Point

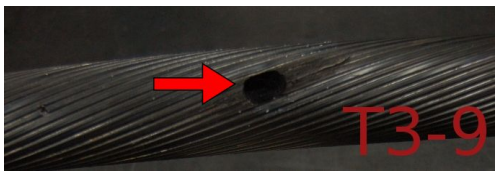

(i) Sample T3-9 Failure Point

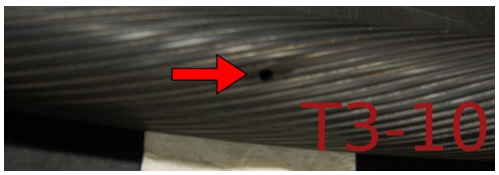

(j) Sample T3-10 Failure Point

Figure 3.13: Photographs of the failure points of the samples from Tank 3.

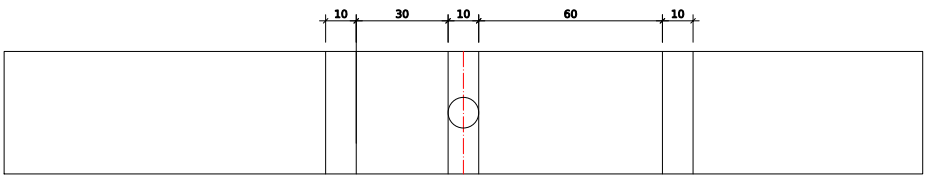

Figure 3.14: The sites at which spiral samples were lathed from the failed cable sample. The 10mm sections were analysed.

the sample was re-stained by repeating the procedure.

After staining, the samples were rinsed thoroughly in tap water and dried by hand. Care was taken to remove any surface stains which could obscure the optical analysis.

Once the samples are cleaned and dried, the inner semiconducting layer was removed, as it interferes with the mechanics of the projecting device. One group of samples in this test had semiconductor layers of the strippable type which can easily be removed by pulling away the semiconductor layer by hand. The fully bonded semiconductor layer was also able to be removed by hand, however it required more care to avoid damaging the insulation in the process.

Most samples were analysed directly after staining; only two sets required a second staining procedure when the temperature was not sufficiently high to adequately stain the sample.

3.7.3 Viewing

In contrast to most published methods, the samples were analysed using a projector rather than a microscope. The field of view of a projector allows for a cross section of the insulation to be visualised at once. The projector screen setup is shown in figure 3.15. As indicated in the figure, the length and location of each water tree can be measured as they pass under the fixed measuring ruler.

Microscope examination of water trees typically happens at 100x, with details of the structure of the water tree often visible (see figure 3.16a). The projected image in this work was magnified 50x. This was the maximum magnification that could fit within the boundaries of the projector screen. While the projector had lenses allowing magnification to 100x, the benefit of this higher level of detail was considered less important than being able to capture both length and spatial information on the samples in a single pass (figure 3.16c). At 50x, water trees > 0.02mm in length (magnified size 1mm) would be visible.

For the segments directly at the failure site, where lathing the sample produced a series of 'C' shaped segments, a microfiche reader was utilised instead of the projector (figure 3.16b). The images from the microfiche reader had somewhat better contrast, albeit at a lower magnification (30x rather than 50x). It was considered that the improved contrast would counteract the reduced magnification of the microfiche. Thus it was considered that a water tree

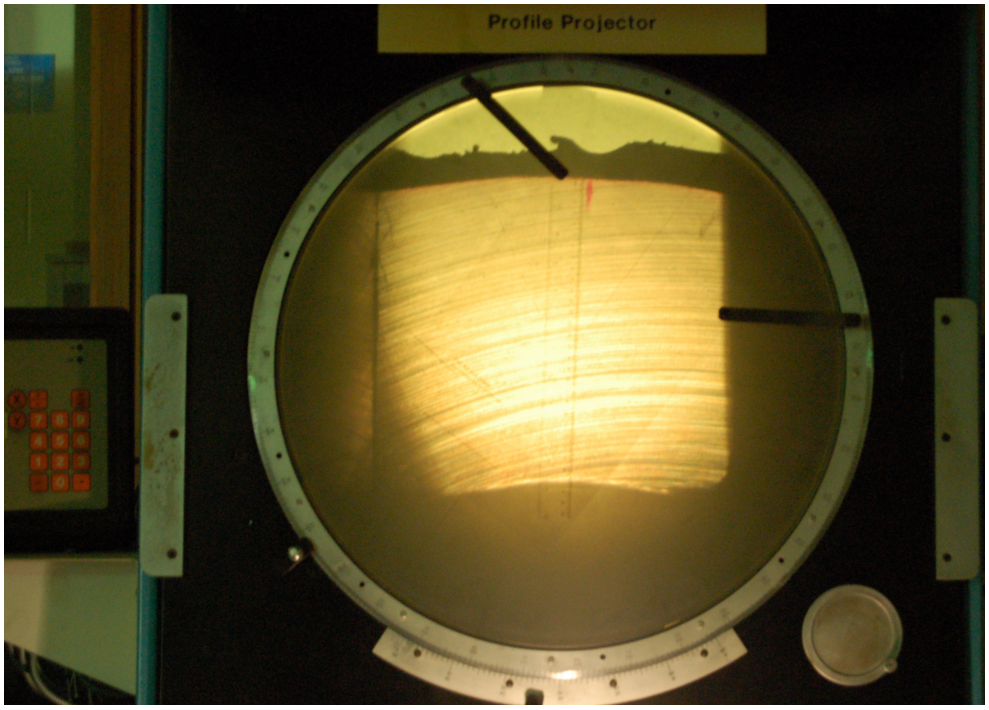

Figure 3.15: The projector setup used for measuring water trees.

0.02mm (1mm on the projector, 0.6mm on the microfiche) would still be visible. This resolution can be compared to a microscope, in which the resolution is approximately 2.5 μm (0.0025 mm) [27].

3.7.4 Measurement Error

There are several opportunities in the measurement of the samples for making measurement errors. The most difficult error to control is the irregular border of water trees. For example, the water trees in figure 2.4 are recorded as being different by 0.02mm in length, but one is hard pressed to draw a clear line indicating the length of these water trees. In a similar fashion, exacerbated by the relatively low contrast nature of the projected image, it is difficult to exactly determine the boundary of a water tree.

This error was controlled in two ways. Firstly, a rule was determined for measuring the length of water trees. The boundary was defined as the point at which the stain was not visible, with the longest vertical length forming the overall length. The second (and arguably most effective) technique was having the same person perform all the measurements.

The magnification was calibrated by using objects of known size. This was

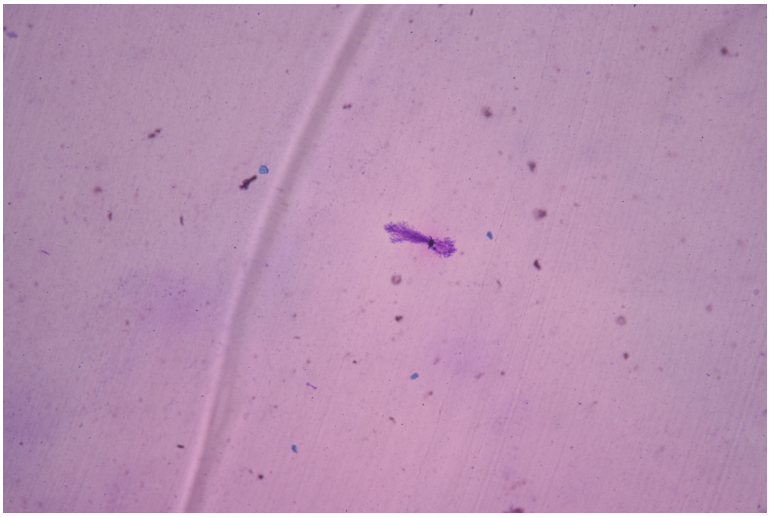

(a) Bow tie water tree as viewed under a medium powered microscope (Methylene Blue stain)

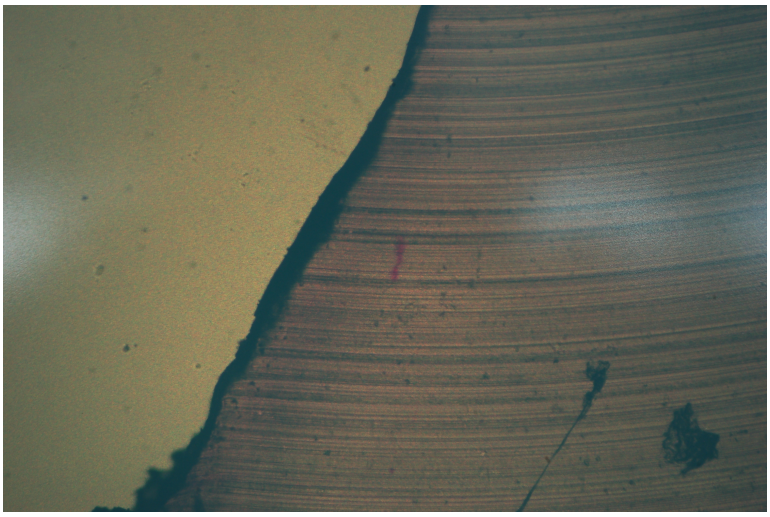

(b) Bow tie water tree as viewed with a microfiche at 30× (Rhodamine B stain)

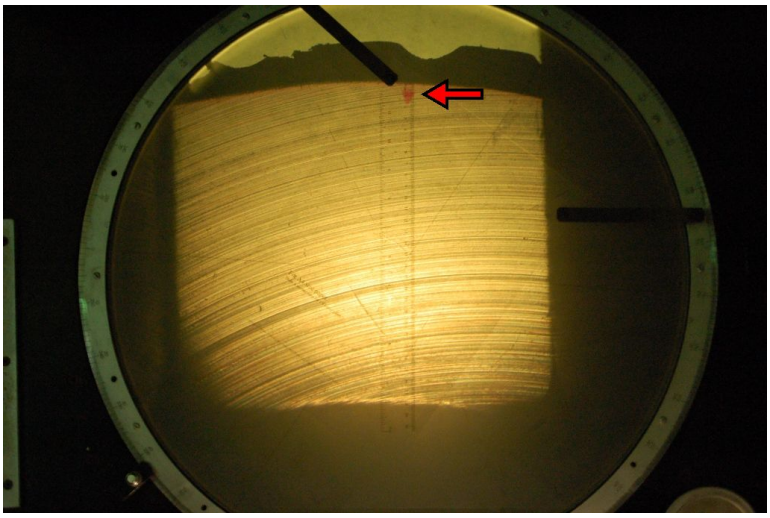

(c) Vented water tree as viewed with the projector described in section 3.7 (Rhodamine B stain)

Figure 3.16: The three methods of visualising water trees utilised in this test.

especially important in the case of the microfiche reader, where the magnification is variable. The projected image was shown to be 50× within the accuracy of the equipment used to test it.

The actual measurements were taken by a transparent ruler with mm markings. Thus there was an error of 1mm (0.5mm at each end) in each measurement. This corresponds to an error of 0.02mm on the projected water trees, and 0.03mm in the measurements made using the microfiche reader.

3.7.5 Ageing Timeline and Downtime

As with any large complex system, there were some issues with the test facility during the course of the test. The unusual requirements for the current transformer put a lot of strain on the custom built transformer, which failed twice in the four years of operation, resulting in a total 400 days of effective ageing.

Furthermore, the transformer was operating very close to its specified limits, and it was discovered that the samples displayed a significant power factor, which was unable to be corrected. As such, the transformer was unable to adequately supply three tanks of ten samples each, and it was decided early in the project to reduce the number of samples to twenty, ten field aged and treated and ten new untreated samples.

The unused field aged samples were used to replace any sample failures, and indeed there were failures in this group (that is, the replacement sample failed). These failed samples were used to establish the post-mortem analysis procedures and the data gained from these samples is included in this thesis, where applicable.

There were some problems with the terminations on the samples overheating - this was solved with the use of shear head lugs rather than crimp type lugs. It was suggested by the manufacturer (of the shear head lugs) that the use of a crimp connector, which compresses to a certain diameter, is less reliable and much more sensitive to wear on the operating parts of the tool compared to shear head connectors. Shear head connectors tightened to a specified torque, theoretically giving a more consistent connection.

Overall, there were a three periods of extensive downtime (more than a month offline), during which some tests were still performed on the samples. The downtime makes interpretation of the testing data a little more complex, and makes it more difficult to draw long-term trends from the measurements.

In contrast to most of the published literature on accelerated ageing, water was not inserted into the conductor strands of the samples in this test. This was due to the use of the treated samples that had been dried, treated and sealed, resulting in a closed environment that would not permit the introduction of water without damaging the terminations.

In order to maintain consistency, water was not applied to the untreated samples, even though this would have been technically feasible with this group. This decision is the most likely cause for the relatively low number of water trees found in this test, and the good condition of the samples at the conclusion of the test.

An interesting side issue was encountered during this test. While the crimp lugs are rated for 400A continuous current without overheating, the actual current that can be maintained is heavily dependent on the workmanship of the joint. While few in-service failures of cable terminations due to joint overheating are reported by maintenance staff at Ergon Energy, thermal issues were encountered in many of the joints employed in this test. It was suggested that in-service cables do not have to carry the rated current continuously for many hours (as this test required) and therefore joint workmanship is less of a problem.

Of the 40 terminations used in this test, thirteen overheated at the joint during this test. In addition, even after replacing the lugs, some joints continued to overheat. Therefore, during the third year of the project (after approximately 150 days of ageing), all the samples were re-terminated with shear head connectors. These connectors utilise a fixed torque technique, as opposed to the crimp lugs which use a fixed diameter. Due to the fixed diameter nature of the crimping process, tool wear and manufacturing variation can have a significant effect on the pressure applied to the joint when using crimp type lugs, and this variation can increase the resistance of the joint.

By contrast, shear head connectors apply a fixed torque regardless of diameter, and always apply a predetermined amount of pressure to the joint. The shear head connectors were much better at handling the current applied in this test, and overheating of the connectors was not a problem once they were changed.

Initial calculations based on previous works suggested that with the parameters outlined above, most samples would fail within 600 days. Thus, it was

expected that most of the samples (if not all) would have failed within the (initial) three year timespan of the project. Unfortunately downtime reduced the effective ageing time to 400 days, and during this period there were only two failures. With only two failures in 400 days, it was considered to be unlikely that the test could conclude in a timely manner.

Therefore the decision was made to break down the samples by AC breakdown after 400 days of ageing, and the forensic analysis linked to the breakdown voltage to analyse the state of the insulation at breakdown. Rather than giving direct lifetime comparisons, the breakdown voltages were analysed (using Weibull extreme value analysis) in order to estimate the condition of the samples at breakdown - this is a proxy for remaining life, but does not give a direct estimation of remaining life.

The extreme value analysis of the breakdown voltages was combined with a similar extreme value analysis of the water tree lengths found in the forensic study. The final dielectric measurements were correlated with the forensic data taken post failure, in order to assess the effectiveness of the degree of nonlinearity as a monitoring tool. Thus, the condition of the samples was assessed for their functional condition as well as their physical state.

This is a slightly different outcome from the original aim of determining the remaining life of a sample from the dielectric measurements, however this information is still valuable when considering the management of an underground XLPE network.

Chapter 4

Results of Accelerated Ageing Test

> In every branch of knowledge the progress is proportional to the amount of facts on which to build, and therefore to the facility of obtaining data.
>
> *James Clerk Maxwell*

Presented in this chapter are the results of the tests performed on the samples described in chapter 3. The samples were broken down by an AC breakdown step test, and then sectioned, stained and water trees were visualised using a projector and screen.

4.1 Results of the ACBD Test

The procedure for the ACBD test is described in chapter 3. The breakdown strength of each sample is shown in table 4.1. By fitting the failure voltages to a Weibull distribution, the 'expected' breakdown voltage of each sample was computed (the Weibull '63%' value). This value gives a summary of the breakdown strength of the samples contained within the tank.

The breakdown strength was compared to the length of the longest water tree in each tank, computed in a similar manner using a Weibull distribution (this value is the Weibull '37%' value). The breakdown strength correlates well

with the length of the longest water tree, with the treated samples having lower breakdown strength and longer water trees than the new samples.

The confidence limits of the voltage estimates do not overlap, suggesting there is a statistically significant difference between the groups. ACBD Strength Tank 1: 86 [84,89], Tank 3: 115 [114.66, 114.69]. The 'spread' of the values is rather higher for the Tank 1 group - this is in keeping with the greater spread of water tree lengths found.

Sample	ACBD Strength	Max WT Length	WB 37%	WB 63%
T3-1	123	0.28	0.34	115
T3-2	124	0.40	0.34	115
T3-3	110	0.36	0.34	115
T3-4	110	0.84	0.34	115
T3-5	103	0.40	0.34	115
T3-6	131	0.54	0.34	115
T3-7	89	0.32	0.34	115
T3-8	96	0.26	0.34	115
T3-9	89	0.50	0.34	115
T3-10	110	0.20	0.34	115
T1-1	61	0.47	0.63	86
T1-2	82	0.78	0.63	86
T1-4	103	0.56	0.63	86
T1-5	82	0.82	0.63	86
T1-7	75	0.66	0.63	86
T1-8	75	0.60	0.63	86
T1-9	89	0.66	0.63	86
T1-10	96	0.69	0.63	86

Table 4.1: Summary of the results from the accelerated ageing test

4.2 Morphology of Water Trees

This test discovered the presence of a subgroup of water trees in the samples examined. The water trees observed in samples taken from the group of treated cables had a noticeably different structure than those observed in the untreated samples. While vented and bow tie water trees were present in both sets of samples, these groups were further classified into 'dark' trees and 'fuzzy' trees.

The untreated samples tended to have more defined trees, with a clearly defined boundary between the bulk insulation and the stained water tree, while

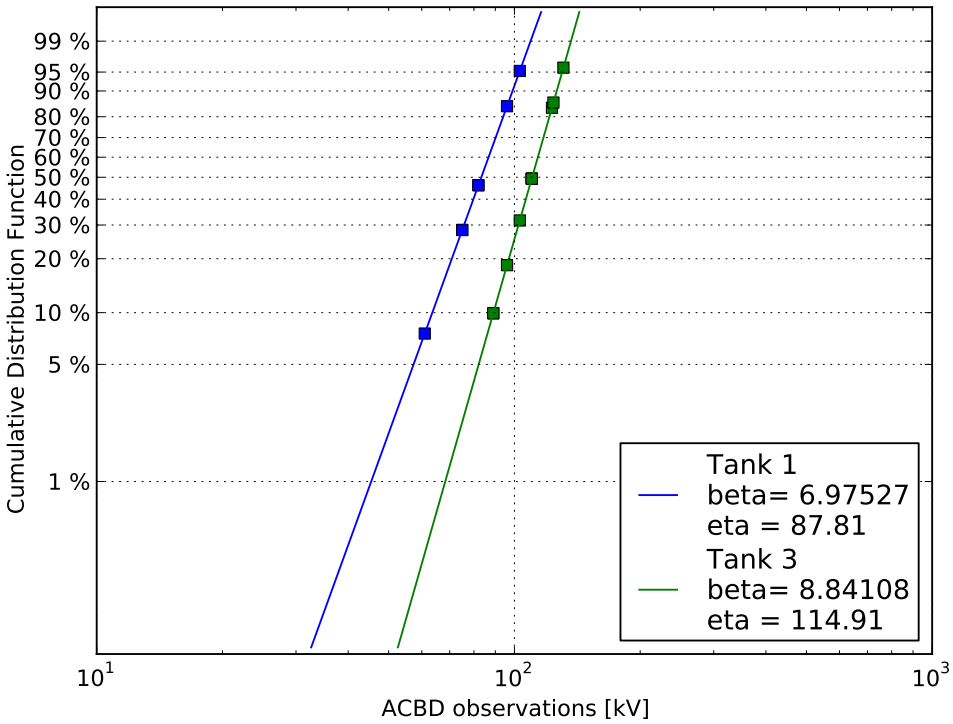

Figure 4.1: Weibull Plot of ACBD voltages.

the treated samples, in addition to these 'dark' trees, had water trees that were shorter, wider and 'fuzzy' (see figure 4.2). This was the basis of classifying the measured trees into two groups.

'Dark' water trees were found in every sample. These could be both bow tie trees or vented, and typically were quite long. They were easily seen on the screen, and there is a high confidence that they were all located and measured.

The 'dark' water trees observed in the untreated samples were similar to those seen in the published literature (for example [105]). They tended to be longer than wider, they had a clearly defined treelike structure, and they were well defined. Fuzzy water trees on the other hand, were still clearly visible as a pink patch, but the boundary between the stained tree and the bulk insulation was indistinct. Additionally the shape of the tree was somewhat compressed; being noticeably wider and shorter than the dark water trees.

'Fuzzy' water trees were of the bow tie type, and were only found in the treated samples. They ranged from somewhat dark (although noticeably lighter than the 'dark' water trees), to very faint, almost invisible. Generally the light-

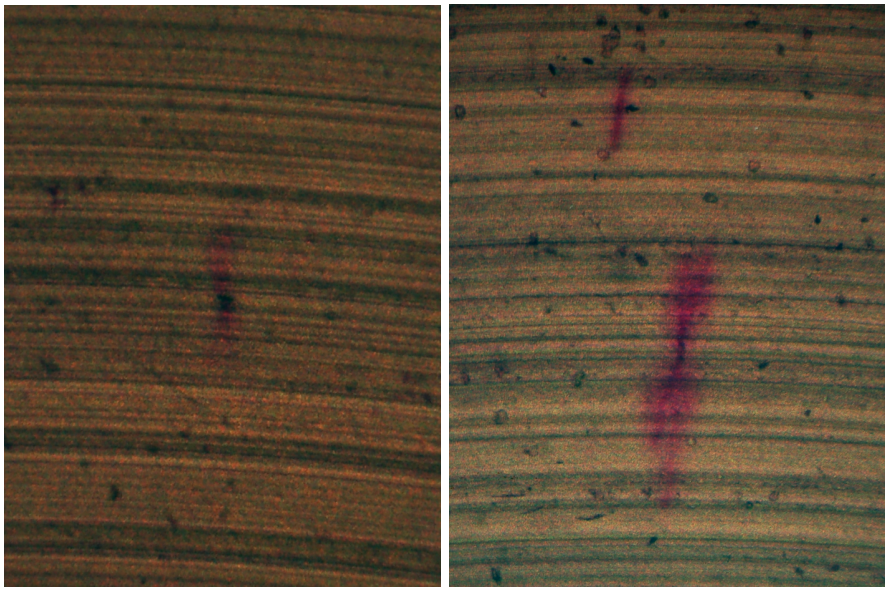

(a) Fuzzy Tree **(b)** Dark Tree

Figure 4.2: A fuzzy water tree (left) compared to a dark water tree (right).

ness of the 'fuzzy' water tree was correlated to its size: the larger trees tended to be darker than the smaller ones.

This fuzziness is possibly due to these trees being 'cured' water trees; water trees that were in the field aged samples prior to the 'curing' treatment. The fluid is intended to bind the water trees into an inert structure, but it is possible that this bound water may retain some of the dye used in staining, and as such show up as a fuzzy water tree - the lightness caused by the lower solubility of the captured water in the dye compared to hydrophilic channels in an untreated water tree.

The presence of two types of water trees suggests that the treatment does not prevent the formation of new water trees, with new trees produced in the ageing test staining to a dark colour due to their high free water content. This raises a possibility that the reason for the field aged samples having many more water trees is due to water trees grown in the field during 30+ years of ageing.

That the more dangerous of the two are the dark water trees is indicated by two properties. Firstly, all the vented trees seen were of the dark type, and vented trees are considered the more dangerous type of water tree. Secondly, the length of the dark trees was generally longer than that of the fuzzy trees. While there were large trees of both types, the fuzzy trees tended to be smaller

and shorter with regards to their width (that is, they tended to be shorter and fatter), while the dark water trees tended to be longer for a given width. This may indicate that the dark water trees are growing faster - for a given volume of water a thinner dark tree will be longer than a fatter fuzzy one.

The breakdown analysis considered the longest water tree, regardless of type, as it was considered that anything that retains the dye is a point of weakness in the insulation. Any tree or defect may contribute to the loss of breakdown strength, but it is hypothesised that the dark water trees increase in length most rapidly, causing premature failure of a cable sample.

Unfortunately clear conclusions cannot be drawn on this data set for several reasons. The different water trees were noticed after sectioning and staining had taken place, and several confounding features were not controlled prior to this stage. The most significant confounding factor is the relatively uncontrolled staining procedure. An effort was made to ensure consistency between the samples, however as the staining procedure was somewhat unrefined, there was some significant difference between the treatment received by each sample in relation to temperature and time in the stain bath.

4.3 Analysis of Length of Vented Water Trees

Vented trees are considered the most dangerous type of water tree, because a vented tree will continue to grow from its initiation point on the boundary of the insulation until the insulation is weakened sufficiently to cause breakdown. The vented tree lengths measured in this test are shown in figure 4.3.

The longest water tree (most frequently a vented water tree) in a sample represents the weakest point of the insulation. As such, it is this tree that creates the source of the breakdown in the breakdown test. The energy released by the breakdown destroys this part of the insulation, so the length of the longest tree in a broken down sample cannot be measured - it must be estimated instead.

Using extreme value theory as outlined in [41], the expected value of the longest water tree was estimated using the '37%' level, the results of this analysis are shown in table 4.2.

The results indicated in this table may appear somewhat counter-intuitive. Each sample in Tank 1 has a relatively short 'longest expected water tree' com-

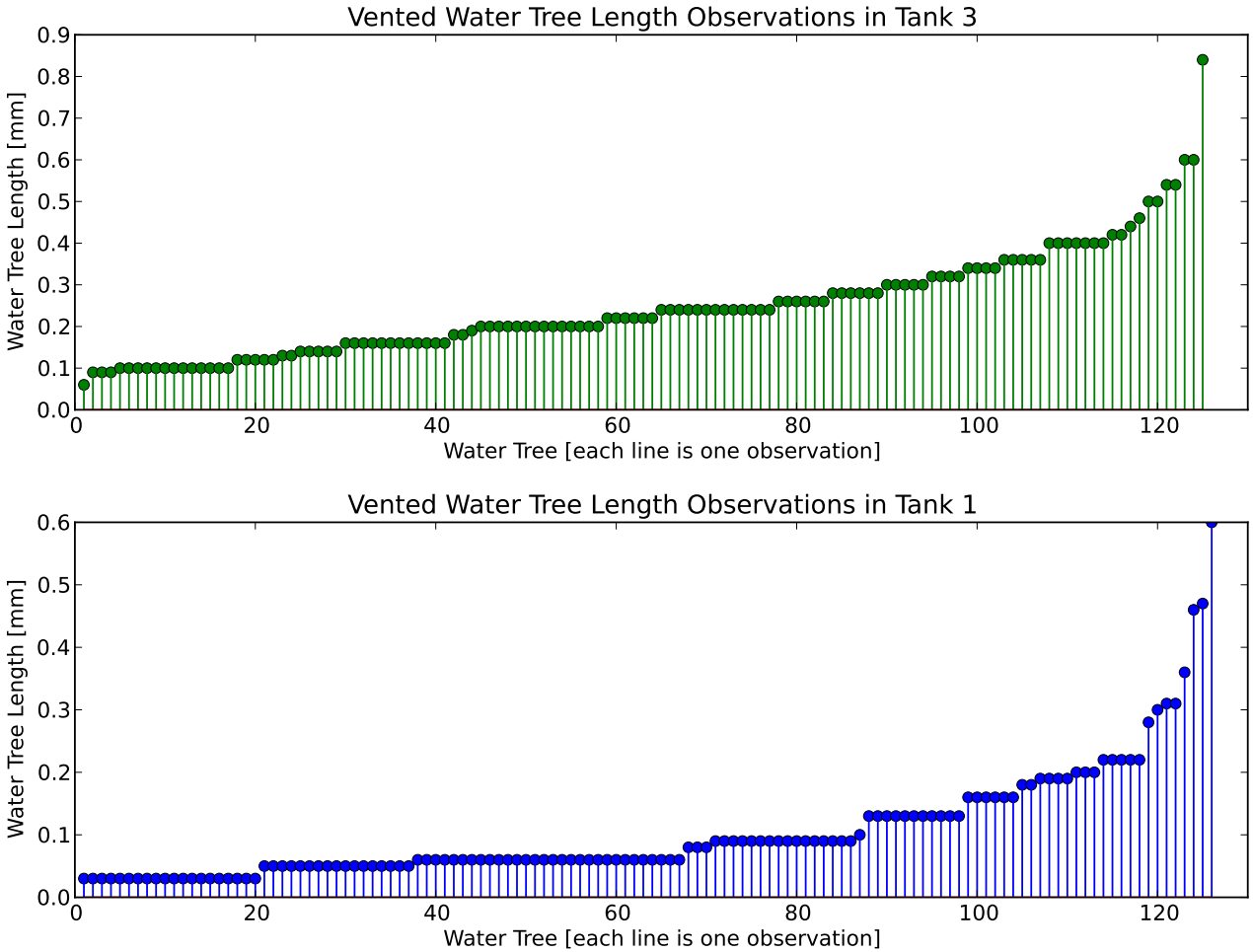

Figure 4.3: The observations of each vented water tree - each line represents a single water tree (there were a similar number of vented trees in each group).

Sample	ACBD Strength	Max WT Length	Sample WB 37%	Tank WB 63%
T3-1	123	0.28	N/A	115
T3-2	124	0.40	0.40	115
T3-3	110	0.36	0.36	115
T3-4	110	0.84	0.19	115
T3-5	103	0.40	0.24	115
T3-6	131	0.54	0.20	115
T3-7	89	0.32	0.20	115
T3-8	96	0.26	0.09	115
T3-9	89	0.50	0.14	115
T3-10	110	0.20	0.10	115
T1-1	61	0.47	0.06	86
T1-2	82	0.78	0.08	86
T1-4	103	0.56	0.04	86
T1-5	82	0.82	0.06	86
T1-7	75	0.66	0.08	86
T1-8	75	0.60	0.12	86
T1-9	89	0.66	N/A	86
T1-10	96	0.69	0.08	86

Table 4.2: The extreme value calculations for each sample, showing the expected longest water tree length for each sample and the expected ACBD strength for each tank, along with the longest measured water tree and the AC breakdown voltage.

pared to Tank 3, however the Tank 1 group has the longest expected water tree overall. This is a result of applying the Weibull method to an entire population, rather than the maxima of a series of populations. As such, the vast number of small water trees cause the longest expected value to decrease, with a very large scatter on the results. These values are included for interest, the overall 'Tank' values are much more reliable estimates.

The vented water trees grown in this test were relatively small in comparison to the thickness of the insulation. The longest water trees were less than 1mm in length, breaching less than 20% of the insulation thickness (see figure 4.16 on page 103). As such, these samples might be considered to be 'middle aged' rather than 'severely degraded'. The relatively good condition of the samples makes the electrical measurements much more difficult to interpret.

This result is confirmed by the ACBD test, which indicated samples in a 'mid-life' condition. The '63%' level of the samples in Tanks 1 and 3 were 86kV and 115kV respectively. This corresponds to stress levels of 15.6 kV/mm and

20.9 kV/mm. In-service insulation must withstand approximately 2.3kV/mm, and a cable that can withstand 12.5kV/mm is almost indistinguishable from a new cable [36].

The proposed reason for the good condition of the samples is twofold: dry central conductors and ageing test downtime. Both of these factors are 'engineering' considerations that relate to the practicality of operating the test, rather than a 'scientific' consideration of the effectiveness of the experiment to highlight a phenomenon. This result provides support for the theory of wet central conductors causing more rapid water treeing, and highlights the need for careful planning and experience in the construction and maintenance of a facility of this type.

One feature this test highlights is the positive effect of creating a dry internal environment. To that end, the CableCure process of drying and sealing the central core would certainly contribute to improving the lifespan of a treated cable, and this benefit may be realised even in cables in near-new condition.

4.4 Analysis of Length of Bow tie Water Trees

Using the techniques outlined in the previous sections, a large population of bow tie trees was sampled. In comparison to other similar tests, the larger number of bow tie trees measured allows for an analysis of the population of water trees with much higher confidence.

One debate with regards to water tree population modelling is the superiority of log-normal or Weibull statistical distributions when modelling water tree length populations. It has been impossible to provide convincing evidence on either side, due to the fact that the two distributions are quite similar and the small number of samples measured are not sufficient to differentiate them [91, 6].

By analysing a much greater length of insulation, and sampling many bow tie water trees, this test has given some evidence for the use of the log-normal population distribution over the Weibull population distribution.

The observations of bow tie water trees are shown in figure 4.4. It can be readily seen that many more bow tie trees were found in the field aged samples, likely due to the time spent ageing in the field, but also possibly due to a greater number of inclusions in this very old cable.

The length of the bow tie trees were analysed in order to assess which statistical distribution gives the best fit for the length of water trees. The data was plotted against a normal distribution, a log-normal distribution, and a Weibull distribution. The probability plots for each sample are presented along with other sample information in appendix B. The probability plots for each tank are shown in Figure 4.5 and Figure 4.6.

The Weibull distribution is used often when discussing the estimated length of water trees found in a sample. The argument for the Weibull distribution stems from the field of reliability statistics, where it is used extensively in analysing the expected life of artefacts, as well as other processes related to ageing and failure [91]. Applying the Weibull distribution to the length of water trees that lead to failure was a logical step.

The Log-normal distribution comes from the field of growth analysis. The growth of fatigue cracking is often modelled well by the log-normal distribution, and the analogy of a water tree being a fatigue induced crack in a material leading to failure yields an argument for the log-normal distribution [28].

The Normal (Gaussian) distribution was included for completeness - in the

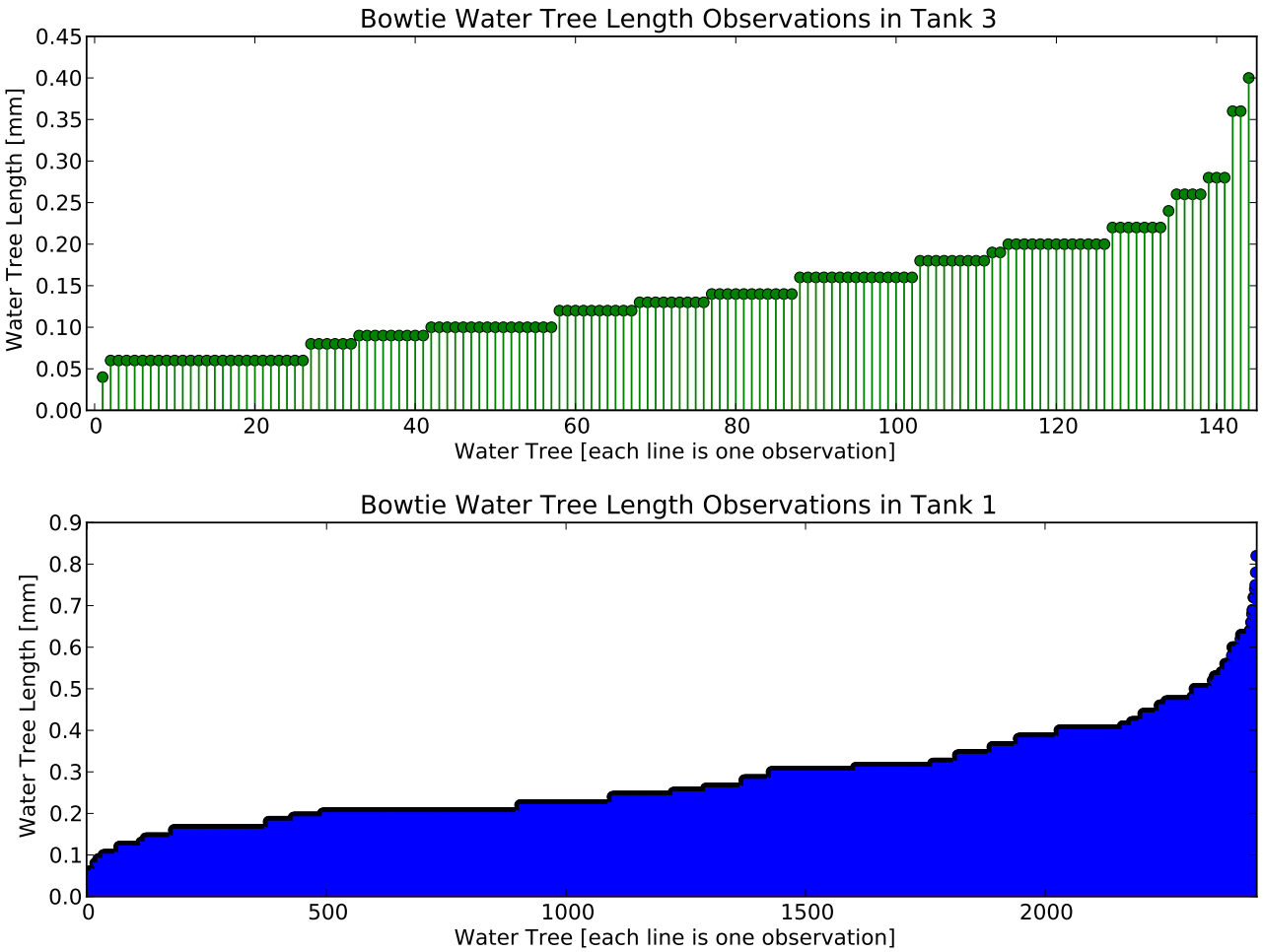

Figure 4.4: The observations of each bow tie water tree - each line represents a single water tree. Note the greater number of bow tie trees found in tank 1.

literature survey other models were typically used, but no evidence was found rejecting the case for a normal distribution of water tree length.

As expected, the curvature seen in the Gaussian probability plots indicate this model is not a good fit for the data; this is confirmed by several of the samples failing the test for normality. This is not a surprising result - most current models of water tree length suggest the use of the Weibull or log-normal probability distribution.

Separating the log-normal probability distribution from the Weibull distribution is somewhat trickier, with some authors resorting to statistical simulation techniques to attempt to separate these models [27]. Probability plots of both distributions with this data suggests either could be a possibility. In both cases there is deviation at the 'base' of the graph (in the 0.1mm range of water tree lengths). This region is of a similar order of magnitude of the detection floor of the equipment used to measure the water tree lengths, and as such is likely to have a significantly higher error of measurement than the longer water tree lengths found. At the longer lengths, the log-normal probability distribution has a slightly better fit, with some minor curvature of the Weibull probability plot.

An additional point of interest may be seen in the probability plots for Tank 1. With a little imagination, one may observe a possibly bi-modal distribution of the lengths of water trees found in Tank 1 in the log-normal probability plot (Figure 4.5 top). If the log-normal probability distribution is an accurate fit (this experiment shows evidence, but it is not conclusive), then this point of flexure at the 0.1 cumulative probability level may indicate a second population within this group of samples.

The presence of a bi-modal population in Tank 1, with a unimodal distribution in Tank 3 could be explained by the two different modes of ageing the samples underwent. While both sets of samples were subjected to the high stress ageing in the accelerated ageing facility, only samples in Tank 1 were aged in the field. This time of 'normal' ageing could reasonably be expected to produce a large number of small to moderately sized water trees, while it would be expected that the high stress accelerated ageing would result in the fewer, but longer water trees.

Continuing with this possibility, a bi-modal population would explain the large number of outlying points on the box-plots in Figure 4.18 (top left). If

this were the case, and the results of the accelerated ageing test were the longer of the two groups of water trees, the medians in this plot would be an underestimate of the higher population.

The presence of two different types of water trees, as outlined in the previous section, further supports the theory that the samples from Tank 1 have a bimodal population distribution. Whether the two populations are related to accelerated ageing vs. field ageing, or pre-treatment vs. post-treatment is not conclusively shown by the data obtained in this experiment. However, it seems likely that the more dangerous dark water trees, with their higher water content and longer length, are the result of ageing under more stressful conditions. As such, this would represent examples of the population grown under accelerated ageing, which is coincidentally also post-treatment.

It should be noted that even if the population is bimodal, the analysis presented in section 4.3 would still be valid. The extreme value method only considers the longest water tree in a group, and this value will most likely be from the 'accelerated ageing' population. Furthermore, the Weibull analysis is valid regardless of the underlying distribution (even an unknown distribution).

Particularly with regards to the length of water trees, a model for the underlying distribution of the length has yet to be determined. One of the most significant contributions of this method of forensic analysis is the large number of points available for statistical testing. The comparatively large number of water trees measured in this test allows for some evidence supporting the use of the log-normal probability distribution for modelling the length of water trees in XLPE.

With the fewer samples typically measured in other tests, it may not be possible to distinguish the difference between the log-normal and Weibull probability plots, however the larger number of samples analysed in this test (especially in Tank 1) provides evidence against the use of the Weibull distribution when modelling the length of bow tie water trees.

In the samples from Tank 1 (of which there were significantly more water trees found), the curvature of the Weibull probability plot is much less noticeable, if it is even present. However, there is some interference from the shorter length water trees - these have noticeably affected the fit line. Whether this is due to measurement noise or an actual population model deficit is not entirely clear from this data.

If only a small number of water trees are examined (as is often the case), the resulting statistical models have a large uncertainty in the estimation of parameters, even when assuming a particular population distribution. An exploration of the underlying distribution is even more difficult, as there are even more degrees of freedom. In many cases, authors use data meta-analysis to infer differences in populations, and while these techniques are well established, the use of a greater number of samples to analyse the quality of a model fit is still the gold standard.

Statistical Tests

While observation of probability plots can give an indication into the goodness of fit of a certain distribution, it is helpful to have a quantitative assessment of the goodness of fit of the models as well. In this way, it may be possible to determine if a certain model is a better fit, even if none of the models offer a perfect fit. Thus, to ascertain the differences between the samples, the data was subjected to two different statistical tests - the Lilliefors test for normality, and the Jarque-Bera test for normality.

Both tests are used for testing if the data is normally distributed, however each uses a different aspect of the data to come to a conclusion. The Lilliefors test is based on the deviation of the cumulative distribution of the data from the cumulative distribution of an ideal normal distribution with parameters identical to those estimated from the data. The Jarque-Bera test for normality is based on estimates of the moments of the data (skewness and kurtosis), both of which are zero in normally distributed data, and significant deviation from zero indicate a loss of normality of the data.

The water trees were divided into four categories that would conceivably have different distributions, as indicated in table 4.3

	Tank 1		Tank 3	
	No. Samples	No. W.T.s	No. Samples	No. W.T.s
Bow Tie	7	2441	10	144
Vented	7	126	9	125

Table 4.3: The four categories and the number of samples and number of water trees in each category.

As can be seen from table 4.3, there were many more bow tie trees found

in the field aged (and treated) samples than the new unaged samples. This has a significant effect on the confidence of the estimated parameters.

The first test was analysing the water tree length for normality. Since it has already been suggested that the length of water trees follows either a log-normal or a Weibull distribution, this test should show deviation from normality. Two methods were used to test for normality - the Lilliefors test (a modification of the Kolmogorov-Smirnov test that can be used when the parameters of the underlying distribution are not known, this test is based on the deviation of the CDF of the samples from the CDF of an ideal normal with the estimated parameters) and the Jarque-Bera test (based on the skewness and kurtosis of the samples, which should be zero in an ideal normal population). The results of these tests are shown in tables 4.4 and 4.5.

The tests for normality indicated that the hypothesis of normality of the data could not be rejected in many cases. Rather than showing an underlying trend in the distribution of the data, these results were likely caused by a lack of data - due to the low number of samples in most cases, the hypothesis of normality could not be rejected. In the samples with many data points (as in bow tie trees in tank 1), there was sufficient deviation to reject the hypothesis of normality. This demonstrates a key property of the 'testing' method of analysis - where the underlying distribution is unknown, it takes many samples to be able to reject a null hypothesis. This highlights the importance of the techniques outlined in this chapter in measuring many more water trees than most similar tests.

Having rejected the hypothesis of normality, the data was analysed to determine what other distribution may give a better fit. This type of analysis must be approached with a high degree of suspicion - as was seen in the tests for normality, it can be difficult to reject the null hypothesis (H0: that the data is distributed according to the distribution under scrutiny) without a significant number of samples. In order to minimise the chance of a spurious false positive result being obtained, the analysis was restricted to the two most commonly used distributions - the log-normal and the Weibull distributions. These distributions were chosen because of their use in the literature to model water trees.

The method of analysis was to fit the data to a CDF with parameters estimated from the data. The errors were then analysed for normality. If the underlying curve of a set of data is estimated correctly, the deviation from the

Tank 1: Vented Trees					
Lilliefors Test					
Name	$X \sim N(\sigma, \mu)$	p-value	$\hat{\mu}$	$\hat{\sigma}$	N
T1 1 vented	0	0.0062	0.1055	0.0984	22
T1 2 vented	0	0.0171	0.1157	0.0733	21
T1 4 vented	0	0.0067	0.0554	0.0273	13
T1 5 vented	0	<0.01	0.0898	0.0771	47
T1 8 vented	1	0.1135	0.1836	0.1581	11
T1 10 vented	1	0.2533	0.1422	0.1250	9
Jarque-Bera Test					
Name	$X \sim N(\sigma, \mu)$	p-value	$\hat{\mu}$	$\hat{\sigma}$	N
T1 1 vented	0	<0.01	0.1055	0.0984	22
T1 2 vented	1	0.0829	0.1157	0.0733	21
T1 4 vented	0	0.0075	0.0554	0.0273	13
T1 5 vented	0	<0.01	0.0898	0.0771	47
T1 8 vented	0	0.0042	0.1836	0.1581	11
T1 10 vented	1	0.1446	0.1422	0.1250	9

Tank 1: Bow tie Trees					
Lilliefors Test					
Name	$X \sim N(\sigma, \mu)$	p-value	$\hat{\mu}$	$\hat{\sigma}$	N
T1 1 bow tie	0	<0.01	0.2737	0.1173	276
T1 2 bow tie	0	<0.01	0.2989	0.1183	285
T1 4 bow tie	0	<0.01	0.2737	0.1100	245
T1 5 bow tie	0	<0.01	0.2824	0.1224	481
T1 7 bow tie	0	<0.01	0.2566	0.1191	528
T1 8 bow tie	0	<0.01	0.2693	0.0979	343
T1 10 bow tie	0	<0.01	0.2850	0.0995	283
Jarque-Bera Test					
Name	$X \sim N(\sigma, \mu)$	p-value	$\hat{\mu}$	$\hat{\sigma}$	N
T1 1 bow tie	0	<0.01	0.2737	0.1173	276
T1 2 bow tie	0	<0.01	0.2989	0.1183	285
T1 4 bow tie	0	<0.01	0.2737	0.1100	245
T1 5 bow tie	0	<0.01	0.2824	0.1224	481
T1 7 bow tie	0	<0.01	0.2566	0.1191	528
T1 8 bow tie	0	<0.01	0.2693	0.0979	343
T1 10 bow tie	0	<0.01	0.2850	0.0995	283

Table 4.4: The tests for normality of the data ($X \sim N(\sigma, \mu)$: Normal distribution, 1 indicating the test showed the population to be normal, 0 indicating the population is *not* normal; p-value the chance of getting this data if the population *is* normally distributed; $\hat{\mu}$: estimate of the mean from the data; $\hat{\sigma}$: estimate of the standard deviation from the data; N the number of samples in this group). Note the significantly smaller p-values for the groups with many samples - these tests are the most reliable. In the groups with only a small number of samples, it is more difficult to reject the null hypothesis (null hypothesis is that the data *is* normally distributed).

Tank 3: Vented Trees					
Lilliefors Test					
Name	$X \sim N(\sigma, \mu)$	p-value	$\hat{\mu}$	$\hat{\sigma}$	N
T3 4 vented	0	0.0022	0.2539	0.1416	69
T3 5 vented	1	0.2233	0.2618	0.0744	17
T3 6 vented	0	0.0184	0.2524	0.1212	21
T3 7 vented	1	0.4656	0.2171	0.0734	7
T3 9 vented	0	0.0082	0.2125	0.1926	4
Jarque-Bera Test					
Name	$X \sim N(\sigma, \mu)$	p-value	$\hat{\mu}$	$\hat{\sigma}$	N
T3 4 vented	0	<0.01	0.2539	0.1416	69
T3 5 vented	1	0.5000	0.2618	0.0744	17
T3 6 vented	1	0.0840	0.2524	0.1212	21
T3 7 vented	1	0.5000	0.2171	0.0734	7
T3 9 vented	0	0.0199	0.2125	0.1926	4
Tank 3: Bow tie Trees					
Lilliefors Test					
Name	$X \sim N(\sigma, \mu)$	p-value	$\hat{\mu}$	$\hat{\sigma}$	N
T3 1 bow tie	1	0.2109	0.1640	0.0641	15
T3 2 bow tie	1	0.1486	0.1550	0.0857	6
T3 3 bow tie	1	0.0767	0.1472	0.0784	18
T3 4 bow tie	1	0.5000	0.2133	0.1086	6
T3 5 bow tie	1	0.1282	0.1381	0.0767	21
T3 6 bow tie	1	0.0738	0.1267	0.0745	12
T3 7 bow tie	1	0.0657	0.0982	0.0475	11
T3 8 bow tie	1	0.5000	0.1328	0.0552	18
T3 9 bow tie	0	0.0113	0.1250	0.0411	22
T3 10 bow tie	1	0.3388	0.1440	0.0503	15
Jarque-Bera Test					
Name	$X \sim N(\sigma, \mu)$	p-value	$\hat{\mu}$	$\hat{\sigma}$	N
T3 1 bow tie	1	0.5000	0.1640	0.0641	15
T3 2 bow tie	1	0.3644	0.1550	0.0857	6
T3 3 bow tie	0	0.0284	0.1472	0.0784	18
T3 4 bow tie	1	0.4510	0.2133	0.1086	6
T3 5 bow tie	0	0.0194	0.1381	0.0767	21
T3 6 bow tie	1	0.3827	0.1267	0.0745	12
T3 7 bow tie	1	0.0850	0.0982	0.0475	11
T3 8 bow tie	1	0.4174	0.1328	0.0552	18
T3 9 bow tie	1	0.4382	0.1250	0.0411	22
T3 10 bow tie	1	0.2949	0.1440	0.0503	15

Table 4.5: Two tests for normality of the data (Name: sample name and type of tree under scrutiny; $X \sim N(\sigma, \mu)$: 1/0 indicating if the data follows a standard normal distribution at the standard 5% level; p-value: The 'significance' of the test - p indicates the probability of this data occurring if the underlying distribution is normal (a higher p-value indicates a higher chance the data is normally distributed); $\hat{\mu}$: the estimate of the sample mean (the first moment); $\hat{\sigma}$: the estimate of the sample variance (the second moment)

Tank 1: Vented Trees						
Sample Name	Normal Distribution		Weibull Distribution		Log-normal Distribution	
	MSE	$Err \sim N(\mu, \sigma)$	MSE	$Err \sim N(\mu, \sigma)$	MSE	$Err \sim N(\mu, \sigma)$
T1 1 vented	0.059	1	0.040	1	0.052	1
T1 2 vented	0.055	1	0.051	1	0.052	1
T1 4 vented	0.086	1	0.069	1	0.064	1
T1 5 vented	0.070	1	0.057	1	0.057	1
T1 8 vented	0.078	1	0.062	1	0.065	1
T1 10 vented	0.059	1	0.063	1	0.076	1
Tank 3: Vented Trees						
Sample Name	Normal Distribution		Weibull Distribution		Log-normal Distribution	
	MSE	$Err \sim N(\mu, \sigma)$	MSE	$Err \sim N(\mu, \sigma)$	MSE	$Err \sim N(\mu, \sigma)$
T3 4 vented	0.040	1	0.037	0	0.039	1
T3 5 vented	0.063	1	0.064	1	0.064	1
T3 6 vented	0.032	1	0.032	1	0.039	0
T3 7 vented	0.071	1	0.077	1	0.049	1
Tank 1: Bow tie Trees						
Sample Name	Normal Distribution		Weibull Distribution		Log-normal Distribution	
	MSE	$Err \sim N(\mu, \sigma)$	MSE	$Err \sim N(\mu, \sigma)$	MSE	$Err \sim N(\mu, \sigma)$
T1 1 bow tie	0.036	0	0.034	0	0.033	0
T1 2 bow tie	0.030	0	0.029	0	0.028	0
T1 4 bow tie	0.056	0	0.056	0	0.055	0
T1 5 bow tie	0.022	0	0.021	0	0.020	0
T1 7 bow tie	0.028	0	0.027	0	0.026	0
T1 8 bow tie	0.049	0	0.049	0	0.048	0
T1 10 bow tie	0.026	0	0.026	0	0.024	0
Tank 3: Bow tie Trees						
Sample Name	Normal Distribution		Weibull Distribution		Log-normal Distribution	
	MSE	$Err \sim N(\mu, \sigma)$	MSE	$Err \sim N(\mu, \sigma)$	MSE	$Err \sim N(\mu, \sigma)$
T3 1 bow tie	0.069	1	0.071	1	0.086	1
T3 2 bow tie	0.052	1	0.064	1	0.080	1
T3 3 bow tie	0.054	1	0.052	1	0.056	1
T3 4 bow tie	0.068	1	0.069	1	0.087	1
T3 5 bow tie	0.067	1	0.059	1	0.059	1
T3 6 bow tie	0.101	1	0.087	1	0.075	1
T3 7 bow tie	0.141	1	0.129	1	0.113	1
T3 8 bow tie	0.047	1	0.043	1	0.049	1
T3 9 bow tie	0.078	1	0.076	1	0.072	1
T3 10 bow tie	0.088	1	0.091	1	0.090	1

Table 4.6: An analysis of the 'goodness of fit' of the data to three different statistical distributions (Normal, Weibull, and Log-normal). MSE: the mean squared difference between the data and the model using parameters estimated from the data; $Err \sim N(\mu, \sigma)$: 1/0 indicating whether the *error* is normally distributed. If a model is a good fit, the residuals should be normally distributed - indicating random noise

fit will be the random noise present in all measurements taken experimentally. Measurement noise is widely accepted as being normally distributed around the 'true' value, as such the error (also referred to as the residuals) of a curve fit to experimental data should be normally distributed. The inclusion of the Gaussian model in the analysis serves to provide a 'control' model - if the test suggests the data can be fit with a Gaussian model, the number of data points is insufficient to make accurate estimates of the underlying distribution.

If there are many samples, it is relatively easy to disprove normality of the errors, but if there are only small numbers of samples, it becomes trickier to analyse. As can be seen from Tables 4.6, once again the small number of samples limits the reliability of testing the hypothesis in some groups. In many cases, the residuals were considered normally distributed by the Lilliefors test (that is, there was not sufficient evidence to reject the hypothesis of normality at the 5% level), however graphical plots of the distributions tell a different story, with the sparse points showing a poor fit to the curve. In the case of the group with the highest number of water trees (T1 Bow tie) the residuals were found not to be normally distributed. This suggests that modelling water trees grown under these conditions with the log-normal or the Weibull distribution gives a poor fit.

An examination of the magnitude of the residuals suggests that there may be two different models for the length of water trees grown in XLPE insulation. The error of the Weibull distribution was lower than the log-normal for the vented water trees and the errors were also indicated to be normally distributed. However, the small number of vented water trees found make it difficult to conclusively state that the errors are normally distributed (in this case, the data must clearly indicate a *rejection* of the null hypothesis - H0: that the errors *are* normally distributed - in order to give a conclusive result). Considering the data set as a whole, combining these two pieces of evidence give some support for the use of the Weibull distribution for modelling the length of vented water trees.

In contrast, there were many bow tie trees measured and analysed, and this gives the analysis of the bow tie tree length a much greater sensitivity to deviations from normality. In this group, the log-normal distribution shows a better fit than either the normal or Weibull distribution in 11 out of 17 samples, with these samples having the most data points. All of Tank 1 (2441 water trees

total), and 5 out of 10 samples (81 of 144 water trees) in tank 3 had a lower error when considering the fit of the data to a log-normal distribution instead of a Weibull distribution.

To restate, Tank 1 had the most bow tie trees, and in this group none of the errors were shown to be normally distributed, and out of the commonly used distributions the log-normal distribution shows a better fit than Weibull.

Thus, while evidence was found for both distributions being systematically different from the 'true' distribution, the log-normal had consistently lower errors associated with the fit of the distribution. This suggests that the log-normal distribution gives a better fit than the Weibull distribution for modelling the length of *bow tie* trees grown in XLPE.

There is a further implication of fitting the data to a log-normal distribution. If this distribution does indeed model some aspect of the growth of water trees, then this suggests that water tree length may be a result of the *product* of several random processes. In a similar manner to the normal distribution modelling the sum of random processes, the log-normal distribution models the product of random processes. If this were the case, it would go some way towards explaining the fact that varying ageing parameters (supply frequency, voltage, temperature, etc.) seems to change the lifespan in a non-linear manner.

If the underlying process were the product of random processes, variables that are unknown or not adequately controlled will exert a disproportionate effect on the results of the test. For example, water tree length has been seen to be related almost but not quite linearly to the frequency of the supply, perhaps the deviation from the linear fit is related to other variables being changed by changing frequency (e.g. changing the frequency will also change the thermal energy dissipated by the sample).

In summary, the analysis of these samples found some evidence for the use of the log-normal distribution for modelling the length of bow tie water trees, weaker evidence for the use of the Weibull distribution for modelling the length of vented water trees, and strong evidence rejecting the use of the normal distribution in both cases.

4.5 Location of Bow tie Water Trees

Another contribution of this study is an examination of the relative location of the bow tie water trees inside the insulation. A study on the location of bow tie water trees within XLPE insulation was not found in the literature search.

The use of a projecting screen with a measuring overlay allowed for the center of each bow tie tree to be located. The center of each bow tie tree was used as a proxy for the initiation point, as observation of bow tie trees suggest they are close to being symmetrical. While it is likely that they will grow more in one direction than another to some extent, the water trees grown in these samples did at least appear symmetrical.

Figures 4.7 4.8 4.9 show the length and location of each bow tie water tree measured. Note the clustering in the center of the insulation of both length and number of bow tie trees. As can be seen, the length and location do not correlate with each other. The data derived from tanks 1 and 2 are very similar, these groups were taken from a single length of field-aged cable. These populations contrast strongly with the population measured in tank 3 (new cable) where much fewer water trees were measured, and they tended to cluster near the central core. As with most of the analysis of bow tie tree populations, the data from tank 3 is somewhat less useful due to the small number of water trees found.

Figure 4.10 and figure 4.11 show that the distribution of bow tie water trees within the insulation is clearly not a uniform distribution, even when corrected for the relative change in volume of the insulation. The uniform distribution is what would occur if the initiation of a water tree was based on the presence of impurities. Instead, the histogram seems to follow a normal or Russian distribution. It is proposed that several of the mechanisms highlighted previously in chapter 2 are at play at the same time. By overlaying the various distributions each process would take, an approximately normal distribution is the result (as the means of the various distributions would approach a normal distribution).

A further consideration then is the ‘fertility’ of the environment for water tree growth. If many overlapping factors cause the initiation of water trees, are there any specific factors that increase the growth rate? This can be assessed by considering the lengths of the bow tie trees at each location.

Figures 4.12 4.13 4.14 show the spread of water trees at each location in-

side the insulation (the thickness is divided into eight segments). This figure shows the central region has longer water trees in tanks 1 and 2. Two possible explanations for these longer trees in the center of the insulation are proposed: older water trees or faster growing water trees. The data from this experiment is unable to determine which of these possibilities took place. However, in either case, the conditions for longer water tree growth are more favourable. As such, this suggests that the processes outlined in chapter 2 may act synergistically and therefore the growth of bow tie trees is promoted in regions where heat, electrical field strength and mechanical strain overlap.

In contrast, the water trees in tank 3 tended to be longer at the boundaries of the insulation. This may represent a requirement of time to 'saturate' the insulation with water, or may indicate a different ageing population entirely. This data does not lend solid support to any conclusions, as the number of data points is rather sparse. However, the measured population would fit with current thinking - that of water penetrating the insulation and electrical stress causing water tree growth.

Initially there will be more water trees close to the boundaries, and over time water trees may begin to grow in the center of the insulation, as the water reaches saturation at this point. Alternatively, the boundaries of the insulation may continue to harbour longer water trees than the center (due to the higher stresses present), and some of these may 'convert' to vented water trees, which continue to grow and lead to failure. Investigation of this process would be better served by a 'truncated time-to-failure' test which would allow analysis of the water tree population as it develops over time.

4.6 Comparison of Water Tree Length Populations in each Tank

The first set of statistical tests compared the mean lengths of the water trees to determine if the samples had statistically different water tree lengths. It was found that most of the the samples from each tank had statistically similar water tree lengths to other samples from the same tank, and statistically different lengths to the samples from the other tank (Figure 4.15).

Figure 4.15 shows that the samples from Tank 1 each had a unique expected value. The increased number of data points in this group allows for relatively

narrow confidence intervals on the parameter estimations in this group. Thus even if the average values of these samples are similar, they may still be statistically different. Furthermore, if the distribution of the lengths in this group is bimodal (as previously discussed), this will skew the estimates of the expected values.

In contrast, the samples from Tank 3 (Figure 4.15, bottom right) were shown as belonging to the same population as other samples from this tank in many cases. This can be explained firstly by the possibility that many of the samples in this group do in fact share their population characteristics, and this group has a unimodal population distribution that is not skewed by having two distinct populations being combined. Alternatively, the relatively small number of measurements in this group causes larger errors in the estimation of population parameters, and this will make the samples harder to distinguish from each other, even if they do have different means.

A significant aspect of the data that is shown in this table is that samples from opposite groups do not correlate well. Even the relatively small number of measurements taken from the samples in Tank 3 are sufficient to differentiate them from the samples in Tank 1. This can be seen by the lack of high p-values in the top right and bottom left. This is the first piece of evidence for the two groups having different populations.

Figure 4.16 shows the length of all water trees measured in tanks 1 and 3. The first thing that is obvious in this figure is the much larger number of water trees grown in tank 3. However, the length of the longest trees found were comparable in both tanks.

In either case, the total insulation breached was only a small part of the whole thickness (Figure 4.16 right). This makes the absolute difference between the groups rather small, and in turn, suggests the insulation to still be in fairly good condition. While small, however, the difference between the groups is statistically significant. The two populations do not share a common average (Figure 4.16 center).

Figure 4.17 shows the contribution of the different types of water trees to the total population. Unfortunately, the results found here are more confusing than enlightening. While Tank 1 with its lower breakdown strength (Figure 4.17 right) has the longest overall water trees (Figure 4.17 center right), it was found to have shorter *vented* water trees overall, and does not possess the

longest water tree, as one might expect.

A possible explanation is that the longer length of bow tie trees found suggests the possibility of Tank 1 having processes at work that cause longer water trees to grow in this group. Furthermore, the larger size of the failure sites in Tank 1 (Figure 3.12) coupled with the small number of vented trees found in both sample groups, allows for the possibility that the longest vented water trees were destroyed in the breakdown process, and the remaining vented water trees are not representative of the longest vented trees in the sample.

This theory is further supported by the analysis in section 4.3, which applies extreme value analysis to the water trees measured in each sample to estimate the longest water tree one might expect to find in a given length of cable. In this analysis (which is based on the longest water tree measured in each individual cable sample, rather than the aggregate of all water trees in a tank) it is shown that one might expect a longer water tree to be found in Tank 1. This matches with the lower breakdown strength, and the lower expected breakdown strength (also in section 4.3).

This apparent inconsistency can be explained in more detail when looking at Figure 4.18 where it can be seen that the samples in Tank 1 had generally longer water trees, with higher median and interquartile values than Tank 3, despite the fact that Tank 3 had the longest water trees overall. This tendency to higher values is consistent with the results from section 4.3 indicating this group has a higher expected value of water tree length.

Considering the information contained in Figures 4.16, 4.17 and 4.18, good evidence was found in this experiment indicating the two tanks did in fact have different populations of water trees. Even without any additional information on the underlying population distribution of each tank or sample, it can be stated with good confidence that the samples in Tank 1 were more degraded than the samples in Tank 3.

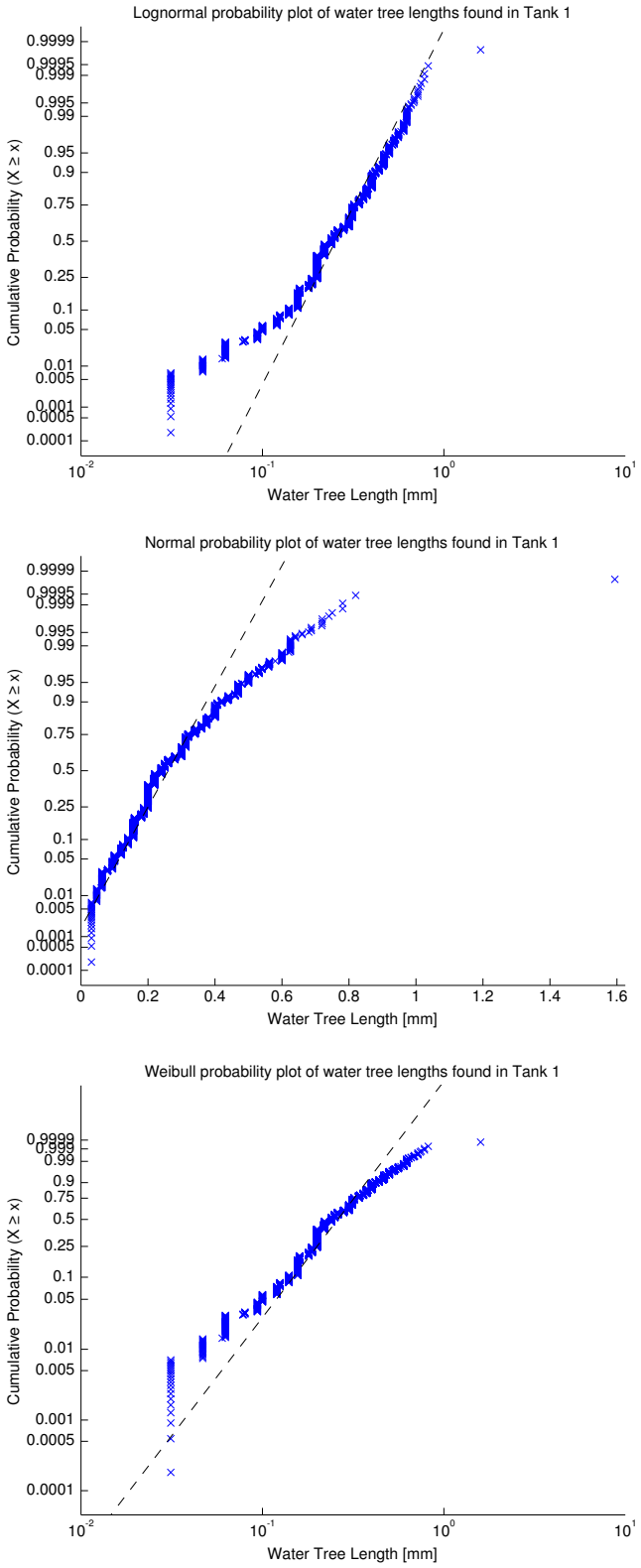

Figure 4.5: The probability plots of Tank 1 (treated samples), from top to bottom: Log-normal probability plot, Normal probability plot, Weibull probability plot.

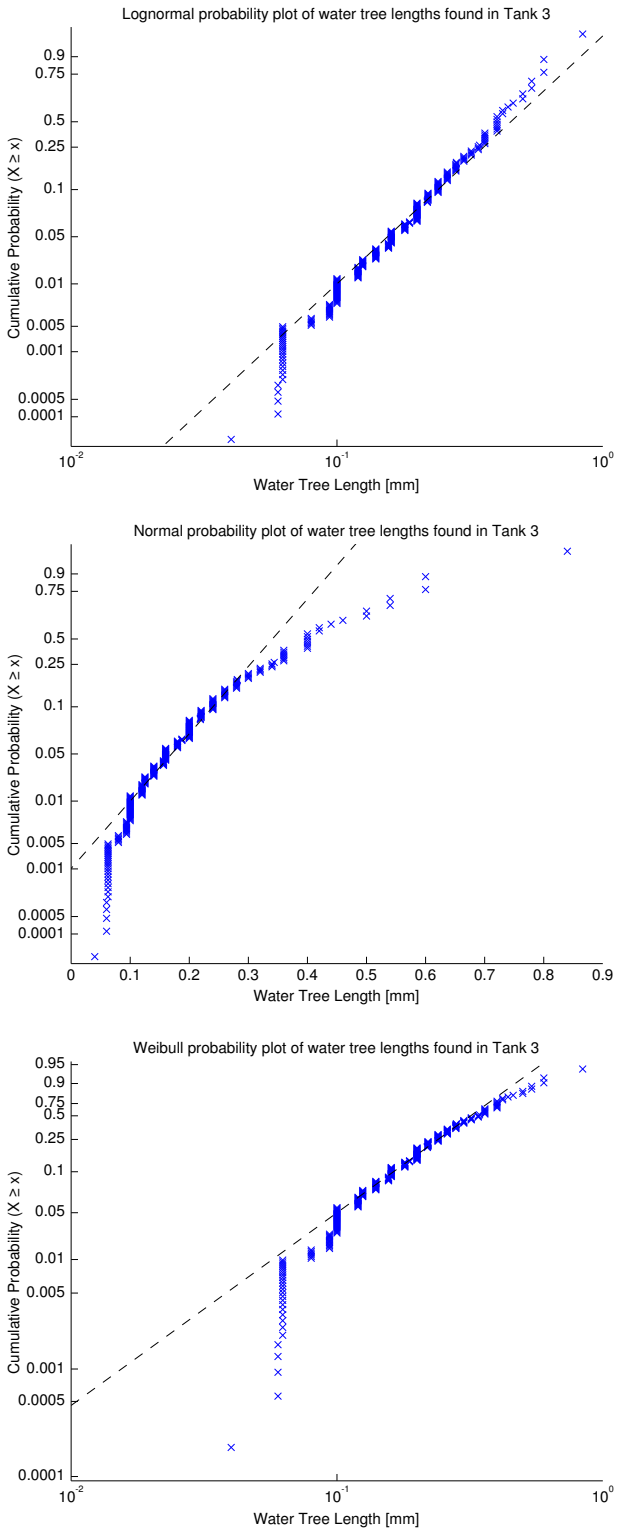

Figure 4.6: The probability plots of Tank 3 (untreated samples), from top to bottom: Log-normal probability plot, Normal probability plot, Weibull probability plot.

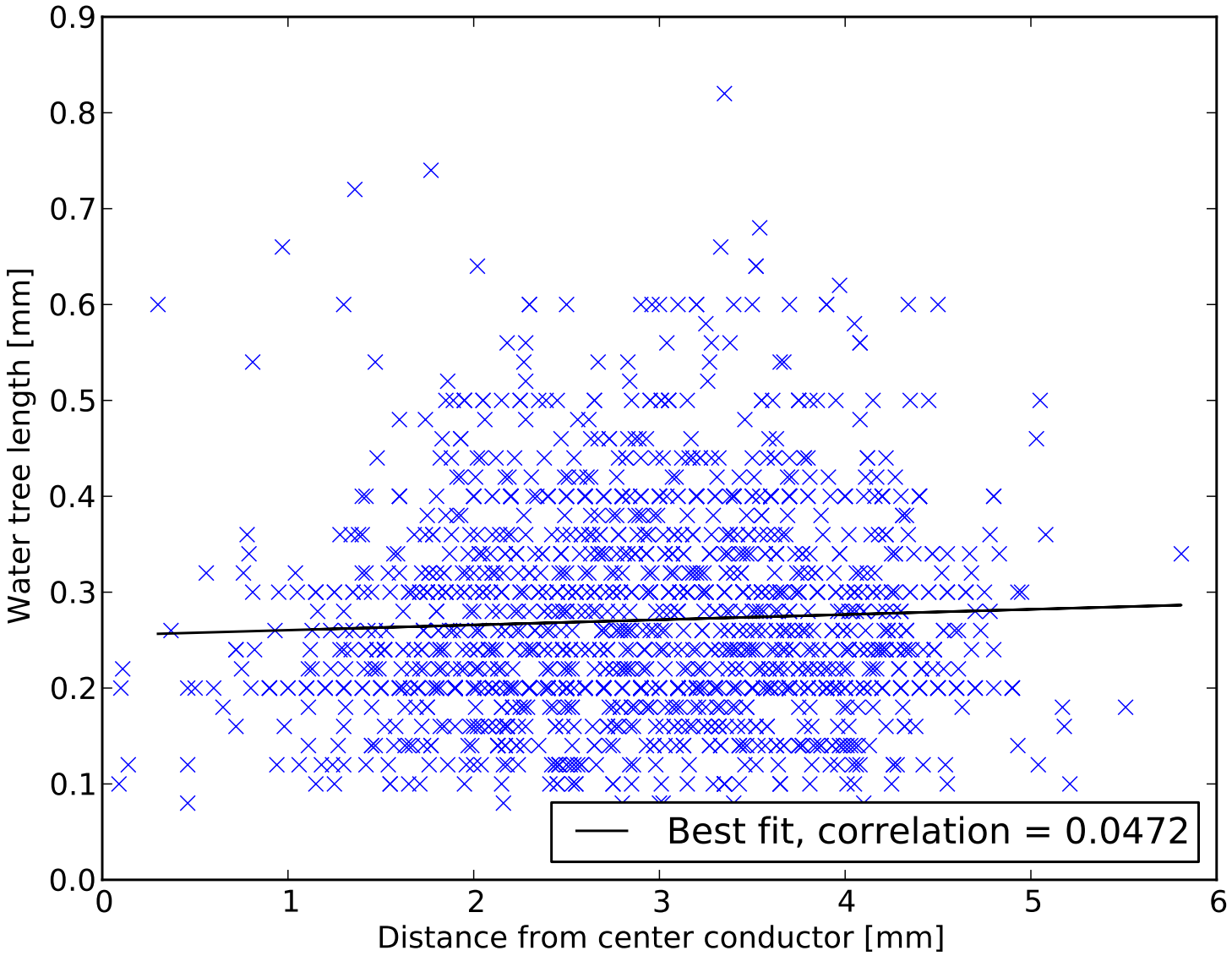

Figure 4.7: The location of the midpoint of each bow tie tree, plotted against its length - each data point represents a single bow tie water tree. The x-axis represents the distance from the inner semiconductor boundary (the 'conductor core' is at the left of the image), while the y-axis represents the length of the measured water tree in mm. From top to bottom: Field aged and treated, field aged untreated, new untreated.

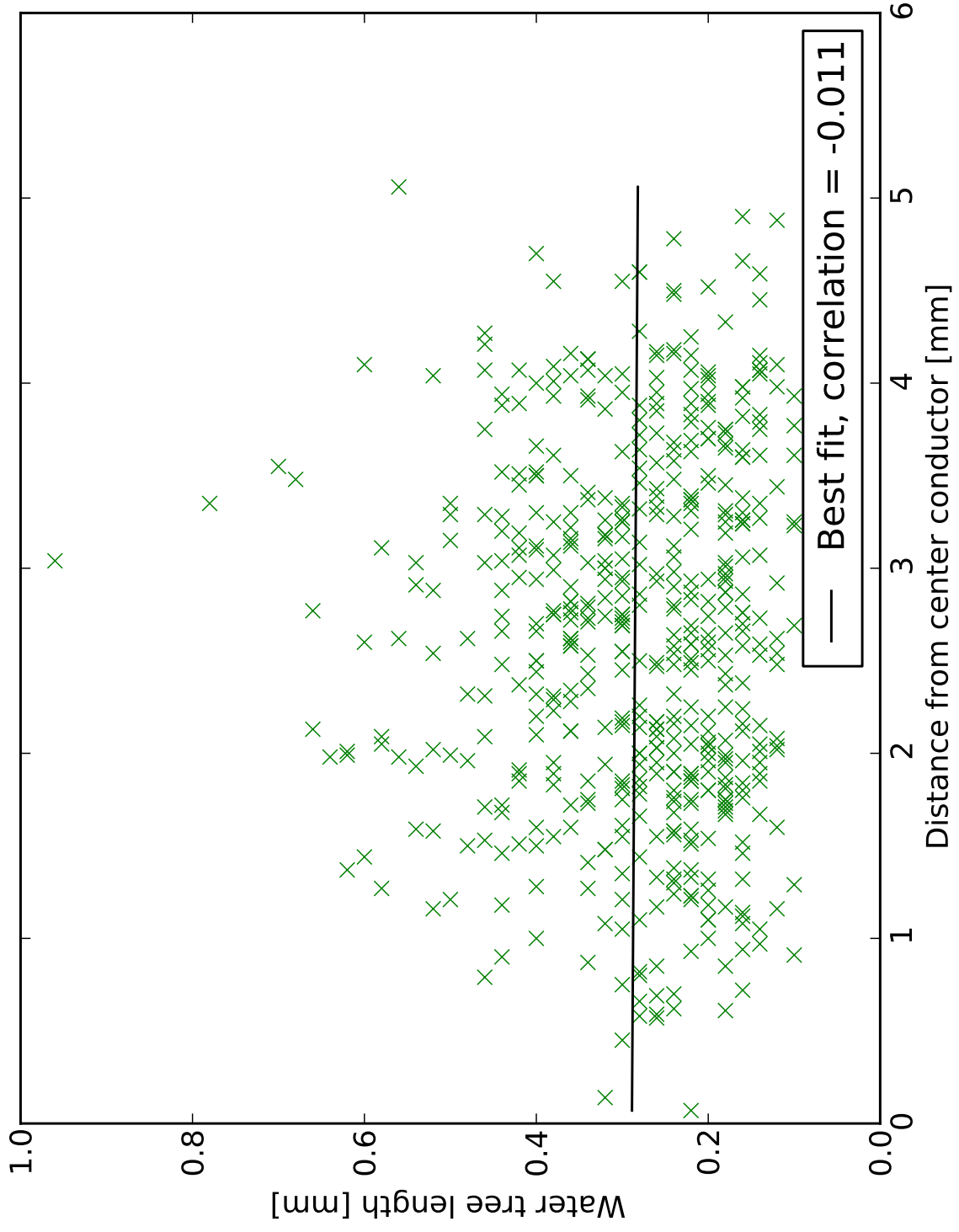

Figure 4.8: The location of the midpoint of each bow tie tree, plotted against its length - each data point represents a single bow tie water tree. The x-axis represents the distance from the inner semiconductor boundary (the 'conductor core' is at the left of the image), while the y-axis represents the length of the measured water tree in mm. From top to bottom: Field aged and treated, field aged untreated, new untreated.

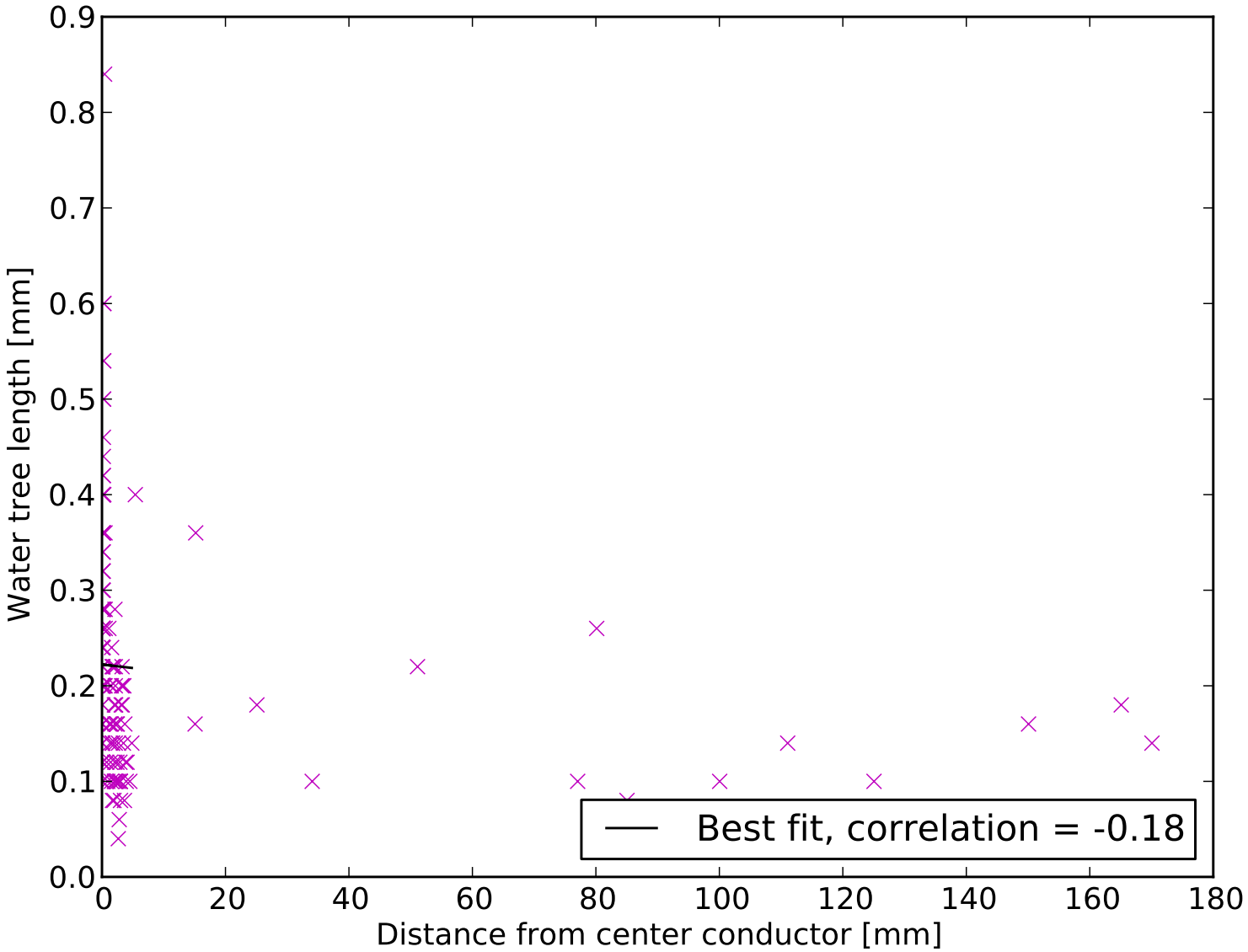

Figure 4.9: The location of the midpoint of each bow tie tree, plotted against its length - each data point represents a single bow tie water tree. The x-axis represents the distance from the inner semiconductor boundary (the 'conductor core' is at the left of the image), while the y-axis represents the length of the measured water tree in mm. From top to bottom: Field aged and treated, field aged untreated, new untreated.

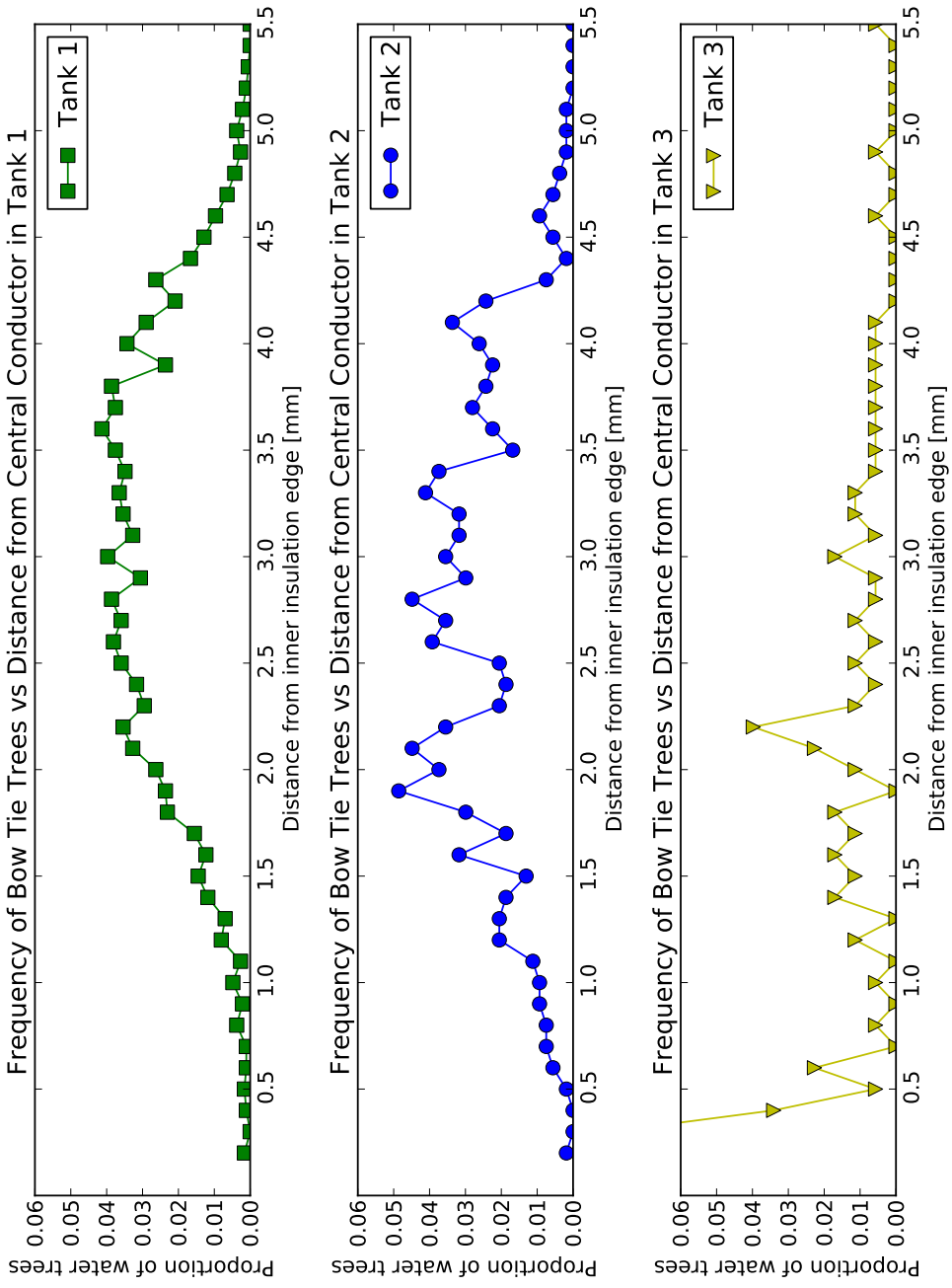

Figure 4.10: Number of bow tie trees at each location in the insulation. From top to bottom: Field aged and treated, field aged untreated, new untreated.

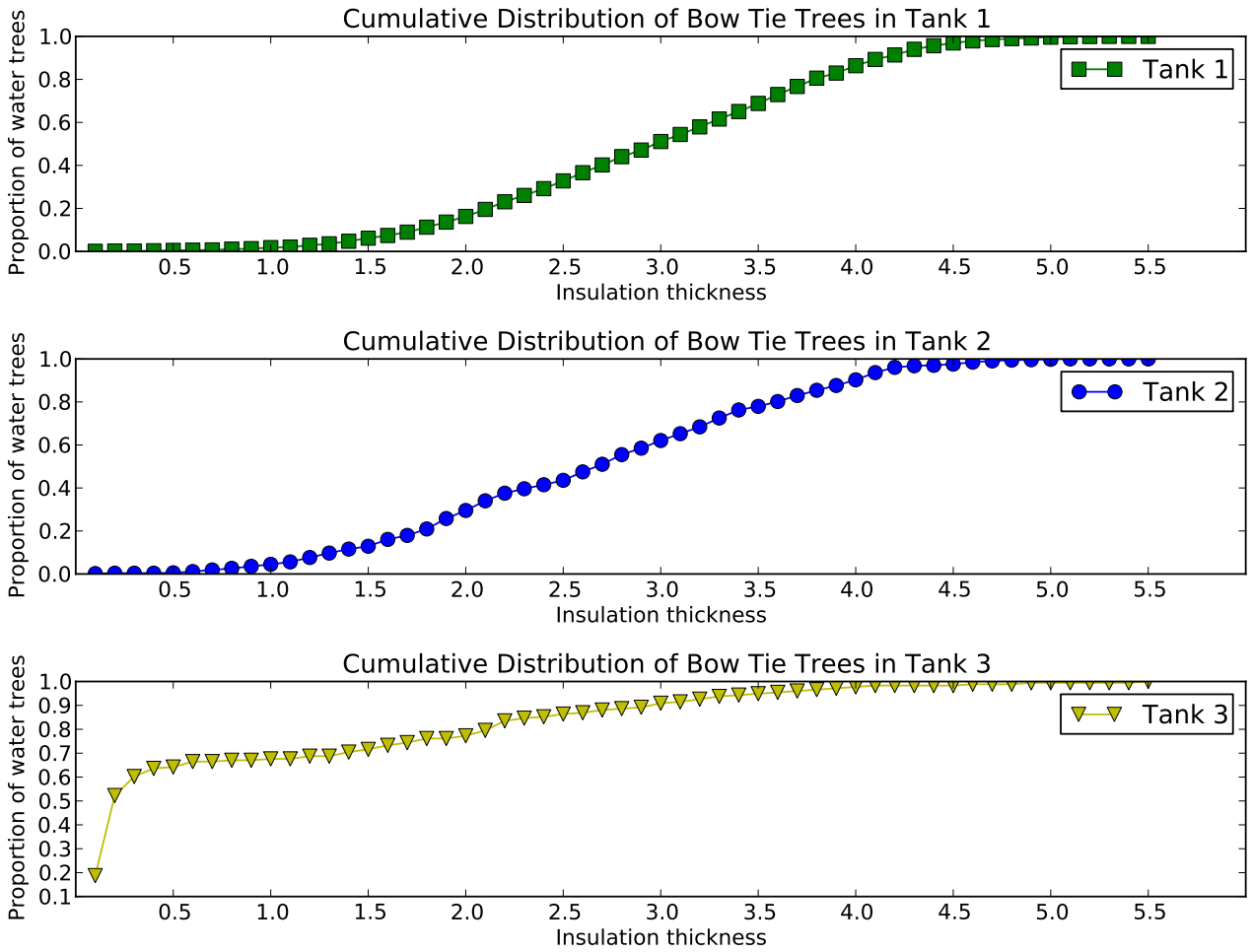

Figure 4.11: Cumulative distribution of bow tie trees from center of insulation. From top to bottom: Field aged and treated, field aged untreated, new untreated.

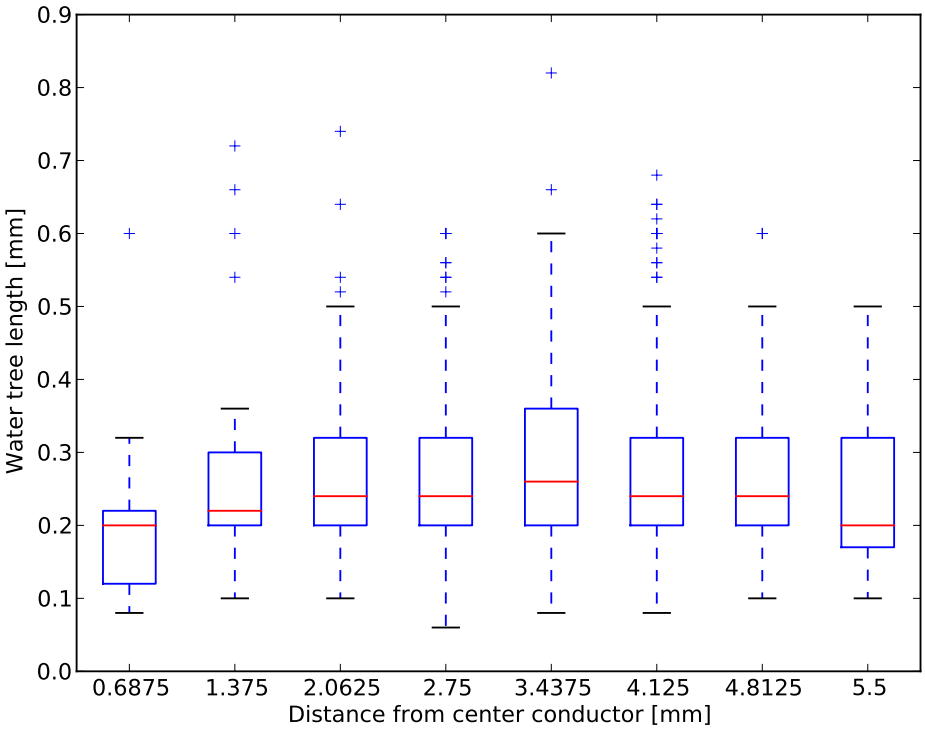

Figure 4.12: Indication of the lengths of bow tie water trees found in each of segment when dividing the insulation into eight concentric rings. Note the trees are somewhat longer in the middle segments.

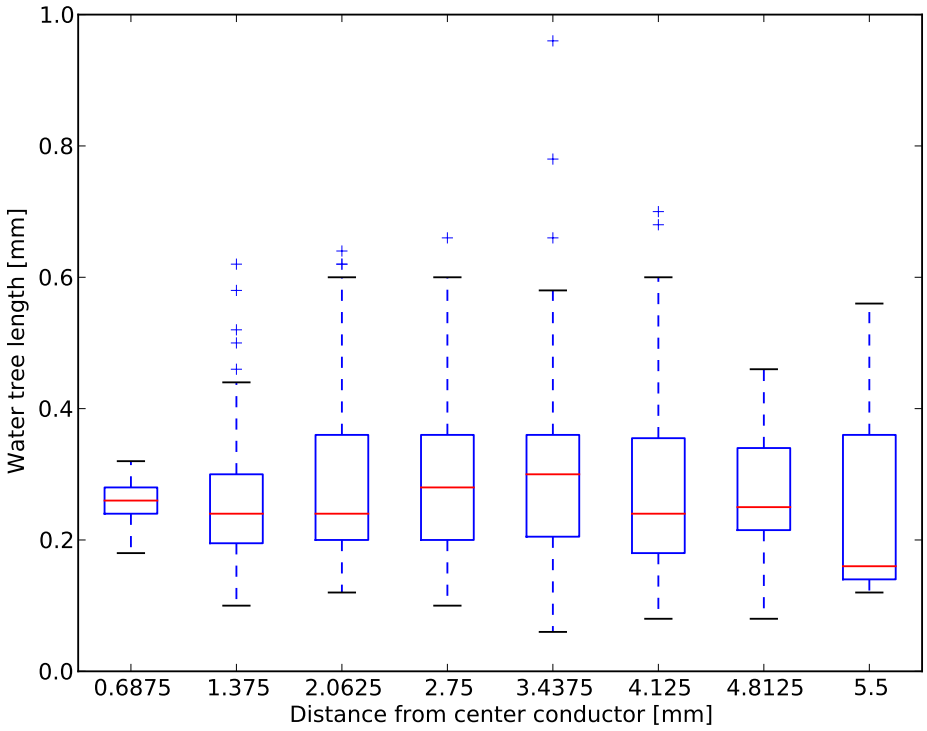

Figure 4.13: Indication of the lengths of bow tie water trees found in each of segment when dividing the insulation into eight concentric rings. Note the trees are somewhat longer in the middle segments.

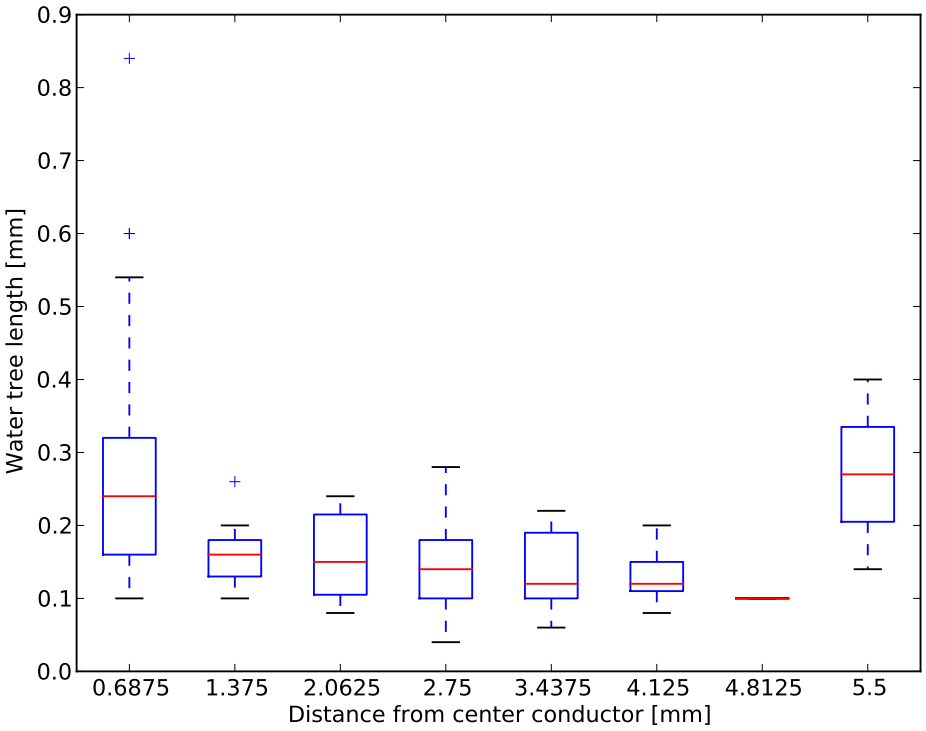

Figure 4.14: Indication of the lengths of bow tie water trees found in each of segment when dividing the insulation into eight concentric rings. In contrast to the preceding two images, note the relatively longer water trees found close to the conductor core in the new untreated samples.

P values for H0:That the two samples have the same mean.

	t1_1	t1_2	t1_4	t1_5	t1_6	t1_7	t1_8	t1_10	t2_7	t2_9	t3_1	t3_2	t3_3	t3_4	t3_5	t3_6	t3_7	t3_8	t3_9	t3_10
t1_1	1.00	0.00	0.00	0.03	0.14	0.16	0.00	0.00	0.00	0.00	0.01	0.02	0.00	0.14	0.02	0.03	0.00	0.00	0.00	0.00
t1_2	0.00	1.00	0.02	0.00	0.00	0.00	0.01	0.16	0.00	0.01	0.00	0.01	0.00	0.02	0.00	0.00	0.00	0.00	0.00	0.00
t1_4	0.00	0.02	1.00	0.02	0.00	0.02	0.58	0.00	0.00	0.01	0.01	0.03	0.00	0.08	0.00	0.01	0.00	0.00	0.00	0.00
t1_5	0.03	0.00	0.02	1.00	0.17	0.07	0.00	0.00	0.00	0.02	0.00	0.04	0.00	0.39	0.01	0.04	0.00	0.00	0.00	0.00
t1_6	0.14	0.00	0.00	0.17	1.00	0.17	0.00	0.00	0.00	0.01	0.01	0.02	0.00	0.07	0.01	0.01	0.00	0.00	0.00	0.00
t1_7	0.16	0.00	0.02	0.07	0.17	1.00	0.00	0.00	0.00	0.00	0.02	0.03	0.00	0.31	0.01	0.07	0.00	0.00	0.00	0.00
t1_8	0.00	0.01	0.58	0.00	0.00	0.00	1.00	0.00	0.00	0.00	0.00	0.01	0.00	0.01	0.00	0.00	0.00	0.00	0.00	0.00
t1_10	0.00	0.16	0.00	0.00	0.00	0.00	0.00	1.00	0.00	0.00	0.00	0.01	0.00	0.00	0.00	0.00	0.00	0.00	0.00	0.00
t2_7	0.00	0.00	0.00	0.00	0.00	0.00	0.00	0.00	1.00	0.00	0.12	0.14	0.01	0.01	0.32	0.44	0.03	0.00	0.00	0.00
t2_9	0.00	0.01	0.01	0.02	0.01	0.00	0.00	0.00	0.00	1.00	0.00	0.01	0.00	0.03	0.00	0.01	0.00	0.00	0.00	0.00
t3_1	0.01	0.00	0.01	0.00	0.01	0.02	0.00	0.00	0.12	0.00	1.00	0.63	0.38	0.02	0.16	0.55	0.13	0.14	0.02	0.61
t3_2	0.02	0.01	0.03	0.04	0.02	0.03	0.01	0.01	0.14	0.01	0.63	1.00	0.94	0.15	0.36	0.32	1.00	0.77	0.71	0.61
t3_3	0.00	0.00	0.00	0.00	0.00	0.00	0.00	0.00	0.01	0.00	0.38	0.94	1.00	0.00	0.20	0.11	0.92	1.00	0.72	0.77
t3_4	0.14	0.02	0.08	0.39	0.07	0.31	0.01	0.00	0.01	0.03	0.02	0.15	0.00	1.00	0.15	0.43	0.00	0.00	0.00	0.00
t3_5	0.02	0.00	0.00	0.01	0.01	0.01	0.00	0.00	0.32	0.00	0.16	0.36	0.20	0.15	1.00	0.99	0.07	0.02	0.00	0.02
t3_6	0.03	0.00	0.01	0.04	0.01	0.07	0.00	0.00	0.44	0.01	0.55	0.32	0.11	0.43	0.99	1.00	0.13	0.01	0.00	0.04
t3_7	0.00	0.00	0.00	0.00	0.00	0.00	0.00	0.00	0.03	0.00	0.13	1.00	0.92	0.00	0.07	0.13	1.00	0.87	0.52	0.72
t3_8	0.00	0.00	0.00	0.00	0.00	0.00	0.00	0.00	0.00	0.00	0.14	0.77	1.00	0.00	0.02	0.01	0.87	1.00	0.93	0.83
t3_9	0.00	0.00	0.00	0.00	0.00	0.00	0.00	0.00	0.00	0.00	0.02	0.71	0.72	0.00	0.00	0.00	0.52	0.93	1.00	0.55
t3_10	0.00	0.00	0.00	0.00	0.00	0.00	0.00	0.00	0.00	0.00	0.61	0.61	0.77	0.00	0.02	0.04	0.72	0.83	0.55	1.00

Grey Level	0.05
Yellow Level	0.13
Green Level	0.67
Black Level	> 0.67

Figure 4.15: The p-values for the hypothesis that the samples are from the same distribution. Note that many of the Tank 1 samples showed them belonging to different populations, while many in Tank 3 showed similar populations. The p-value is the chance of getting this data if the samples being compared have the same mean (note the diagonal '1.0's).

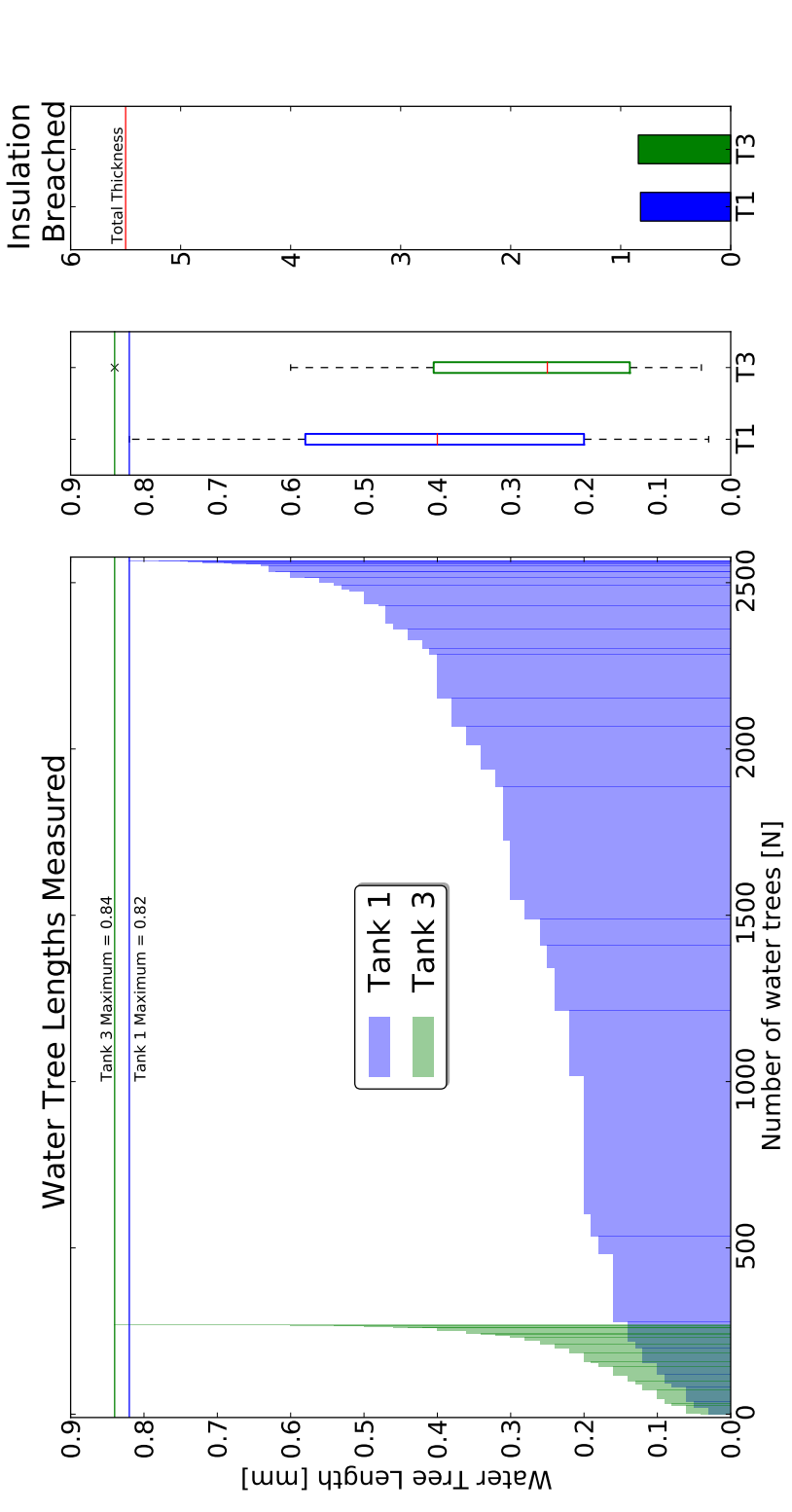

Figure 4.16: The lengths measured in the samples from the ageing test. Note the relatively small proportion of the insulation breached, the relatively similar maximum length and the significant difference in the number of water trees.

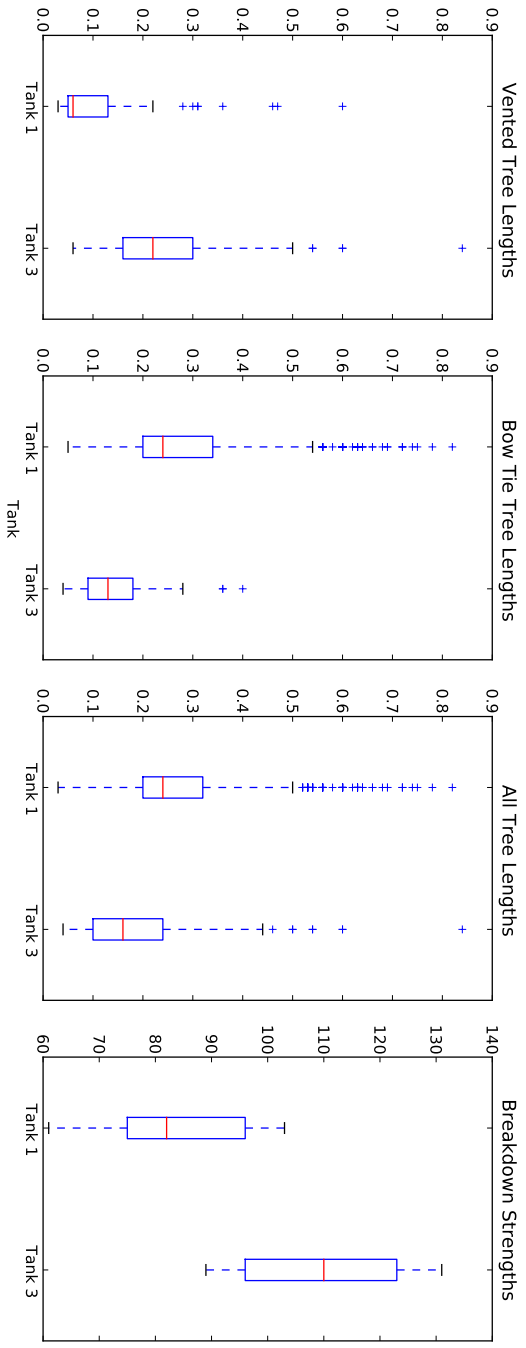

Figure 4.17: Box-plot of water tree lengths compared to AC breakdown strength. Note the reversal of effect between vented and bow tie trees, this is possibly caused by the small number of vented trees measured.

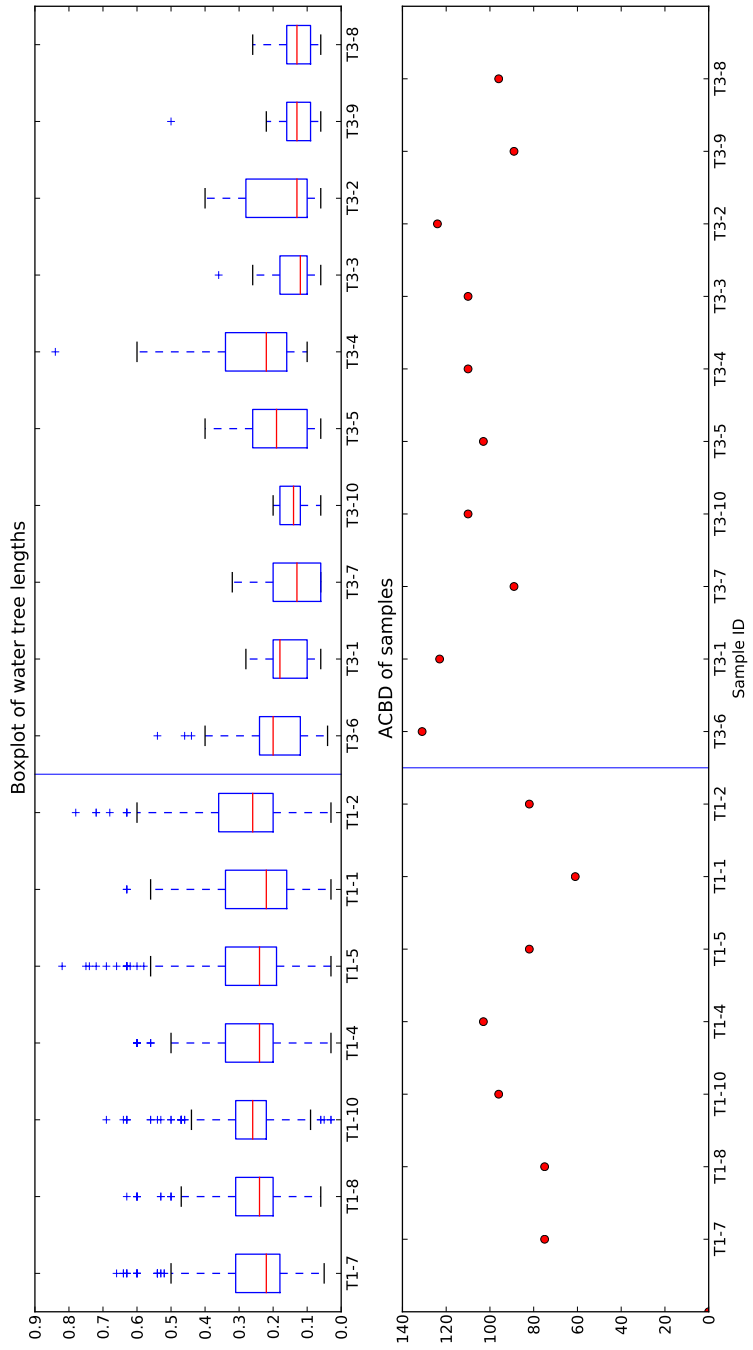

Figure 4.18: Comparison of the water tree length (top) to the AC breakdown strength (bottom) (on identical x axis). Note intra-tank similarities in both water tree length and breakdown strength and inter-tank differences.

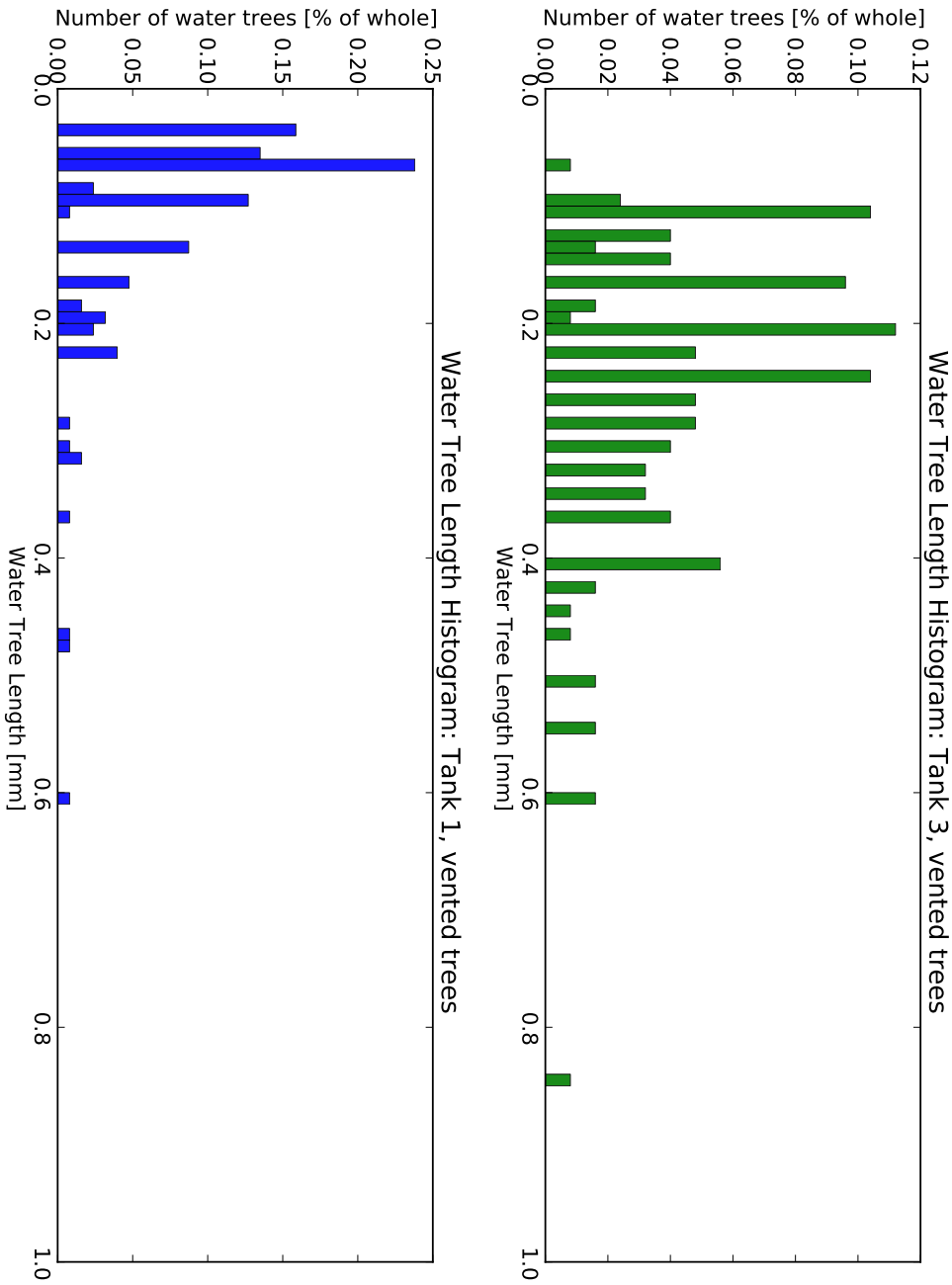

Figure 4.19: Frequency histogram of the vented water trees in each tank.

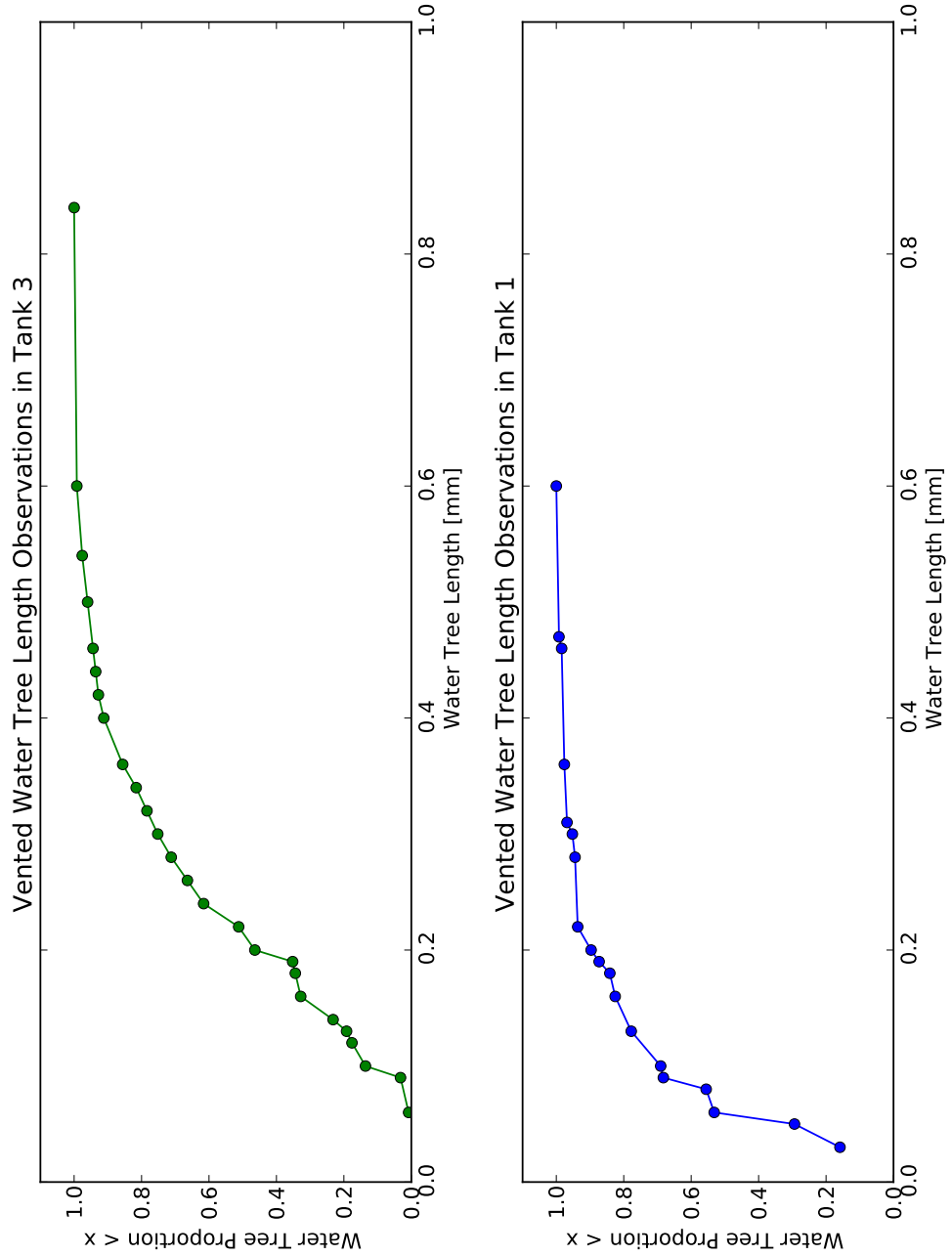

Figure 4.20: Cumulative distribution of vented tree lengths in each tank.

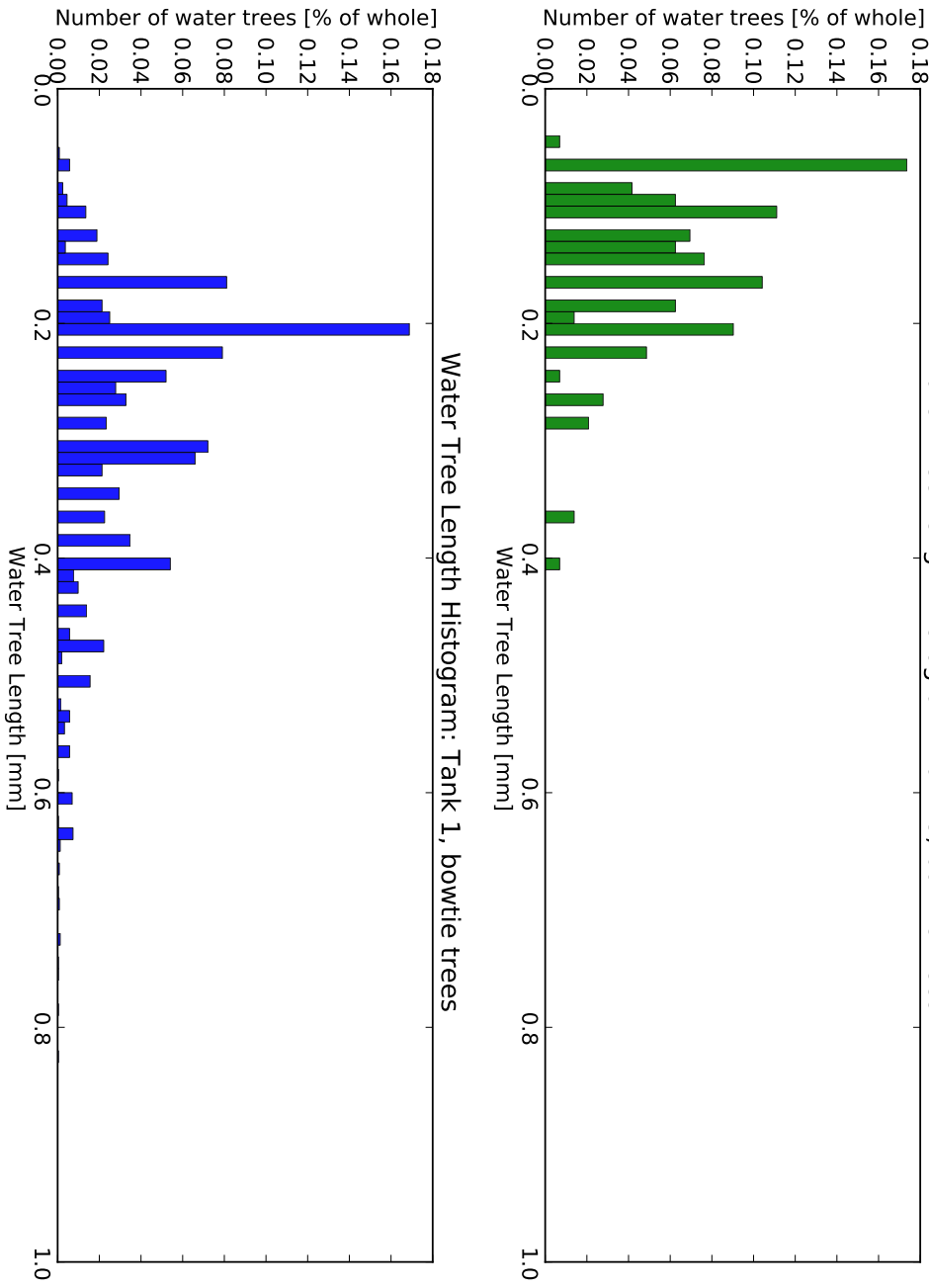

Figure 4.21: Frequency histogram of the bow tie water trees in each tank.

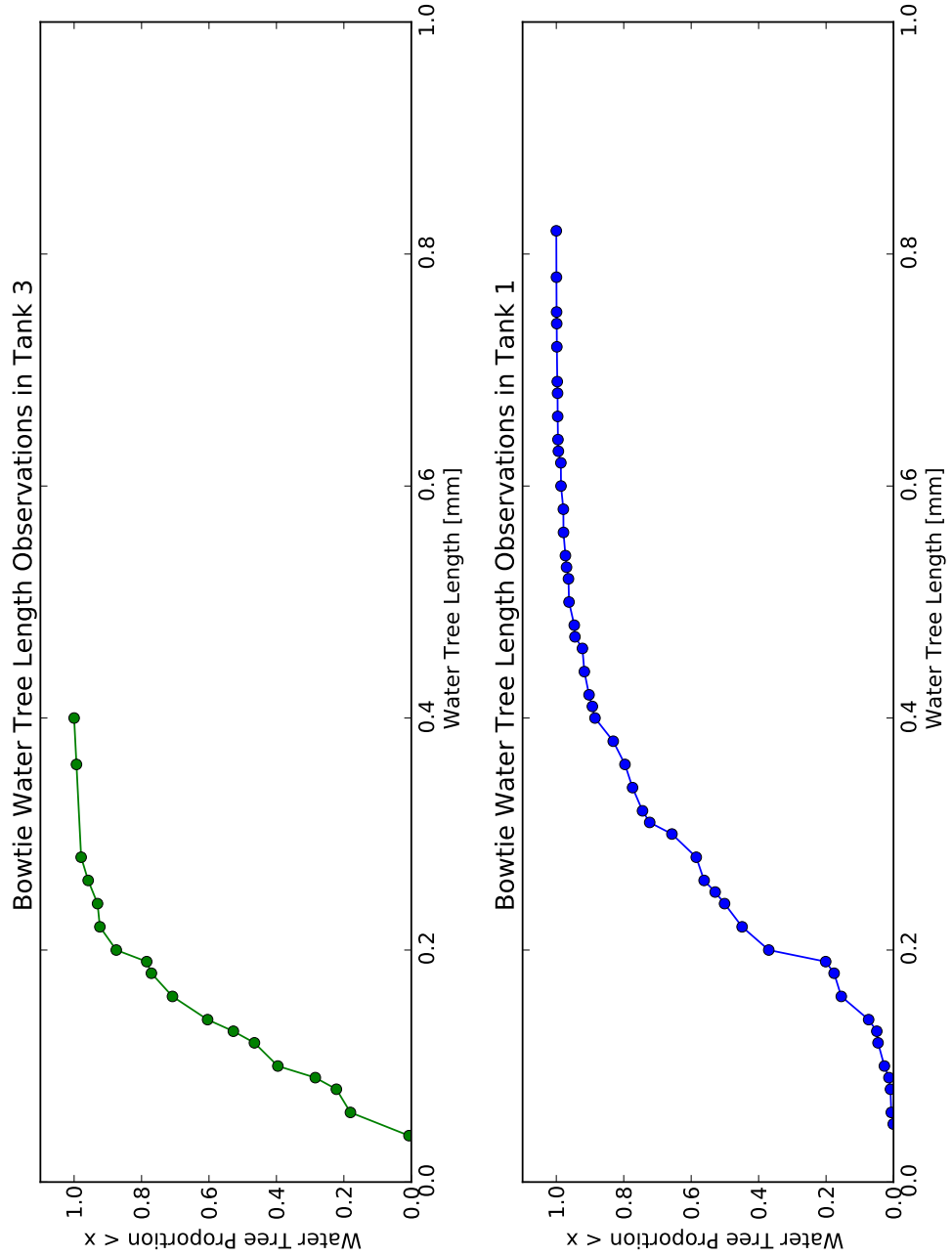

Figure 4.22: Cumulative distribution of bow tie tree lengths in each tank.

Chapter 5

Non-Linear effects of water treed XLPE - A proposed factor for assessing cable age

> Prediction is very difficult, especially if it's about the future.
>
> *Niels Bohr*

5.1 The Effect of Water Treeing on Linearity of Electrical Measurements

This work is primarily concerned with estimating the remaining life of a sample of XLPE by using non-destructive techniques. The means by which the remaining life is estimated is by estimating the length of the longest water tree. This chapter deals with a means of estimating the length of the longest water tree in a sample of XLPE non-destructively.

The method described here is referred to as the *degree of non-linearity* or DONL. The essence of the method is that a change in response of a sample to changing voltage away from the ideal linear response will give an estimate of the longest water tree.

The proposed theory is that changing the voltage will change the internal morphology of a water treed sample, while an untreed sample will not undergo the same change in morphology. The proposed mechanism for this change is the change in dielectrophoretic force on free water.

In an untreed sample, there will be only a single dielectric, and thus the current measured by an appropriate instrument will be linearly related to the applied voltage. In water treed XLPE there are two proposed changes. Firstly, as defined in the very start of this work, water trees represent *permanent* defects, that may or may not be filled with water. Secondly, when taking electrical measurements, there will be an available reservoir of water that may or may not be contained inside the water trees.

When two dissimilar dielectrics are in direct contact, and an electrical field is applied, there is a resulting force on the two dielectrics that may be computed by the theory of dielectrophoresis (see chapter 2, and [86, 85]. Obviously only the 'free' water in the insulation is able to move, and it will be constrained by the internal structure of the insulation.

Over time, ageing stress will cause water filled cracks to gradually appear and grow (water trees). These cracks are permanent deformations of the internal structure (breaking polymer bonds, etc.) and as such will remain even if the ageing stressors are removed. Water, being free to move, will only be found inside the water trees when the forces pushing it out of the insulation (gravity, thermal gradient, plastic deformation/restoration) are balanced by a force pushing it into the water trees.

The proposed force pushing the water into the water trees is dielectrophoresis. The dielectrophoretic force is directly related to the applied voltage (see equation 2.2) [86, 85]. As such, the dynamic balance of forces pushing water into and out of the water trees is related to the applied voltage.

This finally brings us to the theory of the degree of non-linearity. This proposed theory makes use of the changing dynamic force on the water inside water trees to estimate the length of the longest water tree. The means by which a non-linear response is elicited from a sample of XLPE is the change in water tree lengths due to the change in balance of dynamic forces on free water at different electrical field strengths. In short, at low fields, the water trees are relatively shorter than at high fields.

The conductivity of a sample is assumed to be dependant on the length of

the water trees in the sample, by way of shortening the path from one electrode (conducting via the relatively low resistivity water trees) to the other. Thus as the applied voltage rises, the conductivity of water treed XLPE should increase. Analysis of this increase will give an estimate of the condition of the sample. That is, by examining the change in conductivity (a large change in conductivity indicates a large change in water tree length) the state of water treeing in a sample may be deduced.

The degree of non-linearity (DONL) as presented here is computed by calculating the apparent conductivity of the sample, comparing this value at a lower voltage (1kV in this case) with a higher voltage (5kV). The apparent conductivity is computed by analysing the charging and discharging curves of the samples in the time domain.

If a dielectric is modelled as a lossy capacitor, that is a capacitor with a parallel resistance, the charging and discharge measurements can be used to characterise the insulation. In the charging phase, the measured current I_t will be the sum of the capacitive and resistive currents ($I_c + I_r$). In the discharge phase however, the measured current will be entirely due to the discharging of the capacitor, and will result in measuring I_c on its own. Finding the difference between the charging current I_t and the discharge current I_c will give the resistive current I_r. Knowing the applied voltage, current and capacitance of the object, it is then possible to estimate the conductivity of the object under test (equation 5.2).

This analysis is concerned with the change in the resistive component of the sample, as this will be most affected by the change in effective insulation thickness. The conductivity is used to normalise the samples for comparison. The units for conductivity (σ) are Amperes per Volt-Metre ($\frac{A}{Vm}$), and the value is computed by using a co-axial capacitor model of the cable:

$$
\begin{aligned}
I &= \sigma E A \\
A &= 2\pi r L \\
E &= \frac{Q}{\epsilon_m 2\pi r L} \\
&\therefore \\
I &= \sigma \frac{Q}{\epsilon_m 2\pi r L} 2\pi r L \\
I &= \frac{\sigma C V}{\epsilon_m} \\
\sigma &= \frac{\epsilon_m I}{C V}
\end{aligned}
\tag{5.1}
$$

$$
\begin{aligned}
\sigma_{app} &= \frac{\epsilon_m I_r}{C V_{app}} \\
I_r &= I_{charging} - I_{discharging}
\end{aligned}
\tag{5.2}
$$

Where σ_{app} is the apparent conductivity, $I_{charging}$ the charging current ($I_{resistive}$+ $I_{capacitive}$), I_d the discharge current (purely $I_{capacitive}$) and V_{app} the applied voltage. The capacitance of each sample is listed in appendix A. With a value for the material permittivity of XLPE, one may compute the conductivity of the samples directly. However, as this value will not take into account the effects of the semiconducting layer, the samples were compared using their measured capacitance. As the (unknown) material constants will not change, the ratio of the conductivities will remain the same.

In an ideal dielectric, since I_r is directly proportional to V_{app}, the apparent conductivity should not vary with different applied voltages. However, if changing the applied voltage changes the internal morphology of the sample, there will be a deviation of the response from this ideal case. This deviation from the ideal response, causing the current to become non-linear with respect to the applied voltage, is the basis of the theory of the degree of non-linearity.

5.2 Data Collection

The data for all the measurements presented in this chapter was taken from the accelerated ageing test described in chapter 3. The measurements presented here were taken directly before breakdown of the samples by an AC step breakdown test, as it was considered that these measurements would most closely correlate with the forensic data (presented in chapter 4).

Each sample had a time domain DC step test taken at 1kV and 5kV, and the capacitance measured[1]. These measurements were used to compute the conductivity, and thence the degree of non-linearity for each sample. Some samples were removed from the test by early failure - in two cases there were insulation failures due to ageing, and in one case there was a termination failure. In total, there were 17 samples analysed, 7 field aged and treated with restoration fluid before ageing, and 10 samples of new cable.

The charging currents measured, along with the curve fits are detailed in appendix B, the estimates of the apparent conductivity and the variation of this value over time can also be seen there. Of note is the flatness of the plot of I_r after a short time, allowing the fit of a constant resistivity to be made with good confidence.

5.3 Computation of DONL

The conductivity of the sample is assumed to be affected largely by the length of the water trees in the sample due to the nature of water trees being a conductive impurity into the insulation. The lessening of the effective insulation thickness at any point will increase the conductivity of the sample as a whole.

The degree of non-linearity ($DONL$) was computed by dividing the conductivities, as defined by the following equation:

$$DONL = \frac{\sigma_{5kV}}{\sigma_{1kV}} \tag{5.3}$$

Computing the conductivity by subtracting the charging and discharging currents gives a time varying value for the conductivity due to the measure-

[1]The capacitance was measured using a simple LCR meter, giving a version of the DC capacitance. This value is based principally on the geometry of the cable sample (including length, radius, and dielectric material) and is used to compute the conductivity. It does not reflect the complex interplay of the time-varying polarisation measured using the DC step test.

ments containing electrical noise, as well as other physical phenomena not found in the idealised model. The first part of the analysis deals with reducing this time series to a single representative value.

Having chosen a method of representing the time series value, there is a single DONL value for each sample. This value was compared with the water tree length using the estimated longest water tree (see section 4.3) and a box-plot of the water tree lengths. This comparison was used to validate the relationship of the DONL with the length of the longest water tree.

Finally, the DONL value was incorporated into a wider 'ageing landscape' by plotting the DONL for each sample against the conductivity at 1kV. The 1kV conductivity in this case is being used as an estimate of the 'non-water treed' state of the insulation. This ageing landscape is a useful real-world tool that allows all the information gathered to be used to give an idea of the condition of a sample in a real world setting.

The ageing landscape takes into account the effects of joints and terminations in the samples, and gives an indication of the condition of a sample and whether a problem is due to water treeing, or cable accessories.

5.4 Results

When examining the results obtained from this test, it should be kept in mind that the values for the non-linearity computed are rather high when compared to measurements taken on other samples (e.g. [78], which applied the same testing methodology to in-service samples, with a non-linearity of less than 1.2 for samples in good condition). The exact reasons for the large non-linearity measured are not known, but it seems likely that it is the very low conductivity of the samples that may play a part. Another possible factor is that the experimental samples, which have relatively few attached accessories and a controlled environment, may tend to exaggerate the non-linear effects that might otherwise be masked somewhat by leakage currents via other mechanisms.

The simulated non-linearity (chapter 6) was closer in magnitude to the measurements taken from the field (presented in [78]), which suggest that there may in fact be some confounding factor in the experimental samples that is not accounted for. It may be possible that the effect of the terminations (which represent a large fraction of the cable length in these samples, when

compared to installed cable), or temperature effects (experimental measurements are taken at higher temperatures due to the heated water in the tanks) also play a part in enhancing the non-linear response beyond what may be seen practically.

Although the measurements may not give a truly accurate reflection of real-world effects, the trends observed in these samples do follow the trends seen in both the simulations and the real-world measurements. Thus the analysis will give some qualitative indication of the DONL, even if the quantitative effects remain to be discovered.

Figure 5.1 shows the measured charging and discharge current of a sample at 1kV and 5kV, as well as the time-varying DONL ratio. As can be seen from the indicated lines, the ratio quickly approaches a fairly constant value, and there is a relatively small amount of noise. The time varying DONL value for this sample is also represented as a box-plot in figure 5.2

In order to reduce this time-varying function to a representative value, the DONL at each point in time was aggregated into a box-plot to gain an understanding of the spread of the values and the population parameters. The box-plot for each sample is shown in in figure 5.2.

The close clustering of the points in figure 5.2 means that almost any convenient sample can be taken (the DONL at 30s or 60s for example) to represent the DONL of a particular sample. The risk when using simple measures is that random noise may affect the value chosen. Thus for most of the computations presented here, the median of the conductivity was used. In practical terms the choice of value made little difference to the values obtained.

Observing the good fit of the line and the close clustering of the box-plots, for field work the representative value of the DONL may simply be taken as the value at 60 seconds. This value requires no computation, and gives a good representation of the function. In addition, the measurement need only be taken for a relatively short time to obtain this value.

Figure 5.2 shows all the results of these tests. The differences of non-linearity between each sample and each tank are not as clear as the difference between the water tree lengths measured. Firstly, it should be noted that in some cases the degree of non-linearity was less than 1, and in one case (T3-6) the conductivity was negative! This can be explained by the good quality of this sample, as evidenced by its high breakdown strength. When measuring

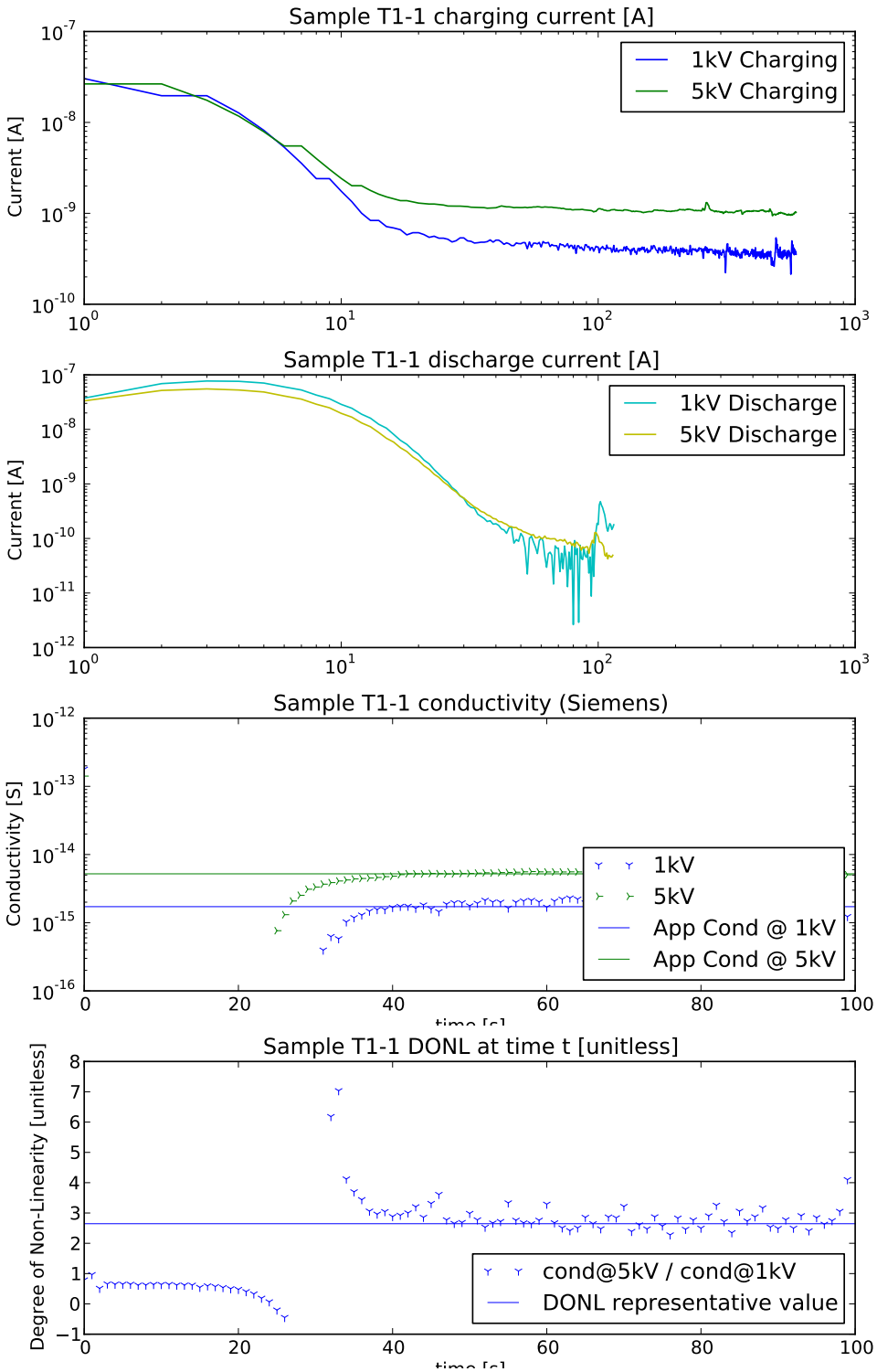

Figure 5.1: Measurements taken on a sample showing the method of computing the degree of non-linearity. From top to bottom, the charging current is measured, the discharge current is measured, the difference between them normalised to the geometric capacitance, and finally the ratio of the conductivity at 5kV to the conductivity at 1kV - the degree of non-linearity.

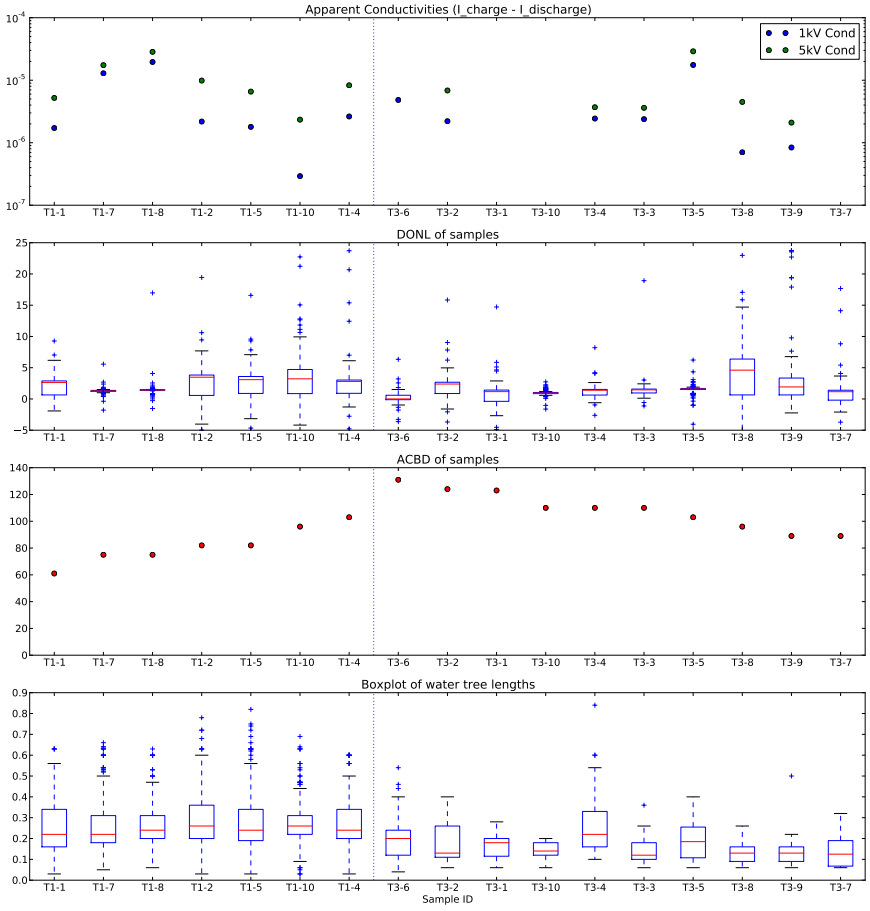

Figure 5.2: The degree of non-linearity for all the samples in the test. From top to bottom: the apparent conductivity, the non-linearity, the breakdown strength of the sample, and finally the water trees measured.

such a low conductivity, the errors in the measurement can overcome the 'true' measurement. Observing the measurements taken on T3-6 (Appendix B.13), one can see that the charging current measurement does not follow the same curve as the other samples, and this may be due to noise or other measurement error overcoming the very small current being measured in this sample.

In other cases, the degree of non-linearity has a wide spread, or a value below unity. This is particularly evident in the 1kV measurements, where the lower currents are more susceptible to ambient noise. Even relatively minor temperature variations in the measurements can affect the absolute value of the conductivity. The degree of non-linearity is used because it is somewhat resistant to such confounding factors, although it is still not a perfect measurement on its own.

Another interesting feature of figure 5.2 is the effect of the conductivity on the non-linearity factor. This is particularly evident in samples T1-7 and T1-8. These samples had significantly lower non-linearity factors than the rest of tank 1, combined with a significantly higher conductivity. This is in the context of a lower breakdown strength and longer water trees found in these samples.

The divergence of the 5kV conductivity from the 1kV conductivity as the sample ages is the means by which the degree of non-linearity assesses the state of the insulation. This value does not tell the whole story however, as the absolute value of the conductivity of the sample is also significant. Besides water treeing, there are other parts to the cable construction that may display a non-linear response, and it is useful to use the absolute conductivity to differentiate some of these phenomena.

The effects of joints and terminations for example, can cause non-linear effects on the measurements due to the changes in field grading and the different paths that may conduct current. In situations where the conductivity is high, the relatively small effect of the change in morphology may easily be swamped by a large conductive current. When taking field measurements, this must be taken into account, as large measured currents give an indication of a poor joint or termination. These must be corrected before an accurate assessment of the water treed state of the insulation may be made.

The second and third graphs in figure 5.2 compare the degree of non-linearity to the breakdown strength, with a tendency to higher non-linearity values in in tank 1 corresponding to a lower AC breakdown strength. Com-

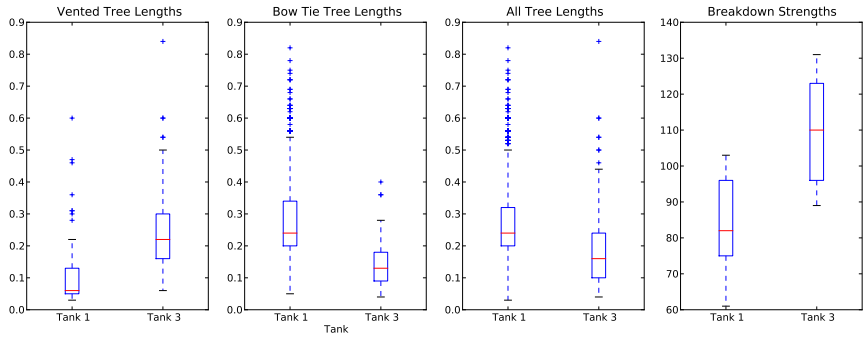

Figure 5.3: Box-plot of the lengths of the water trees measured in the tanks, indicating the slightly longer water trees found in tank 1, and the lower breakdown strength in tank 1.

paring further, the bottom graph in figure 5.3 indicates the length of the water trees (the total population of all water trees) found in tank 1 was also longer.

Further to the above comment relating the conductivity along with the non-linearity, the results of this test were plotted on an 'ageing landscape' (figure 5.4). Plotting the conductivity of the sample on the y axis and the degree of non-linearity on the x axis, the 'ageing' state of the sample may be examined.

In the top right of the ageing landscape, the sample has high degree of non-linearity and high conductivity - this may be due to water treeing, but also may be due to external factors (joint or termination). Samples in this region would warrant further investigation into the quality of the joints and terminations. Notice that none of the samples in this test fell in this area, suggesting the terminations on these samples were still in good shape at breakdown (further supported by their withstanding several times their rated voltage!).

The bottom right, low conductivity and high non-linearity, is suggestive of significant water treeing. While water trees will increase the conductivity, they will increase the non-linearity earlier and to a greater degree. Note the samples extending into this area tended towards lower breakdown strengths (see table 4.1 for details of breakdown strength).

The bottom left region has low degree of non-linearity and low conductivity, this suggests cable in good or new condition. Many of the samples in this test fell in this region, where their similar state and generally good condition make them difficult to differentiate.

Finally the top left area, with low degree of non-linearity and high conductivity, indicates a sample that may have an overwhelming joint or termination

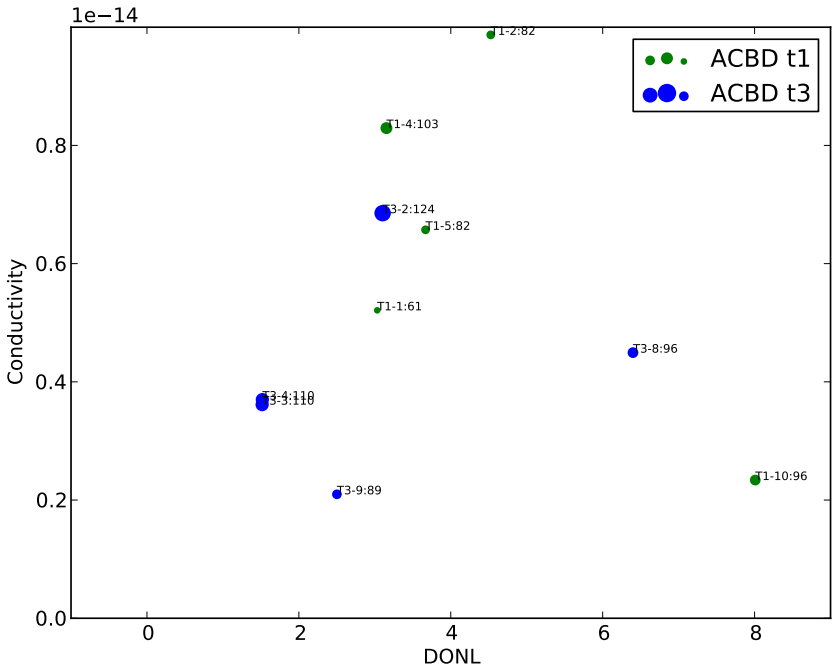

Figure 5.4: The 'ageing landscape' of conductivity vs. DONL. The size of the points indicate the ACBD value - larger points a higher breakdown strength. See appendix A for a larger version of the linear plot.

problem, or other factor affecting the measurement. In this test, a few samples overheated, and this may have caused a structural deformity that affected the electrical measurements (although no changes were visible on inspection, and it was thought the damaged sections were removed when the terminations were replaced). When taking field measurements, samples that respond in this manner will require further measurements to analyse for the presence of water treeing.

In order to remove some of the confounding factors of electrical measurements, a computer simulation was created to further investigate the effects of water treeing on the linearity of the measurements. This model is presented in chapter 6. The goal of this model was to investigate the possibility of dielectrophoresis being responsible for the non-linear effect observed in the samples. The non-linear effect was intended to be simulated by changing the length of water trees in the samples, to see if the effects seen in the real samples could be modelled by changing water tree lengths.

Chapter 6

Modelling of Water Trees in XLPE Cable - Review, Procedure and Comparison of Simulation to Measurements

> To those who ask what the infinitely small quantity in mathematics is, we answer that it is actually zero. Hence there are not so many mysteries hidden in this concept as they are usually believed to be.
>
> *Leonhard Euler*

6.1 Background

When constructing an ageing facility for XLPE samples, it is very difficult (if not impossible) to control for all the variables affecting the ageing process and the measurements taken on the samples. These confounding factors can significantly affect the results of the test, even when they are not known [99]. The value of a testing facility lies in the ability to reproduce real-world conditions,

and study the effects of interventions on real samples under real conditions. In contrast, when attempting to analyse the mechanism of operation of a theory, the many unknown factors make drawing conclusions from real world tests difficult.

One valuable aspect of computer modelling is that it allows the scientist to perform tests on idealised samples to examine the mechanism of a theory under development. In effect, it allows a researcher to isolate a single variable or process and observe how changes in this variable affect the sample as a whole.

Presented in this work is the concept of the degree of non-linearity being related to the phenomenon of dielectrophoresis, and one means by which this theory is presented is the construction of a three dimensional model that allows experiments and calculations of the electric field under time-varying conditions to be performed. By creating a computer model, the effect of polymer morphology on the electric field may be isolated from the many confounding processes that occur in a real world test.

When designing this experiment, it was found that the skills and techniques used in constructing and maintaining a large scale high voltage high power experimental facility did not significantly overlap with the skills required to construct a detailed and nuanced electrical simulation of a complex system.

It was found that the available tools for modelling systems in the engineering field tended to be focused on electromagnetic field simulations with emphasis on the magnetic field or dispersion of high frequency electromagnetic waves. In contrast, what was required for this project is a relatively simple electrostatic model with the ability to extend the model into the time domain.

Rather than spending considerable time and effort examining, testing and modifying existing commercial electromagnetic field simulation software for this purpose, it was decided to make use of a tool that had been developed at QUT for teaching the theory of electromagnetic field theory to undergraduate students. This tool was used to develop a model of the system without requiring the complex mathematical methods employed in most commercially available software.

Development using this tool allowed construction of a model that was customised to the nature of this particular project without many of the extra features that would needlessly complexify analysis of the phenomena under study.

This tool is based on a novel method referred to as *flux modelling* [64] which focuses on a visual/practical method of understanding electrical field properties in order to make conceptualisation of the underlying theory easier - this is the basis of its use as a teaching tool. By basing the model on the theories related to electrical (and magnetic) flux, this method allows the model to sidestep most of the complex high-order mathematics typical of most simulation packages.

6.2 Review of Methods of Modelling Electrical Fields

6.3 Flux Modelling

6.3.1 Basic Method

The aim of this model is to investigate the relationship between a morphological change in water trees and the charge arising from time domain measurements. If a relationship between the measured charge in a sample and the morphology of the water trees in the sample can be established, then it may be possible to analyse multi-voltage degree of non-linearity measurements to establish the likely length of the longest water tree.

The simulation was devised as a means of isolating the effects of changing the internal morphology of the insulation from confounding effects associated with increasing the voltage applied to a sample of aged XLPE. As no commercially available software was found to fit the purpose, the model was based on a teaching tool developed at QUT for teaching field theory to electrical engineering students.

Rather than defining points or cells by partial differential or integral equations, this method uses the theory and properties of electrical flux. The model is divided into small volumes (cells), with each cell assumed to contain uniform flux[1]. In a region where the flux can be assumed to be uniform, the following relationships are defined:

[1] *Uniform* flux has a constant magnitude and direction - the flux density vector of a region having uniform flux is identical in any point in the region.

$$I_n = (V_0 - V_n)\frac{\gamma_m A_n}{d_n}$$
$$\Psi_n = (V_0 - V_n)\frac{\epsilon_m A_n}{d_n} \tag{6.1}$$

Where I_n is the current flowing through the nth boundary of a cell, V_0 is the potential at the centroid of cell, while V_n is the potential of the centroid of the nth neighbour, γ_m is the conductivity of the material within the cell, ϵ_m is the electrical permittivity of the material (in this model, each cell can contain only a single homogeneous material), A_n is the area of the nth boundary of the cell, d_n is the (small) distance between V_0 and V_n and Ψ_n is the electrical flux flowing over the nth border.

By dividing a given structure into a set of cells and assuming the flux is uniform inside each cell, the potential at each point may be computed by solving the set of linear homogeneous equations generated by equations 6.1, rather than the set of differential equations often encountered in electrical field modelling. By combining many simple cells, each with known properties, the 'emergent' behaviour of a complex system may be observed.

The method is interesting because of its flexibility and simplicity. The properties of flux lines and equipotential surfaces are easily visualised, and the complexities of dielectric relaxation of a complex structure may be modelled using a simple and well defined set of processes. By focusing on the requirements of the model instead of the detailed underlying mathematics, a model has been developed that allows analysis of the proposed theory to compare with the results obtained from the electrical measurements.

The model is created in three steps (figure 6.1). Firstly, an array of a size constrained by available computing power is created. Secondly, the environment is sampled at each point in the array. Finally, the relationship between each cell is defined by the material properties and the initial conditions.

The first step, creating the array, has the largest impact on the detail of the simulation. In this work, a cube or rectangular prism was simulated. The simulation 'environment' was bounded by the boundaries of the prism, and sampled homogeneously at each point of the array. The number of points in the array, combined with the size of the environment being simulated, gives the spacing between each point, and thus the smallest detail that can be accurately

simulated.

As an example, one model made use of an array sized $50 \times 50 \times 50$ (figures 6.1 and 6.2). This was used to simulate a cube of a quarter of a sample of XLPE cable. A sample of XLPE occupies approximately 14mm from centre conductor to surrounding earth screen. Thus the spacing in this model is .28mm between each point. This is 280μm, which is somewhat too large for simulating individual water trees, but it gives an initial outline of the gross field inside a sample of XLPE. This method of using a low resolution model is similar to that used in [5] in simulating water treed XLPE segments.

Once the sampling dimensions have been established, the next step is assigning each point in the array a type of material. The model is designed that each cell can contain only a single pure type of material, for which the time domain properties should be well known by some function.

In the case of the model shown in Figure 6.1 (parts 3 and 4), XLPE is material type 1 (cyan and black in parts 3 and 4 respectively), 'conductor' is defined by material type 2 (black, then red), and water by material type 3 (red, white). There is no limit to the number of types of materials, and their properties as long as they can be defined by the resistivity and electrical permittivity.

The issue of material properties was the most problematic in the construction of the model. The properties of some materials are easy to define (e.g. resistivity of copper and aluminium), while the properties of other materials were not able to be located in the literature. Most notably, there was no time-domain function for charging or discharging of XLPE available in the literature surveyed.

In this work, water was modelled as a pure resistor, although it was given a nominal permittivity for reference purposes. Since the conductivity of water is very high compared to XLPE, the resulting field grading would be small (the electrical field $\vec{E}$ is close enough to zero). Thus it was considered that approximating it as a conductive material with an internal field of zero would not degrade the quality of the simulation significantly. This approximation is also used in other works (e.g. [25]).

Defining the properties of pure XLPE was somewhat more problematic. If this issue had been foreseen by the authors, detailed and accurate time domain measurements of pure samples of XLPE may have been performed. However, time and budgetary constraints prevented this, and instead the gross measure-

Figure 6.1: The stages of creating a model for simulation (showing slice number 11 of 50). From left to right, defining the region of interest (boundaries in white, 'free' cells in black), defining the initial potential (white: 10kV, black 0V), defining the resistivity (third image, note the low resistivity of the boundary conductors in black, the higher resistivity of the water trees, and the highest resistivity of XLPE) and permittivity (far right, the conductors are nominally assigned zero permittivity, with the higher permittivity of water being visible on the lower permittivity XLPE, coloured white and black respectively). By observing the 'mask' created by the free cells (first image), one can see that the conducting boundaries are not simulated - these regions are fixed at either V_{app} or $0V$/GND.

Figure 6.2: The result of the simulation on the model presented in figure 6.1. The left image shows the potential at each point, coloured by magnitude. The right image shows the magnitude of the electric field at each point - this is better for visualising the effects of water trees on the electric field. Note the very short distance which is affected by the presence of a water tree, the local field distortion is quickly graded by the surrounding insulation. In order to make the boundaries of the water tree more visible, this method of calculating the field also highlights the slight distortion created by the boundary as a small 'step' near the boundaries of the simulation. The low resolution of this model results in a more marked step, resulting in a spurious 'high field' at the low voltage conductor boundary.

ments of the samples were used to model pure XLPE. This is not an ideal situation, as the measurements taken will include the effects of semiconductors, joints and terminations, but the lack of readily available information made this approximation necessary.

The model has the flexibility in this area for future measurement data to be 'plugged in' to the simulation being performed. Without modification of the software (only the simulation being created) a set of more detailed measurements can be added easily.

Finally, the relationship between each cell and its neighbours is defined by the material properties and the initial conditions of the model. The basis of the model, the flux balance method, allows each cell to be modelled by an ideal capacitor parallel to an ideal resistor (figure 6.7). Typically the network was initialised with the capacitor discharged, however any charge state could be initialised (if, for example one wished to analyse the decay process of a 'space charged' sample of XLPE).

As all the materials being simulated have a linear voltage response over the ranges being considered, the applied voltage can be simplified to a unit value, with the resulting response multiplied by the desired applied voltage post-simulation. Thus, the effect of increasing voltage will be entirely linear.

Conceptually, the basis of the theory is the concept of the 'flux tube'. A flux tube is a volume inside an electrical field containing equipotential surfaces at each end (see figure 6.3). Flux lines entering (and exiting) a flux tube can do so only at an end, and only at right angles. Flux lines cannot cross the surface of the flux tube, because the tube is oriented to be tangential to the flux density vector. By calculating the density of flux within each flux tube, the potential at each end-plate may be solved. The end-plates correspond to the nodes of the simulation, thus computing the potential of each end-plate computes the potential at each point in the simulation.

With equipotential ends, and no flux lines crossing the surface, the total flux within a flux tube must be constant. Thus, if the flux tube has a constant cross sectional area, the flux density within the tube must remain constant. With a constant flux density and equipotential boundaries, the electric field within a flux tube must be uniform. The only caveat to this reasoning is that the flux tube can contain only a single type of material (if it contains different materials, the flux density will still be constant, but the field may change at the

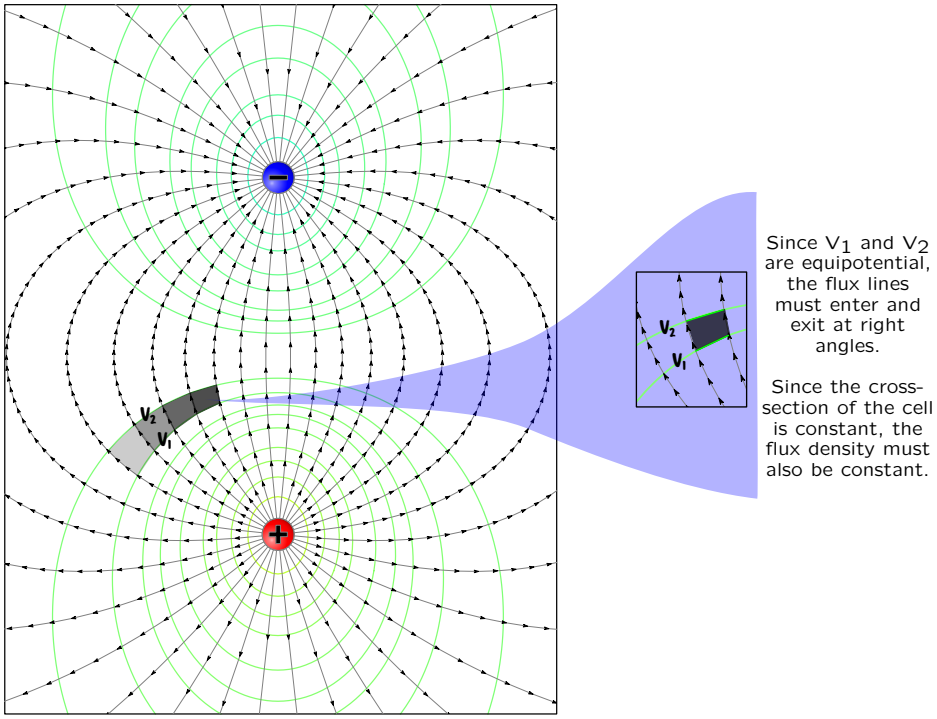

Figure 6.3: The approximation of an electric field by the flux tube. The green lines represent equipotential surfaces, therefore the flux lines must cross at right angles. By keeping the cross sectional area of the cells constant, the flux density in each cell must be uniform. This results in a cell geometry dependant on prior knowledge of the equipotential surfaces.

interface of the materials).

By constraining each cell to have a single common boundary with each neighbour (each boundary surface must join exactly two cells), and contain only a single type of material, the flux tubes connecting neighbouring cells become relatively simple to analyse according to equation 6.1. Since ϵ_m, A_n, and d_n are all known, and $\Delta\vec{E}$ may be approximated by $\frac{V_0 - V_n}{d_n}$, V_0 and V_n become part of a large set of linear homogeneous equations that can be solved by applying boundary conditions.

In more formal terms, the theory is based on three equations:

$$\Psi \equiv Q \tag{6.2}$$

$$\oint \vec{D} \cdot d\vec{S} = Q_{enc} \tag{6.3}$$

$$\vec{E} = -\nabla V = \frac{\vec{D}}{\epsilon_m} \tag{6.4}$$

With equation 6.4 being approximated by:

$$\vec{E} = \frac{\Delta V}{d_n} \tag{6.5}$$

Where Ψ is the electrical flux, Q_{enc} the charge, $\vec{D}$ the flux density vector, V the potential at a point, d_n the (small) distance separating two points within an electrical field, ϵ_m is the electrical permittivity of the material, and $\vec{E}$ is the electrical field vector.

In most cells, the enclosed charge Q_{enc} is zero. Furthermore, if the cells are cuboidal (as they are in this model), and the flux across the boundary is uniform (as it is assumed to be, given a small enough cell), the surface integral may be reduced to the sum of the area of the sides multiplied by the average flux on each side. That is, $\oint \vec{D} \cdot dS$ becomes $\sum_{n=1}^{6}[\vec{D}_n A_n]$. Thus combining equations 6.3, 6.4, and 6.5

$$\begin{aligned}
&\oint \vec{D} \cdot d\vec{S} = 0 \\
&\sum_{n=1}^{6}[\vec{D}_n A_n] = 0 \\
&\sum_{n=1}^{6}[\epsilon_m \vec{E}_n A] = 0 \\
&\sum_{n=1}^{6}[\epsilon_m \frac{\Delta V}{d_n} A_n] = 0 \\
&\sum_{n=1}^{6}[\epsilon_m \frac{V_0 - V_n}{d_n} A_n] = 0 \\
&\frac{\epsilon_m A}{d} \sum_{n=1}^{6}[V_0 - V_n] = 0
\end{aligned} \tag{6.6}$$

Where ϵ_m is the electrical permittivity of the material in the cell under scrutiny, A_n is the area of a side of the cell, d_n the distance from the centroid of this cell to its neighbour, n being the nth neighbour, V_0 the potential at the centroid of this cell, and V_n the potential of the centroid of the nth neighbour.

The area A_n of each boundary is the same in this example, and can be replaced by the constant A, similarly with the distance between each centroid d_n being replaced by d.

The above treatment applies to the most common cells - those surrounded by similar material (XLPE in this case). For the cells with an interface (e.g. water/XLPE or electrode/XLPE), the equation is modified slightly: the distance d_n is adjusted to reflect the fact that conductive cells have an equipotential interior, and therefore the centroid is the same voltage as the boundary.

Thus a set of linear homogeneous equations is created, with the boundaries defined by the model (either an electrode with fixed voltage, an 'infinite' boundary with zero potential, or a line of symmetry). This allows the computation of the potential at any point in the field, under the assumption that the dielectric may be modelled by an ideal (lossless) capacitor.

This is analogous to a network of ideal capacitors connecting the centroid of each cell to its neighbours, with the properties of the capacitor defined by the properties of the material and the geometry of the cells.

The question arises, if the model is based on assuming a uniform flux between equipotential surfaces, how can the computation be performed prior to calculating the location of the equipotential surfaces? As the potential distribution of the simulation must be known in order to calculate the location of the equipotential surfaces, this is not an efficient solution to the problem.

The answer lies in a closer inspection of equation 6.4. While the approximation in equation 6.5 certainly applies in the region between equipotential surfaces, this is not a necessary condition. Rather, what is necessary is that $\vec{E} = -\nabla V$ be approximated by a constant value. This implies a constant potential difference between the surfaces of the cell, rather than the surfaces being constrained to be equipotential. Thus the approximation is valid for cells of any orientation, as long as the cell size is small relative to the gradient of the field (figure 6.4).

One benefit for work in modelling any system is the great strides in computational power recently available to researchers (and indeed, independent experimenters). The last decade has seen great increases in the speed of processors available. However, the *most* recent developments have been focused on creating computers that are ever more parallel in their operation. In this manner, the model has been developed to take advantage of many parallel pro-

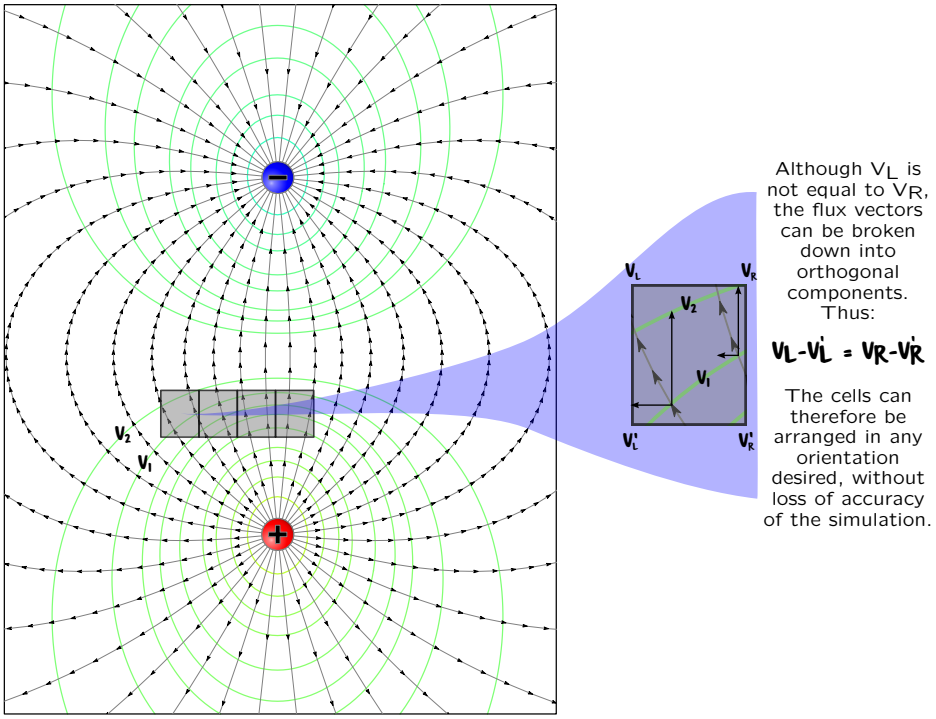

Figure 6.4: Since the equipotential field lines are unknown when dividing the environment into cells, the method must function with any cell orientation. The method correctly computes a result if the *difference* between the cell boundaries may be approximated by a constant value.

cessors, and allow the simulation time to scale well with increasing numbers of processors.

In order to achieve this goal, the model was designed to enable each time-slice to be computed separately from the rest. This technique may seem counter-intuitive when the goal is to analyse the effects of the polarising insulation over time, but this model examines the effects of *interacting* cells where each cell's time domain response is pre-decided. The idea is that the many interacting cells may display some signature behaviour that can be related to real-world test results.

The means by which the parallelisation was achieved is described later in this chapter. In brief, the essence of the method is mapping the time-domain effects of polarisation to a material change that can be computed in advance of the simulation. The result is that each time-step consists of only parallel ideal resistors and capacitors, and therefore require no information on either the preceding or proceeding charge state. As such, each time-step can then be calculated independently of the others, and the system can be computed in

parallel.

The degree to which the computed result follows the actual field is dependant somewhat on the geometry of the problem and the geometry of the cells. Generally speaking, with a fine grained mesh, the solution can be made quite close to the analytical solution. The more rapidly the surfaces change, the smaller the cells must be to maintain accuracy. The effect of resolution is particularly important in water tree modelling, as the structures under scrutiny are very small relative to the bulk insulation.

The work presented here has a relatively abstracted shape of a water tree, limited by available computing power. The nature of the model allows it to take benefit from the modern shift of computing technology to favour many parallel processes. As more computing power becomes available, the model may be extended without modification into higher resolutions, even with the possibility of fractal modelling of individual water trees in the future.

The simulation of a 'new' sample of cable was modelled by a coaxial conductor. Since this is a simple geometry for which the closed form solution is known, this was used as a basis for validating the model. With the addition of water trees to the model, there was an expected deviation from the ideal coaxial capacitive model, and this was analysed for insight into the effect of water treeing on XLPE measurements. The effects of changing morphology on the simulated current are presented in following sections.

6.3.2 Modifications for Lossy Dielectrics

In order to model the time varying properties of a solid dielectric, the change in the material under an electric field must be taken into account. This is in contrast to an 'ideal' capacitor, which may be visualised as a set of parallel conducting plates in free space. In a solid dielectric, the dipoles of the material are somewhat constrained, and so move slowly. As such, the effective capacitance of a block of dielectric will depend not only on its dimensions, but also on the effects of previous applied fields.

Using idealised capacitors will calculate the so-called 'free space' distribution of the modelled structure, but in a purely capacitive system, there is no time-based component of the potential distribution (consider the equation for the potential across a capacitor in an RC circuit: $v(t) = V_0(1-e^{\frac{-t}{RC}})$, with $R = 0$, this reduces to $v(t) = V_0$). Solid dielectrics have a time domain response based

on the changing polarisation field of the dielectric when a driving field remains applied. Thus, it is desirable to compute the time-domain response of the sample, and this requires some time-varying component of the model in order to produce a time-varying distribution that will result in a current flowing across the conductor boundary.

The effect of polarisation on a dielectric may be analysed by considering the initial and final field distribution when a potential is applied to a sample. Initially, (after a few nanoseconds) the internal field may be modelled by the free space permittivity, which is created nearly instantaneously on application of a potential difference to the conductor boundaries. This state may be modelled by a capacitance determined by the free space permittivity ϵ_0.

Over time, the domains become more 'polarised', that is, they line up to oppose the driving field. The internal field, called the polarisation field ($\vec{P}$), opposes the driving field, and lowers the flux gradient inside a dielectric. Examination of 6.4 shows that a change in field magnitude may be modelled as a change in material permittivity. After a long time, the permittivity may be a different value ϵ_m. The flux density inside the dielectric is the sum of the free space field and the opposing polarisation field.

More formally, the flux density $\vec{D}$ inside a dielectric is given by the equation

$$\vec{D} = \epsilon_0 \vec{E} + \vec{P} \tag{6.7}$$

where $\vec{P}$ is the polarisation of the dielectric, $\vec{E}$ the applied electric field, and ϵ_0 is the permittivity of free space.

Considering the polarisation to be linear with respect to $\vec{E}$, the polarisation field varies by material according to the electrical susceptibility χ_m, which is normalised against ϵ_0:

$$\begin{aligned} \vec{P} &= \epsilon_0 \chi_m \vec{E} \\ \vec{D} &= \epsilon_0 \vec{E} + \epsilon_0 \chi_m \vec{E} \\ \vec{D} &= \epsilon_0 \vec{E}(1 + \chi_m) \\ &let \\ \epsilon_m &= \epsilon_0(1 + \chi_m) \\ \vec{D} &= \epsilon_m \vec{E} \end{aligned} \tag{6.8}$$

This can be modelled as a single capacitor, with permittivity of the dielectric being (ϵ_m), and the boundaries being defined by the geometry of the volume. This is the traditional form of the ideal capacitor with a dielectric between the plates.

The modification to this equation for the purpose of this model is to replace the material constant ϵ_m with a time-varying function $\epsilon_m(t)$. In this manner, the time-dependant polarisation can be simulated by a time series of ideal capacitors, with the capacitance changing in time according to a pre-computed time response ($f(t)$, discussed further below). The polarisation function is taken by analysing the time-domain response of the samples from the test. In this way, it is both theoretical and measured. This method was intended to give a closer response of the model to the measurements taken from samples.

In order to realise the simulation, the dielectric function must be computed. This may be calculated by taking measurements of the time-domain response of a samples of XLPE, and using the definition of the dielectric function:

$$f(t) = \frac{d}{dt}[\chi_m] \tag{6.9}$$

Applying a constant voltage to a sample of ideal dielectric will yield a current ($I(t)$) per unit area (displacement current):

$$\begin{aligned} I(t) &= \frac{d}{dt}[\vec{D}] \\ \vec{D} &= \epsilon_0\vec{E} + \epsilon_0\chi_m\vec{E} \end{aligned} \tag{6.10}$$

Assume $\vec{E}$ is constant - as is the case in linear isotropic material under constant applied voltage.

$$\begin{aligned} I(t) &= \frac{d}{dt}[\epsilon_0\vec{E} + \epsilon_0\chi_m\vec{E}] \\ &= \frac{d}{dt}[\epsilon_0\vec{E}] + \frac{d}{dt}[\epsilon_0\chi_m\vec{E}] \\ &= \epsilon_0|\vec{E}|\delta(0) + \epsilon_0\vec{E}\frac{d}{dt}[\chi_m] \end{aligned} \tag{6.11}$$

For the purposes of this experiment, the delta function at time zero can be

neglected:

$$\begin{aligned} \frac{d}{dt}[\chi_m] &= \frac{I(t)}{\epsilon_0 \vec{E}} \\ f(t) &= \frac{I(t)}{\epsilon_0 \vec{E}} \\ I_{measured}(t) &= \oint I(t) d\vec{S} \\ \text{Using: } C_0 &= \frac{\epsilon A}{d} \\ f(t) &= \frac{I_{measured}(t)}{C_0 V} \end{aligned} \tag{6.12}$$

Where C_0 is the capacitance of the sample and V is the (constant) applied voltage. In this manner, the measurements (applying a constant known voltage and measuring the current and capacitance) taken on the samples in the test may be used to determine $f(t)$. Having determined $f(t)$, it is possible to determine χ_m and use equation 6.8 to determine $\epsilon_m(t)$ for XLPE.

In the model, the time varying $\epsilon_0(1 + \chi_m)$ was collected into a single term $\epsilon_m(t)$, which was defined for each material. Thus, equation 6.6 is modified by the information gained in applying equation 6.12: [Note that the cells are assumed to be identical in this case, therefore A_n and d_n are replaced by the constant terms A and d]

$$\frac{A}{d} \sum_{n=1}^{6} [V_0 - V_n] \epsilon_m(t)_n = 0 \tag{6.13}$$

Since the change in polarisation is a property of the material rather than the specific system being modelled, the field computations of a charging dielectric may be separated in time; each time step may be computed independently of the others. The significance of this separation is the increase in processing speed allowed by utilising a parallel processing setup.

This result may be surprising, considering the RC network that is being analysed might be expected to have a time-dependant or memory component based on the charging of capacitors over time. The result given here can be imagined by firstly considering the charging time of an ideal capacitor connected directly to a voltage source. Since in this ideal system $R = 0$, the charging time of the capacitor must also be zero (the time constant of the network is zero). The

addition of a resistance might cause a finite time constant and result in a finite charging time, but only if the resistance is in *series* with the capacitor. A quick observation of the equivalent circuit (figure 6.7) of the network defined in this model will show that there are no series RC components, only parallel. Therefore, the charging time of the whole system will be zero, and the system will be memoryless. The charge on the boundary of each cell will be defined by the geometry of the cell and the material within the cell, and likewise the current flowing into the cell will be equal to the current flowing out of the cell - crossing the boundaries via a resistive path.

Furthermore, the presence of a resistive component in each cell serves to ensure the potential across each capacitor will remain constant (assuming all resistances are constant), and therefore the polarisation of each cell may be computed independently in time.

Having determined the polarisation function for a material from careful laboratory experiments, complex dielectric systems may be simulated in a concurrent manner. This provides substantial gains in simulation speed, as current technology is towards many concurrent processors rather than a single high speed processor.

The function used to model the dielectric response was based on measurements taken from the samples in the accelerated ageing test. Polarisation and depolarisation currents were measured on the samples, and these currents were curve-fit to a triple exponential model (of the form $A_1e^{k_1t} + A_2e^{k_2t} + A_3e^{k_3t}$). Initially, a means of combining the responses of the samples was tested (using averages and medians), however the slight variations in the samples caused significant differences in the measurements, and this method did not give good estimates of the variables.

Instead, the samples which displayed a response that was modelled well by the triple exponential curve were examined, and a representative sample was chosen (figure 6.5, samples T1-1 and T3-2). The values from this sample were then compared to the other samples, and values that were similar were incorporated into the model. The resulting curve did not closely follow any of the samples, but gave a reasonable estimate of the collection as a whole.

In particular, this method of curve fitting did not give a good fit of the variation in the current found in the samples. While the current varied by two to three orders of magnitude from the peak at around 5s, to the lowest point

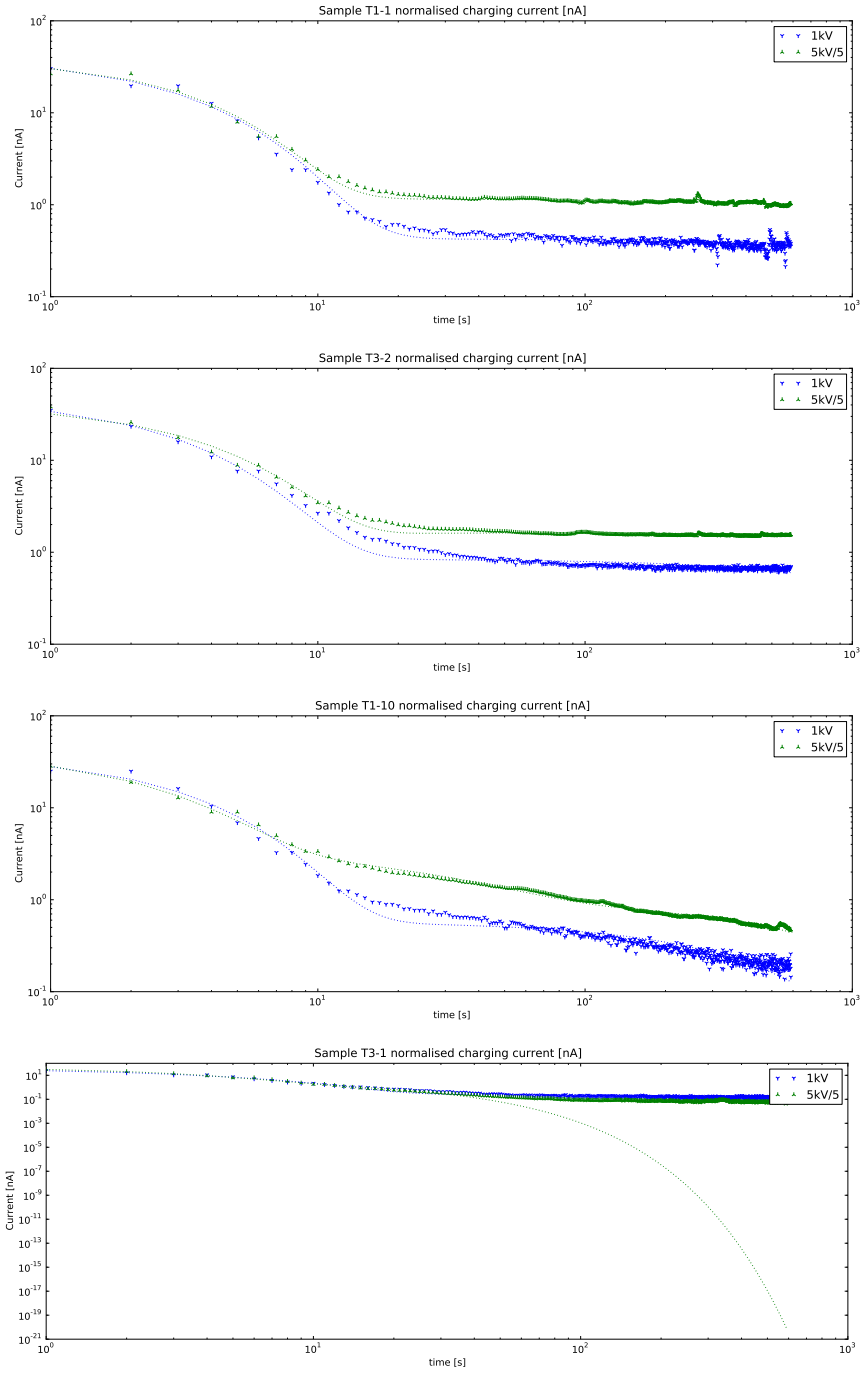

Figure 6.5: Samples with good fits and poor fits respectively. T1-1 and T3-2 show a good fit of the model (dashed line) with the measured data (symbols). In contrast, samples T1-10 shows significant deviation at later times, and T3-1 shows a continuing gradient that is suspect.

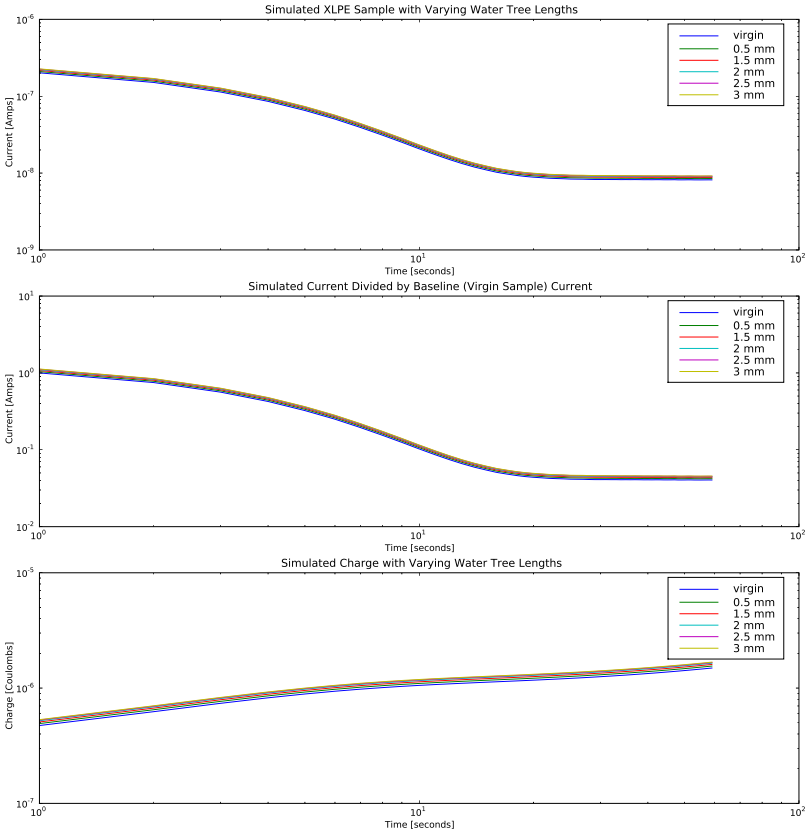

Figure 6.6: The current and charge resulting from various simulated water tree lengths.

at the end of the measurement, the simulated responses remained close to one order of magnitude of the starting value (see figure 6.6, the current ranges from 10^{-6} to 10^{-8}, and compare with figure 6.5 where the current varies from 10^{-7} to 10^{-10}). The use of the triple exponential model for fitting these samples does not seem to give a good fit overall.

This function was chosen based on the suggestions and experience of the members of the team. Function fitting to non-linear models is a project in itself. The techniques often used in other areas (regression, least squares) are not as effective in this case, and this is reflected in the results obtained using these methods in this project. This is a specific area that would inform any future developments of this model, as time constraints prevented a rigorous analysis of the curve fitting process.

This model would benefit from a series of detailed measurements on pure samples of XLPE in order to more fully establish the 'true' nature of the time-domain response. However, the fit-curve method used here was adequate for examining the phenomenon under scrutiny, even if the exact function is not well known, the ratio of conductivity estimates should still produce similar effects in simulation as in measurements.

When modelling a dielectric material, the in-phase component of the permittivity results in dissipation of energy in the material (typically as heat). This loss of energy is grouped with other effects of conduction (such as electron hopping) into a single term that represents the conductive losses of the material. This conduction current (sometimes also called pseudo-DC current) may not precisely reflect the physical processes at work (this measurable current is partially related to electron hopping rather than 'normal' conduction), but it may be approximated by giving the material a finite resistivity.

In order to add conduction effects to the model, it was extended to include a resistive component, the value for which was taken from published data defining the conductivity of pure XLPE. If a parallel resistance is added, there will be unbound charges (Q_r) crossing the cell boundary due to the conduction of electrons via the resistive pathway. The total flux crossing the boundary will therefore represent both the 'free' charges moving across the boundary (the time integral of this flux will equal the current) and the flux generated by any enclosed charge. This is represented by the continuity equation:

$$\oint \vec{J} \cdot d\vec{S} = -\frac{d}{dt}[\int_v \rho_v dv] \tag{6.14}$$

Where $\vec{J}$ is the current density, and ρ is the volume charge density.

$$Q_{enc} = \int_v \rho_v dv \tag{6.15}$$

Typically, the enclosed charge Q_{enc} is zero in almost all cells, however this is not a necessary condition.

$$\oint \vec{J} \cdot d\vec{S} + \frac{d}{dt}[Q_{enc}] = 0 \tag{6.16}$$

In order for the parallelisation method to correctly produce a result, the

charge in each cell must remain constant (always zero in the case of the simulations presented here), thus equation 6.14 is equal to zero, and $\oint \vec{J} \cdot d\vec{S}$ must also be zero. This is not an absolute requirement of the model - accumulating charge can be simulated correctly, however the advantages of parallelisation are lost.

In a cell of cuboidal shape, where I_n is the current flowing over the nth face:

$$\sum_{n=1}^{6}[I_n] + \frac{d}{dt}[Q_{enc}] = 0 \tag{6.17}$$

Using the properties of the material, it is a simple task to solve the first half of this equation, since I_n may be calculated directly from $(V_0 - V_n)/R_n$ (where V_0 is the potential of the centroid of the cell under scrutiny, V_n is the potential of the centroid of the cell that shares face n, and R_n the resistance of the material over the same space). In order to solve the second half of the equation, we apply the principles of flux modelling - that of uniform flux within the cell:

(A_n is the surface area of the face n)

$$\begin{aligned} Q_{enc} &= \Psi \\ \oint \vec{D} \cdot d\vec{S} &= \Psi \\ \vec{D} &= \epsilon_m \vec{E} \\ \vec{E} &\approx \frac{\Delta V}{d_n} \\ Q_{enc} &= \sum_{n=1}^{6}[A_n \frac{(V_0 - V_n)}{d_n} \epsilon_m] \end{aligned} \tag{6.18}$$

Which allows both Q_{enc} and I_n to be expressed in terms of V_n.

This is approximated over a time step by assuming that the current is constant over the period Δt:

$$0 = \sum_{n=1}^{6}[I_n] + \frac{d}{dt}[\Psi_{enc}]$$

Performing a 'Riemann style' integration in time: (6.19)

$$0 = \sum_{n=1}^{6}(I_n \Delta t) + \Delta\Psi_{enc}$$

Thus, the final set of equations for a model implementing N neighbours all having resistive and capacitive components is (in a cell with no enclosed charge):

$$0 = \sum_{n=1}^{N}\frac{(v_0 - v_n)\Delta t}{r_n} + \sum_{n=1}^{N}\frac{(v_0 - v_n)\Delta\epsilon_n A_n}{d_n} \tag{6.20}$$

Unlike the method used to compute the permittivity (the basis for the polarisation function $f(t)$), the resistivity was taken from published data ([26, 25]). The value for the resistivity of XLPE was taken as $1.5 \times 10^{14}\Omega$m.

The model has the capability for adding bound charges to cells, and with relaxation of the requirement for parallel processing, each cell may store or release charge. This feature would be particularly helpful in allowing a model to accumulate space charges and assess the effect on the field (and therefore the electrical measurements) of space charge. This feature was not used in this work, the measurements were made in such a way as to minimise the effect of space charges, and for the model they were not added in order to focus on the effects of morphology.

By observation of equation 6.20, it may be seen that an analogue may be produced using ideal resistors and capacitors, where the values are given at each time (making the circuit non-linear in the sense that the values of the components may change in time, but linear in the sense that the circuit displays the expected behaviour within each time step). The model ultimately can be expressed by an equivalent circuit as shown in figure 6.7.

Where R is the resistance of the material (calculated by the dimensions of the cell, and the resistivity taken from published data); and $C(t)$ is the time varying capacitance that is defined by the dielectric function (ideally taken

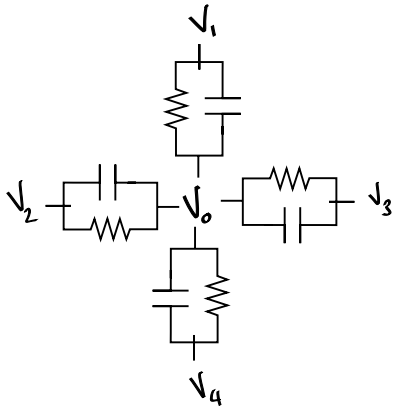

Figure 6.7: The equivalent circuit, used to model a single small volume of insulation.

from laboratory measurements, but taken from gross sample measurements in this work). This mesh is the basis of the implemented model.

6.4 Model of Water Treed XLPE

The simulation of water treed XLPE presents an interesting challenge in the construction of a structural model. The goal of the XLPE cable model is to model the effects of a micro structure in a somewhat macro sense. That is, while cable insulation thickness may be measured in millimetres (e.g. 22kV insulation as used here is 5.5mm thick), the dimensions of a water tree may often be measured in micrometers (μm). Furthermore, while water tree length may be measured in mm, the thickness of its parts will typically still be in the micrometer range.

This large range of sizes to be simulated tends to produce a model with a very large number of elements. If a 5.5mm cable sample is divided isotropically into cells 0.1mm in size, the result is a model containing approximately 55^3 cells. As the cell size decreases, the number of cells rises cubically: with each halving of cell length there are eight times the number of cells (0.1mm = 166,375 cells, 0.05mm = 1,331,000 cells, and so on). In order to simulate water tree structure with any significant detail, a mesh in the 1μ range is necessary - this results in a simulation space in the region of 166×10^9 points.

The most detailed models created in this project had a size of approximately 2 million simulation points. This model took a 3mm thin slice of quarter-symmetry XLPE and simulated it with a grid of $256 \times 256 \times 60$, in order to get

a good sense of the field distortion of individual water trees. This model had a cell spacing of 20μm, which is still somewhat coarse when modelling individual water trees.

The high resolution model was used in the 'Degree of Non-Linearity' calculations, and to produce figures 6.9 6.8, and forms the basis for the conclusions in this chapter. The lower resolution model shown above was used for conceptual testing. The results of these two models were identical in idealised test cases, with subtle changes being visible in the higher resolution model when the water treed models were simulated.

This cell size used was considered sufficient to model the effects of longer water trees, with a usable degree of accuracy. As available computing power increases, the resolution may be improved. Even at this somewhat modest resolution, effects of changing the morphology can be seen, giving some interesting results for comparison to the measurements taken.

The proposed theory is that there will be a noticeable change in the length of water trees as the applied voltage varies from zero to a multiple of the operational voltage. This change in length is due to the dielectrophoretic force on the water inside the water trees and should change the wet length, and therefore the charge accumulated on the tip of, any vented water trees present. Furthermore, the increased length of water trees will raise the conductivity of the sample as a whole, as this represents a shorter path for the conductive processes to allow a DC current.

Thus a deviation of the current from the expected linear response to increasing applied voltage gives an indication of the presence of vented water trees inside the insulation. The challenge then is to distinguish the change in current due to water tree length from the change in current due to other processes.

In the field this poses a very challenging problem, as the effect of joints, terminations and measuring equipment cannot be easily accounted for. In the case of a computer model, however, these elements may be removed, allowing for a study specifically related to the effect of the variable under scrutiny. In this manner, the model was used to isolate the effects of changing morphology of the insulation from other effects found in the time domain measurements.

An accurate correlation of the model with real world measurements is dependant on having accurate information regarding the properties of the materials present in the desired structure. Unfortunately detailed time-domain data

on solid XLPE is scarce; the properties of XLPE used in this model were based on the measurements taken from the ageing test. This data has various factors that may influence the response (terminations, environment, equipment, etc.). There is scope for improvement of the model by making laboratory time-domain measurements of various materials.

Water was modelled as a purely resistive material. While water does act as a dielectric, the capacitive effect is negligible compared to the effect of the resistivity of the material in this context. Other authors also model water as a resistive substance, and this model is in keeping with the general theme of reviewed literature (e.g. [26, 25, 101]).

In order to model an inhomogeneous environment, the different material properties of each substance must be known in some detail. Then each cell is assigned a single material type, and the equivalent network for each cell is defined by the material of the cell. In this way, the model may simulate any type of environment, provided the morphology of the environment can be ascertained, and the properties of the materials present may be estimated.

The goal of this model was to investigate the possibility of dielectrophoresis being responsible for the non-linear effect observed in the samples. The non-linear effect was intended to be simulated by changing the length of water trees in the samples, to see if the effects seen in the real samples could be modelled by changing water tree lengths.

To this end, the charging current was used to compute a variation of the degree of non-linearity. The essence of the method is dividing the current measured when the water trees are 'long' by the current measured when they are 'short'. In real-world samples, long water trees are created by increasing the test voltage, which increases the dielectrophoretic force on water, which causes the trees to fill with water. In the simulation, the means by which a higher voltage was simulated was by the addition of longer water trees to the model.

If this change in morphology of the insulation is significant, there will be a non-linear response of the insulation to longer water trees, and this will be detectable as a higher current flowing when the water trees are longer. The ultimate goal of the model is to predict the length of water trees that give rise to a certain amount of non-linearity. This can then be the basis of a 'look-up' table that will allow an estimate of the longest water tree in a sample by

knowing the non-linearity of the sample.

Due to the relatively short lengths of water trees grown in this project (figure 4.16), and the relatively good condition the samples were in, the differences between samples was rather subtle. While the correlation between the model and the measurements was not good enough to detect the small difference, the effects observed in the model were broadly similar to the measurements, giving some support to the theory that it is the change in length of water trees that gives rise to the non-linear response of the sample in the time domain.

The degree of non-linearity was computed on simulated samples using the same techniques as used when computing the non-linearity of measured data from real samples (e.g. [78]). However, since the model has precisely known dimensions, it is not necessary to compute the conductivity of the sample; it is sufficient to compare the currents.

Having simulated the electrical field of the model at each time step, the flux crossing each boundary of each cell was known. The measured current is the flux crossing the boundary of the conductor - in the resistive case, this represents charges crossing out of the conductor and into the insulation, and in the capacitive case, the change in flux over time results in a displacement current flowing across the boundary.

The current is therefore calculated by adding the resistive current flowing across the conductor boundary to the rate of change of flux over the time-step. This gives the charging current of the sample.

$$DONL_{simulated} = \frac{I_{charging_{5kV}}}{5I_{charging_{1kV}}} \tag{6.21}$$

In the case of the simulation, the presence of a higher voltage was simulated by lengthening the water trees in the model. By assuming the effect of dielectrophoresis was at play, the model computes the charging non-linearity by the following mechanism:

$$DONL_{simulated} = \frac{I_{long}}{I_{virgin}} \tag{6.22}$$

If the change in the length of water trees does not introduce a non-linearity into the measurement, the simulated charge should not change and the ratio between the water treed model and the non-water treed model ('virgin' model)

should remain at unity. By extension, the ratio of a short water treed model (as a means of representing a lower voltage measurement) to the longer water treed model should also be unity if the length of water trees does not have an effect on the measured current.

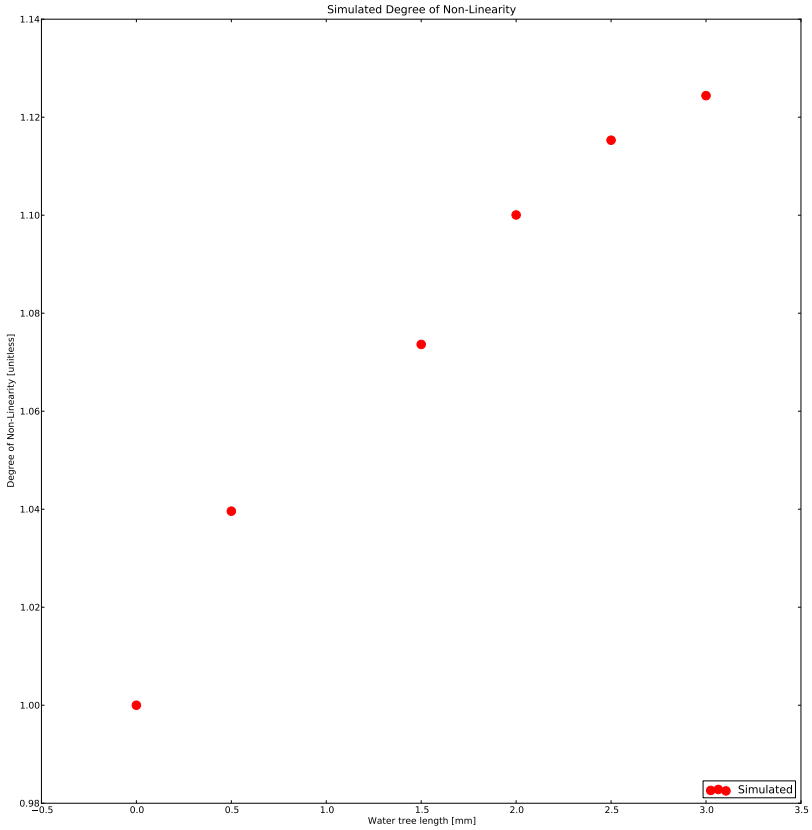

Figure 6.8: The simulated degree of non-linearity, computed by $\frac{I_{long}}{I_{short}}$. The non-linearity increases with increasing water tree length, but note the small range of the y-axis. A non-linearity of unity indicates a linear response (no non-linearity).

Figure 6.8 contains a plot of the non-linearity of each simulated water tree length (current in a simulation with water trees of length indicated divided by the current in a simulation with no water trees). In contrast to the measurements taken from the samples, there is no change of the non-linearity with time (see for example, fig 5.1). The whole time-series can be represented by a single DONL value. These values were computed by dividing the sample with a water tree of a given length (say 0.5mm) with the values taken from a simulation of

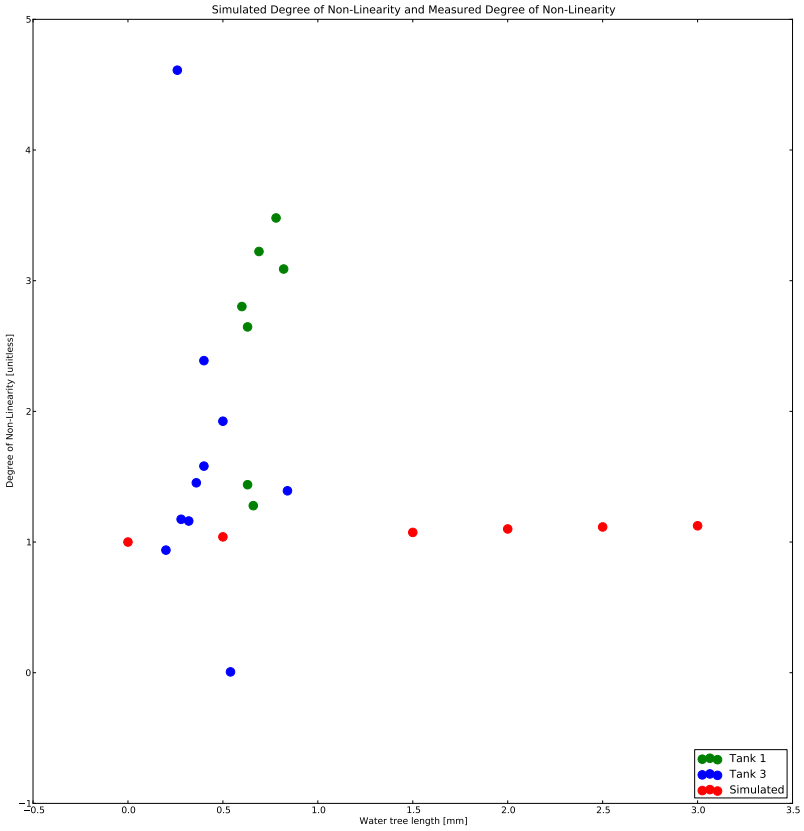

Figure 6.9: The simulated degree of non-linearity, combined with the measured degree of non-linearity. Note the upward trend of the non-linearity as the water tree length increases. The measured water tree length is the longest water tree found. See appendix A for an overview of the non-linearity and other properties of each sample.

a sample with zero water treeing ('virgin' sample). Thus, a plot of non-linearity vs. water tree length is created.

Although the method developed for field work computes the conductivity of the sample (thereby eliminating the effect of the polarising field), and uses this as a basis for comparison, the method described for computing the degree of non-linearity on simulated samples includes the polarisation component. The reason for this is the timing of the development of each technique. As the model was being developed concurrently with the measurement techniques, the model was designed to compare the total current. When it became apparent that field measurements would be more reliable if the conductivity of the

sample was used, it was too late to perform the necessary modifications for modelling this part of the technique. It is a logical next step, and would not require modification to the underlying software, but would require generation of a new set of models and simulations.

If the low-voltage measurements taken on a sample can be likened to the 'virgin' state of insulation (that is, all water in water trees collapsed into the environment), and the high voltage measurements taken to be the 'maximum' water tree length (sufficient potential applied to fully 'inflate' all water trees), then plotting the water tree length against the non-linearity should show an increase in non-linearity as the length of water trees in the sample increases.

This can be seen in figure 6.9, where there is a definite trend of increasing non-linearity as water tree length increases. Note the rather conservative estimate of the non-linearity given by the model, varying from 1 to around 1.12 vs. measured non-linearity up to 8. There is a similar trend in the measured data (see figure 6.9), that of increasing non-linearity with increasing water tree length (the value for water tree length is the longest water tree found).

The simulated non-linearity indicates that the measured non-linearity should be close to unity for new insulation, and rise to about 1.10 for heavily water treed insulation. This finding is similar to the results taken from real world measurements using the same technique ([78]), which describes a non-linearity of $>$ than 1.2 being found in heavily water treed cable.

The results of this test do not closely match those taken from the accelerated ageing test however, and the reasons for this are unknown. It is notable that the measured conductivity of the samples was very low, and this makes the measurements more susceptible to noise or other dielectric effects that can manifest as very small perturbations in the measured current. The measurements were taken with great care, and guarding was used to minimise the effects of terminations and creepage current, however even small changes (e.g. due to field distorting effects at the conductor terminals) may have a significant effect.

Furthermore, the model is based on using gross cable measurements to estimate the properties of 'perfect' bulk insulation. As such, there is almost certainly an error introduced by the dielectric and other factors that contribute to measurements on real cables. As such, while the similarity of the general patterns seems to give evidence for dielectrophoresis as the mechanism for the

changes in aged cables, this model would benefit from further careful laboratory measurements in order to more fully simulate real samples.

The use of the non-linearity is only applicable in the absence of other significant cable pathology. Other factors that reduce the resistivity of the insulation will mask this effect (for example damaged joints or terminations), while conversely, very good samples may potentially have high amounts of non-linearity due to the relatively large amount of noise on the measurements.

The effects noticed in the simulation resulted in somewhat conservative estimates of the effect of water treeing on samples, giving some evidence that the effect of changing morphology can be analysed by non-destructive measurements. This provides support for the theory of dielectrophoresis being a cause of this change in morphology.

6.5 Discussion and Future Directions

A major unforeseen obstacle in the construction of the model was the lack of carefully analysed material constants for XLPE made on pure samples under laboratory conditions. While values for the physical properties and resistivity were finally found, there seems to be an opportunity for a project in taking detailed measurements of the complex permittivity and resistivity constants of the material. Lacking this detailed material data, the constants were estimated from measurements taken from real samples. These estimates do not provide a reliable source of information relating to pure XLPE, as they include the effects of the semiconducting layer, joints, terminations, and environment.

However, even with these issues, there is a clearly similar trend seen in the simulations and the measurements of the current in the samples. This gives some confidence in the results of the simulations. While the 'scale' of the simulations seems somewhat different to the measurements, the shape is quite similar.

In a similar manner, the effects of changing the water tree length were not as significant in the simulations as discovered in the measurements. It is possible that, due to the rather conservative estimates of the resistive currents, the amount of non-linearity is similarly conservative. However, there was a definite relationship found, and this gives support to the theory of dielectrophoresis changing the length of the water trees in the sample, and therefore creating a

non-linear response of the insulation with respect to the applied voltage.

The nature of a simulated test is that it removes confounding factors that may influence the interpretation of data obtained. In some cases, the factors removed prove to be integral to the properties of measured data. Therefore, though there was good correlation of the simulation to the field tests taken during the project ([78]), this similarity should be considered with caution. Nevertheless, having similar changes in both datasets highlights the importance of small change in the non-linearity being significant indication of water treeing.

While the ultimate goal of creating a simulation that could accurately correlate a level of non-linearity to a measured water tree length in a sample of real XLPE was not reached, this model provides a good starting point for reaching this goal. With more detailed material properties, increasing computing power, and additional development of the model, this goal becomes more possible.

The next major step is to include the effects of conductivity into the final analysis, as found in the 'ageing landscape' proposed in chapter 4. By characterising the causes of increased conductivity as well as increased non-linearity, the goal of sifting out the effects of water trees from other confounding effects may become realisable.

Chapter 7

Conclusion

> I have discovered a truly remarkable proof of this theorem which this margin is too small to contain.
>
> *Pierre de Fermat*

This work has presented the details and results of a large scale ageing test that operated for 4 years, albeit with many periods of downtime, resulting in an effective ageing time of 400 days. Electrical measurements were performed on the samples and a novel technique of forensic analysis was applied to the failed samples. A teaching tool in use at QUT was demonstrated as a useful research tool, able to simulate the effect of dielectrophoresis and give some correlation to real world measurements on water treed XLPE.

The first part of this project, construction and maintenance of an accelerated ageing facility, is a part that could significantly benefit from more information in the literature. While work in this area is not considered research in the sense that the details of the setup, and problems and solutions encountered during this process, are not generally publishable, and information especially related to staining methods and dyes would be a valuable addition to the IEEE Standard 1407 to ensure tests are more comparable across sites, and assist those embarking on similar undertakings in the future.

In particular, Standard 1407 outlines many of the electrical and environ-

mental characteristics of the test set - specifying terminations, water impurities/additions, and temperatures. While it may be somewhat outside the scope of a 'typical' standard, it may be useful to outline the impedance of other established test-sets, in order to allow for the sizing of appropriate current supply for a new facility.

Specifying the tank material seems to be a crucial aspect (although the exact mechanism is unknown), as outlined in [99]. A worthy addition to the Standard would also be an outline of the 'expected' life of samples under various ageing stresses (if such could be compiled), in order to project time lines of accelerated ageing. Furthermore, the outline of the statistical basis of the choice of test might be expanded (this project changed from time-to-failure to ACBD, however a truncated time-to-failure test would likely have provided better quality data). Specifying the temperature of the samples at breakdown would also be a useful addition.

Finally, the aspect of the Standard that would most benefit from further review is the staining process. While it is rather straightforward in many aspects, the fact that most sites perform the process using 'local' techniques make comparison of water tree morphology across sites somewhat tricky. Indeed, this is an area of deficit in this test - that of evolving the method of staining preventing effective assessment of the 'dark' vs. 'fuzzy' water trees.

An unfortunate aspect of a technically demanding project taking place in a busy commercial workshop are issues relating to access and resource allocation. This is not a criticism of the staff of the Ergon workshop where the project was housed, rather an acknowledgement that high quality research requires some unusual demands on time and resources, which can become very expensive in a commercial environment. By way of example, many of the measurements during this test were taken after hours, however the use of certain equipment (such as access to high voltage control panels) was not routinely made available after hours for safety concerns. In comparison, a research institution will tend to have procedures and facilities in place for 24/7 operation that simply would not be cost effective in a commercial environment where staff are often paid by the hour (and penalty rates apply).

Much of the knowledge and equipment for creating this facility was not available at QUT, however, and there are no institutions in Brisbane with the capability of a test of this size. Indeed, one wonders if there are any public

institutions in Australia that could house such a project! This test could not have been executed and completed without the skills and dedication of the staff of Ergon Energy.

It is the nature of projects such as this, that push many components to their limits, to encounter equipment failures over time. All in all, equipment failures and maintenance accounted for approximately two years of the four year project. The main equipment issues were related to the high current supply for the samples, and the high voltage supply for the frequency domain test set.

After the initial prototype current transformer overheated and caught fire, a custom oil cooled transformer was ordered. The transformer supplied did not meet the requirements, and suffered a thermal failure, requiring refurbishing and modification of the test facility to accommodate a lower current supply. This was the principal reason for the removal of Tank 2 (field aged, non-treated samples) to be removed from this test.

Procurement and commissioning of the high voltage supply for the frequency domain spectrometer used in [103, 104] also occupied several months. The initial procurement process was complicated by issues with supply of the equipment, and in the commissioning tests, the high voltage unit flashed over and required repairs lasting several months.

Ultimately, the work here was based on the use of a cheaper and more readily available DC testing tool that could be supplied immediately with replacement parts and units available quickly if necessary. While the use of variable frequency spectroscopic measurements did form useful part of the project, the equipment does not seem quite ready for large scale use.

These issues of facility design and construction, equipment procurement and policy creation represent a sunk cost that is required for performing research of this kind, but could greatly benefit future projects on the same facility. This project would have been an ideal candidate for a long term laboratory at a larger public institution, and it seems unfortunate that the systems will be dismantled and the facilities decommissioned.

The experimental setup provided a serviceable facility for examining the effects of time and water on XLPE, with the results of the water tree population study and the effects of water tree length on breakdown strength the most reliable useful parts of the test.

The method of forensic analysis outlined in chapter 4 is an incremental

improvement on currently employed methods, but nevertheless gave significant information that allowed for the statistical analysis to be performed. This method, using a projector and screen rather than a microscope, could be adapted into a fully automatic water tree analysis setup, and indeed steps were taken in this direction, however time constraints limited this to a non-functional prototype.

The forensic analysis of the samples post-mortem, and the resulting statistical analysis of the populations of water trees represents the most scientifically rigorous part of this work, and the evidence supporting the use of the log-normal distribution when modelling the lengths of water trees (particularly bow tie water trees) is the most reliable contribution from this test.

In the literature, there was little information found regarding the population distribution of water trees, and the examination of bow tie trees performed here appears to be the first of its kind. The statistical evidence for the use of the log-normal distribution is one of the most significant contributions of this work.

The implications of establishing the population distribution are not well understood at this stage, however it may be possible to use this knowledge to estimate the chance of finding water trees over a certain length in water treed XLPE based on forensic analysis of a part of the sample. This may prove useful in reliability analysis, as analysis of failed segments removed from service could potentially provide an insight into the condition of the cable as a whole.

The analysis of the samples by extreme value theory was performed in line with currently accepted methodologies, with the unsurprising result of the more heavily water treed samples having a lower breakdown strength. The main point of information gained from this study is that there is a real measurable difference between the sample groups, and this is borne out in their different water tree lengths and breakdown strengths.

In contrast to the more established techniques above, the comparison of treated aged samples with new samples did not give conclusive results. There is evidence that water trees will grow in XLPE post-treatment, and a suggestion that there is a 'point of no return' after which treatment has limited benefit. The only in-service failures were from the treated group, and the presence of fuzzy and clear water trees in the treated sample group serve as evidence of this.

What is less clear is whether the treatment program will be beneficial for

in-service cables that are subjected to more moderate stresses. The costs and expected gains will need to be measured against the improvements of cable technology gained by replacing cable. The tests performed here suggest improvement in cable condition - in keeping with electrical cable utility experiences - however, the treatment program is not a 'silver bullet'. Treated cables will require replacement in time, and assessing their condition is both difficult and necessary.

The effects of this treeing on the electrical measurements is even less clear. There was certainly a suggestion that increasing water tree length increases the non-linearity of the sample when measured at 1kV and 5kV, however the exact relationship remains elusive. This relationship is further complicated by the effects of changing conductivity on the non-linearity; the relationship between water treeing, non-linearity and conductivity has yet to be fully elucidated.

There is evidence from this test that the degree of non-linearity can form a basis for assessing the presence and danger of water trees in XLPE. This measure, which is based on a morphological change of water trees under an applied voltage, may be used to assess the condition of an underground cable in-situ, using relatively cheap and simple time-domain based equipment.

The means by which this can be used to predict failure is unique to each sample, as each installed cable will have different properties, different attached accessories, and a different environment in which the ageing will occur. By analysing each sample on an individual basis, the change in ageing factors with time can be analysed to compute an 'ageing trajectory', which will enable the organisation to manage the asset based on condition and estimated remaining life.

The use of flux modelling as a means of teaching and research is a contribution that may have less significance with time, as powerful computational models, along with skilled programmers and mathematicians to operate them, become more commonplace. Nevertheless, in the current environment, with the available models being beyond the realm of the individual to install and operate, flux modelling as a means of creating a custom model for electrostatic field modelling is a useful tool. It is especially useful in teaching the theory of electromagnetic fields, as it provides a good visualisation of the concepts without sacrificing mathematical rigour or accuracy.

The results of the simulation in this work gave somewhat conservative esti-

mates of the effect of water treeing on the non-linearity of XLPE. It is likely the main diverging factor of the model from the real samples is the conductivity and the effect of various processes on the conductivity of water treed XLPE. This limitation could be overcome with careful measurements of XLPE samples in different stages of ageing. Ultimately, discovering the specific causes of the increased conductivity of aged XLPE could provide the missing key to the model.

Finally, the effects of non-linearity were combined with the effects of increasing conductivity to produce an 'ageing landscape'. This plot takes into account both of these factors and attempts to classify the samples accordingly. As a real world test, this is the most useful part of this work - this can be used immediately by utility companies, using only simple off the shelf test equipment. While the data points presented in this work are only the beginning of a complete picture, with many measurements on many samples (as might be performed in a condition-monitoring maintenance program), the expected state of samples at various locations in the landscape can be established by comparing measurements to those from samples taken out of service and analysed.

Further developments in computer simulation may give greater insight into the results of electrical measurements taken on in-service samples. If this advancement can be combined with an improved model of the population of water trees in a cable, it may become possible to assign probabilities of localised ageing causing failure. In essence, it may be possible to interpret measurements on a cable in such a way as to describe the population parameters of the water trees in the cable.

Reaching this goal would give utilities a powerful tool for managing cable replacement and refurbishment priorities. Establishing the log-normal distribution as a population model is a first step, and more detailed forensic analysis will confirm or elucidate the nature of the underlying distribution of water trees in XLPE cable. With a firm grasp of the population model, and its effect on electrical measurements, the expected lifetime of a cable will be a fairly simple statistical computation.

Finally, an understanding of the factors that create a fertile environment for water treeing will uncover targets for future modifications to the composition of XLPE cable, improving again the resistance of this material to water treeing. While it seems unlikely that the detrimental effects of water on XLPE can ever

be conquered, the task of managing an ageing network will become just that little bit easier.

Appendix A

Tank details and data

A.1 Cable Capacitance

Sample Name	Measured Capacitance [nF]
Tank 1	
T1-1	1.70
T1-2	1.69
T1-3	1.70
T1-4	1.70
T1-5	1.74
T1-6	1.70
T1-7	1.73
T1-8	1.75
T1-9	1.76
T1-10	1.74
Tank 3	
T3-1	1.69
T3-2	1.71
T3-3	1.72
T3-4	1.73
T3-5	1.77
T3-6	1.80
T3-7	1.79
T3-8	1.86
T3-9	1.82
T3-10	1.93

A.2 Cable Thermal History

The temperature effects discussed here apply only to the termination lugs on the samples. This was discovered to be a problem area early in the test, with several of the lugs overheating. While some of the lugs exceeded 110°C, the thermal effects were somewhat localised (as visualised by a thermal camera),

due partly to the cooling effect of the water on the sample below the waterline. The thermal events listed here were not observed more than 600mm from the termination.

The sample lugs were monitored by thermal camera first, followed by colour-change stickers that would permanently change colour at temperatures of 70°C, 80°C, 90°C. 'Excessive temperature' was recorded if a sticker had indicated the termination had exceeded 90°C.

Sample Name	Thermal Events
Tank 1	Termination split - possibly due to overheating and presence of injected flu
T1-1	Experienced excessive temperature
T1-2	Experienced excessive temperature
T1-3	Experienced excessive temperature
T1-4	Experienced excessive temperature
T1-5	No events
T1-6	No events
T1-7	Experienced excessive temperature
T1-8	Experienced excessive temperature
T1-9	Experienced excessive temperature
T1-10	No events
Tank 3	
T3-1	No events
T3-2	No events
T3-3	Experienced excessive temperature
T3-4	Experienced excessive temperature
T3-5	No events
T3-6	No events
T3-7	No events
T3-8	No events
T3-9	Experienced excessive temperature
T3-10	Experienced excessive temperature

Sample	ACBD Strength	Max WT Length	DONL	σ_{5kV}	σ_{1kV}
T3-1	123	0.28	1.99	-1.50e-15	-7.52e-16
T3-2	124	0.40	3.10	6.07e-15	1.96e-15
T3-3	110	0.36	1.52	3.22e-15	2.12e-15
T3-4	110	0.84	1.52	3.32e-15	2.18e-15
T3-5	103	0.40	1.65	2.66e-14	1.61e-14
T3-6	131	0.54	-0.14	-6.23e-16	4.51e-15
T3-7	89	0.32	1.73	-1.46e-15	-8.44e-16
T3-8	96	0.26	6.40	4.33e-15	6.77e-16
T3-9	89	0.50	2.50	1.98e-15	7.91e-16
T3-10	110	0.20	2.61	-1.46e-16	-5.59e-17
T1-1	61	0.47	3.03	4.59e-15	1.51e-15
T1-2	82	0.78	4.53	8.64e-15	1.91e-15
T1-4	103	0.56	3.15	2.32e-15	7.30e-15
T1-5	82	0.82	3.67	5.92e-15	1.62e-15
T1-7	75	0.66	1.35	1.56e-14	1.16e-14
T1-8	75	0.60	1.45	2.58e-14	1.78e-14
T1-9	89	0.66	-	-	-
T1-10	96	0.69	8.01	2.11e-15	2.63e-16

Table A.1: Overview of sample data.

A.3 Sample Data Overview

A.4 Ageing Landscape

Plot of conductivity vs degree of non-linearity. Sample name and breakdown strength are listed at each point.

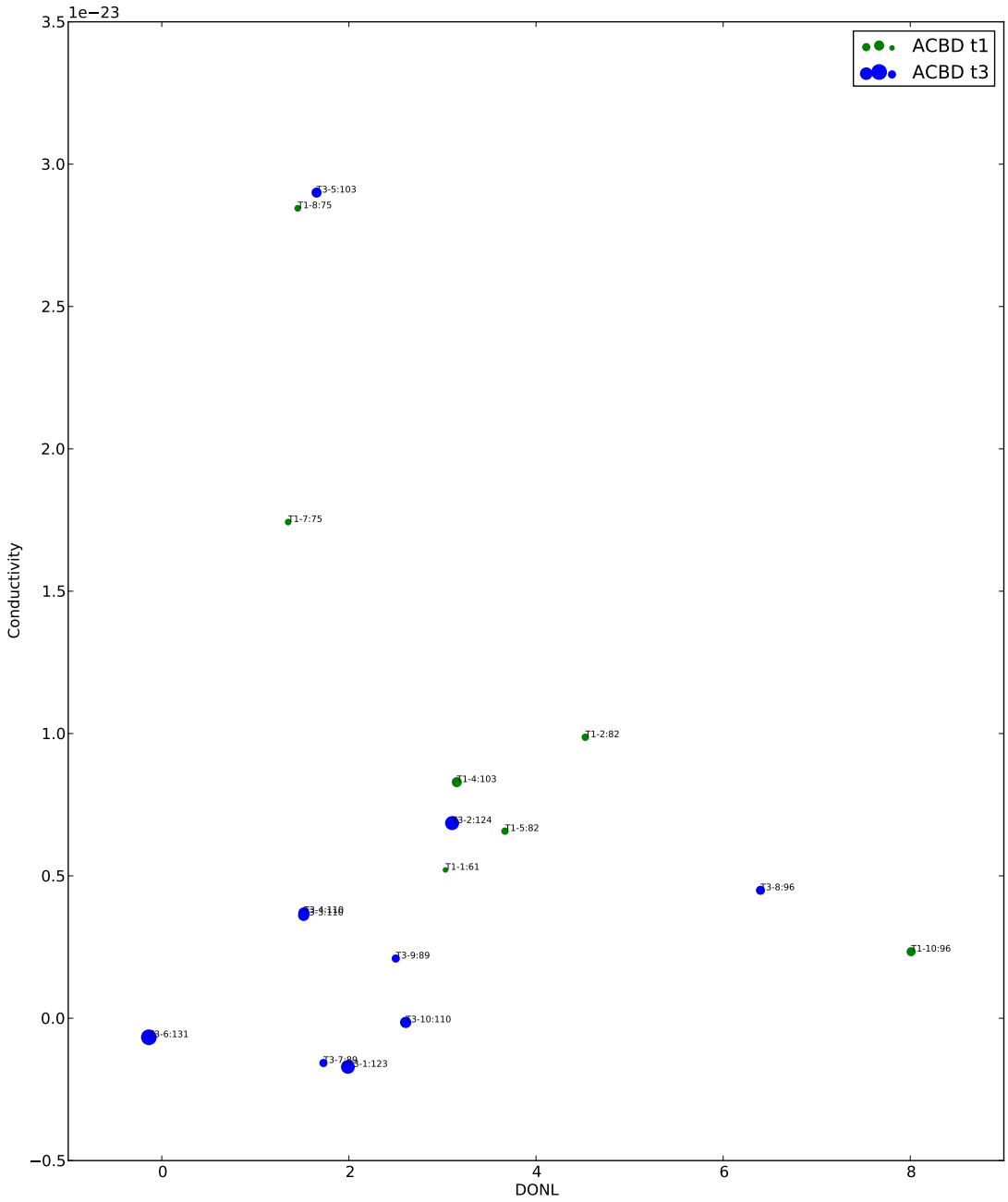

Figure A.1: The 'ageing landscape' of conductivity vs. DONL. The size of the points indicate the ACBD value - larger points a higher breakdown strength.

Appendix B

Sample details and data

B.1 Tank 1 Sample 1

T1-1

Sample Name	T1-1
Sample AC Breakdown Strength [kV]	61
Longest Vented Tree [mm]	0.47
Longest Bow Tie Tree [mm]	0.63
Number of Bow Tie Trees	276
Number of Vented Trees	22
Length of Insulation Analysed [mm]	30
Sample Water Tree Density [trees/mm]	9.00
Sample Measured Capacitance [nF]	1.70
Sample Apparent Conductivity @ 5kV [S/m]	5.21e-15
Sample Apparent Conductivity @ 1kV [S/m]	1.72e-15
DONL [conductivity]	3.03
DONL (charging) @ 30s [$\frac{I_{5kV}}{5I_{1kV}}$]	2.22
DONL (charging) @ 60s [$\frac{I_{5kV}}{5I_{1kV}}$]	2.74
DONL (discharge) @ 30s [$\frac{I_{5kV}}{5I_{1kV}}$]	1.01
DONL (discharge) @ 60s [$\frac{I_{5kV}}{5I_{1kV}}$]	0.99

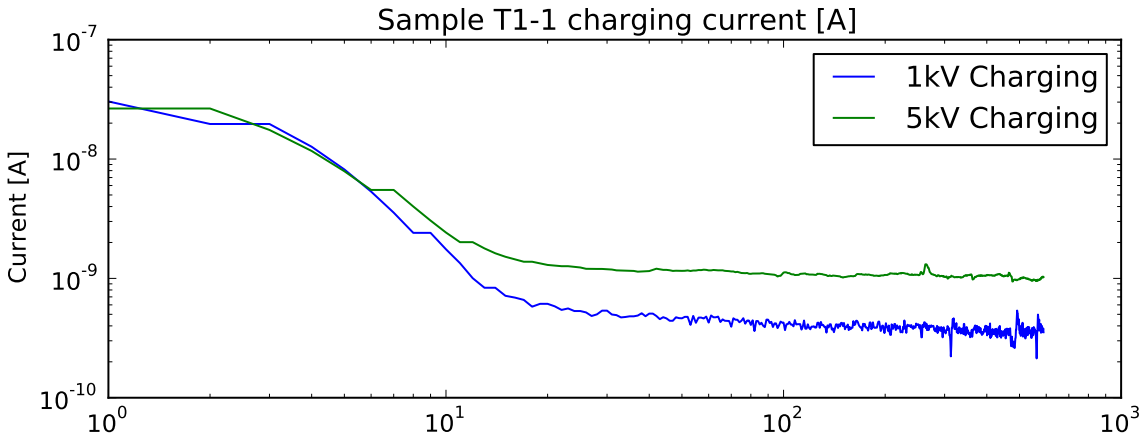

Figure B.1: Charging current of sample T1-1.

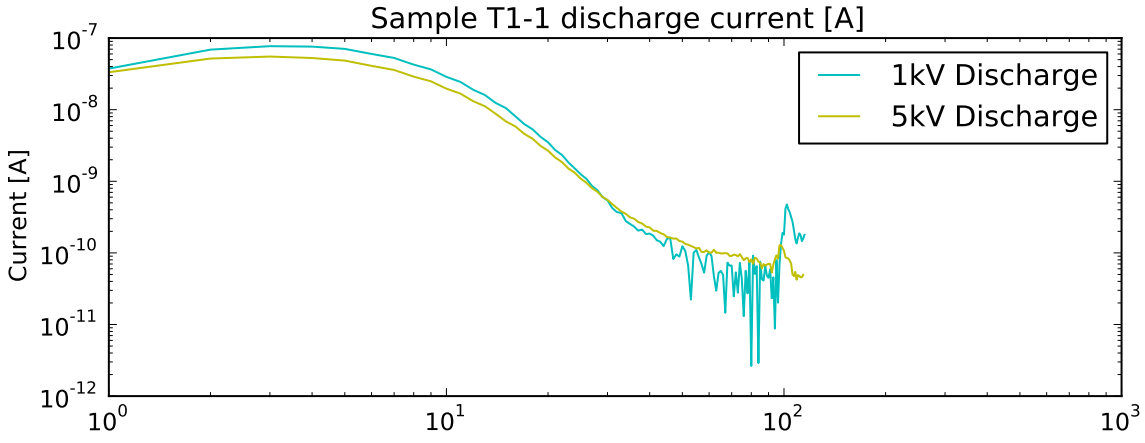

Figure B.2: Discharge current of sample T1-1.

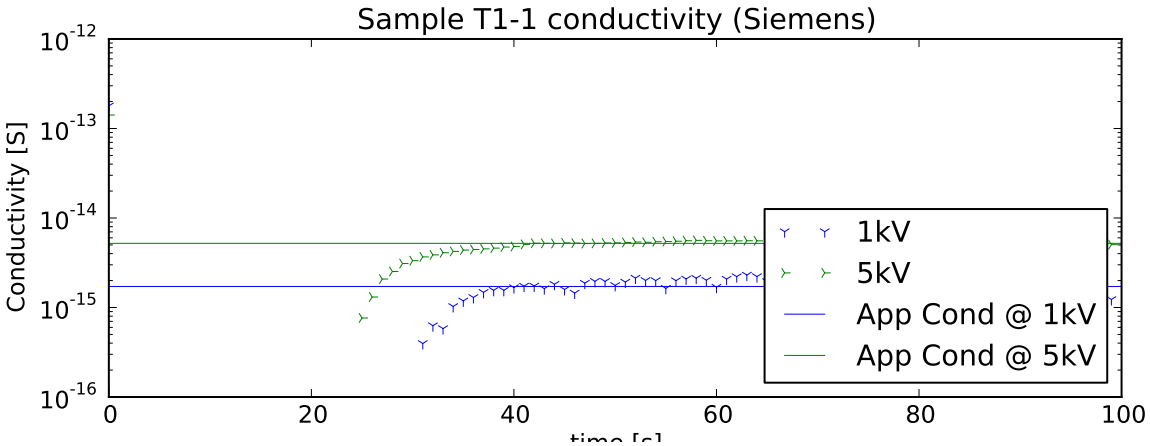

Figure B.3: Difference between charging and discharge current in sample T1-1, normalised by sample capacitance.

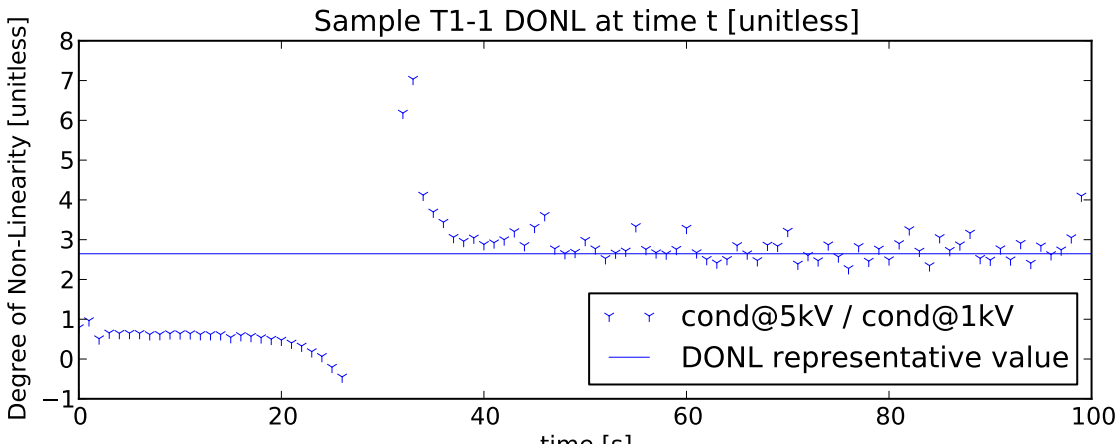

Figure B.4: Degree of Non-Linearity of sample T1-1.

B.2 Tank 1 Sample 2

T1-2

Sample Name	T1-2
Sample AC Breakdown Strength [kV]	82
Longest Vented Tree [mm]	0.30
Longest Bow Tie Tree [mm]	0.78
Number of Bow Tie Trees	285
Number of Vented Trees	21
Length of Insulation Analysed [mm]	30
Sample Water Tree Density [trees/mm]	10.00
Sample Measured Capacitance [nF]	1.69
Sample Apparent Conductivity @ 5kV [S/m]	9.87e-15
Sample Apparent Conductivity @ 1kV [S/m]	2.18e-15
DONL [conductivity]	4.53
DONL (charging) @ 30s [$\frac{I_{5kV}}{5I_{1kV}}$]	2.59
DONL (charging) @ 60s [$\frac{I_{5kV}}{5I_{1kV}}$]	2.61
DONL (discharge) @ 30s [$\frac{I_{5kV}}{5I_{1kV}}$]	0.80
DONL (discharge) @ 60s [$\frac{I_{5kV}}{5I_{1kV}}$]	0.79

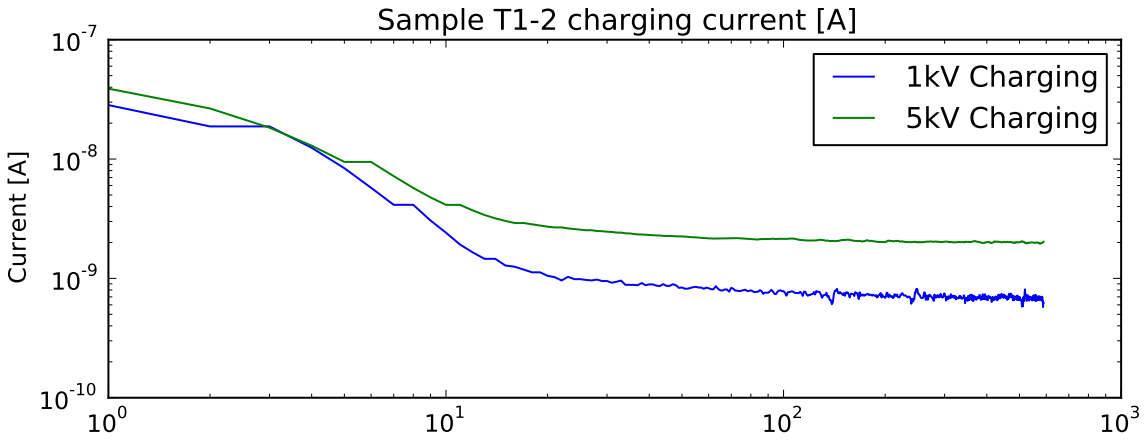

Figure B.5: Charging current of sample T1-2.

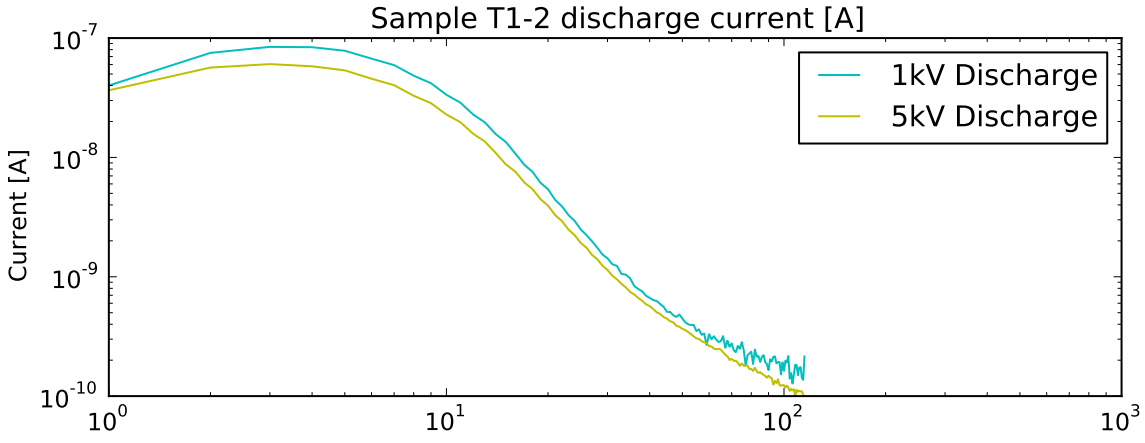

Figure B.6: Discharge current of sample T1-2.

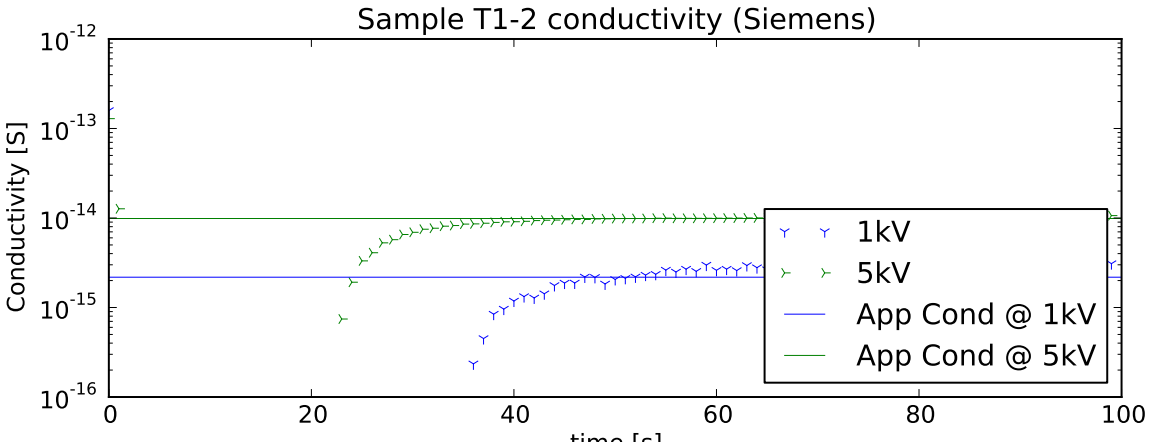

Figure B.7: Difference between charging and discharge current in sample T1-2, normalised by sample capacitance.

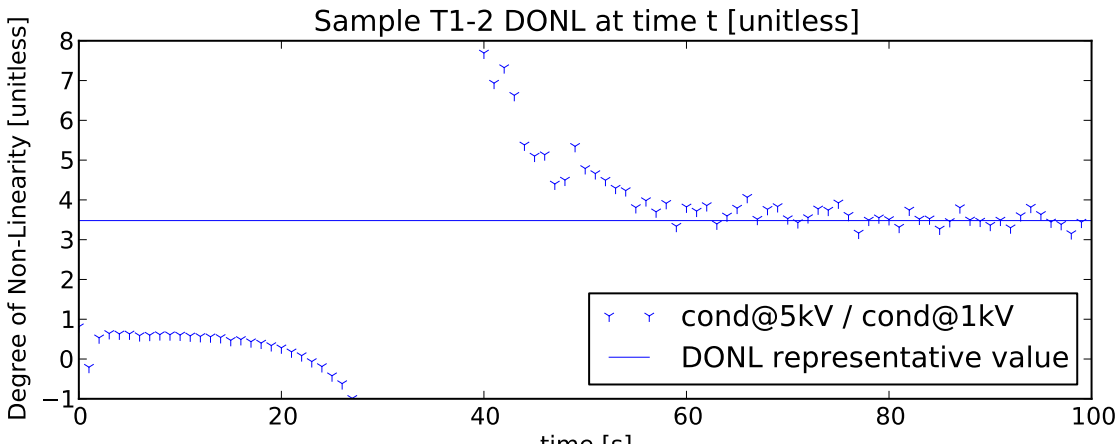

Figure B.8: Degree of Non-Linearity of sample T1-2.

B.3 Tank 1 Sample 4

T1-4

Sample Name	T1-4
Sample AC Breakdown Strength [kV]	103
Longest Vented Tree [mm]	0.13
Longest Bow Tie Tree [mm]	0.60
Number of Bow Tie Trees	245
Number of Vented Trees	13
Length of Insulation Analysed [mm]	30
Sample Water Tree Density [trees/mm]	8.00
Sample Measured Capacitance [nF]	1.70
Sample Apparent Conductivity @ 5kV [S/m]	8.29e-15
Sample Apparent Conductivity @ 1kV [S/m]	2.63e-15
DONL [conductivity]	3.15
DONL (charging) @ 30s [$\frac{I_{5kV}}{5I_{1kV}}$]	2.29
DONL (charging) @ 60s [$\frac{I_{5kV}}{5I_{1kV}}$]	2.50
DONL (discharge) @ 30s [$\frac{I_{5kV}}{5I_{1kV}}$]	0.86
DONL (discharge) @ 60s [$\frac{I_{5kV}}{5I_{1kV}}$]	0.80

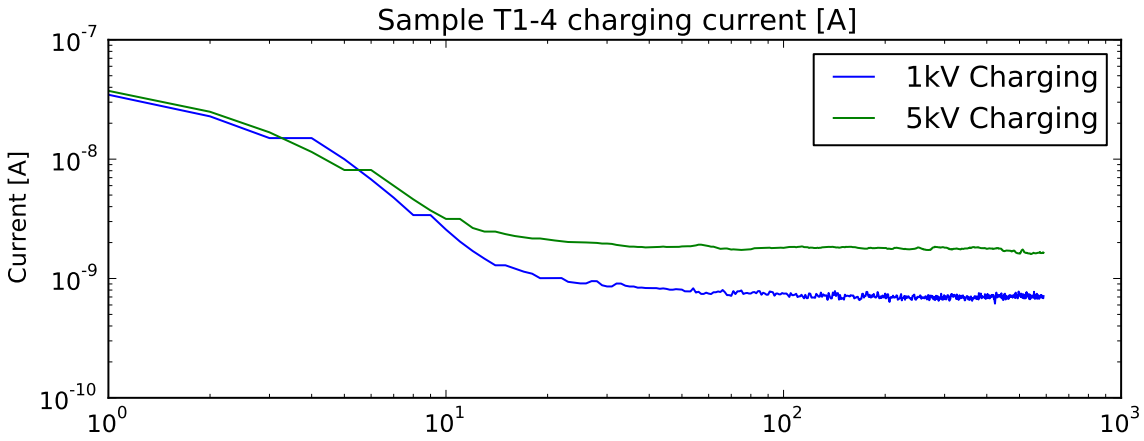

Figure B.9: Charging current of sample T1-4.

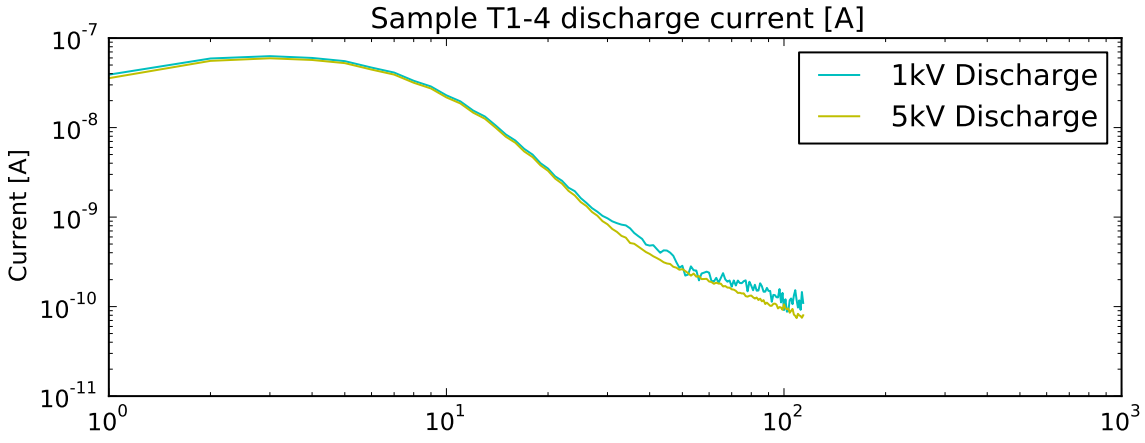

Figure B.10: Discharge current of sample T1-4.

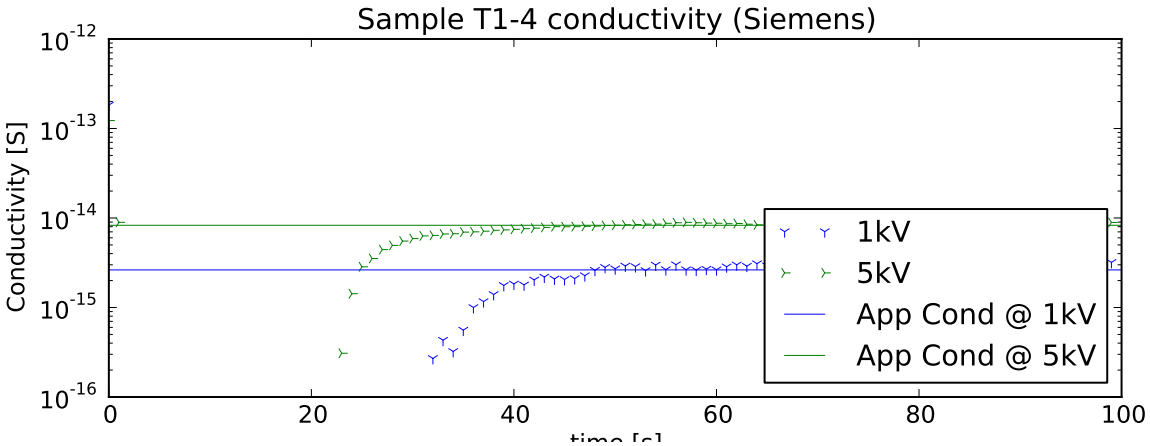

Figure B.11: Difference between charging and discharge current in sample T1-4, normalised by sample capacitance.

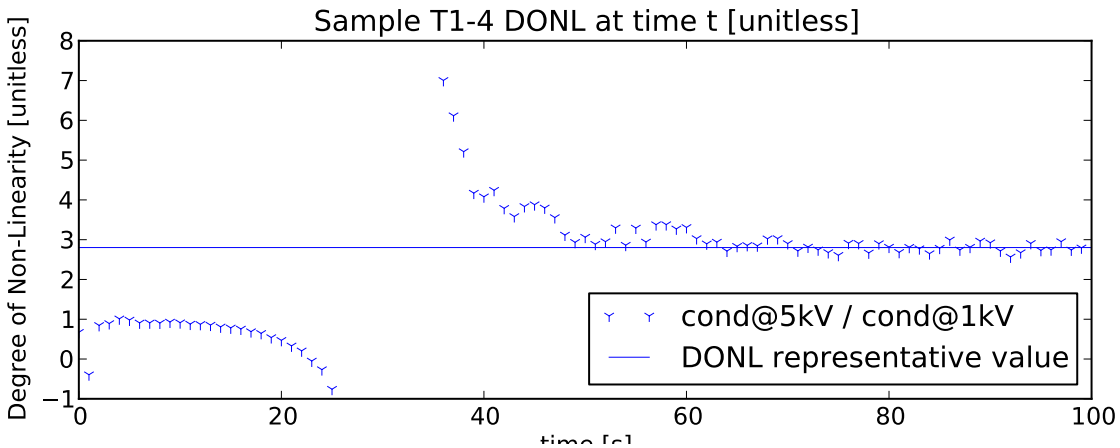

Figure B.12: Degree of Non-Linearity of sample T1-4.

B.4 Tank 1 Sample 5

T1-5

Sample Name	T1-5
Sample AC Breakdown Strength [kV]	82
Longest Vented Tree [mm]	0.46
Longest Bow Tie Tree [mm]	0.82
Number of Bow Tie Trees	481
Number of Vented Trees	47
Length of Insulation Analysed [mm]	30
Sample Water Tree Density [trees/mm]	17.00
Sample Measured Capacitance [nF]	1.74
Sample Apparent Conductivity @ 5kV [S/m]	6.57e-15
Sample Apparent Conductivity @ 1kV [S/m]	1.79e-15
DONL [conductivity]	3.67
DONL (charging) @ 30s [$\frac{I_{5kV}}{5I_{1kV}}$]	2.34
DONL (charging) @ 60s [$\frac{I_{5kV}}{5I_{1kV}}$]	2.58
DONL (discharge) @ 30s [$\frac{I_{5kV}}{5I_{1kV}}$]	0.90
DONL (discharge) @ 60s [$\frac{I_{5kV}}{5I_{1kV}}$]	1.02

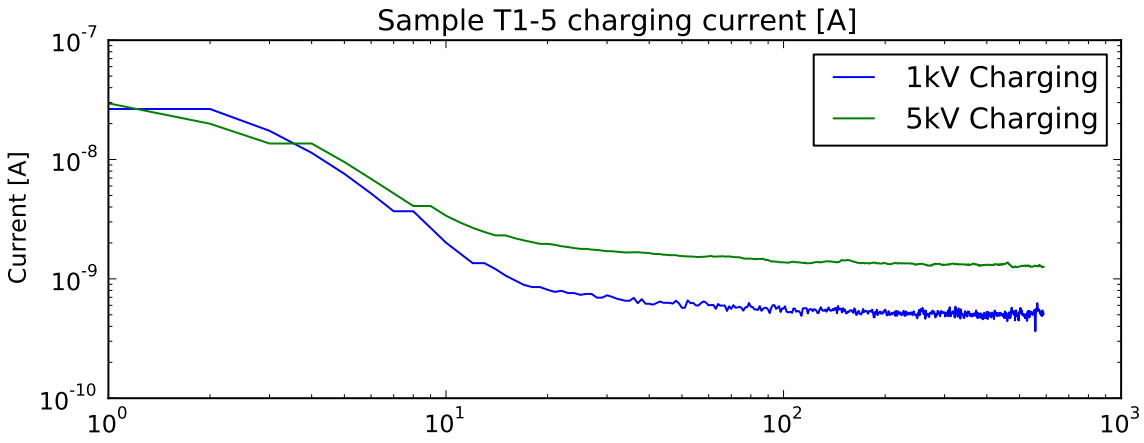

Figure B.13: Charging current of sample T1-5.

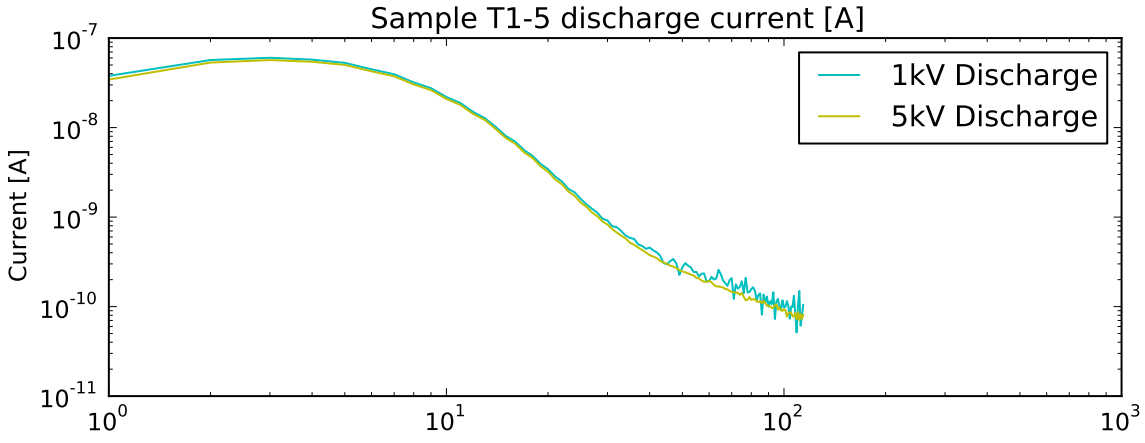

Figure B.14: Discharge current of sample T1-5.

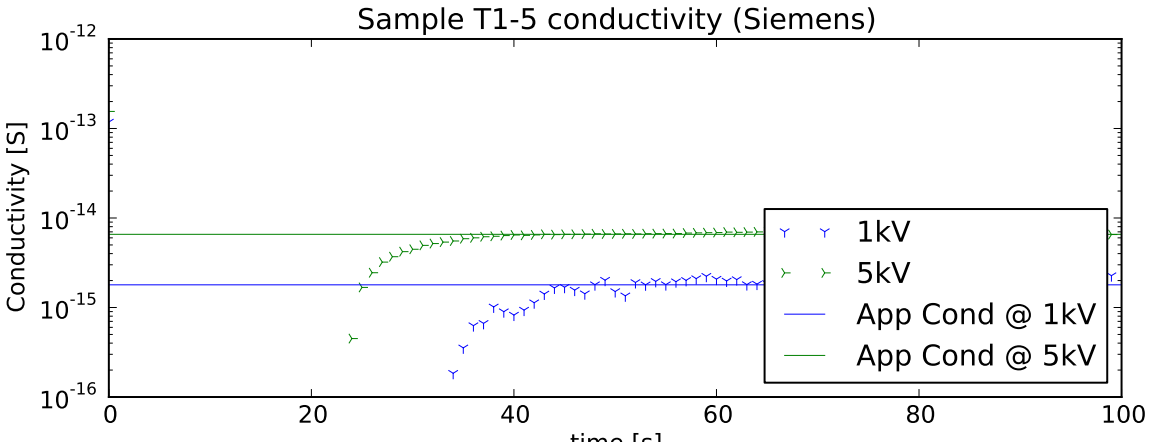

Figure B.15: Difference between charging and discharge current in sample T1-5, normalised by sample capacitance.

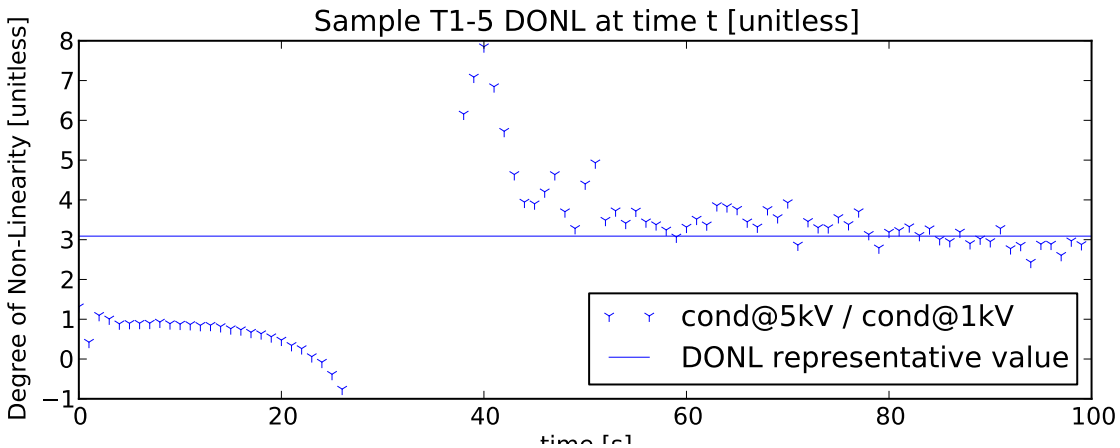

Figure B.16: Degree of Non-Linearity of sample T1-5.

B.5 Tank 1 Sample 7

T1-7

Sample Name	T1-7
Sample AC Breakdown Strength [kV]	75
Longest Vented Tree [mm]	0.22
Longest Bow Tie Tree [mm]	0.66
Number of Bow Tie Trees	528
Number of Vented Trees	3
Length of Insulation Analysed [mm]	30
Sample Water Tree Density [trees/mm]	17.00
Sample Measured Capacitance [nF]	1.73
Sample Apparent Conductivity @ 5kV [S/m]	1.74e-14
Sample Apparent Conductivity @ 1kV [S/m]	1.29e-14
DONL [conductivity]	1.35
DONL (charging) @ 30s [$\frac{I_{5kV}}{5I_{1kV}}$]	1.33
DONL (charging) @ 60s [$\frac{I_{5kV}}{5I_{1kV}}$]	1.29
DONL (discharge) @ 30s [$\frac{I_{5kV}}{5I_{1kV}}$]	1.10
DONL (discharge) @ 60s [$\frac{I_{5kV}}{5I_{1kV}}$]	1.26

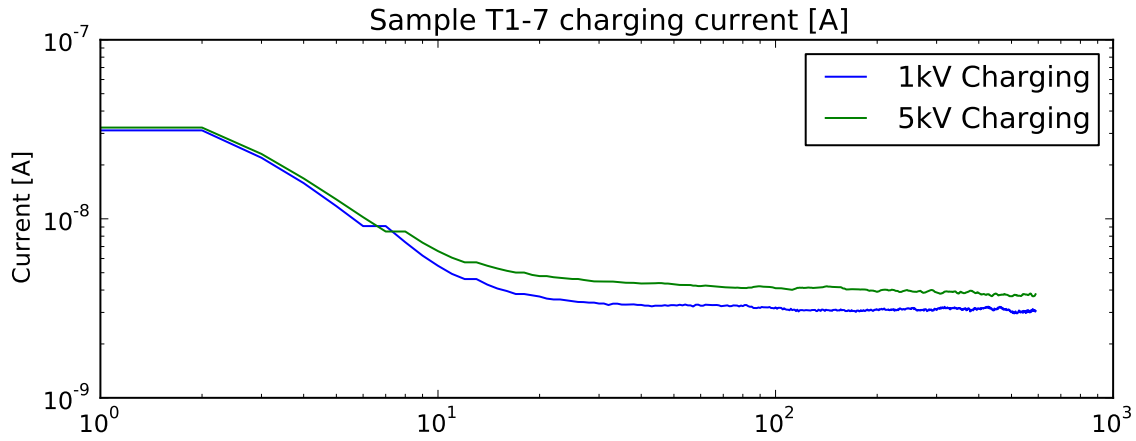

Figure B.17: Charging current of sample T1-7.

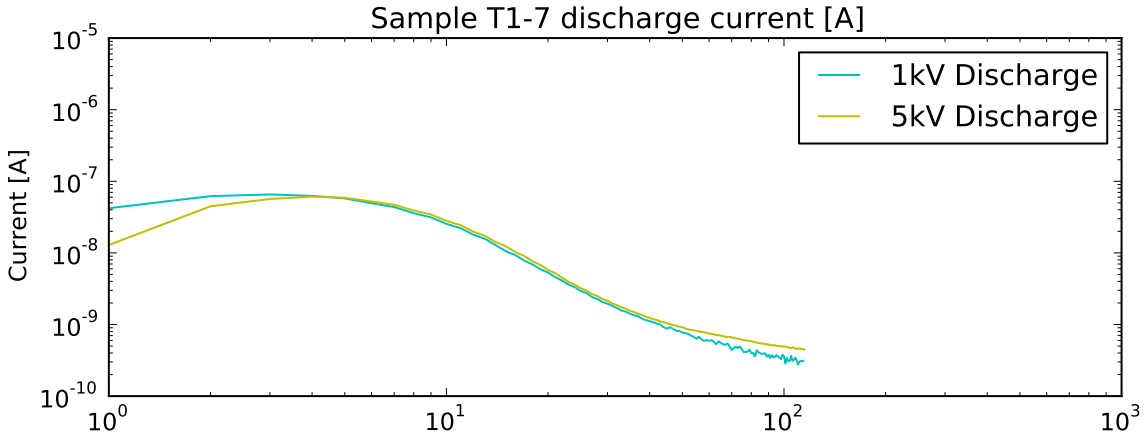

Figure B.18: Discharge current of sample T1-7.

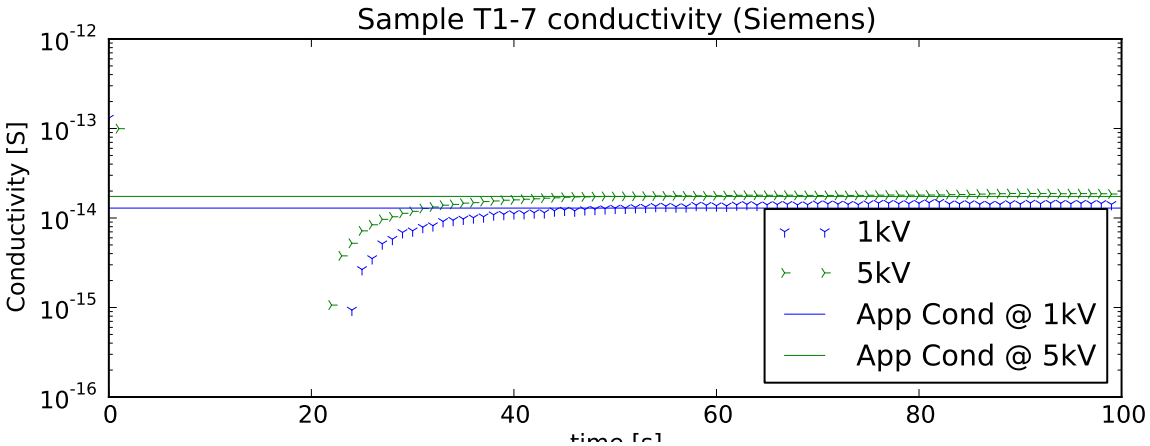

Figure B.19: Difference between charging and discharge current in sample T1-7, normalised by sample capacitance.

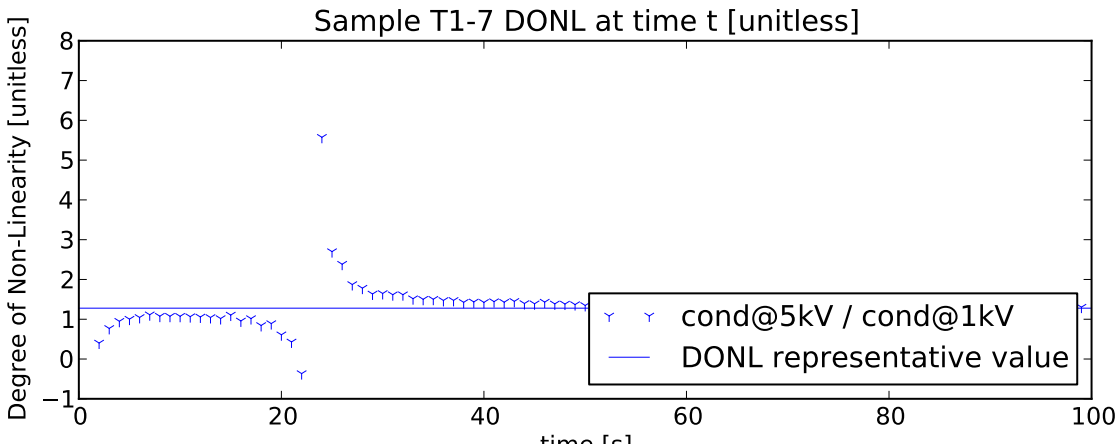

Figure B.20: Degree of Non-Linearity of sample T1-7.

B.6 Tank 1 Sample 8

T1-8

Sample Name	T1-8
Sample AC Breakdown Strength [kV]	75
Longest Vented Tree [mm]	0.60
Longest Bow Tie Tree [mm]	0.63
Number of Bow Tie Trees	343
Number of Vented Trees	11
Length of Insulation Analysed [mm]	30
Sample Water Tree Density [trees/mm]	11.00
Sample Measured Capacitance [nF]	1.75
Sample Apparent Conductivity @ 5kV [S/m]	2.84e-14
Sample Apparent Conductivity @ 1kV [S/m]	1.96e-14
DONL [conductivity]	1.45
DONL (charging) @ 30s [$\frac{I_{5kV}}{5I_{1kV}}$]	1.32
DONL (charging) @ 60s [$\frac{I_{5kV}}{5I_{1kV}}$]	1.33
DONL (discharge) @ 30s [$\frac{I_{5kV}}{5I_{1kV}}$]	0.87
DONL (discharge) @ 60s [$\frac{I_{5kV}}{5I_{1kV}}$]	0.75

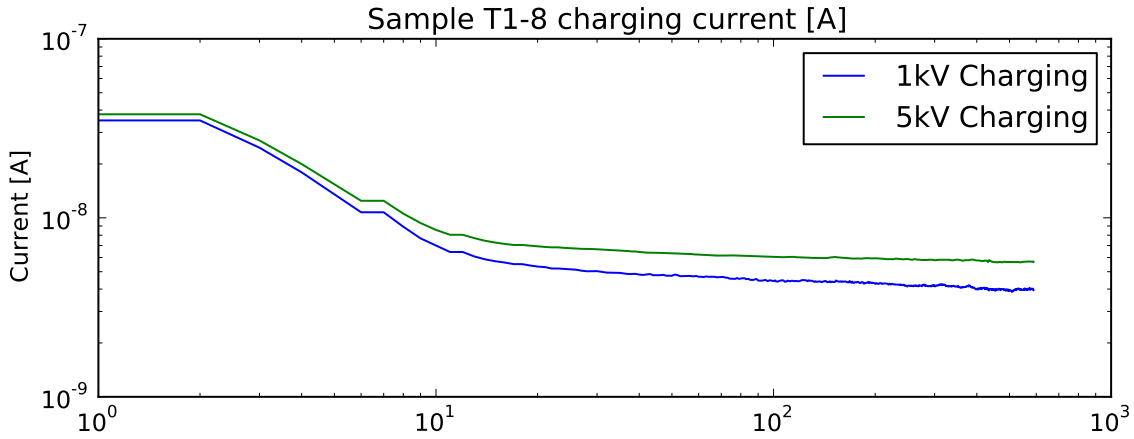

Figure B.21: Charging current of sample T1-8.

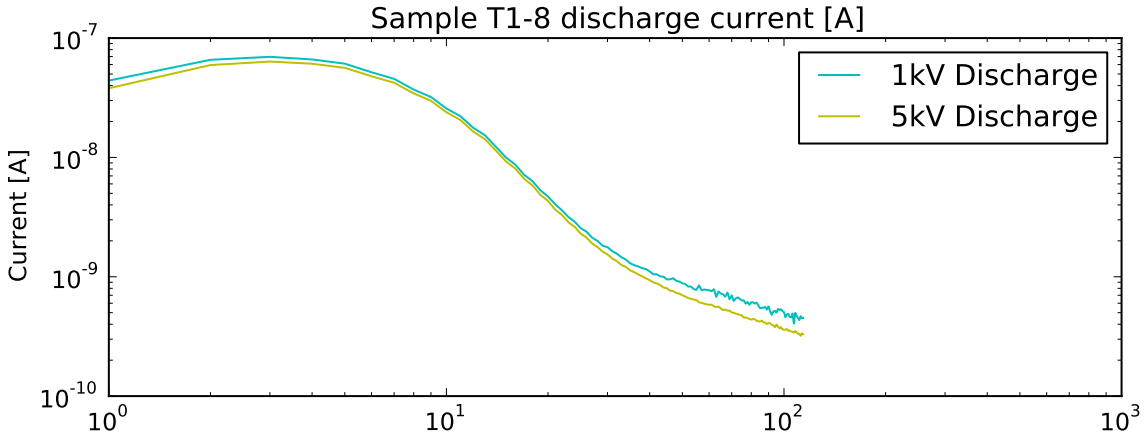

Figure B.22: Discharge current of sample T1-8.

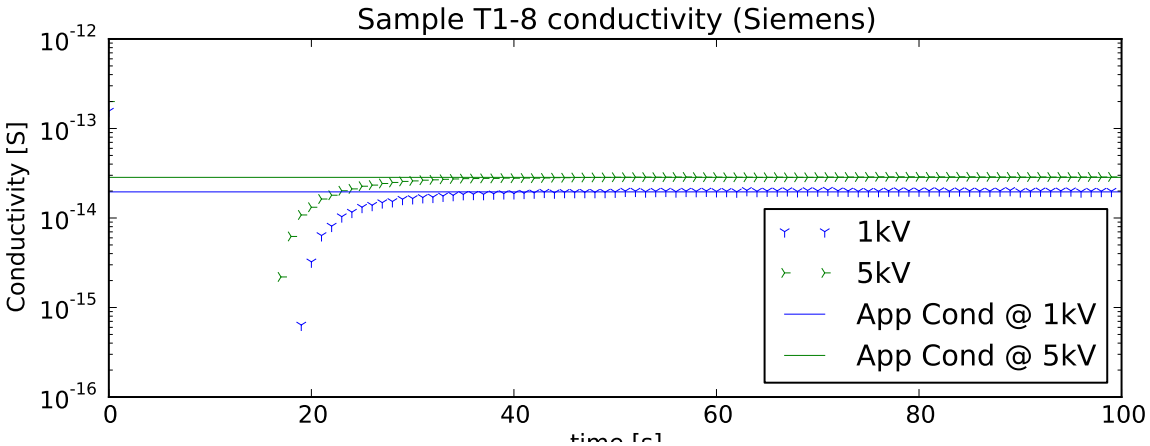

Figure B.23: Difference between charging and discharge current in sample T1-8, normalised by sample capacitance.

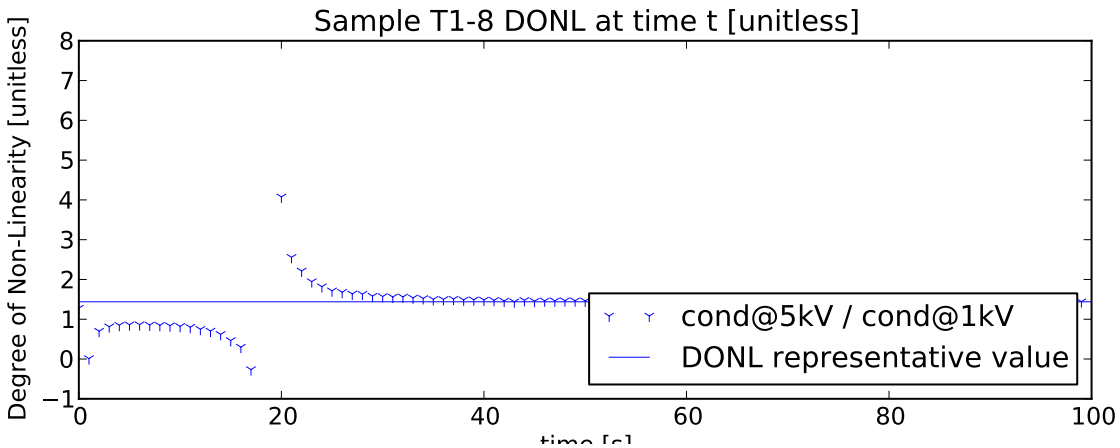

Figure B.24: Degree of Non-Linearity of sample T1-8.

B.7 Tank 1 Sample 10

T1-10

Sample Name	T1-10
Sample AC Breakdown Strength [kV]	96
Longest Vented Tree [mm]	0.36
Longest Bow Tie Tree [mm]	0.69
Number of Bow Tie Trees	283
Number of Vented Trees	9
Length of Insulation Analysed [mm]	30
Sample Water Tree Density [trees/mm]	9.00
Sample Measured Capacitance [nF]	1.74
Sample Apparent Conductivity @ 5kV [S/m]	2.34e-15
Sample Apparent Conductivity @ 1kV [S/m]	2.92e-16
DONL [conductivity]	8.01
DONL (charging) @ 30s [$\frac{I_{5kV}}{5I_{1kV}}$]	2.28
DONL (charging) @ 60s [$\frac{I_{5kV}}{5I_{1kV}}$]	2.57
DONL (discharge) @ 30s [$\frac{I_{5kV}}{5I_{1kV}}$]	1.53
DONL (discharge) @ 60s [$\frac{I_{5kV}}{5I_{1kV}}$]	1.69

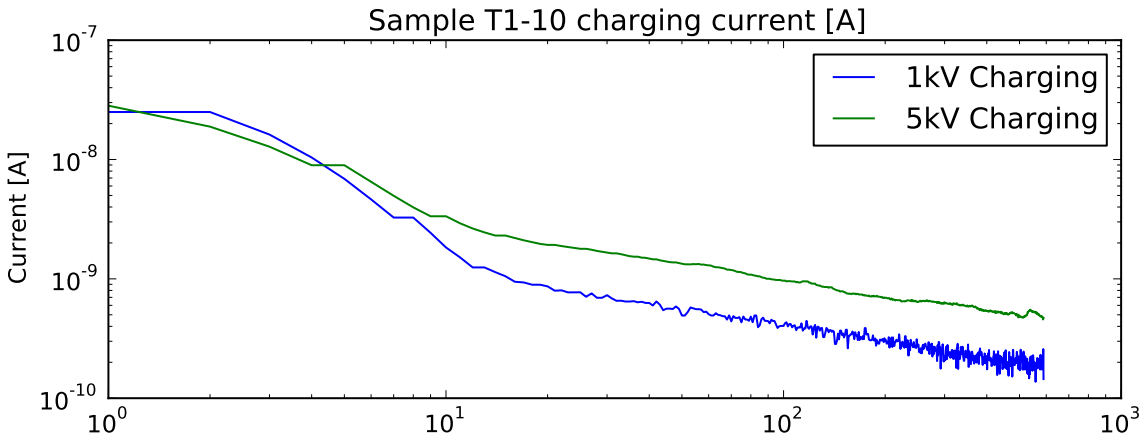

Figure B.25: Charging current of sample T1-10.

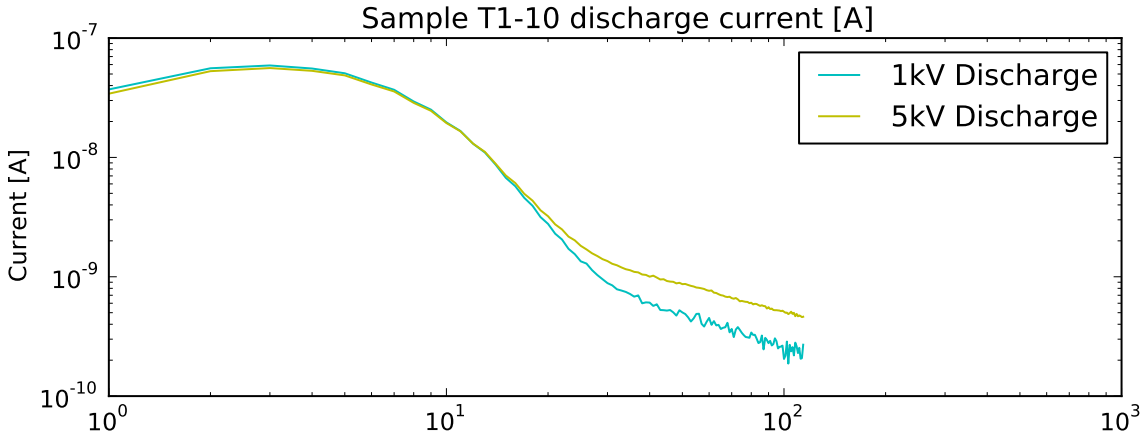

Figure B.26: Discharge current of sample T1-10.

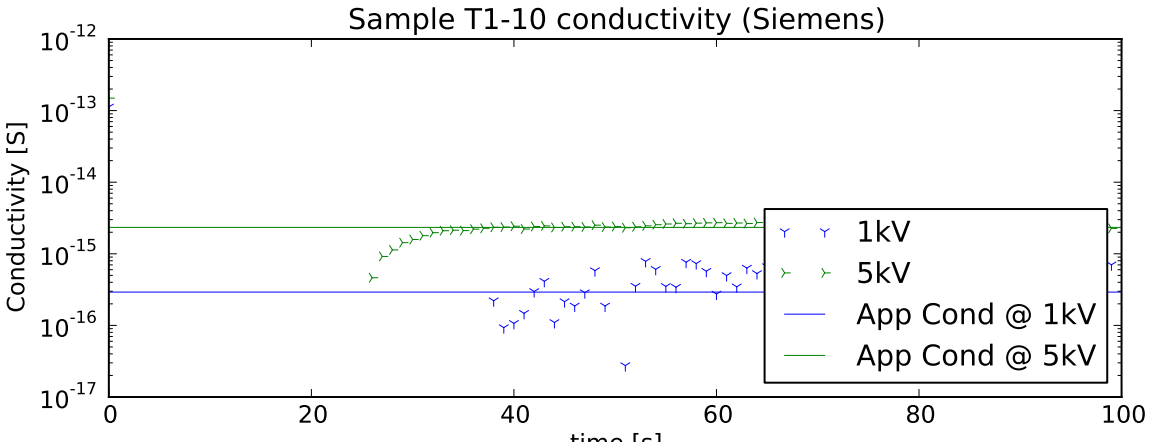

Figure B.27: Difference between charging and discharge current in sample T1-10, normalised by sample capacitance.

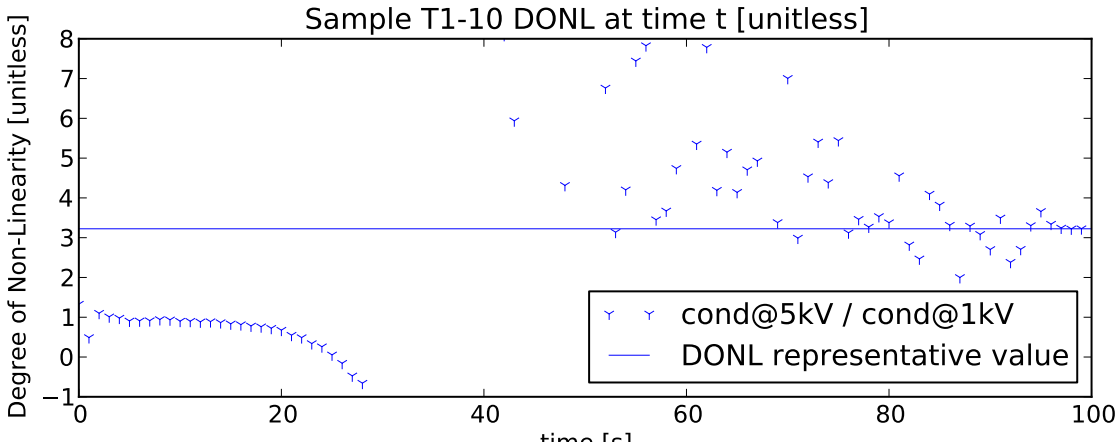

Figure B.28: Degree of Non-Linearity of sample T1-10.

B.8 Tank 3 Sample 1

T3-1

Sample Name	T3-1
Sample AC Breakdown Strength [kV]	123
Longest Vented Tree [mm]	0.00
Longest Bow Tie Tree [mm]	0.28
Number of Bow Tie Trees	15
Number of Vented Trees	0
Length of Insulation Analysed [mm]	30
Sample Water Tree Density [trees/mm]	0.00
Sample Measured Capacitance [nF]	1.69
Sample Apparent Conductivity @ 5kV [S/m]	-1.71e-15
Sample Apparent Conductivity @ 1kV [S/m]	-8.59e-16
DONL [conductivity]	1.99
DONL (charging) @ 30s [$\frac{I_{5kV}}{5I_{1kV}}$]	0.76
DONL (charging) @ 60s [$\frac{I_{5kV}}{5I_{1kV}}$]	0.58
DONL (discharge) @ 30s [$\frac{I_{5kV}}{5I_{1kV}}$]	1.08
DONL (discharge) @ 60s [$\frac{I_{5kV}}{5I_{1kV}}$]	1.46

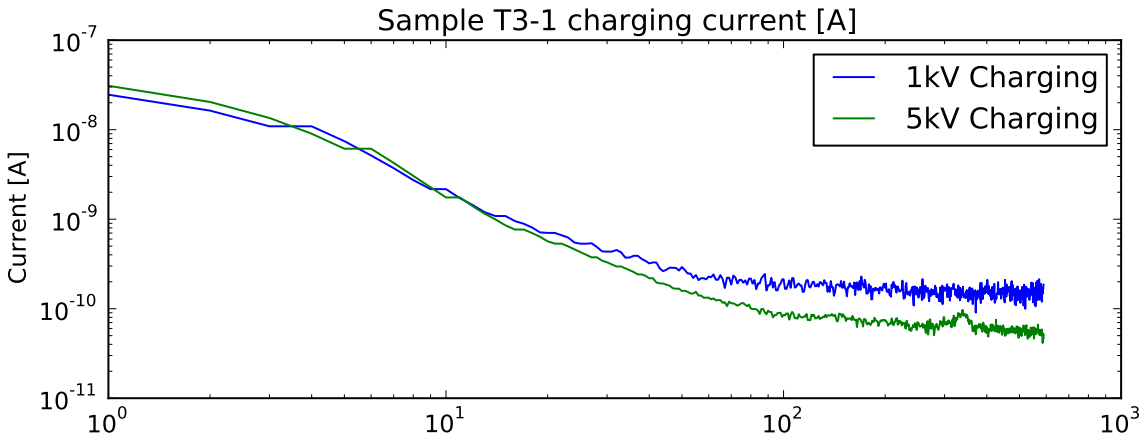

Figure B.29: Charging current of sample T3-1.

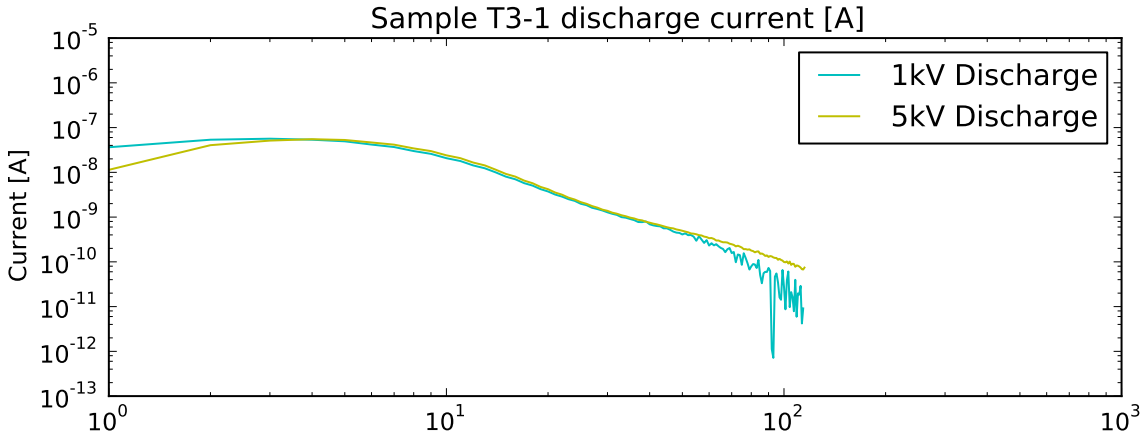

Figure B.30: Discharge current of sample T3-1.

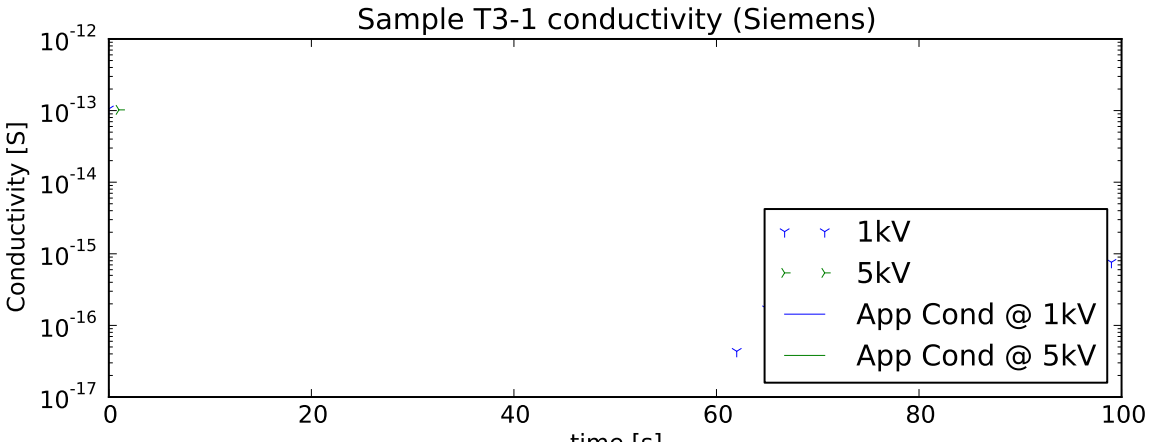

Figure B.31: Difference between charging and discharge current in sample T3-1, normalised by sample capacitance.

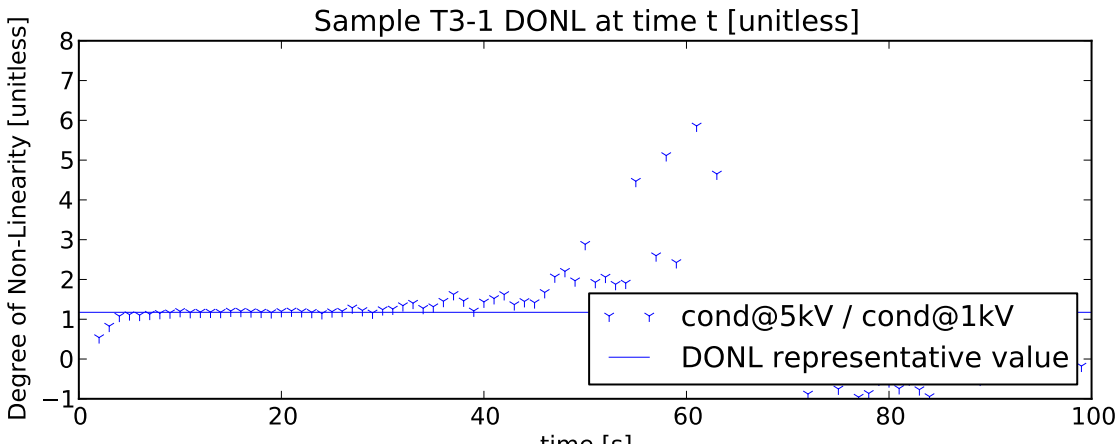

Figure B.32: Degree of Non-Linearity of sample T3-1.

B.9 Tank 3 Sample 2

T3-2

Sample Name	T3-2
Sample AC Breakdown Strength [kV]	124
Longest Vented Tree [mm]	0.40
Longest Bow Tie Tree [mm]	0.28
Number of Bow Tie Trees	6
Number of Vented Trees	1
Length of Insulation Analysed [mm]	30
Sample Water Tree Density [trees/mm]	0.00
Sample Measured Capacitance [nF]	1.71
Sample Apparent Conductivity @ 5kV [S/m]	6.85e-15
Sample Apparent Conductivity @ 1kV [S/m]	2.21e-15
DONL [conductivity]	3.10
DONL (charging) @ 30s [$\frac{I_{5kV}}{5I_{1kV}}$]	1.89
DONL (charging) @ 60s [$\frac{I_{5kV}}{5I_{1kV}}$]	2.08
DONL (discharge) @ 30s [$\frac{I_{5kV}}{5I_{1kV}}$]	0.89
DONL (discharge) @ 60s [$\frac{I_{5kV}}{5I_{1kV}}$]	0.87

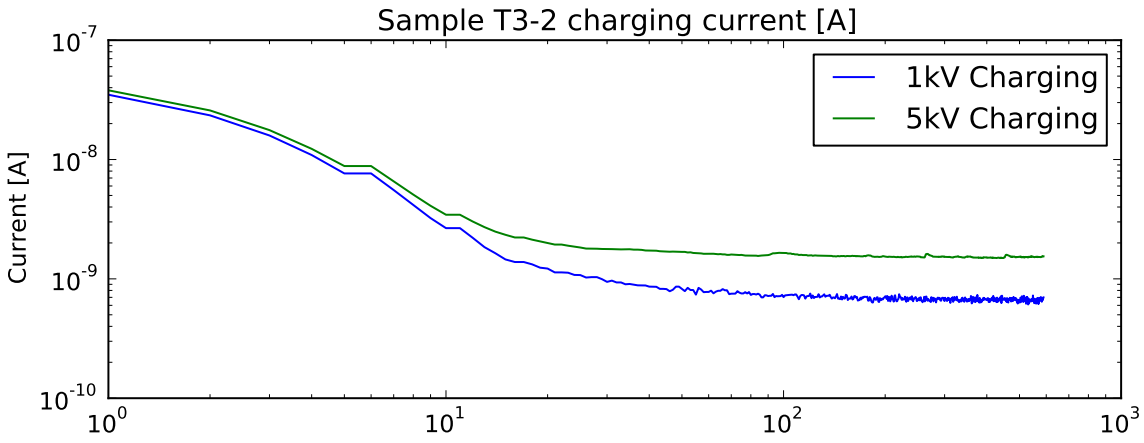

Figure B.33: Charging current of sample T3-2.

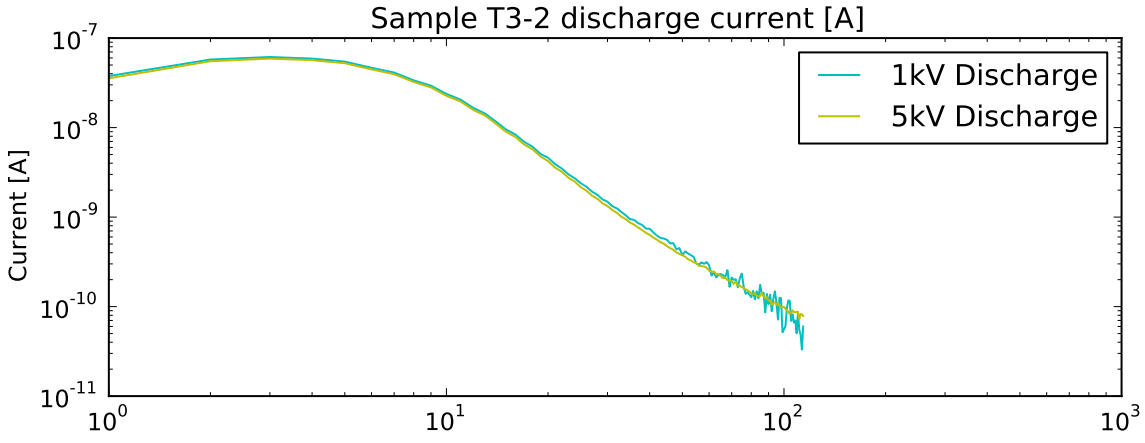

Figure B.34: Discharge current of sample T3-2.

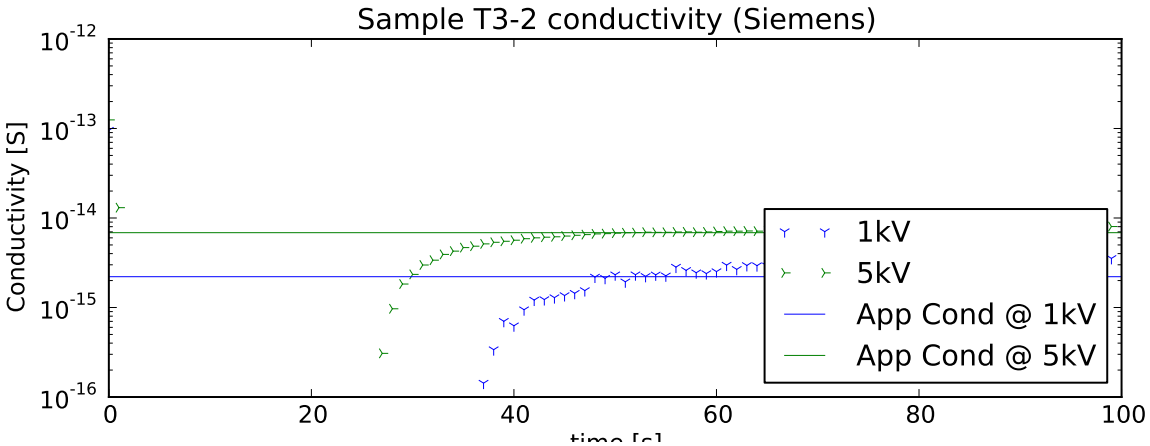

Figure B.35: Difference between charging and discharge current in sample T3-2, normalised by sample capacitance.

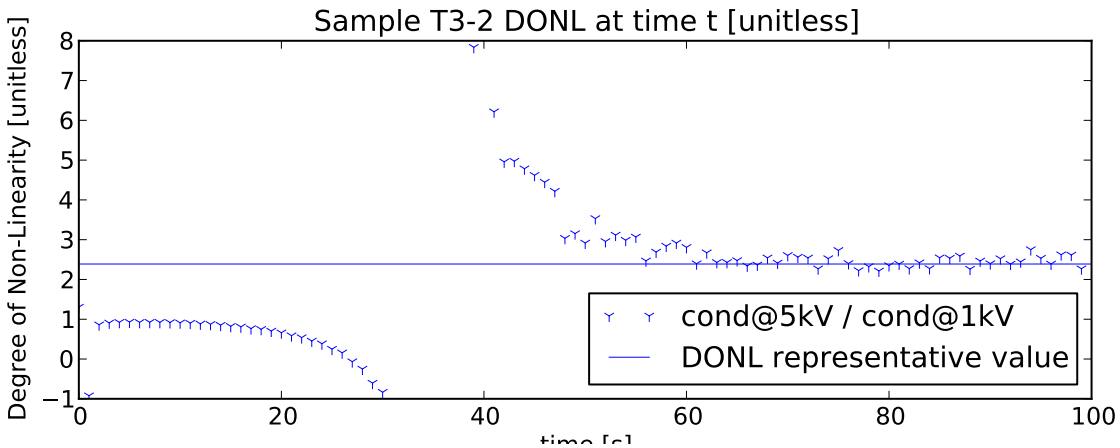

Figure B.36: Degree of Non-Linearity of sample T3-2.

B.10 Tank 3 Sample 3

T3-3

Sample Name	T3-3
Sample AC Breakdown Strength [kV]	110
Longest Vented Tree [mm]	0.16
Longest Bow Tie Tree [mm]	0.36
Number of Bow Tie Trees	18
Number of Vented Trees	1
Length of Insulation Analysed [mm]	30
Sample Water Tree Density [trees/mm]	0.00
Sample Measured Capacitance [nF]	1.72
Sample Apparent Conductivity @ 5kV [S/m]	3.61e-15
Sample Apparent Conductivity @ 1kV [S/m]	2.38e-15
DONL [conductivity]	1.52
DONL (charging) @ 30s [$\frac{I_{5kV}}{5I_{1kV}}$]	1.43
DONL (charging) @ 60s [$\frac{I_{5kV}}{5I_{1kV}}$]	1.44
DONL (discharge) @ 30s [$\frac{I_{5kV}}{5I_{1kV}}$]	1.07
DONL (discharge) @ 60s [$\frac{I_{5kV}}{5I_{1kV}}$]	2.08

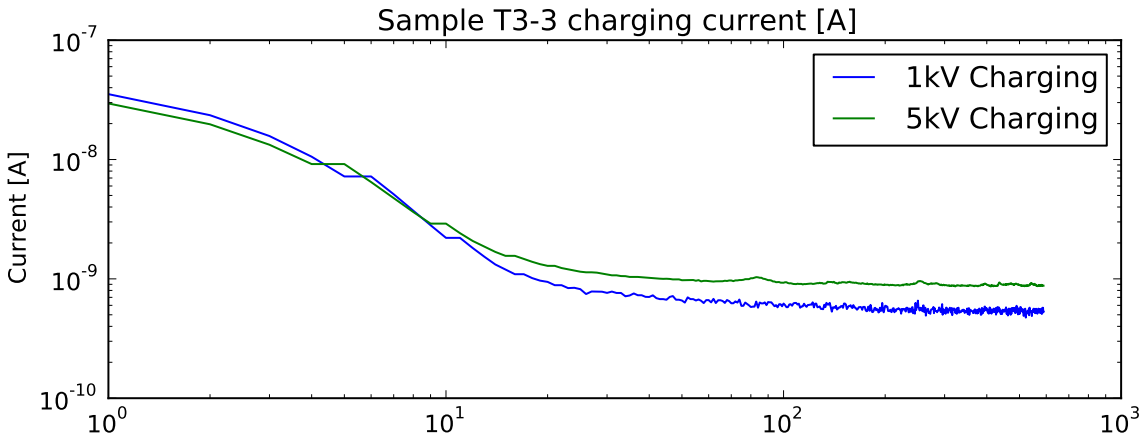

Figure B.37: Charging current of sample T3-3.

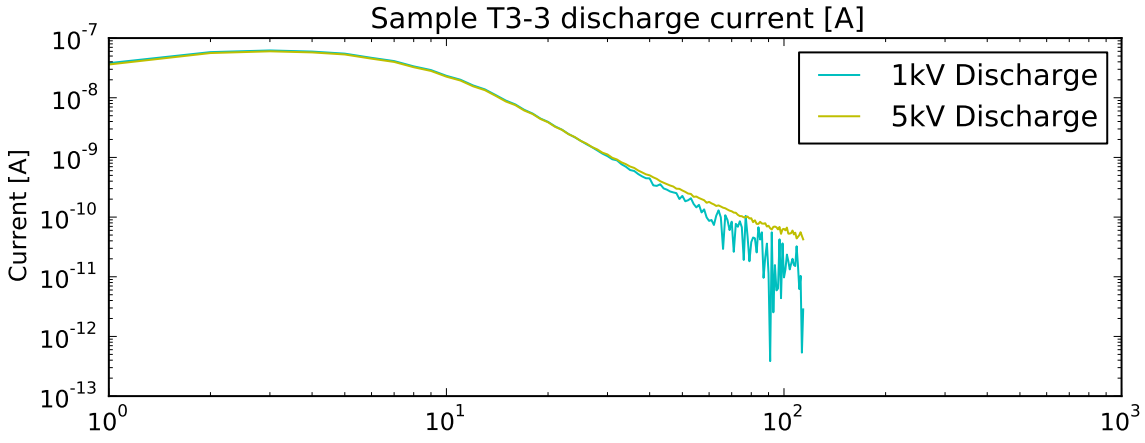

Figure B.38: Discharge current of sample T3-3.

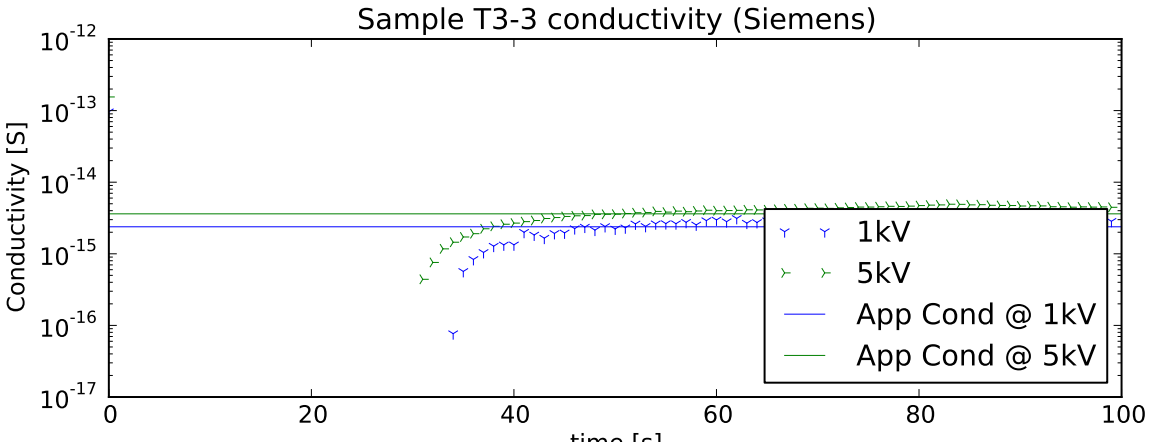

Figure B.39: Difference between charging and discharge current in sample T3-3, normalised by sample capacitance.

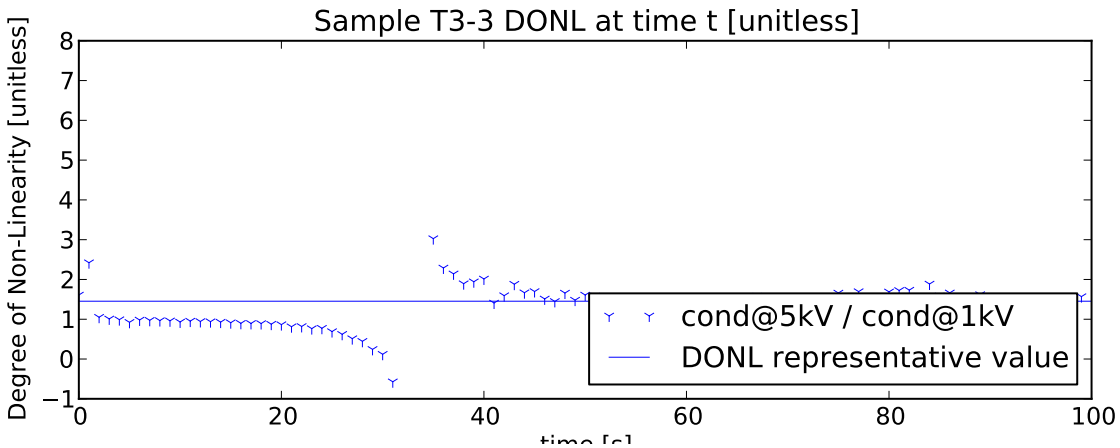

Figure B.40: Degree of Non-Linearity of sample T3-3.

B.11 Tank 3 Sample 4

T3-4

Sample Name	T3-4
Sample AC Breakdown Strength [kV]	110
Longest Vented Tree [mm]	0.84
Longest Bow Tie Tree [mm]	0.40
Number of Bow Tie Trees	6
Number of Vented Trees	69
Length of Insulation Analysed [mm]	30
Sample Water Tree Density [trees/mm]	2.00
Sample Measured Capacitance [nF]	1.73
Sample Apparent Conductivity @ 5kV [S/m]	3.70e-15
Sample Apparent Conductivity @ 1kV [S/m]	2.44e-15
DONL [conductivity]	1.52
DONL (charging) @ 30s [$\frac{I_{5kV}}{5I_{1kV}}$]	1.60
DONL (charging) @ 60s [$\frac{I_{5kV}}{5I_{1kV}}$]	1.38
DONL (discharge) @ 30s [$\frac{I_{5kV}}{5I_{1kV}}$]	0.86
DONL (discharge) @ 60s [$\frac{I_{5kV}}{5I_{1kV}}$]	1.71

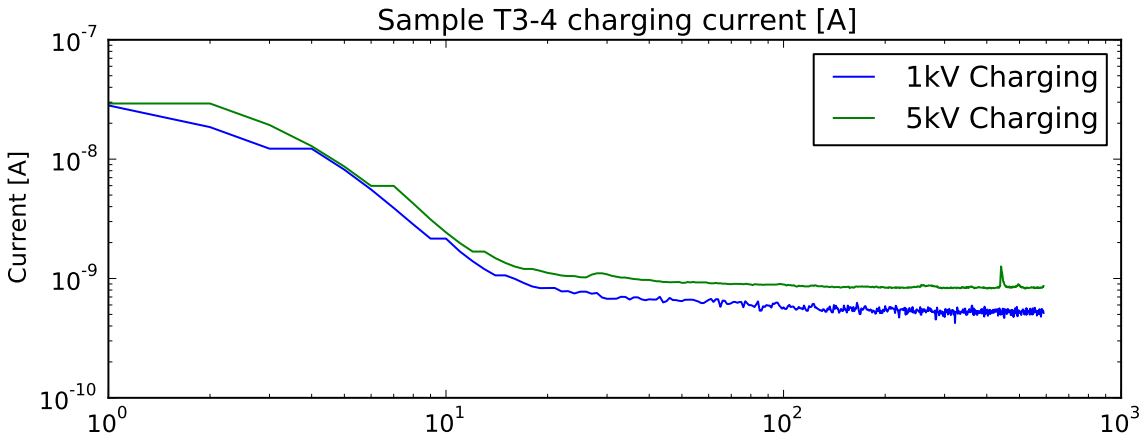

Figure B.41: Charging current of sample T3-4.

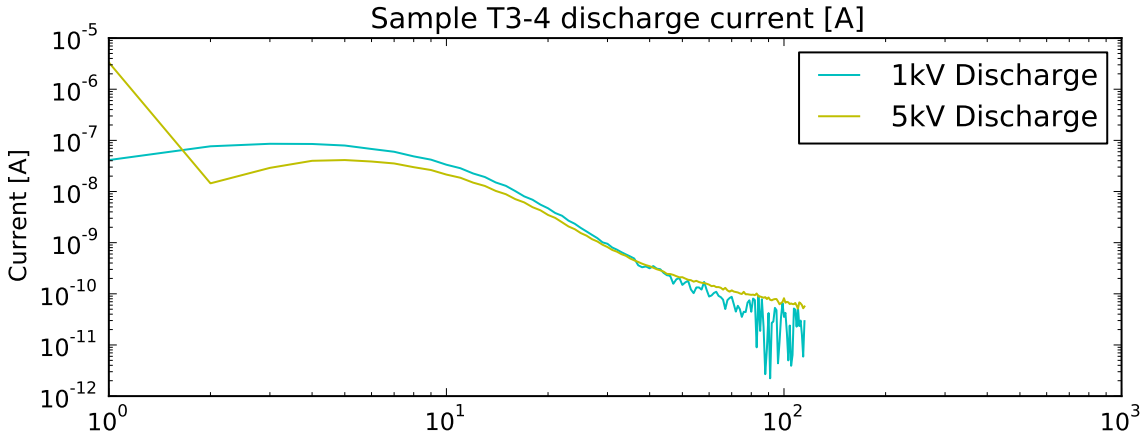

Figure B.42: Discharge current of sample T3-4.

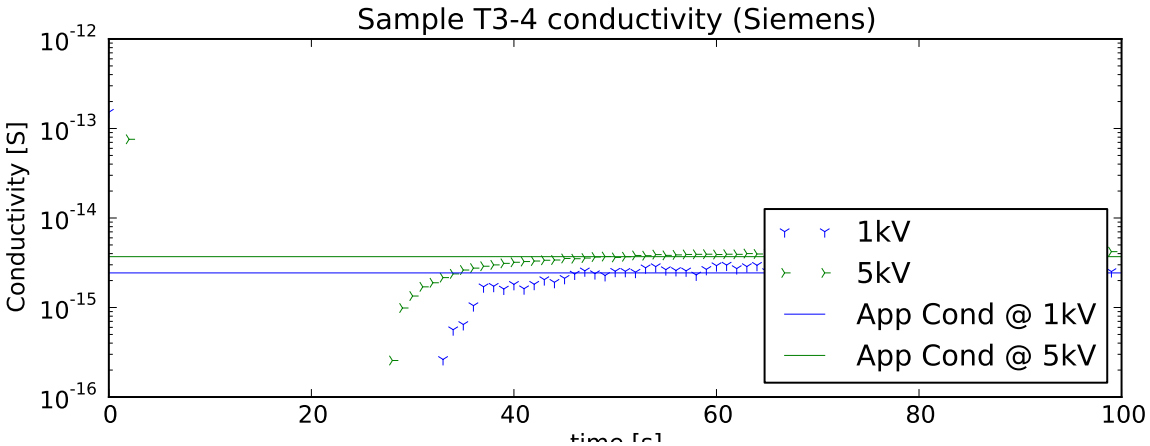

Figure B.43: Difference between charging and discharge current in sample T3-4, normalised by sample capacitance.

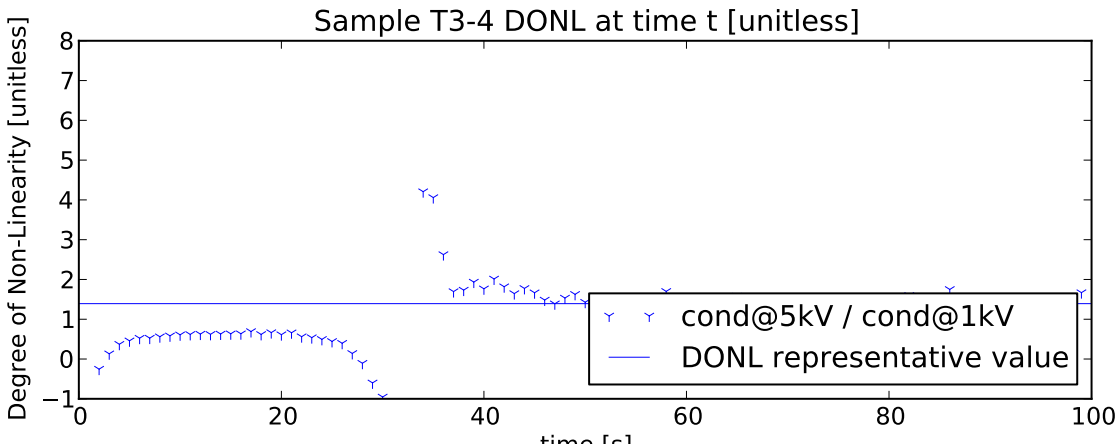

Figure B.44: Degree of Non-Linearity of sample T3-4.

B.12 Tank 3 Sample 5

T3-5

Sample Name	T3-5
Sample AC Breakdown Strength [kV]	103
Longest Vented Tree [mm]	0.40
Longest Bow Tie Tree [mm]	0.36
Number of Bow Tie Trees	21
Number of Vented Trees	17
Length of Insulation Analysed [mm]	30
Sample Water Tree Density [trees/mm]	1.00
Sample Measured Capacitance [nF]	1.77
Sample Apparent Conductivity @ 5kV [S/m]	2.90e-14
Sample Apparent Conductivity @ 1kV [S/m]	1.75e-14
DONL [conductivity]	1.65
DONL (charging) @ 30s [$\frac{I_{5kV}}{5I_{1kV}}$]	1.48
DONL (charging) @ 60s [$\frac{I_{5kV}}{5I_{1kV}}$]	1.51
DONL (discharge) @ 30s [$\frac{I_{5kV}}{5I_{1kV}}$]	0.94
DONL (discharge) @ 60s [$\frac{I_{5kV}}{5I_{1kV}}$]	1.11

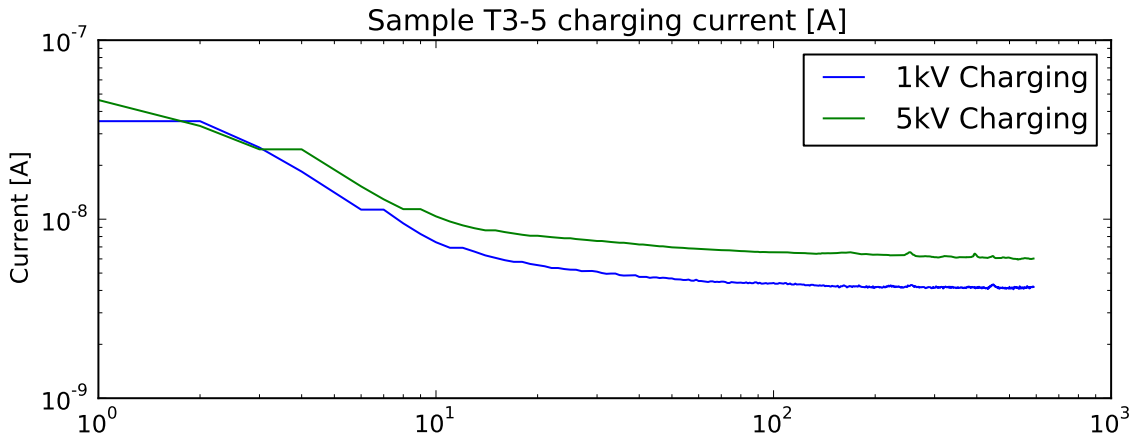

Figure B.45: Charging current of sample T3-5.

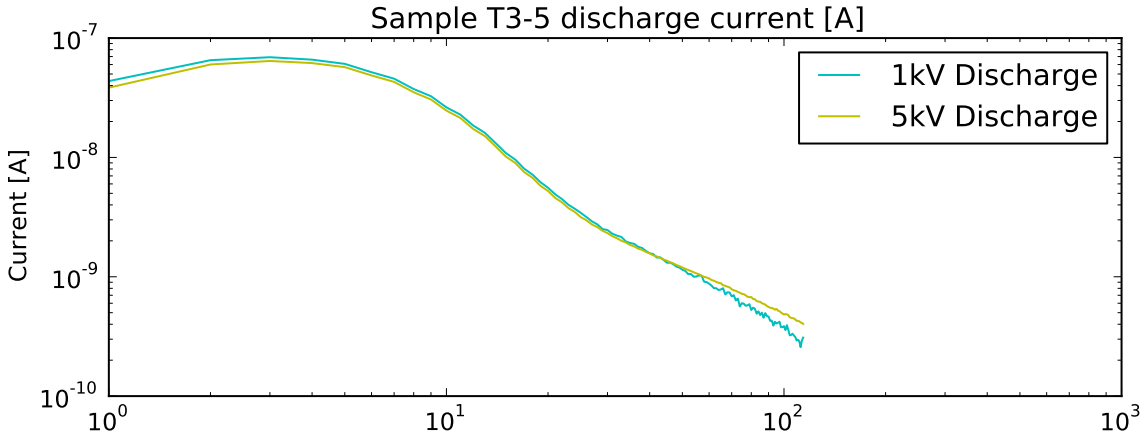

Figure B.46: Discharge current of sample T3-5.

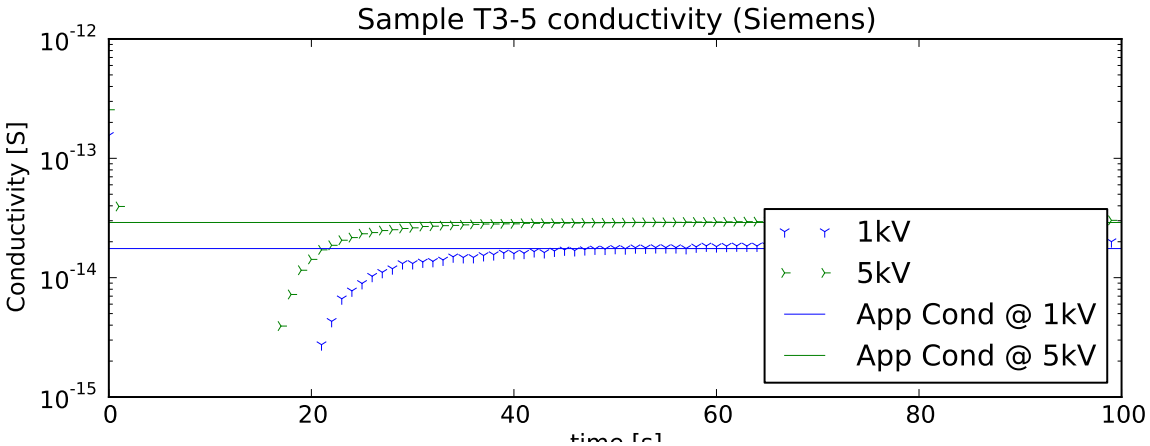

Figure B.47: Difference between charging and discharge current in sample T3-5, normalised by sample capacitance.

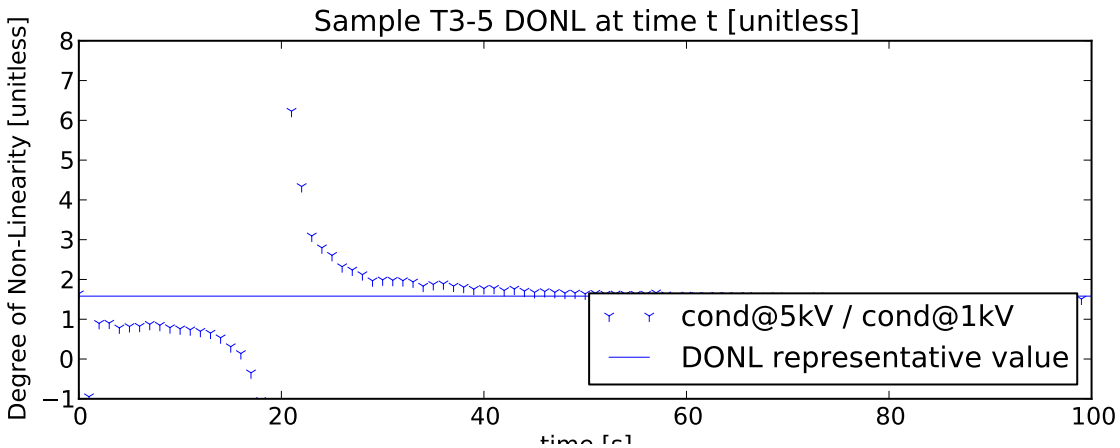

Figure B.48: Degree of Non-Linearity of sample T3-5.

B.13 Tank 3 Sample 6

T3-6

Sample Name	T3-6
Sample AC Breakdown Strength [kV]	131
Longest Vented Tree [mm]	0.54
Longest Bow Tie Tree [mm]	0.28
Number of Bow Tie Trees	12
Number of Vented Trees	21
Length of Insulation Analysed [mm]	30
Sample Water Tree Density [trees/mm]	1.00
Sample Measured Capacitance [nF]	1.80
Sample Apparent Conductivity @ 5kV [S/m]	-6.68e-16
Sample Apparent Conductivity @ 1kV [S/m]	4.84e-15
DONL [conductivity]	-0.14
DONL (charging) @ 30s [$\frac{I_{5kV}}{5I_{1kV}}$]	0.14
DONL (charging) @ 60s [$\frac{I_{5kV}}{5I_{1kV}}$]	0.16
DONL (discharge) @ 30s [$\frac{I_{5kV}}{5I_{1kV}}$]	0.83
DONL (discharge) @ 60s [$\frac{I_{5kV}}{5I_{1kV}}$]	1.20

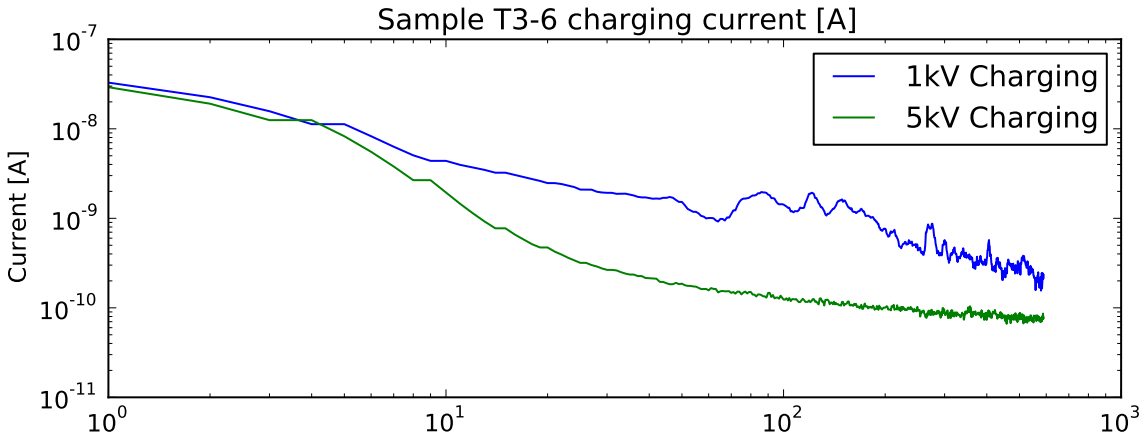

Figure B.49: Charging current of sample T3-6.

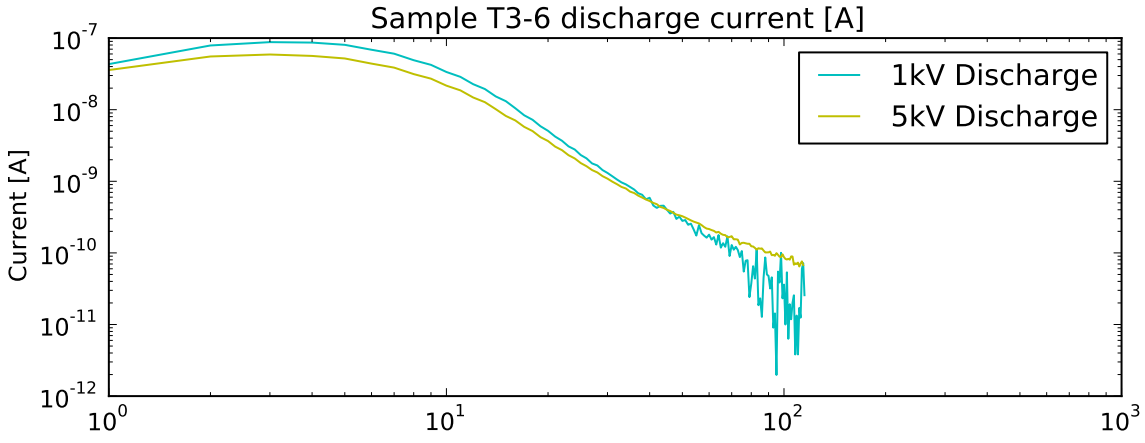

Figure B.50: Discharge current of sample T3-6.

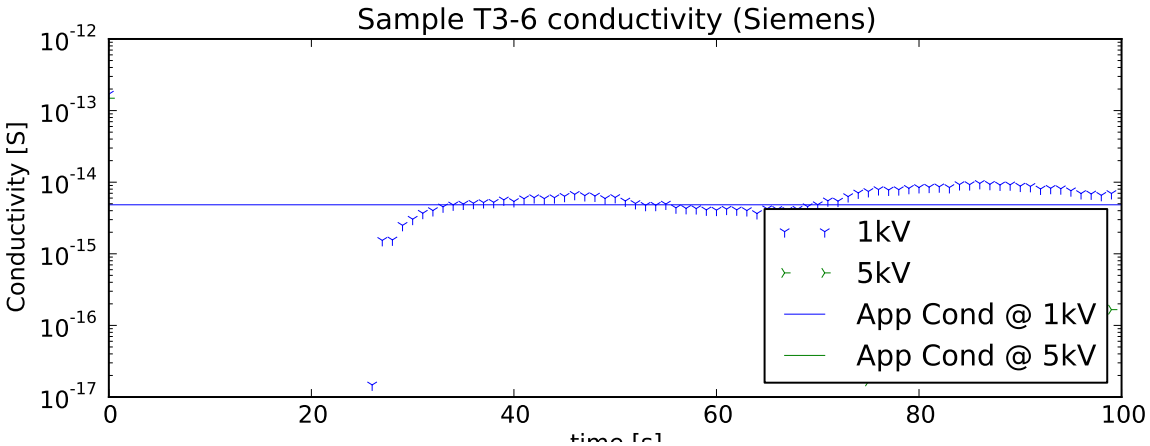

Figure B.51: Difference between charging and discharge current in sample T3-6, normalised by sample capacitance.

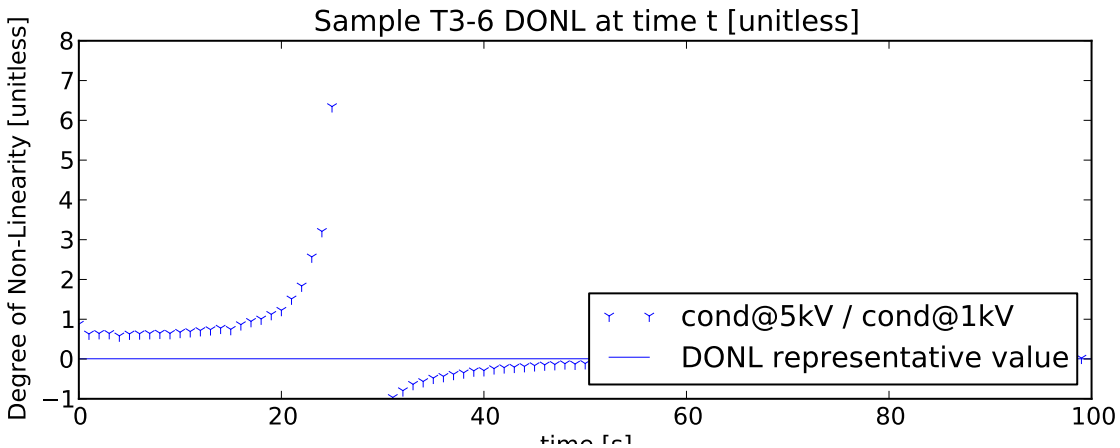

Figure B.52: Degree of Non-Linearity of sample T3-6.

B.14 Tank 3 Sample 7

T3-7

Sample Name	T3-7
Sample AC Breakdown Strength [kV]	89
Longest Vented Tree [mm]	0.32
Longest Bow Tie Tree [mm]	0.20
Number of Bow Tie Trees	11
Number of Vented Trees	7
Length of Insulation Analysed [mm]	30
Sample Water Tree Density [trees/mm]	0.00
Sample Measured Capacitance [nF]	1.79
Sample Apparent Conductivity @ 5kV [S/m]	-1.57e-15
Sample Apparent Conductivity @ 1kV [S/m]	-9.10e-16
DONL [conductivity]	1.73
DONL (charging) @ 30s [$\frac{I_{5kV}}{5I_{1kV}}$]	0.91
DONL (charging) @ 60s [$\frac{I_{5kV}}{5I_{1kV}}$]	0.61
DONL (discharge) @ 30s [$\frac{I_{5kV}}{5I_{1kV}}$]	1.04
DONL (discharge) @ 60s [$\frac{I_{5kV}}{5I_{1kV}}$]	1.10

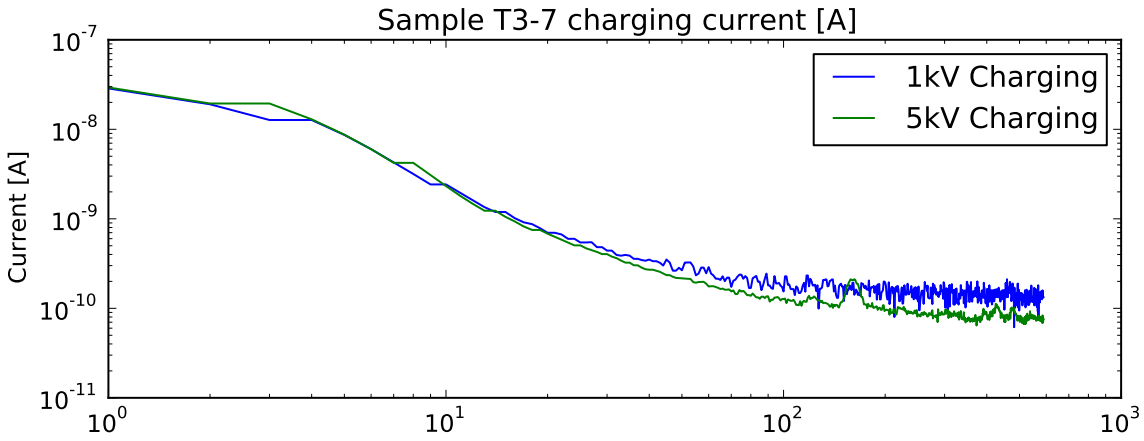

Figure B.53: Charging current of sample T3-7.

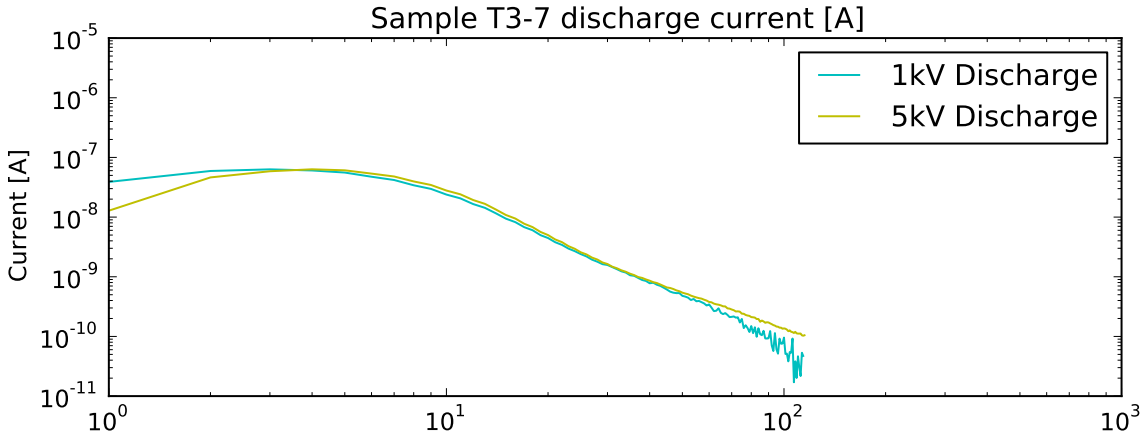

Figure B.54: Discharge current of sample T3-7.

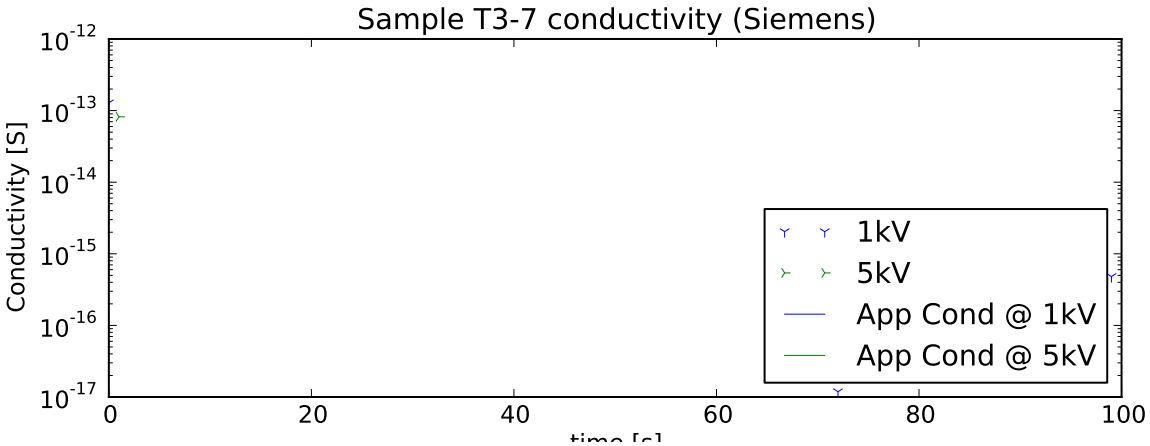

Figure B.55: Difference between charging and discharge current in sample T3-7, normalised by sample capacitance.

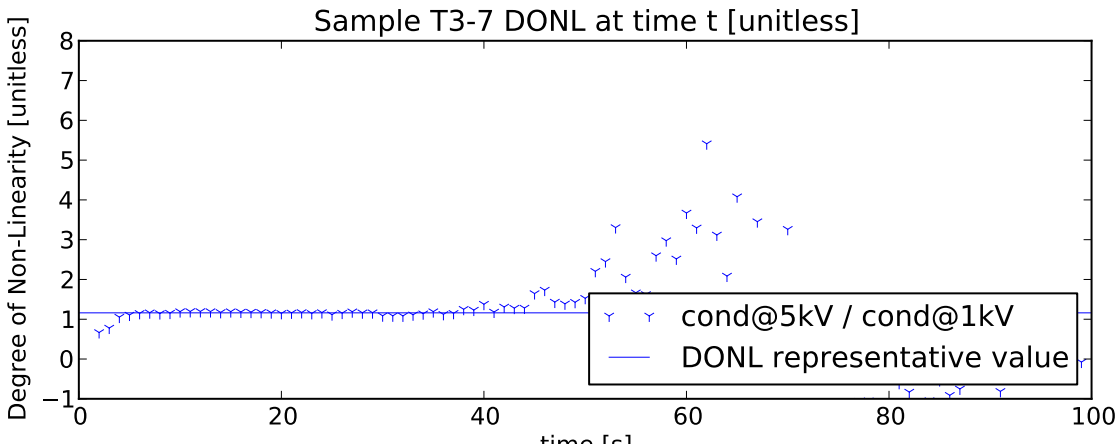

Figure B.56: Degree of Non-Linearity of sample T3-7.

B.15 Tank 3 Sample 8

T3-8

Sample Name	T3-8
Sample AC Breakdown Strength [kV]	96
Longest Vented Tree [mm]	0.16
Longest Bow Tie Tree [mm]	0.26
Number of Bow Tie Trees	18
Number of Vented Trees	3
Length of Insulation Analysed [mm]	30
Sample Water Tree Density [trees/mm]	0.00
Sample Measured Capacitance [nF]	1.86
Sample Apparent Conductivity @ 5kV [S/m]	4.49e-15
Sample Apparent Conductivity @ 1kV [S/m]	7.02e-16
DONL [conductivity]	6.40
DONL (charging) @ 30s [$\frac{I_{5kV}}{5I_{1kV}}$]	2.98
DONL (charging) @ 60s [$\frac{I_{5kV}}{5I_{1kV}}$]	4.88
DONL (discharge) @ 30s [$\frac{I_{5kV}}{5I_{1kV}}$]	1.37
DONL (discharge) @ 60s [$\frac{I_{5kV}}{5I_{1kV}}$]	6.26

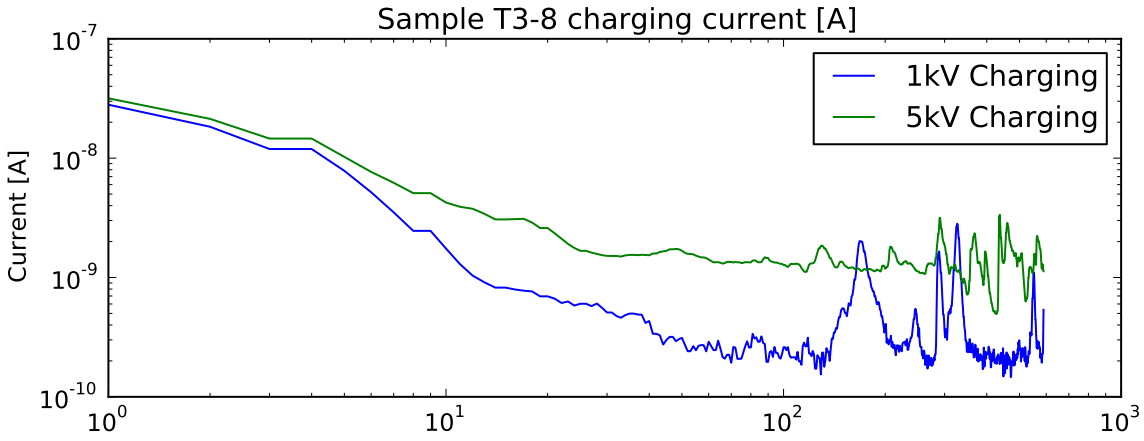

Figure B.57: Charging current of sample T3-8.

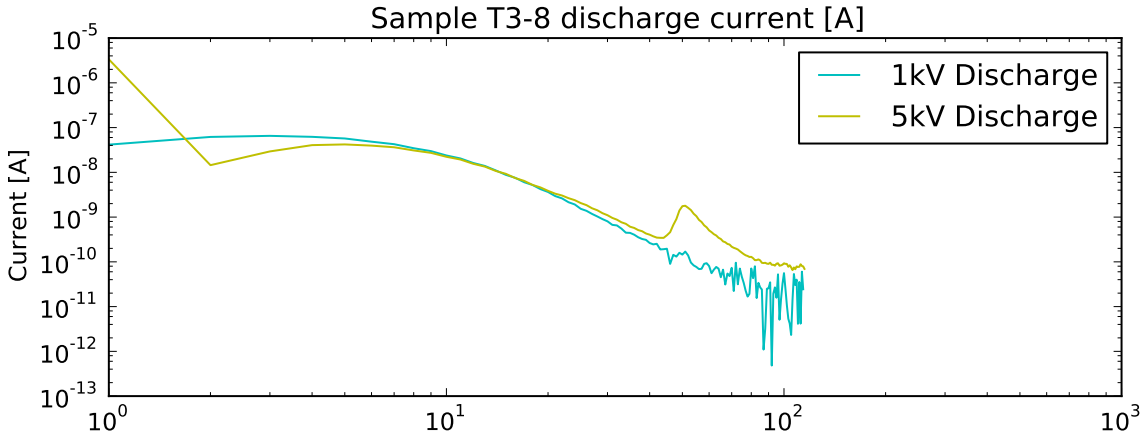

Figure B.58: Discharge current of sample T3-8.

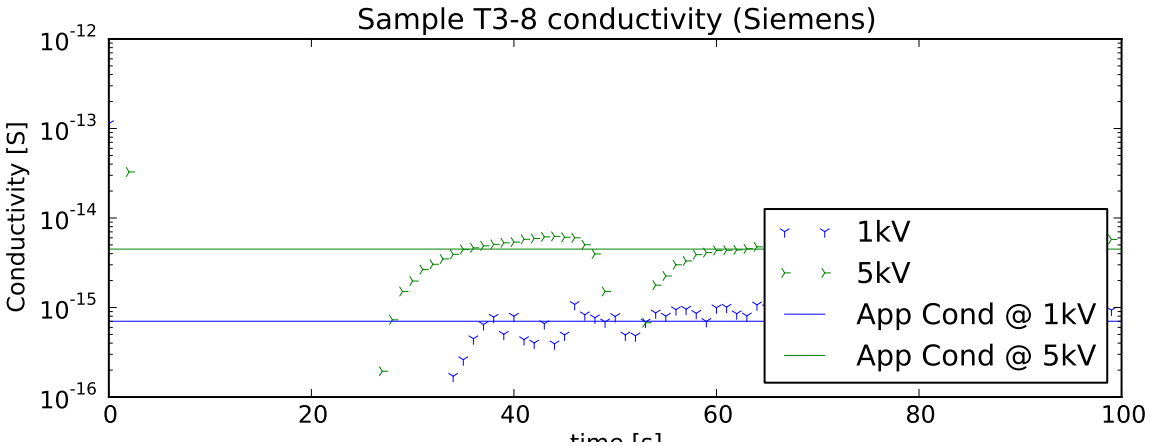

Figure B.59: Difference between charging and discharge current in sample T3-8, normalised by sample capacitance.

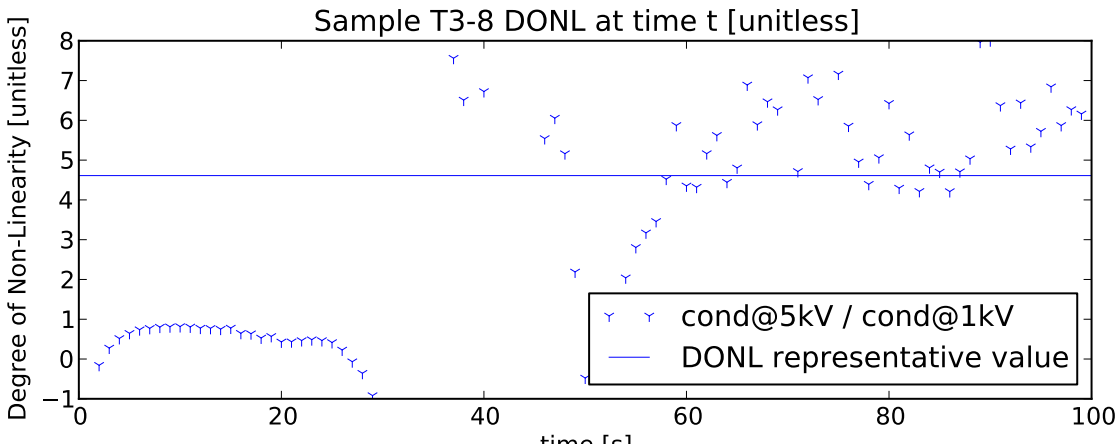

Figure B.60: Degree of Non-Linearity of sample T3-8.

B.16 Tank 3 Sample 9

T3-9

Sample Name	T3-9
Sample AC Breakdown Strength [kV]	89
Longest Vented Tree [mm]	0.50
Longest Bow Tie Tree [mm]	0.22
Number of Bow Tie Trees	22
Number of Vented Trees	4
Length of Insulation Analysed [mm]	30
Sample Water Tree Density [trees/mm]	0.00
Sample Measured Capacitance [nF]	1.82
Sample Apparent Conductivity @ 5kV [S/m]	2.10e-15
Sample Apparent Conductivity @ 1kV [S/m]	8.39e-16
DONL [conductivity]	2.50
DONL (charging) @ 30s [$\frac{I_{5kV}}{5I_{1kV}}$]	1.35
DONL (charging) @ 60s [$\frac{I_{5kV}}{5I_{1kV}}$]	2.36
DONL (discharge) @ 30s [$\frac{I_{5kV}}{5I_{1kV}}$]	0.91
DONL (discharge) @ 60s [$\frac{I_{5kV}}{5I_{1kV}}$]	1.92

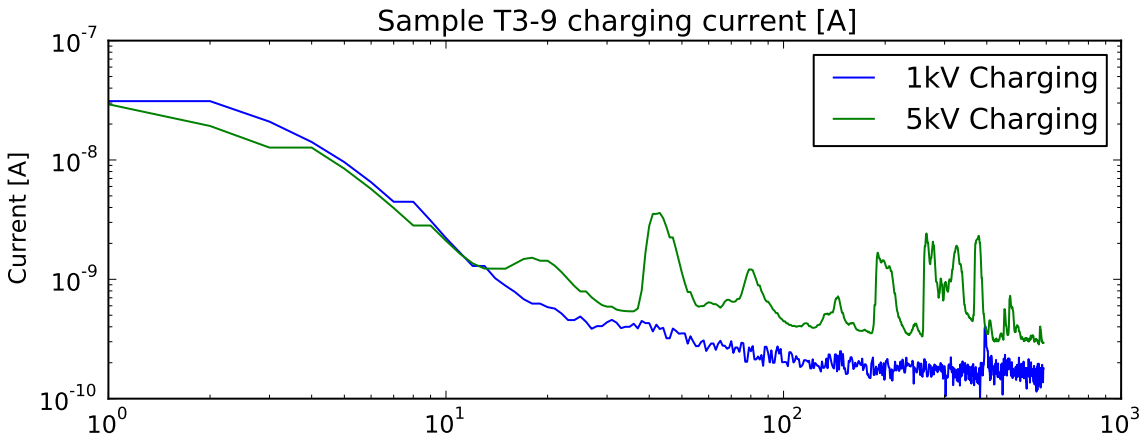

Figure B.61: Charging current of sample T3-9.

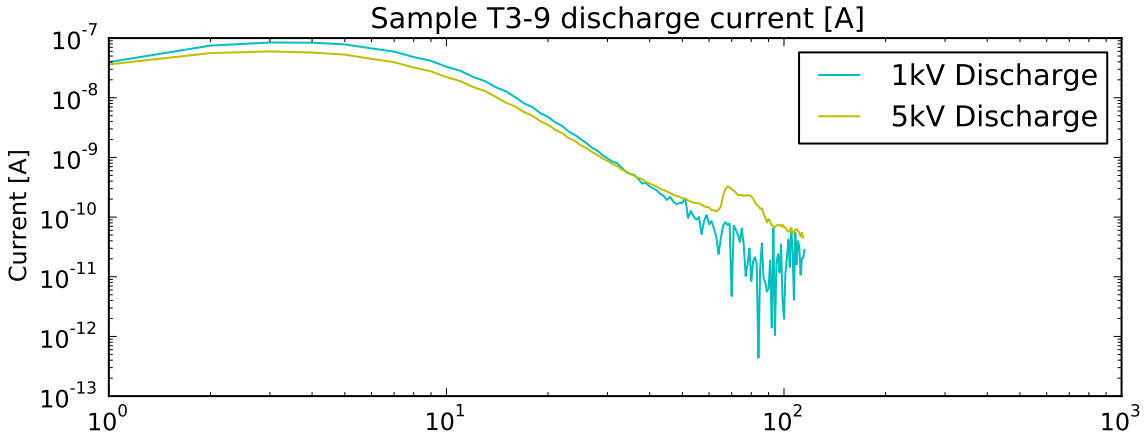

Figure B.62: Discharge current of sample T3-9.

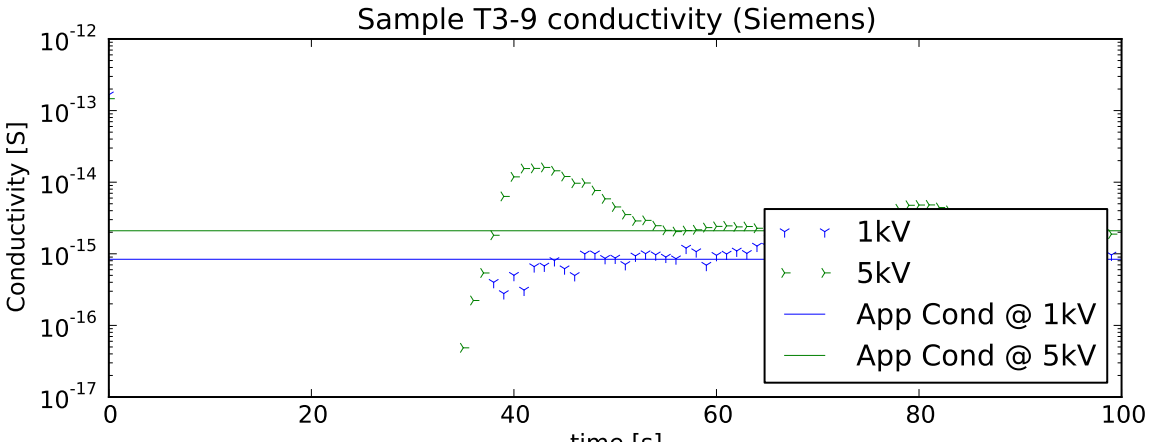

Figure B.63: Difference between charging and discharge current in sample T3-9, normalised by sample capacitance.

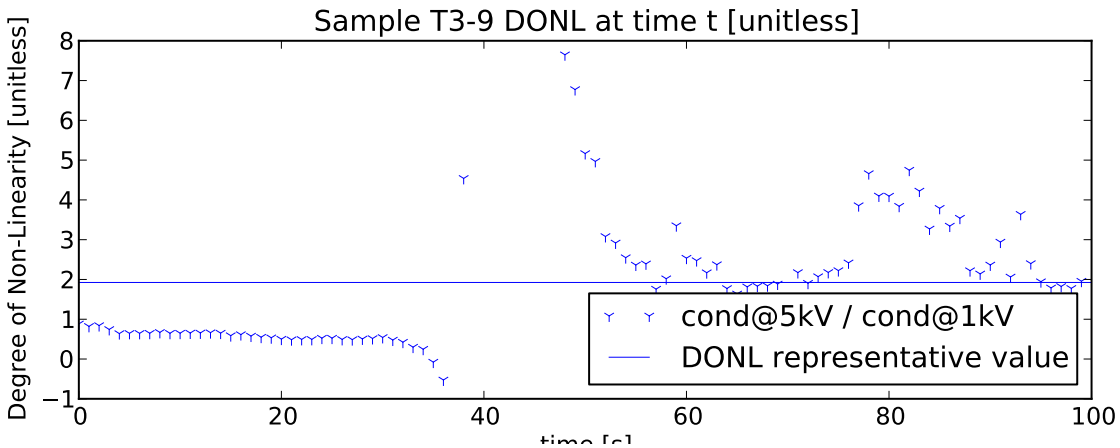

Figure B.64: Degree of Non-Linearity of sample T3-9.

B.17 Tank 3 Sample 10

T3-10

Sample Name	T3-10
Sample AC Breakdown Strength [kV]	110
Longest Vented Tree [mm]	0.14
Longest Bow Tie Tree [mm]	0.20
Number of Bow Tie Trees	15
Number of Vented Trees	2
Length of Insulation Analysed [mm]	30
Sample Water Tree Density [trees/mm]	0.00
Sample Measured Capacitance [nF]	1.93
Sample Apparent Conductivity @ 5kV [S/m]	-1.46e-16
Sample Apparent Conductivity @ 1kV [S/m]	-5.59e-17
DONL [conductivity]	2.61
DONL (charging) @ 30s [$\frac{I_{5kV}}{5I_{1kV}}$]	0.96
DONL (charging) @ 60s [$\frac{I_{5kV}}{5I_{1kV}}$]	1.12
DONL (discharge) @ 30s [$\frac{I_{5kV}}{5I_{1kV}}$]	0.98
DONL (discharge) @ 60s [$\frac{I_{5kV}}{5I_{1kV}}$]	1.33

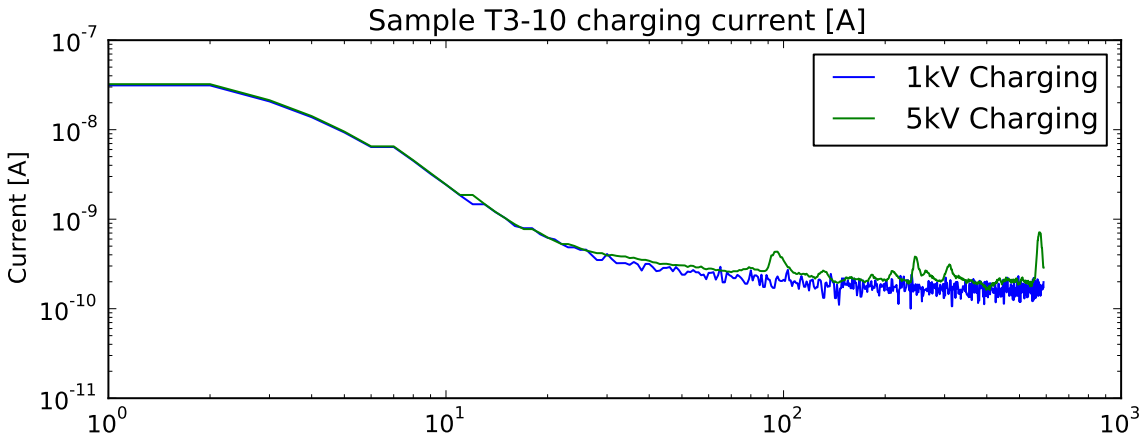

Figure B.65: Charging current of sample T3-10.

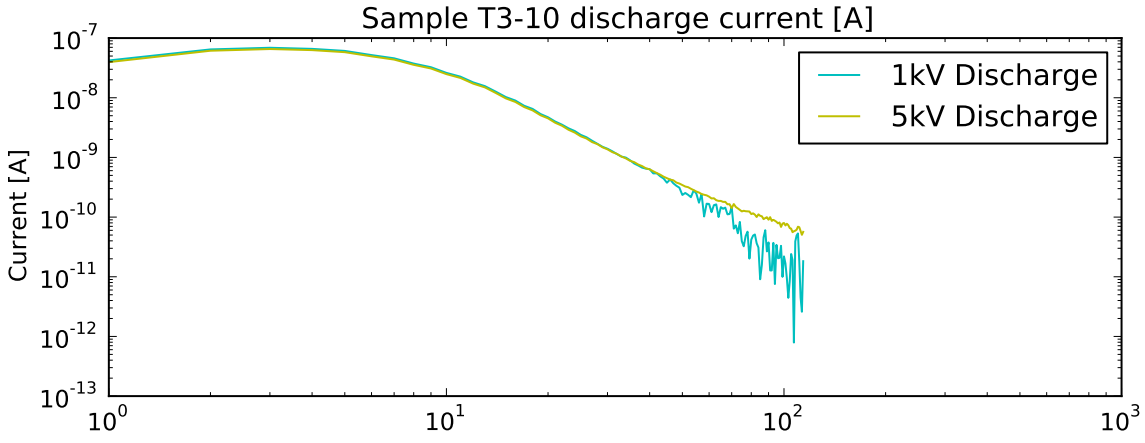

Figure B.66: Discharge current of sample T3-10.

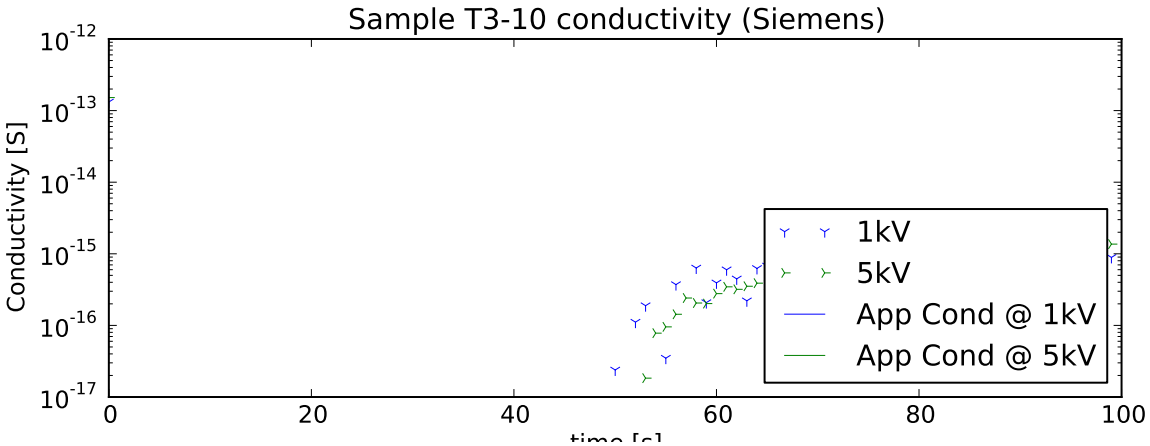

Figure B.67: Difference between charging and discharge current in sample T3-10, normalised by sample capacitance.

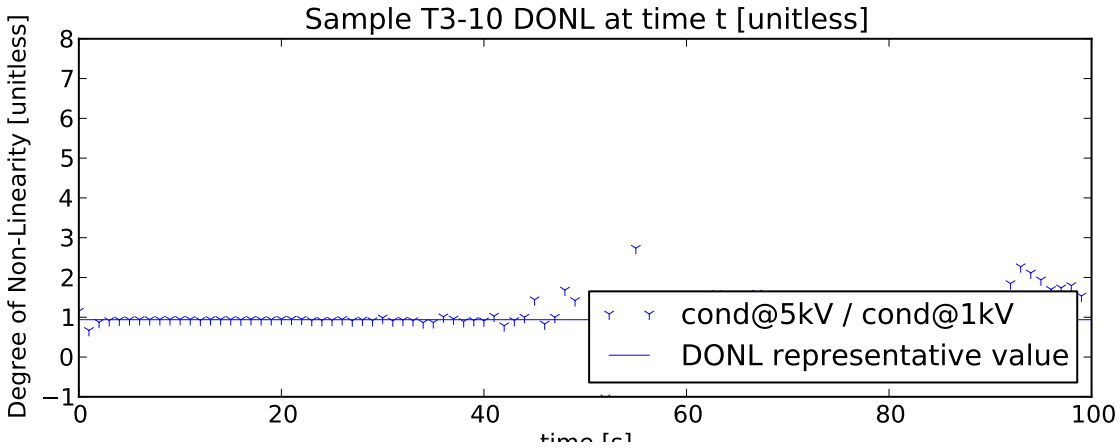

Figure B.68: Degree of Non-Linearity of sample T3-10.

Bibliography

[1] Ieee trial-use guide for accelerated aging tests for medium-voltage extruded electric power cables using water-filled tanks. *IEEE Std 1407-1998*, 0:–, 1999.

[2] Ieee guide for accelerated aging tests for medium-voltage (5 kv-35 kv) extruded electric power cables using water-filled tanks. *IEEE STD 1407-2007 (Revision of IEEE Std 1407-1998)*, pages C1 –44, feb. 2008.

[3] K. Abdolall, G. Halldorson, and D. Green. Condition assessment and failure modes of solid dielectric cables in perspective. *Power Delivery, IEEE Transactions on*, 17(1):18 –24, jan 2002.

[4] M. Abou-Dakka, A. Bulinski, and S. Bamji. Space charge evolution in xlpe with long-term aging under dc voltage - the effect of temperature and polarity reversals. In A. Bulinski, editor, *Electrical Insulation and Dielectric Phenomena, 2006 IEEE Conference on*, pages 537–540, 2006.

[5] M. Acedo, I. Radu, F. Frutos, J. Filippini, and P. Notingher. Water treeing in underground power cables: modelling of the trees and calculation of the electric field perturbation. *Journal of Electrostatics*, 53(4):267–294, October 2001.

[6] A. Al-Arainy, A. Ahaideb, M. Qureshi, and N. Malik. Statistical evaluation of water tree lengths in xlpe cables at different temperatures. *Dielectrics and Electrical Insulation, IEEE Transactions on [see also Electrical Insulation, IEEE Transactions on]*, 11(6):995–1006, 2004.

[7] A. Ashcraft and R. Eichhorn. Method for visualization of water trees by staining. *Electrical Insulation, IEEE Transactions on [see also Dielectrics and Electrical Insulation, IEEE Transactions on]*, EI-13(3):198–199, 1978.

[8] D. Auckland, J. Cooper, and B. Varlow. Factors affecting electrical tree testing. *Science, Measurement and Technology, IEE Proceedings A*, 139(1):9–13, Jan 1992.

[9] D. Auckland, A. McGrail, C. Smith, and B. Varlow. The use of ultrasound for the detection of water trees in xlpe. In A. McGrail, editor, *Conduction and Breakdown in Solid Dielectrics, 1995. ICSD'95., Proceedings of the 1995 IEEE 5th International Conference on*, pages 681–684, 1995.

[10] R. Bartnikas, R. Densley, and R. Eichhorn. Accelerated aging tests for polymer insulated cables under wet conditions. *Power Delivery, IEEE Transactions on*, 6(3):929–937, Jul 1991.

[11] R. Bartnikas, R. Densley, and R. Eichhorn. Long term accelerated aging tests on distribution cables under wet conditions. *Power Delivery, IEEE Transactions on*, 11(4):1695–1701, 1996.

[12] R. Bartnikas, H. Doepken, R. Eichhorn, G. Rittmann, and W. Wilkens. Accelerated life testing of wet cable specimens at frequencies above 60 hz. *IEEE Transactions on Power Apparatus and Systems*, PAS-99(4):1575–1585, July 1980.

[13] G. Bertini. Advancements in cable rejuvenation technology. *Power Engineering Society Summer Meeting, 1999. IEEE*, 2:0, 1999.

[14] T. Bialek and S. Grzybowski. Investigation of the performance of new xlpe and epr cables. In *Electrical Insulation and Dielectric Phenomena, 1999 Annual Report Conference on*, volume 2, pages 546–549 vol.2, 1999.

[15] P. Birkner. Field experience with a condition-based maintenance program of 20-kv xlpe distribution system using irc-analysis. *Power Delivery, IEEE Transactions on*, 19(1):3–8, Jan. 2004.

[16] S. Boggs, J. Densley, and J. Kuang. Surge induced temperature rise in water containing defects in xlpe: Mechanism for conversion of water trees to electrical trees. In *Electric Insulation and Dielectric Phenomena*, 1996.

[17] S. Boggs, J. Densley, and J. Kuang. Mechanism for impulse conversion of water trees to electrical trees in xlpe. *Power Delivery, IEEE Transactions on*, 13(2):310–315, Apr 1998.

[18] A. Bulinski, S. Bamji, B. J.-M., and J. Densley. Water treeing degradation under combined mechanical and electrical stresses. *Electrical Insulation and Dielectric Phenomena, 1992. Annual Report.*, 0:0, 1992.

[19] A. Bulinski, J.-P. Crine, B. Noirhomme, R. Densley, and S. Bamji. Polymer oxidation and water treeing. *Dielectrics and Electrical Insulation, IEEE Transactions on*, 5(4):558–570, Aug 1998.

[20] P. Caronia, J. Furno, K. Pang, and S. Szaniszlo. Advances in tr-xlpe insulation. In J. Furno, editor, *Transmission and Distribution Conference, 1999 IEEE*, volume 1, pages 56–61 vol.1, 1999.

[21] P. Caronia, A. Mendelsohn, L. Gross, and J. Kjellqvist. Global trends in mv utility cables. In A. Mendelsohn, editor, *Transmission and Distribution Conference and Exhibition, 2005/2006 IEEE PES*, pages 621–625, 2006.

[22] J. Chen and J. Filippini. The morphology and behavior of the water tree. *Electrical Insulation, IEEE Transactions on [see also Dielectrics and Electrical Insulation, IEEE Transactions on]*, 28(2):271–286, 1993.

[23] R. Coelho, P. Jestin, L. Levy, and D. Sarrail. On the return-voltage buildup in insulating materials. *Electrical Insulation, IEEE Transactions on*, EI-22(6):683–690, Dec. 1987.

[24] J.-P. Crine. Electrical, chemical and mechanical processes in water treeing. *Dielectrics and Electrical Insulation, IEEE Transactions on*, 5(5):681–694, Oct 1998.

[25] T. Czaszejko. A network model of water tree. *IEEE 1993 Annual Report, CEIDP'93*, 0:726 – 731, 1993.

[26] T. Czaszejko. 3-d electrical network model of water tree. *ANNUAL REPORT CONFERENCE ON ELECTRICAL INSULATION AND DIELECTRIC PHENOMENA*, 2:799 – 802, 1996.

[27] T. Czaszejko. Determination of statistical distribution of water tree lengths: Monte carlo simulation. *Conduction and Breakdown in Solid Dielectrics, 1998. ICSD '98. Proceedings of the 1998 IEEE 6th International Conference on*, 0:333–336, Jun 1998.

[28] T. Czaszejko. Statistical analysis of water tree lengths. *Electrical Insulation, 1998. Conference Record of the 1998 IEEE International Symposium on*, 1:89–92 vol.1, Jun 1998.

[29] R. Eichhorn. Treeing in solid extruded electrical insulation. *Electrical Insulation, IEEE Transactions on [see also Dielectrics and Electrical Insulation, IEEE Transactions on]*, EI-12(1):2–18, 1977.

[30] H. Faremo and E. Ildstad. The efi test method for accelerated growth of water trees. *Electrical Insulation, 1990., Conference Record of the 1990 IEEE International Symposium on*, 0:191–194, 1990.

[31] H. Faremo and E. Ildstad. Rehabilitation of water tree aged xlpe cable insulation. *Electrical Insulation, 1994., Conference Record of the 1994 IEEE International Symposium on*, 0:188–192, 1994.

[32] T. Fukui, K. Hirotsu, and T. Uozumi. The improved voltage life characteristics of ehv xlpe cables. *Power Delivery, IEEE Transactions on*, 14(1):31–38, 1999.

[33] J. Gulmine and L. Akcelrud. Correlations between structure and accelerated artificial ageing of xlpe. *European Polymer Journal*, 42(3):553–562, Mar. 2006.

[34] S. Hagen and E. Ildstad. Reduction of ac breakdown strength due to particle inclusions in xlpe cable insulation. *Third Conference on Power Cables and Accesories 10kV - 500kV*, 1:165–168, 1993.

[35] O. Hestad and S. Hvidsten. Condensation of water vapour in xlpe insulation at different cooling rates and pressures. *Electrical Insulation, 2006. Conference Record of the 2006 IEEE International Symposium on*, 0:515–518, 2006.

[36] J. Hvidsten, S. Benjaminsen. Diagnostic testing of mv xlpe cables with low density of water trees. In *Electrical Insulation, 2002. Conference Record of the 2002 IEEE International Symposium on*, 2002.

[37] S. Hvidsten. Nonlinear dielectric response of vented water treed xlpe insulation. *Electrical Insulation and Dielectric Phenomena, 1999 Annual Report Conference on*, 2:617–621 vol.2, 1999.

[38] S. Hvidsten, E. Ildstad, B. Holmgren, and P. Werelius. Correlation between ac breakdown strength and low frequency dielectric loss of water tree aged xlpe cables. *Power Delivery, IEEE Transactions on*, 13(1):40–45, Jan 1998.

[39] S. Hvidsten, E. Ildstad, J. Sletbak, and H. Faremo. Understanding water treeing mechanisms in the development of diagnostic test methods. *Dielectrics and Electrical Insulation, IEEE Transactions on*, 5(5):754–760, Oct 1998.

[40] E. Ildstad, U. Gafvert, and P. Tharning. Relation between return voltage and other methods for measurements of dielectric response. In *Electrical Insulation, 1994., Conference Record of the 1994 IEEE International Symposium on*, pages 25–28, Jun 1994.

[41] E. Ildstad, J. Sletbak, and A. Bruaset. Estimating the maximum length of water trees using extreme value statistics. *Properties and Applications of Dielectric Materials, 1991., Proceedings of the 3rd International Conference on*, 1:226–231 vol.1, 1991.

[42] A. K. Jonscher. *Dielectric relaxation in solids*. Chelsea Dielectrics Press, 1983.

[43] A. K. Jonscher. *Universal Relaxation Law*. Chelsea Dielectrics Press, 1996.

[44] J. Jung and R. Patsch. Selective detection of water trees in cables. *Dielectric Materials, Measurements and Applications, 2000. Eighth International Conference on (IEE Conf. Publ. No. 473)*, 0:53–56, 2000.

[45] J. Jung, R. Patsch, and D. Kamenka. Return voltage-a reliable diagnosis for water treed cables? In *Electrical Insulation and Dielectric Phenomena, 1999 Annual Report Conference on*, volume 2, pages 626–629 vol.2, 1999.

[46] S. Katakai. Design of xlpe cables and soundness confirmation methods to extra high voltage xlpe cables. *Transmission and Distribution Conference and Exhibition 2002: Asia Pacific. IEEE/PES*, 2:1411–1415 vol.2, Oct 2002.

[47] G. Katsuta, A. Toya, Y. Li, M. Okashita, F. Aida, Y. Ebinuma, and Y. Ohki. Experimental investigation on the cause of harmfulness of the blue water tree to xlpe cable insulation. *Dielectrics and Electrical Insulation, IEEE Transactions on*, 6(6):887–891, Dec 1999.

[48] C. Katz and M. Walker. Evaluation of service aged 35 kv tr-xlpe urd cables. In M. Walker, editor, *Transmission and Distribution Conference, 1996. Proceedings., 1996 IEEE*, pages 411–416, 1996.

[49] C. Katz, M. Walker, and B. Fryszczyn. Comparative laboratory evaluation of tr-xlpe and xlpe cables with super-smooth conductor shields. *Power Delivery, IEEE Transactions on*, 19(4):1532–1537, 2004.

[50] T. Kawashima, T. Maki, T. Takahashi, and K. Maeda. Study on water treeing retardant xlpe insulations. In T. Maki, editor, *Properties and Applications of Dielectric Materials, 1991., Proceedings of the 3rd International Conference on*, pages 222–225 vol.1, 1991.

[51] C. Kim, J. Jang, X. Huang, P. Jiang, and H. Kim. Finite element analysis of electric field distribution in water treed xlpe cable insulation (1): The influence of geometrical configuration of water electrode for accelerated water treeing test. *Polymer Testing*, 26(4):482–488, June 2007.

[52] C. Kim, Z. Jin, X. Huang, P. Jiang, and Q. Ke. Investigation on water treeing behaviors of thermally aged xlpe cable insulation. *Polymer Degradation and Stability*, 92(4):537–544, Apr. 2007.

[53] C. Kim, Z. Jin, P. Jiang, Z. Zhu, and G. Wang. Investigation of dielectric behavior of thermally aged xlpe cable in the high-frequency range. *Polymer Testing*, 25(4):553–561, June 2006.

[54] S. Kotz and S. Nadarajah. *Extreme Value Distributions: Theory and Applications*. World Scientific, 2000.

[55] T. Kubota, Y. Takahashi, S. Sakuma, M. Watanabe, M. Kanaoka, and H. Yamanouchi. Development of 500-kv xlpe cables and accessories for long distance underground transmission line-part i: insulation design of cables. *Power Delivery, IEEE Transactions on*, 9(4):1741–1749, 1994.

[56] M. Kuschel and W. Kalkner. Dielectric response measurements in time and frequency domain of different xlpe homo- and copolymer insulated medium voltage cables. *Science, Measurement and Technology, IEE Proceedings -*, 146(5):243–248, 1999.

[57] M. Kuschel, B. Kryszak, and W. Kalkner. Investigation of the 'non-linear' dielectric response of water tree-aged xlpe cables in the time and frequency domain. *Conduction and Breakdown in Solid Dielectrics, 1998. ICSD '98. Proceedings of the 1998 IEEE 6th International Conference on*, 0:85–88, Jun 1998.

[58] M. Lanca, M. Fu, E. Neagu, L. Dissado, J. Marat-Mendes, A. Tzimas, and S. Zadeh. Space charge analysis of electrothermally aged xlpe cable insulation. *Journal of Non-Crystalline Solids*, 353(47-51):4462–4466, Dec. 2007.

[59] M. R. Leadbetter, G. Lindgren, and H. Rootzn. *Extremes and Related Properties of Random Sequences and Processes*. Springer-Verlag, 1983.

[60] E. Leguenza, G. Silva, J. Gulmine, P. Scarpa, and D. Das-Gupta. Dielectric behaviour of ac aged xlpe cables. In G. Silva, editor, *Dielectric Materials, Mea-*

surements and Applications, 2000. Eighth International Conference on (IEE Conf. Publ. No. 473), pages 241–246, 2000.

[61] Y. Li, J. Kawai, Y. Ebinuma, Y. Fujiwara, Y. Ohki, Y. Tanaka, and T. Takada. Space charge behavior under ac voltage in water-treed pe observed by the pea method. *Dielectrics and Electrical Insulation, IEEE Transactions on*, 4(1):52–57, 1997.

[62] F. Lim, R. Fleming, and R. Naybour. Space charge accumulation in power cable xlpe insulation. *Dielectrics and Electrical Insulation, IEEE Transactions on [see also Electrical Insulation, IEEE Transactions on]*, 6(3):273–281, 1999.

[63] R. Luebbers, F. Hunsberger, K. Kunz, R. Standler, and M. Schneider. A frequency-dependent finite-difference time-domain formulation for dispersive materials. *Electromagnetic Compatibility, IEEE Transactions on*, 32(3):222 – 227, aug. 1990.

[64] J. Lyall. A new approach to the introduction of electromagnetic field theory. *Australian Journal of Engineering*, 2(1):53–61, 1991.

[65] Y. Makishi and H. Kato. Mechanism of water tree generation and propagation in xlpe. In Y. Makishi, editor, *Properties and Applications of Dielectric Materials, 1991., Proceedings of the 3rd International Conference on*, pages 147–151 vol.1, 1991.

[66] G. Matey, F. Nicoulaz, J. Filippini, Y. Poggi, and R. Bouzerara. Water treeing: interaction between test temperature and other test parameters. In *Conduction and Breakdown in Solid Dielectrics, 1989., Proceedings of the 3rd International Conference on*, pages 500–506, 1989.

[67] T. McGrail and C. Smith. Acoustic and ultrasonic techniques for condition monitoring. In C. Smith, editor, *Monitoring Technologies for Plant Insulation, IEE Colloquium on*, pages 1/1–1/3, 1994.

[68] E. Moreau, C. Mayoux, C. Laurent, and A. Boudet. The structural characteristics of water trees in power cables and laboratory specimens. *Electrical Insulation, IEEE Transactions on [see also Dielectrics and Electrical Insulation, IEEE Transactions on]*, 28(1):54–64, 1993.

[69] M. Muhr, E. Neges, R. Woschitz, and C. Sumereder. Aging behaviour of crosslinked polyethylene (xlpe) as an insulating material for high (hv)- and extra-high voltage cables (ehv). In E. Neges, editor, *Electrical Insulation and Dielectric Phenomena, 2004. CEIDP '04. 2004 Annual Report Conference on*, pages 232–236, 2004.

[70] S. Nikolajevic. Investigation of water effects on degradation of crosslinked polyethylene (xlpe) insulation. *Power Delivery, IEEE Transactions on*, 8(4):1682–1688, 1993.

[71] S. Nikolajevic. Accelerated aging of xlpe and epr cable insulations in wet conditions and its influence on electrical characteristics. In *Conduction and Breakdown in Solid Dielectrics, 1998. ICSD '98. Proceedings of the 1998 IEEE 6th International Conference on*, pages 337–340, 1998.

[72] S. Nikolajevic. The influence of the water on water absorption and density of xlpe cable insulation. *Power Delivery, IEEE Transactions on*, 13(2):297–303, Apr 1998.

[73] S. Nikolajevic. The behavior of water in xlpe and epr cables and its influence on the electric characteristics of insulation. *Power Delivery, IEEE Transactions on*, 14(1):39–45, 1999.

[74] K. Ohata and T. Taneichi. The application of new technologies on ehv xlpe cables. *Power Delivery, IEEE Transactions on*, 5(2):753–759, 1990.

[75] T. Okamoto, H. Suzuki, K. Uchida, T. Tanaka, M. Inami, and J. Shinagawa. Interfacial diffusion method to improve the breakdown strength of xlpe power cable joints. In H. Suzuki, editor, *Power Engineering Society Winter Meeting, 2000. IEEE*, volume 1, pages 712–717 vol.1, 2000.

[76] R. H. Olley, A. S. Vaughan, D. C. Bassett, S. M. Moody, and B. V. A. A. Electron microscopy of water trees in xlpe. *International Conference on Conduction and Breakdown in Solid Dielectrics*, 0:676 – 680, 1995.

[77] B. Oyegoke, D. Birtwhistle, and J. Lyall. New techniques for determining condition of xlpe cable insulation from polarization and depolarization current measurements. In *Solid Dielectrics, 2007. ICSD '07. IEEE International Conference on*, pages 150–153, July 2007.

[78] B. Oyegoke, D. Birtwhistle, and J. Lyall. Condition assessment of xlpe cable insulation using short-time polarisation and depolarisation current measurements. *IET Science, Measurement & Technology*, 2:25–31, 2008.

[79] B. Oyegoke, F. Foottit, D. Birtwhistle, J. Lyall, and P. Wickramasuriya. Condition assessment of xlpe insulated cables using isothermal relaxation current technique. In *Power Engineering Society General Meeting, 2006. IEEE*, page 6 pp., 0-0 2006.

[80] B. Oyegoke, P. Hyvonen, M. Aro, and N. Gao. Application of dielectric response measurement on power cable systems. *Dielectrics and Electrical Insulation, IEEE Transactions on*, 10(5):862–873, 2003.

[81] T. Ozaki, N. Ito, J. Kawai, and S. Nakamura. Relative permittivity and conductivity of water-treed region in xlpe estimated by an equivalent circuit. *Electrical Engineering in Japan*, 148(3):7–14, 2004.

[82] R. Patsch. Water trees-growth rate and model concept. In *Conduction and Breakdown in Solid Dielectrics, 1989., Proceedings of the 3rd International Conference on*, pages 489–493, 1989.

[83] R. Patsch. Electrical and water treeing: a chairman's view. *Electrical Insulation, IEEE Transactions on*, 27(3):532–542, Jun 1992.

[84] R. Patsch and J. Jung. Improvement of the return voltage method for water tree detection in xlpe cables. *Electrical Insulation, 2000. Conference Record of the 2000 IEEE International Symposium on*, 0:133–136, 2000.

[85] R. Patsch and A. Paximadakis. Water trees in cables-experimental findings and theoretical explanations. *Power Delivery, IEEE Transactions on*, 5(2):767–773, Apr 1990.

[86] R. Patsch, A. Paximadakis, and P. Romero. The role of dielectrophoresis in the water treeing phenomenon. *Electrical Insulation, 1990., Conference Record of the 1990 IEEE International Symposium on*, 0:160–164, Jun 1990.

[87] F. Petzold and M. Beigert. Experiences of pd diagnosis on mv cables using oscillating voltages (owts). In *Transmission and Distribution Conference and Exhibition: Asia and Pacific, 2005 IEEE/PES*, pages 1 –7, 2005.

[88] J. Piling and G. Bertini. Incorporating cablecure injection into a cost-effective reliability program. *Industry Applications Magazine, IEEE*, 6(5):52–56, 2000.

[89] G. Platbrood, S. Agnel, and A. Toureille. Application of the thermal step method to characterize the charge ability of xlpe insulation with and without ethylacrylate copolymer. In S. Agnel, editor, *Electrical Insulation and Dielectric Phenomena, 2001 Annual Report. Conference on*, pages 508–511, 2001.

[90] Y. Qiliang, W. Dong, G. Xiaoqing, L. Yigang, and C. Ping. Development of high voltage xlpe power cable system in china. In W. Dong, editor, *Properties and Applications of Dielectric Materials, 2000. Proceedings of the 6th International Conference on*, volume 1, pages 247–253 vol.1, 2000.

[91] M. Qureshi, N. Malik, and A. Al-Arainy. Effects of different ionic solutions on statistical length distribution of water trees in xlpe cable insulation. In *Properties and Applications of Dielectric Materials, 2000. Proceedings of the 6th International Conference on*, volume 1, pages 513 –516 vol.1, 2000.

[92] A. Rakowska and I. Sosnowski. Selection for dielectric enhancement technology of polyethylene insulation of mv cables evaluated by means of infrared spectrophotometric analysis. In *International Symposium on High Voltage Engineering Conference Proceedings*, 2005.

[93] C. Robertson, M. Wertheimer, D. Fournier, and L. Lamarre. Study on the morphology of xlpe power cable by means of atomic force microscopy. *Dielectrics and Electrical Insulation, IEEE Transactions on [see also Electrical Insulation, IEEE Transactions on]*, 3(2):283–288, 1996.

[94] R. Ross. Inception and propagation mechanisms of water treeing. *Dielectrics and Electrical Insulation, IEEE Transactions on*, 5(5):660–680, Oct 1998.

[95] R. Ross and W. Geurts. Application of polyethylene sheath and swelling powder against water treeing. *Conduction and Breakdown in Solid Dielectrics, 1998. ICSD '98. Proceedings of the 1998 IEEE 6th International Conference on*, 0:345–348, Jun 1998.

[96] R. Ross, W. Geurts, and J. Smit. Ftir microspectroscopy and dielectric analysis of watertrees in. In W. Geurts, editor, *Dielectric Materials, Measurements and Applications, 1988., Fifth International Conference on*, pages 313–317, 1988.

[97] R. Ross and J. Smit. Composition and growth of water trees in xlpe. *Electrical Insulation, IEEE Transactions on [see also Dielectrics and Electrical Insulation, IEEE Transactions on]*, 27(3):519–531, 1992.

[98] J. Saetbak. A theory of water tree initiation and growth. *IEEE Transactions on Power Apparatus and Systems*, PAS-98(4):1358–1365, 1979.

[99] H. Sarma, E. Cometa, and J. Densley. Accelerated ageing tests on polymeric cables using water-filled tanks - a critical review. *Electrical Insulation Magazine, IEEE*, 18(2):15–26, 2002.

[100] J. Sletbak. The mechanical damage theory of water treeing-a status report. *Properties and Applications of Dielectric Materials, 1991., Proceedings of the 3rd International Conference on*, 1:208–213 vol.1, Jul 1991.

[101] F. Stucki and J. Rhyner. Physical properties of single water trees extracted from field aged cables. *Properties and Applications of Dielectric Materials, 1994., Proceedings of the 4th International Conference on*, 1:0, 1994.

[102] A. Thomas and T. Saha. Frequency domain dielectric relaxation in water tree degraded xlpe cables. In *Universities Power Engineering Conference, 2007. AUPEC 2007. Australasian*, pages 1–6, Dec. 2007.

[103] A. Thomas and T. Saha. A new dielectric response model for water tree degraded xlpe insulation - part a: model development with small sample verification. *Dielectrics and Electrical Insulation, IEEE Transactions on DOI - 10.1109/TDEI.2008.4591236*, 15(4):1131–1143, 2008.

[104] A. Thomas and T. Saha. A new dielectric response model for water tree degraded xlpe insulation - part b: dielectric response interpretation. *Dielectrics and Electrical Insulation, IEEE Transactions on DOI - 10.1109/TDEI.2008.4591237*, 15(4):1144–1152, 2008.

[105] P. Werelius. *Development and Application of High Voltage Dielectric Spectroscopy for Diagnosis of Medium Voltage XLPE Cables*. PhD thesis, Royal Institute of Technology (KTH), Stockholm, Sweden, 2001.

[106] P. Werelius, P. Tharning, R. Eriksson, B. Holmgren, and U. Gafvert. Dielectric spectroscopy for diagnosis of water tree deterioration in xlpe cables. *Dielectrics and Electrical Insulation, IEEE Transactions on [see also Electrical Insulation, IEEE Transactions on]*, 8(1):27–42, 2001.

[107] J. Xu and S. Boggs. The chemical nature of water treeing: theories and evidence. *Electrical Insulation Magazine, IEEE*, 10(5):29–37, 1994.

[108] J. Xu and A. Garton. The chemical composition of water trees in epr cable insulation. *Dielectrics and Electrical Insulation, IEEE Transactions on*, 1(1):18 –24, feb 1994.

[109] H. Yamada, S. Nakagawa, S. Katakai, K. Kishi, T. Nakanishi, and Y. Murata. Development of heat-resistant xlpe cable and accessories. In S. Nakagawa, editor, *Properties and Applications of Dielectric Materials, 2003. Proceedings of the 7th International Conference on*, volume 2, pages 776–781 vol.2, 2003.

[110] C. Yonghong, C. Xiaolin, R. Mingzhe, and Y. Bo. Study on the partial discharge characteristics of the xlpe insulation samples during electrical treeing ageing. In C. Xiaolin, editor, *Properties and Applications of Dielectric Materials, 2003. Proceedings of the 7th International Conference on*, volume 1, pages 211–214 vol.1, 2003.

[111] T. Yoo, M. J. Ackerman, W. E. Lorensen, W. Schroeder, V. Chalana, S. Aylward, D. Metaxes, and R. Whitaker. Engineering and algorithm design for an image processing api: A technical report on itk - the insight toolkit. *Proc. of Medicine Meets Virtual Reality*, 1:586–592, 2002.

[112] B.-H. Youn, D.-H. Cho, and S.-I. Shim. Improvement of breakdown strength by additives and curing conditions on xlpe insulation for power cable. In D.-H. Cho, editor, *Electrical Insulation, 2004. Conference Record of the 2004 IEEE International Symposium on*, pages 347–350, 2004.

[113] W. Zaengl. Dielectric spectroscopy in time and frequency domain for hv power equipment. i. theoretical considerations. *Electrical Insulation Magazine, IEEE*, 19(5):5–19, Sep-Oct 2003.